Author:
Clarke, M. P

Title:
The effect of low velocity impact damage on the compressive properties of carbon fibre reinforced composites.

THE EFFECT OF LOW VELOCITY IMPACT DAMAGE ON THE COMPRESSIVE PROPERTIES OF CARBON FIBRE REINFORCED COMPOSITES.

A thesis submitted to the University of Bristol in accordance with the requirements of the degree of Doctor of Philosophy in the Faculty of Engineering

Mechanical Engineering Department, January 1997

M.P.Clarke

ABSTRACT

In this thesis the behaviour of T800/5245 and T300/913c laminates after low velocity impact is examined, both experimentally and theoretically. The loadings used were static tensile and compressive, stepped compressive and compressive fatigue loading.

Impact energies in the range 3 to 12 joules were investigated and the damage caused was mapped using x-ray, ultrasonic c-scan and deply techniques. These procedures revealed that the majority of the damage was in the region of the 0° plies close to the rear surface.

Preliminary work was carried out to demonstrate the validity of using various inserts and cuts to replicate impact damage. Implanting thin PTFE films allowed a known amount of artificial delamination damage to be introduced. Cutting plies before cure and pre-stressing in tension allowed artifical crack damage to be created in a controlled fashion.

As an aid to understanding the processes involved in structural failure after impact, specimens were damaged artificially by the introduction of artificial delaminations and ply cracks. The implanted damage was based on a 7 joule impact and the results of different implant configurations were compared to those for actual impact damage. Inserted damage that followed closely the configuration of real impact damage gave a similar reduction in strength, while simple square delaminations with a single ply cut gave a reasonable approximation—this was the geometry used for finite element analysis.

Stepped loading in compression in combination with penetrant enhanced X-radiography was used to monitor crack and delamination growth. A novel technique of resin injection was also used to determine the position of internal plies under compressive load.

X-radiography was used again, in conjunction with C-scans to follow the growth of damage in coupons subjected to compressive-compressive fatigue loading.

Large-displacement finite element analysis of the simplified replica of impact damage was used to determine the stress state of the damaged coupon under load, and to follow the deformation of the coupon as plies buckled. The out-of-plane displacement matched that from experiments and the stress state of the deformed plate calculated using the computer model showed highest compressive stresses at the point of failure. The values of stress at failure derived from the model matched closely with the ultimate compressive stress of the material.

The work indicates that the failure is linked to the breaking of the 0° fibres under the combination of in-plane compressive loading and bending-compressive loading caused by localised buckling of the coupon and may be predicted by finite element analysis of simplified damage, using multi-layer semi-loof elements, to calculate compressive stresses within the laminate.

ACKNOWLEDGEMENTS

This work was carried out in the Mechanical Engineering Department of the University of Bristol, with the support of the Defence Research Agency (DRA), Farnborough, and the Procurement Executive, Ministry of Defence.

I would like to thank my supervisor, Dr M. J. Pavier, for his support and guidance during the course of this research. I would also like to thank Dr M. Kemp of DRA Farnborough for useful discussions and advice.

Thanks are due to fellow workers in the Composites and Adhesives Group for their comments and suggestions and their willingness to be a sounding board for my ideas.

I am grateful to members of the technical staff of the mechanical engineering department at Bristol who helped at various stages during the project. They include Mr D. Jordan, Mr J. Skinner and the late Mr B. Smith.

Finally I would like to thank my wife, Carol, for her continual encouragement to complete this work.

AUTHOR'S DECLARATION

This dissertation presents the results of research studies carried out in the Mechanical Engineering Department of the University of Bristol between July 1991 and July 1994. The content is original, except where specific reference is made to the work of others, and includes nothing that is the outcome of work done in collaboration.

No part of this dissertation has been submitted for a degree at any other university.

The views expressed in this thesis are those of the author and not of the university.

Michael Clarke

University of Bristol

Mechanical Engineering Department

CONTENTS

PAGE

MISSING

IN

ORIGINAL

LIST OF FIGURES

Page *Item* *Description*

LIST OF PLATES

LIST OF TABLES

CHAPTER 1.

INTRODUCTION

1.1. Aims of research

This section looks at the reasons for the use of carbon fibre composites in structures and some of the general difficulties that arise when using composites. Problems associated with the impact damage of composites are dealt with in detail and the aim of this research is explained.

The use of carbon fibre composites

The use of carbon fibre composites has increased greatly in recent years. The main reason is the reduction in mass that can be attained while retaining adequate stiffness and strength. This is due primarily to the lower density of composites compared to metals. The higher manufacturing costs associated with using composites may be offset by savings made in operating costs, or a performance gain can be achieved.

The specific strength and stiffness of these composites, which allows them to displace metals in aerospace structures in particular, are due mainly to the enhanced tensile properties of the carbon fibre component of the composite.

The benefits that can be gained by using composites in the place of metals are numerous—reduced weight is the most obvious, but there are others, for example: reduced conduction (to heat and electricity), resistance to chemical attack and transparency to radar.

The combination of constituents used in the composite affect the properties of the final composite. There are many factors that come into play in the choice of fibre, matrix, coatings and construction method when making the basic composite, before it is even made into a component. The relationship between the material properties of the component parts and the final composite is still an area in which considerable research effort is being undertaken.

Problems specific to impact damage

Before carbon fibre reinforced plastics can be used in the primary structure of an aircraft it is necessary that the performance of the component can be predicted or proven by test. Given the expense of the material the advantages of prediction are obvious. In this context the performance of the component cannot be judged purely on its ability to perform its designed function in laboratory conditions. The behaviour of the component under non-ideal conditions must also be known—conditions that will apply in real life—and for the extent of its working life.

All components can suffer reduction in properties due to defects in manufacture or from fatigue during use. In the case of metallic components, the good understanding of the growth of damage in metals and the ability to predict the effect of defects, mean that, in the aircraft industry as an example, a regimen of inspection is deemed sufficient to ensure that safety is not compromised. If a defect is detected its present and future effect on the structure can be predicted,

Carbon fibre reinforced plastics, on the other hand, are susceptible to accidental damage by low energy impacts that can lead not only to a significant reduction in strength (particularly compressive) but the damage itself can be very difficult to

detect visually. These impacts could result from dropped tools during maintenance, or stones thrown up from the runway. The resulting damage contains varying proportions of fibre cracks, delaminations and matrix cracks. This variability in amount and type of damage, combined with the complexity of the geometry of this damage, has meant that it has been difficult to discern the mechanism of failure. This results in difficulties in predicting the precise amount of strength reduction, leading to conservative structures that do not make full use of the materials advantages, and to time consuming and expensive test validation.

The growth of damage under cyclic loading is also of critical interest, as many of the environments in which carbon fibre reinforced plastics are used can lead to fatigue failure. In addition to the difficulties associated with predicting behaviour under monotonic loading, cyclic loading introduces extra problems—the effect of loading history, the interaction of different types of damage and strain-rate dependent behaviour.

1.2. The Approach

This thesis covers work carried out as an investigation into the effect of low velocity impact damage on the residual strength of carbon fibre composites.

This work is aimed at reducing the restrictions on the use of composite materials in structures, particularly those imposed by lack of a full understanding of the effect of impact damage on structural behaviour.

The significance of low velocity impacts and their causes has already been mentioned, but this work does not intend to investigate or predict the generation of

damage from impact events. The aim is to study the effect of the resulting damage on the structural properties. Some investigation into the configuration of impact damage was necessary to characterise the damage for further study, but this involved standard methods only for creating damage in order to gain data particular to the materials being used in this work.

The information gained from experimental impact enabled selection of suitable arrangements of damage for further study. In order to separate the effects of fibre cracks, matrix cracks and delaminations, artificially implanted damage was used.

In order to allow simplification of the complex damage produced by actual impacts artificially inserted delaminations and ply cracks have been used. Delaminations are modelled by inserting thin films between plies, and cracks are modelled by cutting fibres prior to curing the composite.

The results of experiments involving actual impacts were used as the basis for implanting damage, and the effectiveness of different types of artificial damage was verified and compared to real damage. This enables a clearer understanding to be gained of the roles of these two types of damage in the process of failure.

Finite Element modelling of these artificially damaged specimens allows the effects of the damage on the stresses around the impact zone to be seen. The buckling of the various blocks of plies with increasing load can be followed and hence the post-buckling behaviour of composites with embedded damage ascertained.

Some fatigue testing of damage specimens was carried out to determine whether the findings from the static tests were applicable to cyclic loading. The range of these tests was limited, but were sufficient to show that the mechanisms of damage growth in fatigue loading were different to those in static loading.

1.3. Format of thesis

The thesis starts with a background to composites and in particular carbon fibre composites. A brief description is given of their manufacture and the properties that give them advantages over other structural materials.

The work carried out relies heavily on the ability to replicate impact damage by using artificially created damage, therefore chapter 3 of the thesis looks at the validity of the artificial damage techniques that were used, as well as describing the criteria and tests used in choosing suitable materials for inserts.

Chapter 4 covers the experimental methods used in the main body of the work, as well as the details of manufacture of specimens and insertion of damage. The materials used, their stacking sequence, curing regimes and dimensions of specimens are described. The method for inflicting actual impact damage is detailed, as are the investigative techniques for assessing the extent and type of damage (using penetrant enhanced x-ray and deply methods). Testing regimes to measure the effect of damage on strength (static tests in tension and compression) are listed. Also explained are the methods used for stepped loading and fatigue testing, carried out to show how the growth of damage may contribute to loss of strength. Typical results from the inspection of impact damaged composite plates are shown.

The results from tensile and compressive static tests, including some discussion of their significance, are dealt with in the fifth chapter.

The next two chapters deal with the numerical modelling side of the work. First, in chapter 6, a description is given of the specialised finite element that was used in the numerical analysis. Secondly, in chapter 7, the usage of the element is described. A

CHAPTER 2.

LITERATURE REVIEW

2.1. Introduction

The strength of a composite structure in compression depends on many factors, including some which can not be defined as material properties. Predictions for the properties of composites based on the components' material properties indicate that they can give significant improvements over traditional materials in terms of specific properties. It is known, however, that it is difficult to achieve the theoretical compressive strength of fibre reinforced plastics in real structures. Even in test specimens it is difficult [Wisnom 1991,1992; Curtis *et al.*, 1991]. In addition to the difficulties this poses in designing composite components, experimental results indicate that impact damage can seriously affect the compressive properties of carbon fibre reinforced plastics [Strait *et al.*, 1992; Bishop *et al*, 1984]. In this chapter some background information on composite materials and low velocity impacts is given, and previous work on impact and compressive properties of carbon fibre reinforced plastics is reviewed.

Firstly, a review of the properties of carbon fibres is given, and a description of how these can be used to advantage in composites. Following this is a description of some of the design difficulties posed when using composites. The next section looks at the importance of impact properties of composites and then each of the factors that can influence post-impact strength is dealt with in turn.

Further reviews of previous work specific to the topic under discussion are included in subsequent chapters.

2.2. Background to Carbon Fibre Reinforced Plastics

Carbon-fibre reinforced composites are only a part of a larger selection of composites. Even materials that might be considered as homogeneous on the macroscopic scale, such as some metal alloys, when viewed at the microscopic level are in fact a combination of a high strength phase with a tough ductile phase. The term 'composite' is usually used in reference to a material in which the two (or more) component materials have been combined in a controlled fashion. The aim is to take advantage of the physical properties of the two parts with the aim of producing a material that is superior, in some respect, to the two components.

The advantages of fibre-reinforced composites have lain mainly in the improved tensile properties of the fibres, though this can only be attained in very fine fibres (of the order of 10μm). In glass fibres it was found that the strength of freshly drawn fibres was far superior to old fibres - due to the presence of micro cracks on the older fibres. It is in situations such as this, where the use of another component (in this case the matrix, which protects the surface of the fibres) makes it is possible to attain a structural material with a strength close to that of the raw material.

Even with the improvement in the strength of glass and carbon fibres in recent years, they still do not compete with metals purely in terms of strength and modulus, as can be seen from the values in table 2.1.

Material	Density [kgm^{-3}]	Strain to failure %	Young's Modulus [MPa]	Tensile Strength [MPa]	Specific Young's Modulus [MPa/ kgm^{-3}]	Specific Tensile Strength [MPa/ kgm^{-3}]
Low alloy steel (quenched and tempered)	7850	11	207 000	2 000 - 2 600	26.4	0.261 - 0.276
Aluminium alloy (High strength)	2800	12-28	72 000	503	25.7	0.180
Unidirectional carbon fibre reinforced epoxy resin (Vf=0.6) (Vf=0.6) Parallel to fibres Perpendicular to fibres	1620	 0.8 0.6	 165 000[1] 7 000	 2 600[1] 38	 135[1] 4.3	 0.865[1] 0.023
Unidirectional glass fibre reinforced epoxy resin (V_f=0.5) (V_f=0.5) Parallel to fibres Perpendicular "	1930	 1.8 0.2	 38 000 10 000	 750 22	 19.7 5.2	 0.390 0.011
Random short fibre glass reinforced polyester	1550	2	8 500	110	5.5	71
Carbon fibres (only) PAN based type 1 Parallel to fibres Perpendicular to fibre	1950	 0.5	 390 000 12 000	 2 200	 200 6.15	 1.13
Pure graphite [2] parallel to basal plane perpendicular to basal plane	2260		910 000 30 000		402 15.3	

Table 2.1. Typical values for material properties—comparison of metals and composites. [Hull, 1981, with additional information]

---

[1] From BASF Material Data Sheet SPE-J-513-E-3001

[2] Included for comparison—it can be seen that there is still room for improvement in fibre manufacture. These values are theoretical, based on bond strength and typical spacing between the basal planes.

The advantage is gained when considering the *specific* strengths and moduli, when the lower density of composites swings the balance in their favour. Unfortunately, the properties transverse to the fibre length are relatively poor, and so the alignment of the fibres relative to the loading direction can make a large difference to the properties of the composite structure. This is particularly true of carbon fibres where the transverse modulus of the unidirectional composite is less than 10% of the longitudinal modulus.

Carbon fibres exhibit almost pure elastic behaviour. They are brittle and have a low strain to failure, typically less than one percent (see table 2.1). This value is for tensile failure, and similar results are quoted for compressive failure, although it is difficult to avoid fibre buckling failure when testing composites in compression. Recent work by Wisnom [1992] has achieved a strain to failure in compression of 2.5% by using a combination of bending and compression loading.

If a structure were made purely of unidirectional fibres without matrix the tensile properties would be very good, but in compression the fibres would buckle and so compressive strength would be low. With the addition of the matrix this effect is reduced (although compressive strength is still controlled by buckling), but designs for structures still require multi-directional fibre orientations to cover the possibility of off-axis loading.

In contrast, the tensile property of a fibrous composite depends on the tensile properties of the fibres. If the loading is sufficient to cause one fibre to break the load is redistributed to the unbroken fibres, this distribution being dependent on the matrix and interface properties.

The use of glass fibre reinforced plastics has become common in many situations because of the cost and improved corrosion performance over metals. Glass fibre

reinforced composites range from low strength composites of short randomly oriented fibres to medium strength continuous-fibre reinforced composites with specific strength (in the fibre direction) similar to that of steels; but it was not until the manufacture of carbon fibres that a serious competitor to metal in terms of specific strength was found.

Carbon fibres have a very high specific strength and are relatively easy (if expensive) to manufacture in quantity. The fibres are made in a continuous process by the reduction of a polymer chain (such as **p**oly**a**crylo**n**itrile, PAN) to leave a chain of carbon ring structures: (basal plane in plane of paper)

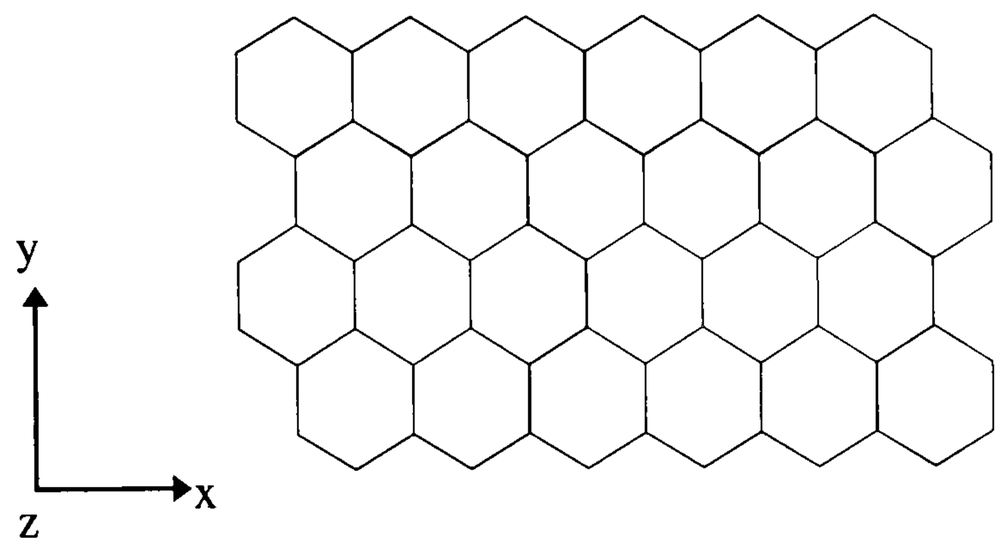

Figure 2.1. The basal plane of graphite layers. Graphite is made of many planes, stacked in the z-direction.

The Young's modulus of graphite parallel to the basal plane is about 900 GPa, normal to the planes it is 30 GPa [Hull, 1981]. The fibres are effectively a cylinder of graphite with the basal planes aligned along the fibre (and approximately concentrically in the case of fibres made from PAN). The Young's modulus of the fibre will depend on the alignment of the graphite crystals within the fibre, which is a rough cylinder of 'rolled up' planes aligned approximately parallel to the fibre axis (see Figure 2.2), and is typically in the range 140 - 250 GPa depending on the manufacturing process. This is similar to steel, but in a material that has a density of approximately 20% that of steel.

Alignment of the graphite planes can be improved by stretching polymer precursors, melt spinning pitch based precursors or by stretching during the graphitisation stage of the manufacturing process.

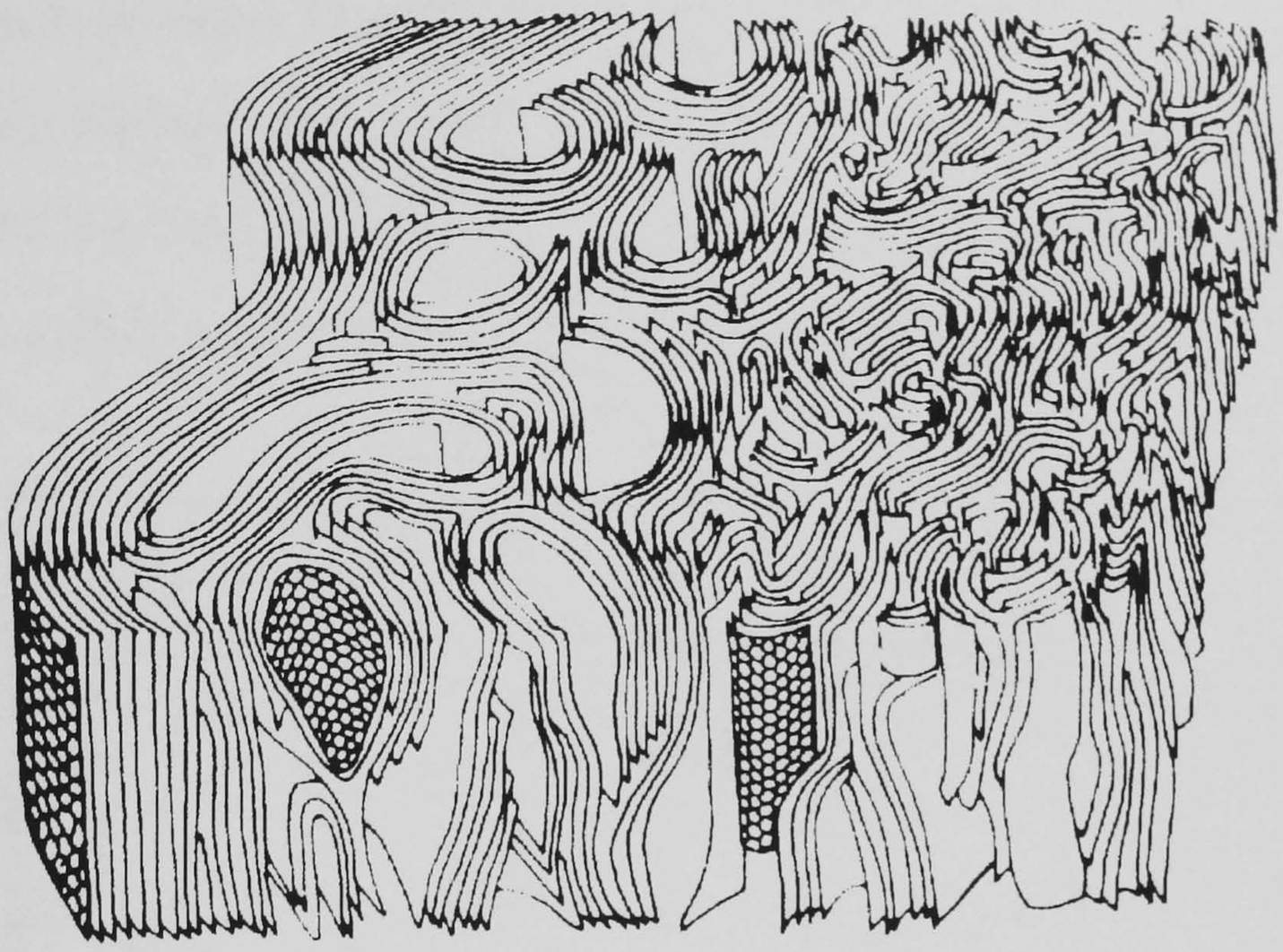

Figure 2.2. A schematic representation of the structure of carbon fibres based on X-ray diffraction and electron microscopy—hexagonal mesh indicates basal plane of graphite layers. [Bennet, 1976]

Carbon fibre composites can thus be used to make structures of similar stiffness to steel (in one direction) but with a weight saving of up to 75%. This is of particular benefit in any application where components are moving or accelerating because of the energy savings possible. Applications for carbon-fibre reinforced composites include aircraft wings, fuselage, landing gear, helicopter blades and propellers (a composite skin over a foam core), tanks and pressure vessels—from fire-fighters' air bottles to space shuttle booster tanks.

The manufacture of components and structures from fibre composites involves using this improvement in properties in one direction to advantage. To gain the full strength advantage of fibre reinforcement continuous fibres are needed in the structure. Composite starter material is available in many forms: chopped strand

matting, pre-impregnated tapes and woven fabric have the fibres already coated in a pre-cured matrix; woven fabric and reels of carbon fibre strands are available without matrix. This means manufacturing components from tapes of unidirectional fibres or fabric stacked in layers (lamina) and then resin injection (if fibre is not pre-impregnated) followed by curing, or by filament winding. The properties of unidirectional laminates made in this way are strongly dependent on the fibre angle with respect to the load, as shown in Figure 2.3 [Sinclair & Chamis, 1979].

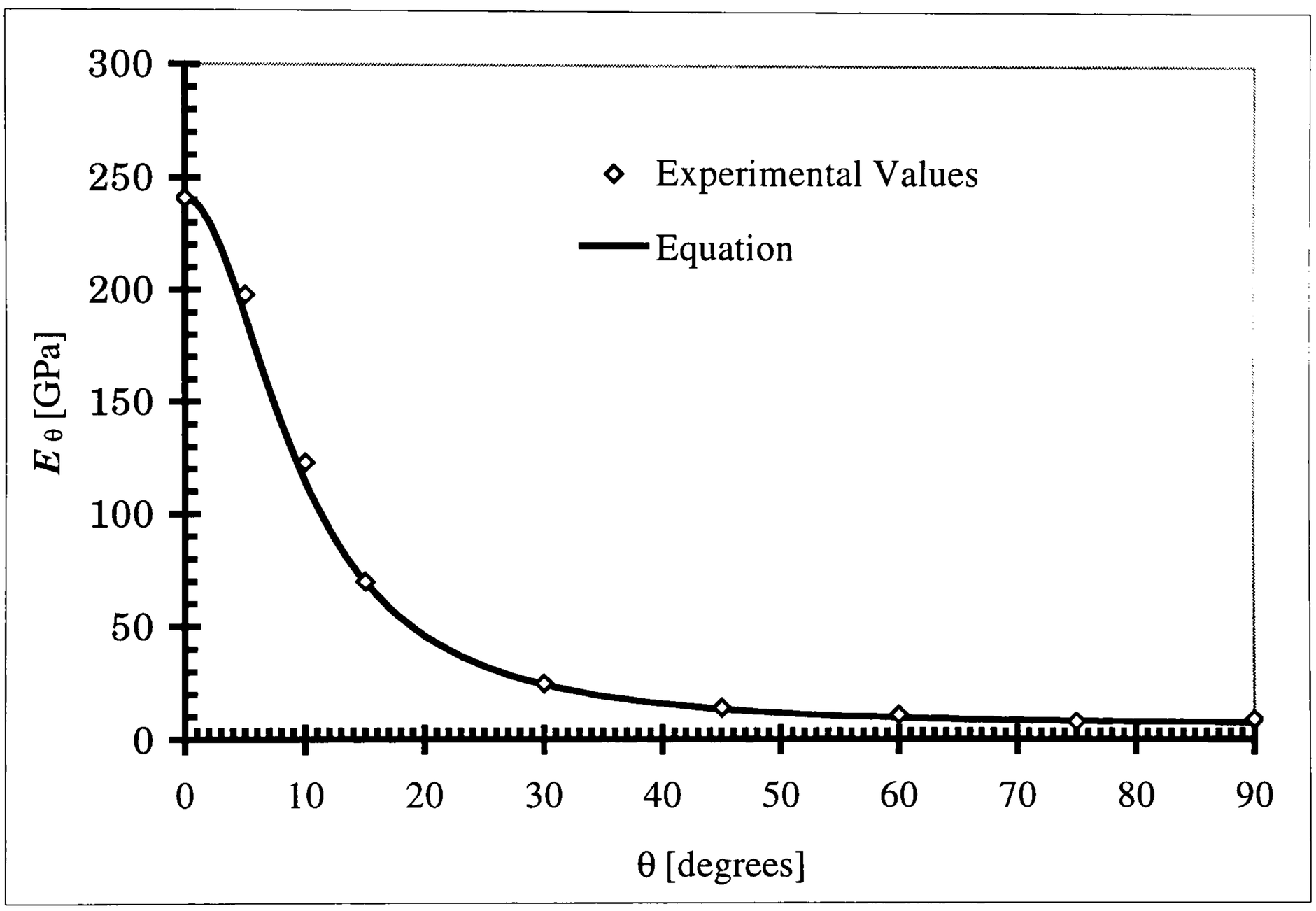

Figure 2.3. *Moduli E_θ of a carbon-epoxy resin unidirectional laminate tested at various angles to the fibre direction [Sinclair & Chamis, 1979] compared to theoretical values, equation used:*

$$\frac{1}{E_\theta} = \frac{1}{E_1}\cos^4\theta + \left(\frac{1}{G_{12}} - \frac{2\nu_{12}}{E_1}\right)\sin^2\theta\cos^2\theta + \frac{1}{E_2}\sin^4\theta$$

where $E_1 = 241$ GPa, $E_2 = 7.7$ GPa, $G_{12} = 6.1$ GPa and $\nu_{12} = 0.27$.

To avoid problems with failure because of loading in more than one direction, composites are invariably made with the fibres aligned in several directions. This is achieved in a laminate by having plies oriented in different directions. The interface between layers is a point of weakness because of the lack of fibre reinforcement. Changing the orientation of plies in the lay-up of a laminate can improve the

minimum strength of the structure but it will reduce the maximum strength, so careful design is needed to balance the transverse and longitudinal properties. (Improving the transverse strength by increasing the proportion of fibres in the 90° direction reduces the proportion in the 0° direction.)

A particular problem in the present day is the lack of strength criteria in design. Predictions of strength need to take into account not only the material properties of the composite, and these can take some time to become firm figures, but also scaling effects from experiment to implementation in a design, stress concentration in the final component and non-uniform loading. To date the properties of a plate made from carbon fibre composite have been determined by experiment, but the use of new materials in the manufacture of composites means that experiments need to be repeated for each of many combinations of component materials. This will continue to be the case until there is a fuller understanding of how the properties of the fibres and matrix relate to the properties of the final structure. Even for a simple structure, such as a flat plate, it is difficult to predict the strength of the composite from the material properties of the constituents because of the many variables—strength and moduli of both matrix and fibre, fibre volume fraction, ply thicknesses and ply angles, manufacturing variables and environmental factors.

A significant disadvantage of carbon fibre composites when compared to metals is the difficulty designing with a material where the behaviour is not fully understood. In the case of metals, imperfections in the structure, such as holes or cracks, affect the strength of the whole in a relatively well understood way, enabling the reduction in strength or stiffness to be allowed for in the design.

Until recently, the use of carbon fibre components has either been limited to secondary structures, where failure of the component will not affect the integrity of the whole structure, or where the use of flat or simply curved plates has taken advantage of the ease of manufacture of these forms from tape or cloth without the

likelihood of stress concentrations. As the move is made towards the use of composites in primary structures, components will have more complex geometries and will require the ability to carry concentrated loads. The presence of fixing holes in a composite has an effect on the strength that is difficult to predict compared to metal structures. The stress concentration round a hole in a metal structure is relatively simple to describe, whereas the anisotropic nature of a composite complicates the analysis of the effect of defects, either manufactured (e.g. drilled holes) or due to damage.

In the realm of composites the mechanisms of failure are less well defined. Clearly it is undesirable that safety factors for strength should be too large as the advantage of possible weight reductions is lost.

2.3. Background to Low Velocity Impact Damage

In the context of this work, a low velocity or low energy impact is considered to be in the region of 1-10 m/s and less than 15 Joules. For any material there is likely to be a range of energies/velocities for which the impact leaves no permanent damage. Above this threshold damage is inflicted, but the material remains intact. At greater energies/velocities still (for example ballistic impacts) the impactor will penetrate the structure. In this range the impact leaves an easily identifiable trace (and also, typically, a well defined damage zone), allowing repair or replacement of the component.

The range of impacts specified here includes an impact from a spanner dropped though a height of one metre, which may be sufficient to exceed the damage threshold for composites. The effect of this impact on a plate will depend not only on the material, but also on the thickness and fixing conditions - a thinner plate may flex causing one type of damage, whereas a thicker or more firmly fixed plate that cannot flex would receive a different type of damage. The prediction of damage from impact is outside of the scope of this work

A comparison of 7 Joule impacts for 2mm thick aluminium and 2mm thick carbon composite reveals the following: a clear and measurable dent in the aluminium, and a barely visible slight surface mark on the composite. The composite shows significant *impact resistance,* by which we mean the ability to absorb impact energy. This is one reason for using composites in engine nacelles, where they would (hopefully) help to contain turbine blades in the event of failure of a jet engine. Returning to the comparison, a detailed inspection of the two plates internally would reveal significantly more damage in the composite than in the metal. Testing the plates to failure in compression would allow measurement of the post-impact compressive strength (PICS), which gives a totally different picture. A material may have a low energy threshold for penetration during impact (low *impact resistance*), yet the

compressive strength may be hardly affected (high *residual compressive strength*), or vice versa.

It is an established fact that the effect of impact damage in composites, even at low energy, is quite significant. Figure 2.4 shows the residual compressive strength after low energy impact—the level of impact from, say, a dropped tool [Bishop *et al.*, 1984]

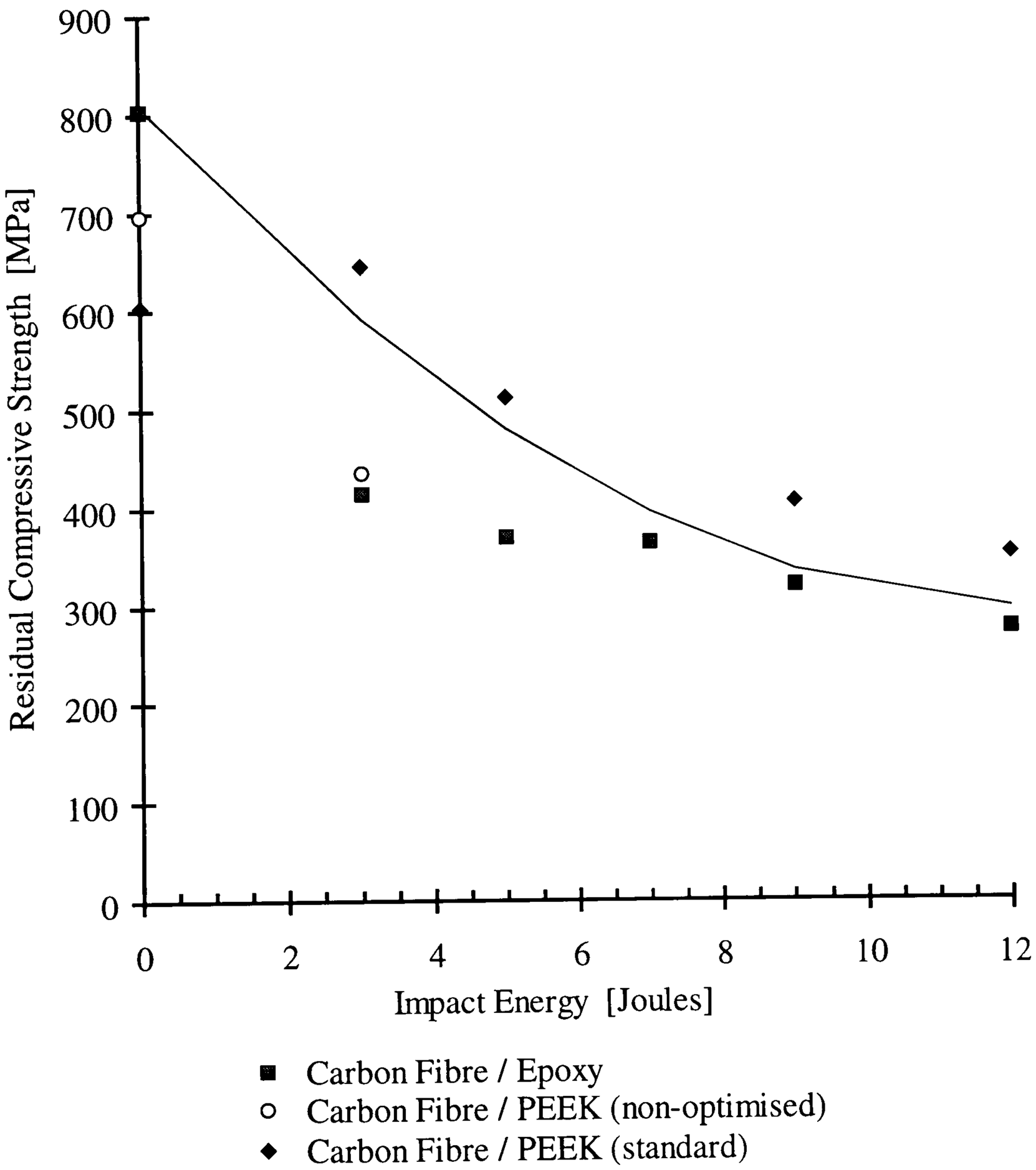

Figure 2.4. *The effect of low energy impacts on compressive strength of carbon-fibre reinforced composites. (From Bishop et al.,* 1984)

It is clear that if carbon fibre reinforced composites are to be used in primary structures the mechanisms that cause this strength reduction need to be understood, since this level of impact energy (of the order of 10 Joules) is quite likely to occur - either during maintenance of the structure or during everyday service.

The first problem is with quantifying the effect of impacts. High velocity or high energy impacts can be easier to deal with than low energy impacts because they produce clearly visible damage and often neat punctures of thin plates, in other words a simpler geometry for the damage. Here the extent and position of the damage are clear, and the growth of the damage, if it occurs, can be monitored. On the other hand, low velocity impacts are both difficult to detect and variable in content (containing a mix of fibre and matrix damage), giving rise to Barely Visible Impact Damage (BVID) on the front face, with a complex combination of fibre breakage, matrix cracks and delaminations within the composite [Davies & Robinson, 1982, Demuts & Sandhu, 1992, Kumar, 1993; Hull and Shi, 1993]. The general pattern for thin plates is for the damage to predominate towards the rear surface of the impacted target. In a structure such as the skin of a wing this means that, since the rear surface is inaccessible, the damage may escape detection. This pattern can be seen in the deply map of a seven Joule impact (Figure 2.5), and in a cross section through an impacted plate. (Figure 2.6)

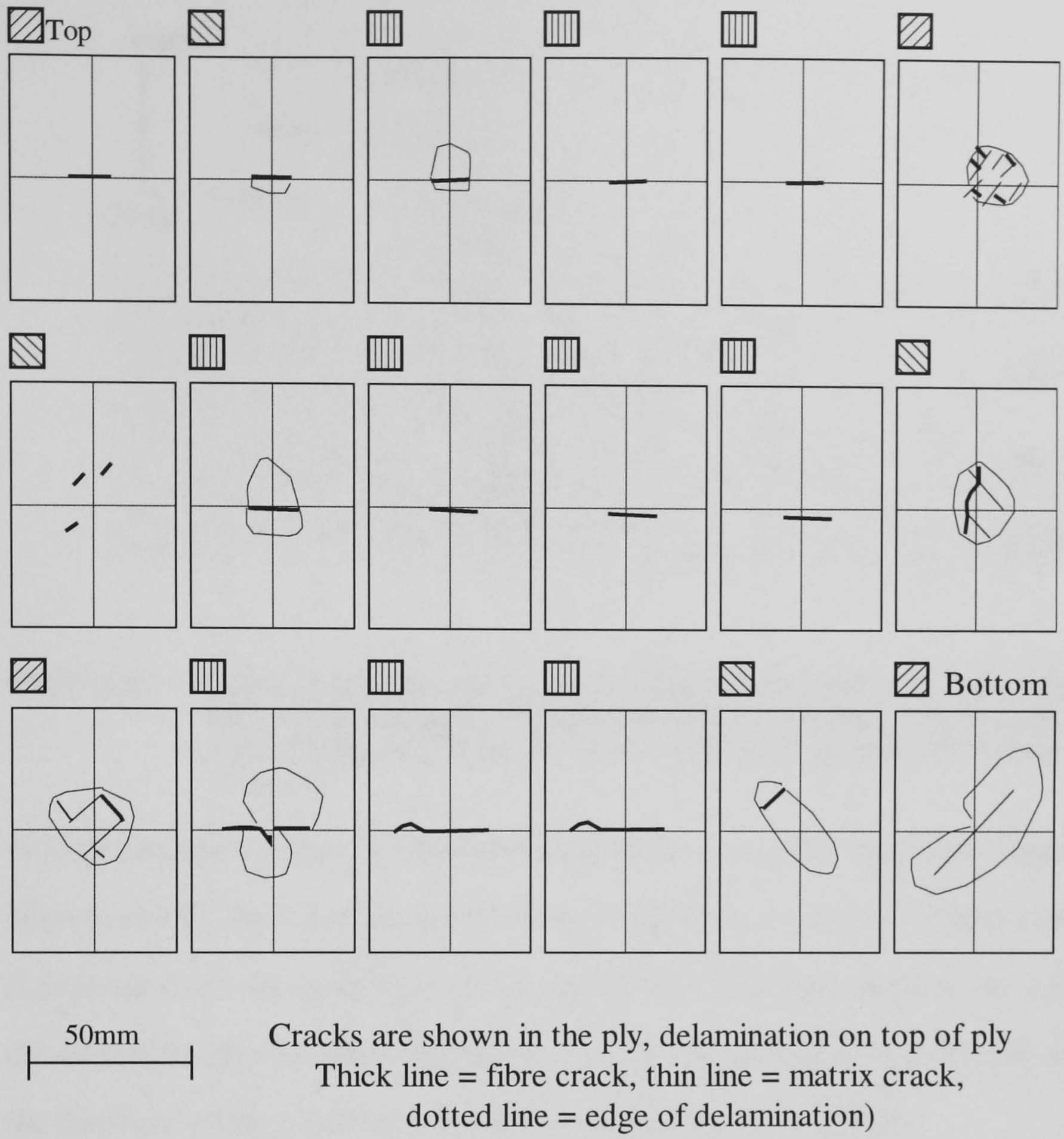

Figure 2.5 *Damage map from a 7 Joule impact, using deply to separate the laminae. Dotted lies indicate extent of delamination, solid lines indicate fibre cracks.*

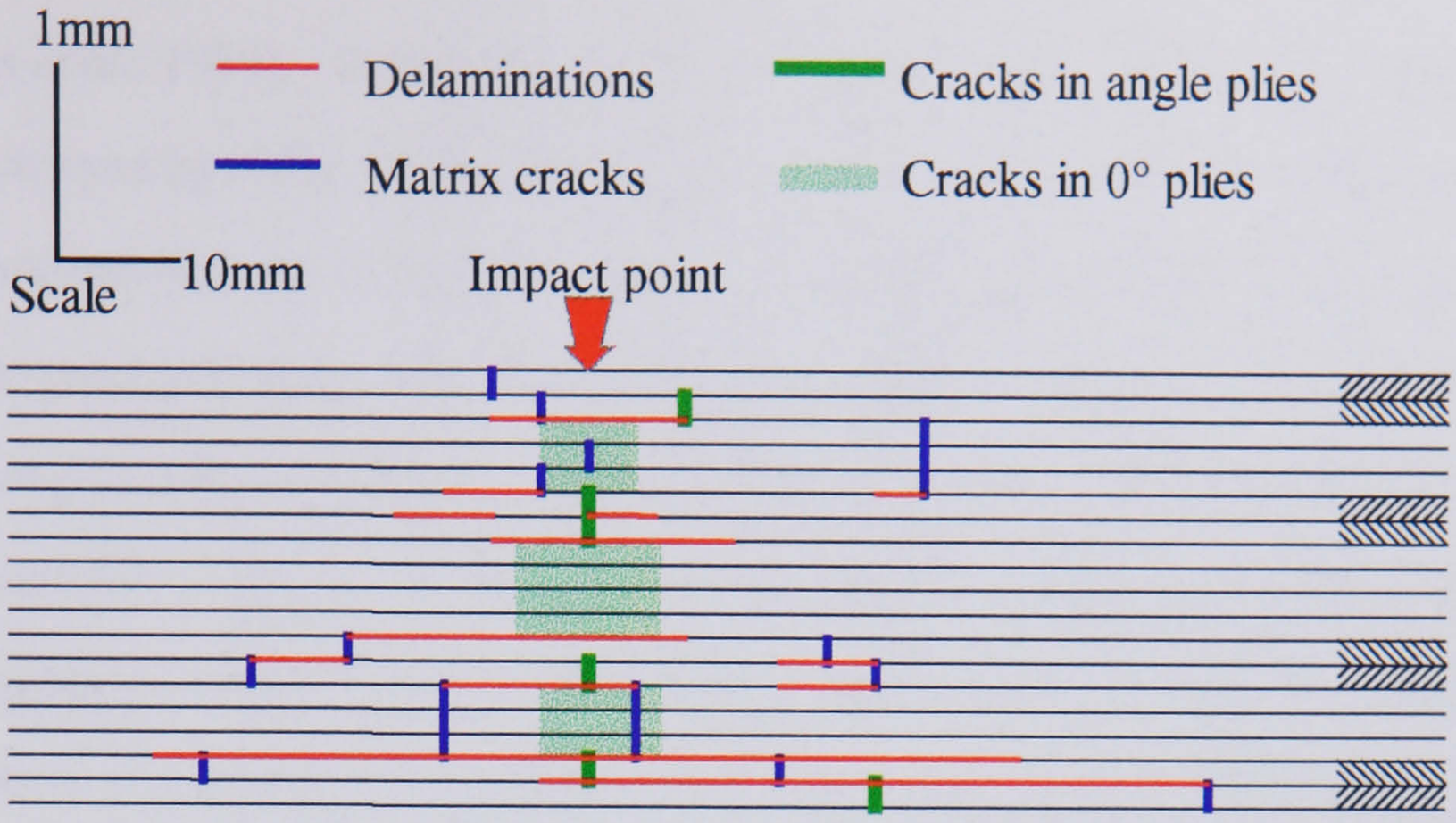

Figure 2.6. *Cross section through an 18-ply T300/913c laminate (±45°, $0°_3$, ±45°,$0°_2$)$_s$ after a 9 Joule impact, cut is perpendicular to 0° plies. Cracks in plies indicate fractured fibres, whereas matrix cracks are cracks in matrix parallel to fibres.*

In their extensive review of impact resistance of composite materials, Cantwell and Morton [1991] show that the actual damage that impacts cause to fibrous composites is dependent on: the material properties of the fibre and matrix used in the composite; the interphase between fibre and matrix; the impact energy and velocity; the supports; the thickness of the plate and also on the stacking sequence of plies.

The following sub-sections look in detail at the factors that affect the post-impact compressive strength of carbon fibre reinforced plastics.

2.3.1. Material properties and post impact compressive strength

Even if only carbon-epoxy composites are considered, there are thousands of different combinations of fibre and matrix that could be used to create a composite. With this wide choice of components for a composite it is still difficult to determine the exact contribution that each part makes to the impact resistance. The fibres in a composite carry a significant proportion of the load, and in terms of their contribution to impact resistance their most important property is strain to failure

[Davies *et al.*, 1989]. Improvements in the tensile strain to failure of fibres have been achieved by reducing the fibre diameter. This reduces the work associated with fibre pull-out and debonding, but in the low energy regime these micro-mechanical fracture processes contribute less to energy absorption, since the energy thresholds for these processes are higher. The effect of changing the fibre properties are shown in Figure 2.7. As far as this thesis is concerned there is another apparent disadvantage—thinner fibres mean a reduced stability of the fibres in compression and poorer compressive properties [Lesser and Leach, 1989]. Whether or not the post impact compressive strength is better or worse will depend on the relative effects of the lower initial compressive strength and the reduction in damage from impact.

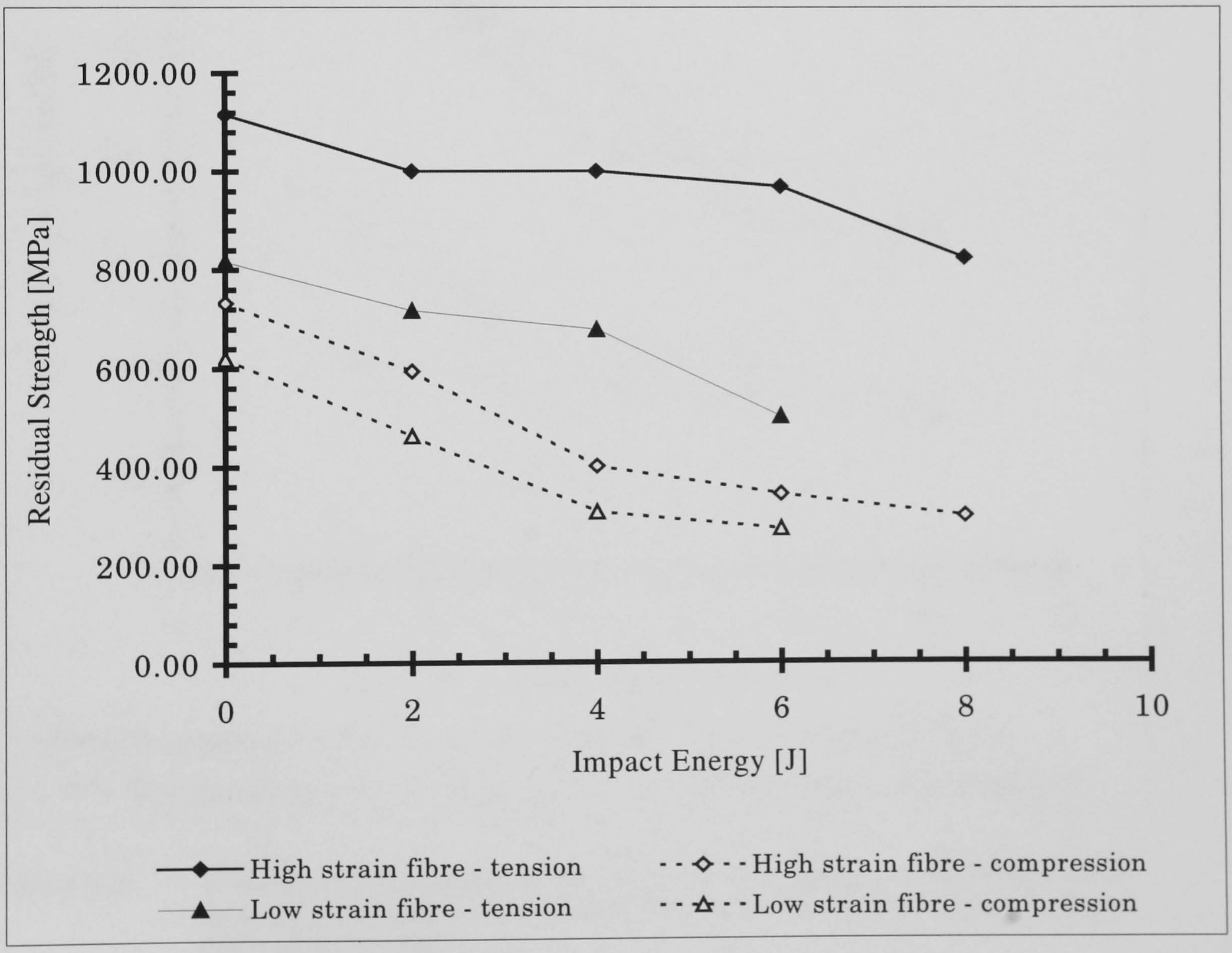

Figure 2.7. *The effect of varying fibre properties on post impact compressive strength. (From Cantwell* et al, *1986)*

The changes that can be made to the matrix in order to improve composite properties under impact include the use of additives (plasticisers, rubber or thermoplastic particles), reduction in cross-linking density of thermosetting matrix materials, the use of thermoplastics and the use of thin interlayers between plies. The aim in all these cases is to increase the toughness of the matrix. The effect of changing the toughness of the matrix can be seen in Figure 2.8. Clearly the effect is much more obvious for compression tests. It is harder to see any effect in tension, and this is likely to be because of the greater contribution to the strength from the fibres.

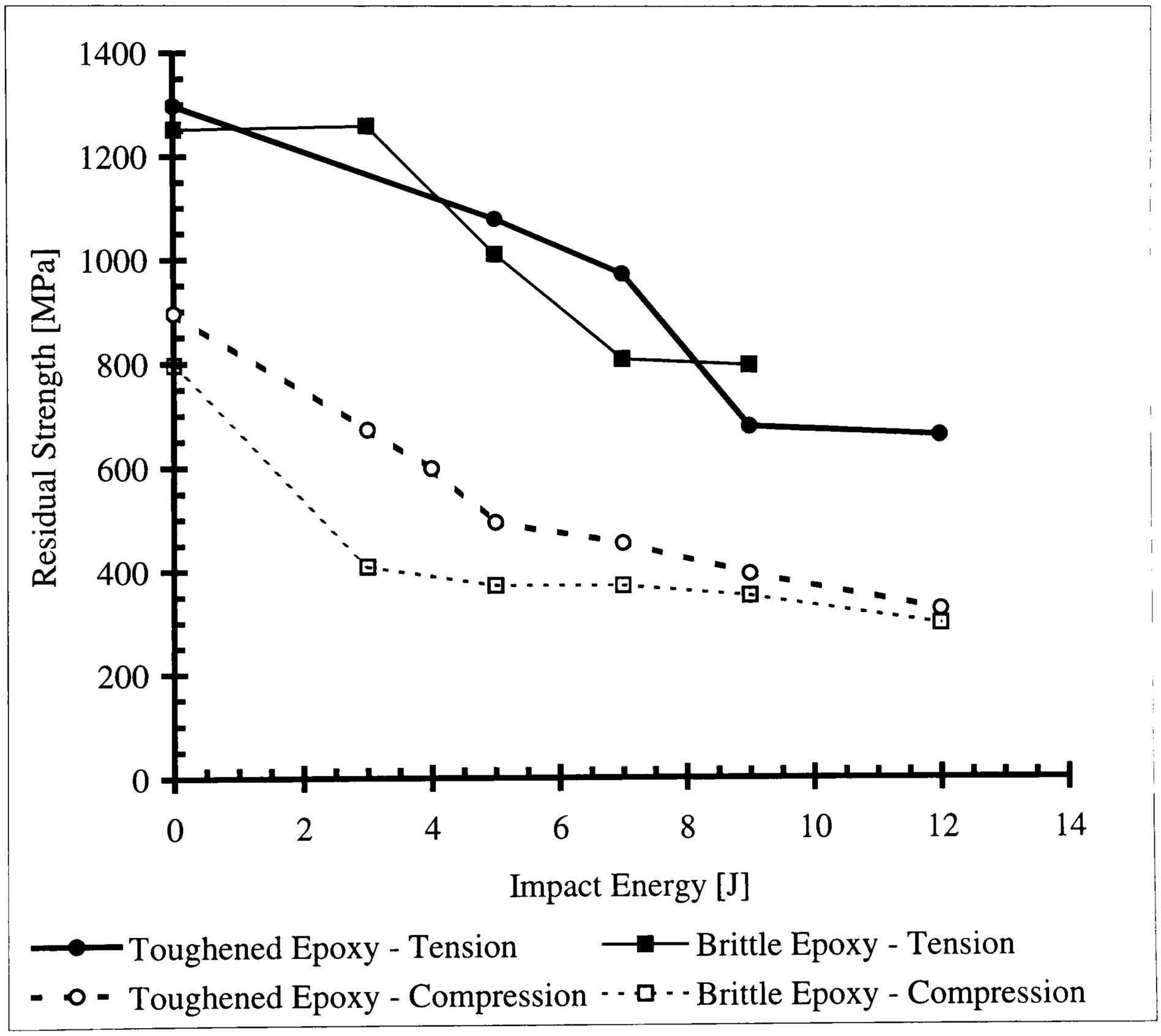

Figure 2.8. *The effect of varying the matrix property - post impact compressive strength as a function of impact energy for composites with different matrix materials. (From Dorey, 1989)*

The residual compressive strength of composites also increases with flexural strain to failure of the neat resin [Cantwell and Morton, 1991]

The final component of a fibre matrix composite is the interface between fibre and matrix. Fibres are generally surface treated (by an oxidative process) to improve adhesion between matrix and fibre. The level of treatment can be varied, with the general trend being that the fibre-matrix bond improves as the surface treatment is increased. This change in the fibre-matrix bond strength can have a dramatic affect on the impact resistance of the composite, as shown by Rogers *et al* [1971]. Alternative surface treatments have been investigated, such as coating the fibres with substances such as carboxyl-terminated butadiene-acrylonitrile rubber [McGarry *et al.*, 1985]. Dorey [1972, 1975] has shown that the effect of increasing the level of surface treatment on residual strength is to reduce the tensile strength and improve the compressive performance. His explanation is that increasing the fibre-matrix bond reduces the transverse fracture energy (from as high as 60kJ $m^{-2}$to as low as 30 kJ m^{-2}). This causes localisation of the damage and a reduced threshold for perforation. Since the damage zone is smaller, the post impact compressive strength is greater. However, the suppression of damage formation also reduces the tensile strength because it increases the notch sensitivity of the composite.

2.3.2. Impact energy and post impact compressive strength

The various types of damage have different 'threshold' energies and also absorb different amounts of energy [Srinivasan, 1992]. The threshold levels are less for matrix type failures (splitting, delamination and debonding) and orders of magnitude greater for fibre based failure modes (fibre fracture, fibre pull out). For example, a quasi-isotropic laminate of IM7/977-2, $[90°,\pm45°,0°]_{6s}$, requires an impact energy of approximately 10J before impacts caused delaminations, but about 60J is required to cause fibre fracture [Strait *et al.*, 1992].

The actual damage caused by an impact will be critical to the components' post impact behaviour. Any predictions of the likely effect of impacts on residual strength must take into account the impact resistance of the material.

2.3.3. Specimen geometry and post impact compressive strength

The effect of a given impact energy also depends on the dimensions of the component. In studies on size effects for impact damage, Swanson [1993] scaled the specimens and impactor in order to give constant surface strain on impact. He varied thickness and size of plates and cylinders and showed that the scaling of damage caused was greater than expected for larger specimen size. Extrapolation of his results (of delamination damage area versus impact velocity) to zero damage indicates different threshold values for initiation of damage—indicating there is a size effect. What this means is that damage threshold is not an absolute material property, but depends in some way on the dimensions of the specimen under test. Not only the scale and type of damage vary with size: the location of damage also varies with the plate thickness. At low incident energies thin target plates can flex on impact and damage is initiated in the plies on the rear surface due to flexural stresses, whereas in thicker plates the damage is concentrated on the impact surface due to the contact stresses around the impactor [Cantwell and Morton, 1985].

2.3.4. Stacking sequence and post impact compressive strength

Many studies have carried out experiments with different ply stacking sequences, in an attempt to understand how damage depends on laminate configuration and therefore produce composites which have greater impact resistance. Invariably, delamination damage in multi-directional laminates is concentrated between plies

with different orientation angle. Work has been done on predicting damage patterns for different stacking sequences [Choi and Chang, 1992], with some success, but there is still a need to compromise between lay-ups for impact resistance and lay-ups for undamaged structural properties. For example, switching the ordering of a $(0°,\pm45°)_s$ laminate so that the 45° plies are on the outside improves the residual compressive strength (~10%)[Cantwell *et al*, 1983], but moving the 0° plies to the inside of a laminate reduces the bending stiffness and allows out-of-plane buckling of the laminate, so the undamaged performance is compromised. Having 0° plies on the outside means that fibres have reduced support against in-plane buckling.

2.3.5. Fatigue and post impact compressive strength

In practise, the loading on a composite structure, a wing panel for example, cycles with time, undergoing both tension and compression. In this example, these cycles come about due to the different loads present at take off, landing, in flight (manoeuvering, level flight turbulence), and have separate characteristic time periods.

Damage growth from initial impact damage may occur if the magnitude of the cyclic loads is sufficient and the increase in damage will be unnoticed unless extensive non-destructive evaluation of the wing is carried out—a time consuming task for a large structure. Damage growth due to fatigue stressing of a damaged area may proceed at loads well below failure loads. The damage growth that occurs will depend on the properties of both the fibre and the matrix, as well as on the loads that are applied. In the matrix this will be in the form of matrix cracks and delaminations.

The growth of a delamination depends on the cyclic strain energy release rate—a measure of the energy required to create fresh delamination surface—and the applied load. For simple geometries it is possible to calculate the relationship between

applied load and strain energy release rate, when the critical value is reached crack growth occurs (the delamination increases in size). Fatigue studies where the strain energy release rate is varied indicate that the delamination growth (in mode II) follows the Paris equation:

$$\frac{da}{dN} = A(\Delta G_{II})^B$$

where $\frac{da}{dN}$ is the crack propagation rate per cycle, ΔG_{II} is the cyclic strain energy release rate and A and B are constants [Hiley and Curtis, 1992]. This work also indicates that there may be a threshold value for cyclic strain energy release rate below which no growth occurs. Hiley and Curtis report that the results show that increasing the toughness of the matrix, as measured by the static critical strain energy release rate (mode II), resulted in reduced crack growth rate. In this work the crack growth proceeded in a controlled manner by delamination growth. Damage growth after real impacts is likely to be complicated due to the interactions of mode I and mode II delamination growth and the presence of matrix and ply cracks.

A review of the literature has not revealed any studies of damage growth by increased fibre breakage. This may be due to the difficulty of restricting damage growth to fibre breakage, or that the thresholds for delamination and matrix growth being much lower than that for fibre crack growth.

2.4. Modes of failure

Information already presented on impact and residual strength has shown that the effect is much more critical for compressive loading. (See Figures 2.7 and 2.8.) Under tensile loading the response of a component is governed by the tensile properties of the fibre. The compressive behaviour of composites after impact is

more complex and it is worth considering the manner in which compressive failure occurs. For fibre-reinforced composites with fibres in the loading direction, compressive failure is dominated by buckling; either microscopic buckling of the individual fibres, or macroscopic buckling of the structure. Whether or not micro-buckling of fibres occurs will depend on the state of the surrounding matrix. If there is insufficient support, individual fibres can buckle on a small scale (i.e. displacements of the order of micrometers) and this can lead to the fibre breaking.

2.4.1. Unidirectional Laminates

Compressive failure of a fibrous composite can be controlled by a combination of the matrix properties and the fibre properties. Different combinations of matrix and fibre strength and modulus cause different modes of failure. In this section examination of the literature will show that failure is dominated by microbuckling, and that this is controlled by matrix properties and initial fibre waviness.

Studies from the literature suggest that the failure of composite plates in compression is by fibre microbuckling. This idea was first introduced by Dow and Gruntfest [1960]. Rosen [1964] expanded on this when he predicted that a composite made of alternating flexible and stiff laminae could buckle in one of two possible modes: shear and extension. (see Figure 2.9). This idea has been extended by Davis [1975] to include initial curvature of the fibres. He also sectioned a nominally unidirectional composite in order to plot the position of fibres along the length. This showed that the fibres did exhibit waviness (in this case there were out-of-line displacements of 15-30μm over a length of 8.64mm - equivalent to a radius of curvature of the order of a metre, or a fibre misalignment ~ 0.2°).

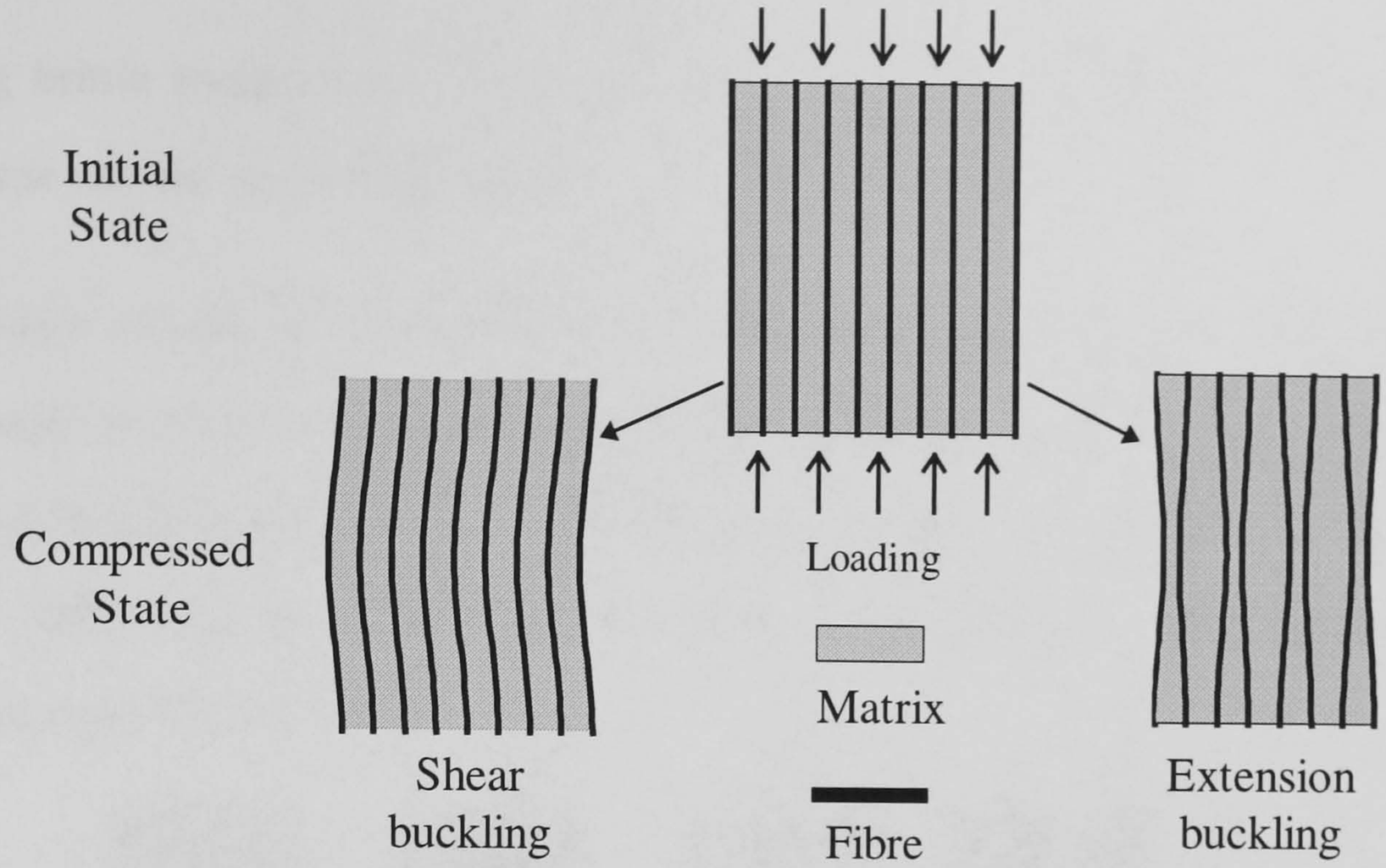

Figure 2.9. The microbuckling modes for fibres (from Rosen, 1964).

The microbuckling of the fibres is resisted by the presence of the matrix. This suggests that the fibres carry the compressive loads until they buckle due to a loss of support from the matrix as it yields. One consequence of shear buckling of the fibres is the possibility of delaminations between the fibres, which can be shown by measuring the reduction in shear modulus as compressive load is increased [Davis, 1975].

Studies of the effect of fibre and matrix properties on the compressive strength of unidirectional composites [Greszczuk, 1972,1975; Ewins and Ham,1973] show that as the stiffness and strength of the matrix is increased relative to the fibre, the failure switches from a microbuckling mode to shear failure of the fibres. This has been shown by two methods: by varying the matrix material used and by changing the temperature of the test (the matrix properties are sensitive to temperature).

Current advances in fibre manufacture (manufacturing methods, fibre diameters, new materials as precursors, fibre finish to name a few) have greatly increased the strength and stiffness of carbon fibres. In the same period the properties of matrix materials used in composites have not changed as significantly (partly to avoid

creating brittle composites), which has effectively moved the failure mode of the composite into the microbuckling region.

Microscopic examination of carbon fibre reinforced plastics that have been subjected to uniaxial compression, while confined by hydrostatic pressure to prevent the specimen buckling, show failure of the fibres by microbuckling [Weaver & Williams, 1975]. The fibres show fractures either side of a 'kink band' of displaced fibre segments (see Figure 2.10).

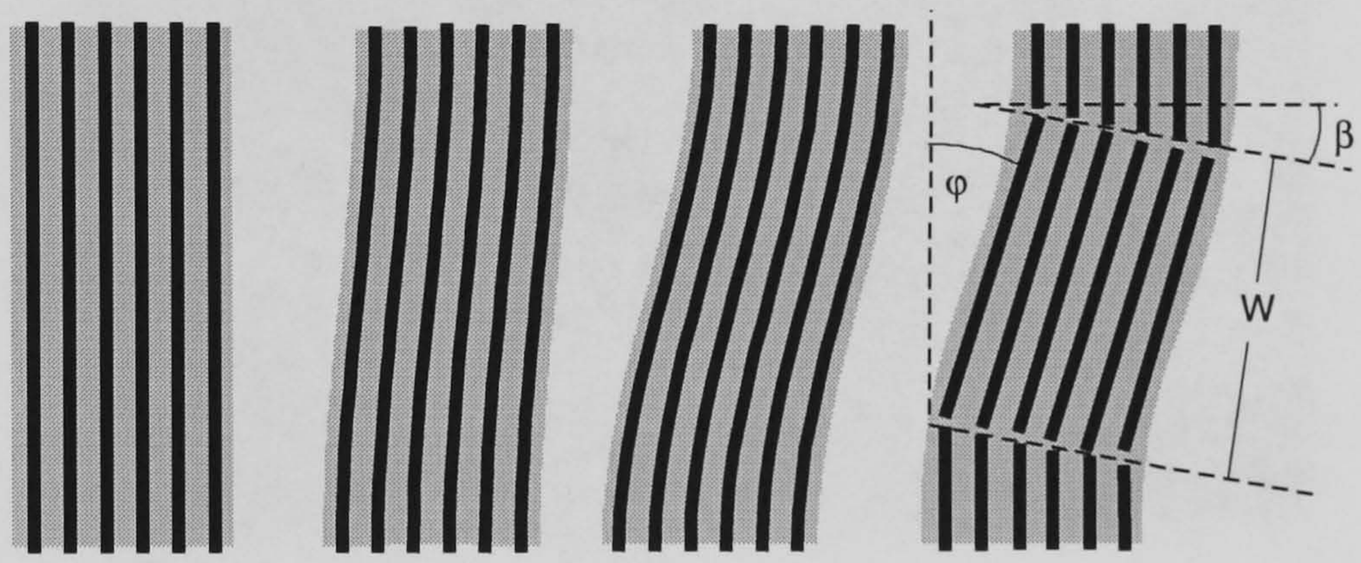

Figure 2.10. Kink band failure of buckled fibres, showing the geometry in-plane

This form of failure has been observed by many researchers [Chaplin, 1977; Evans and Adler, 1977; Hahn, 1986] and the kink is well defined with geometries in the range of 45° to 60° for φ, the kink orientation angle, and 20° to 30° for β the boundary angle (and $\beta \approx \frac{\varphi}{2}$). An example is shown in plate 2.1. Each fibre fractures due to the compressive and tensile forces set up in bending, as shown in plate 2.2, when the fibres buckle.

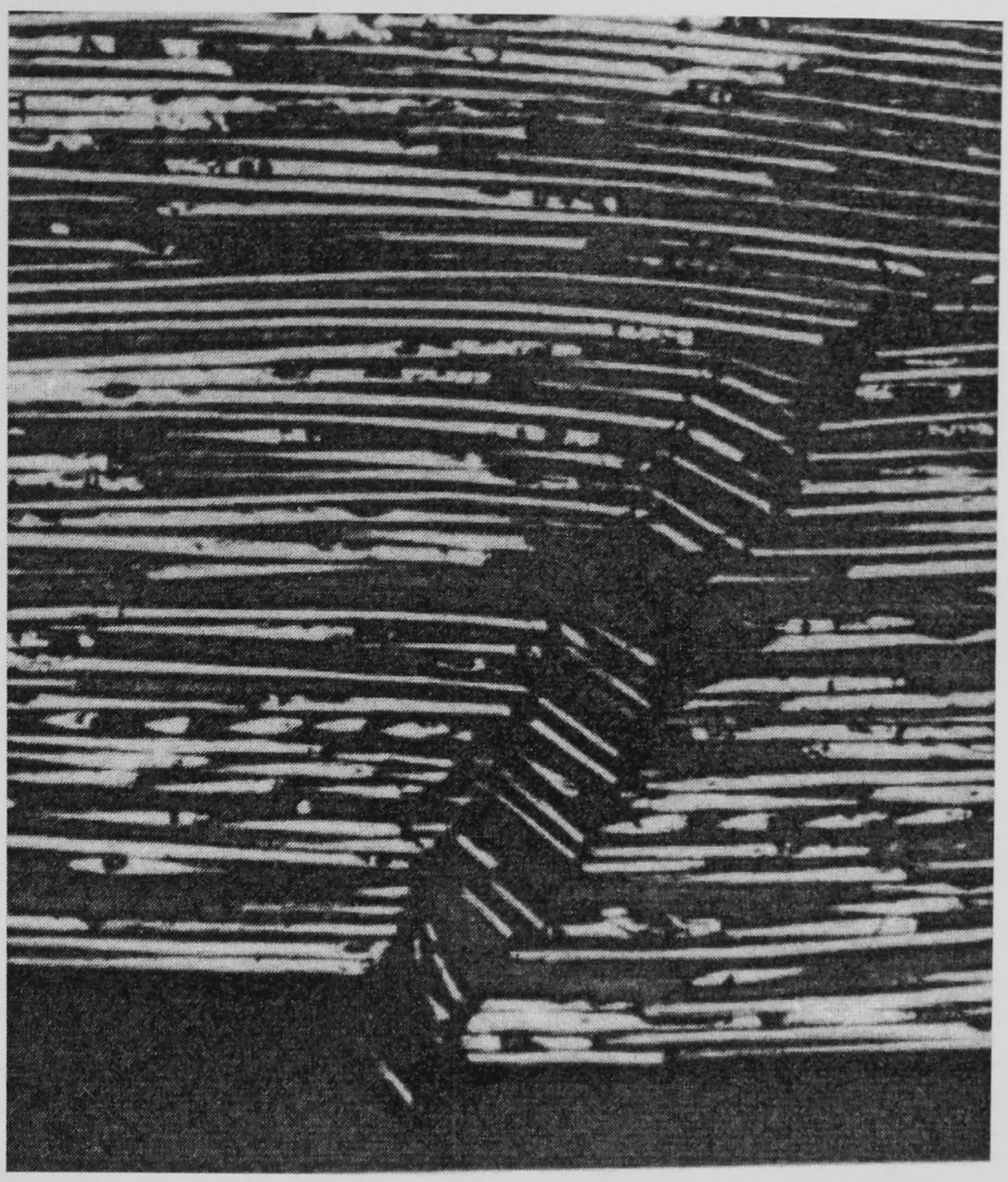

Plate 2.1. *A kink band formed in the compressive zone of a four point bend test sample (Polished section of carbon-fibre resin pultruded specimen) [Parry & Wronski, 1980]*

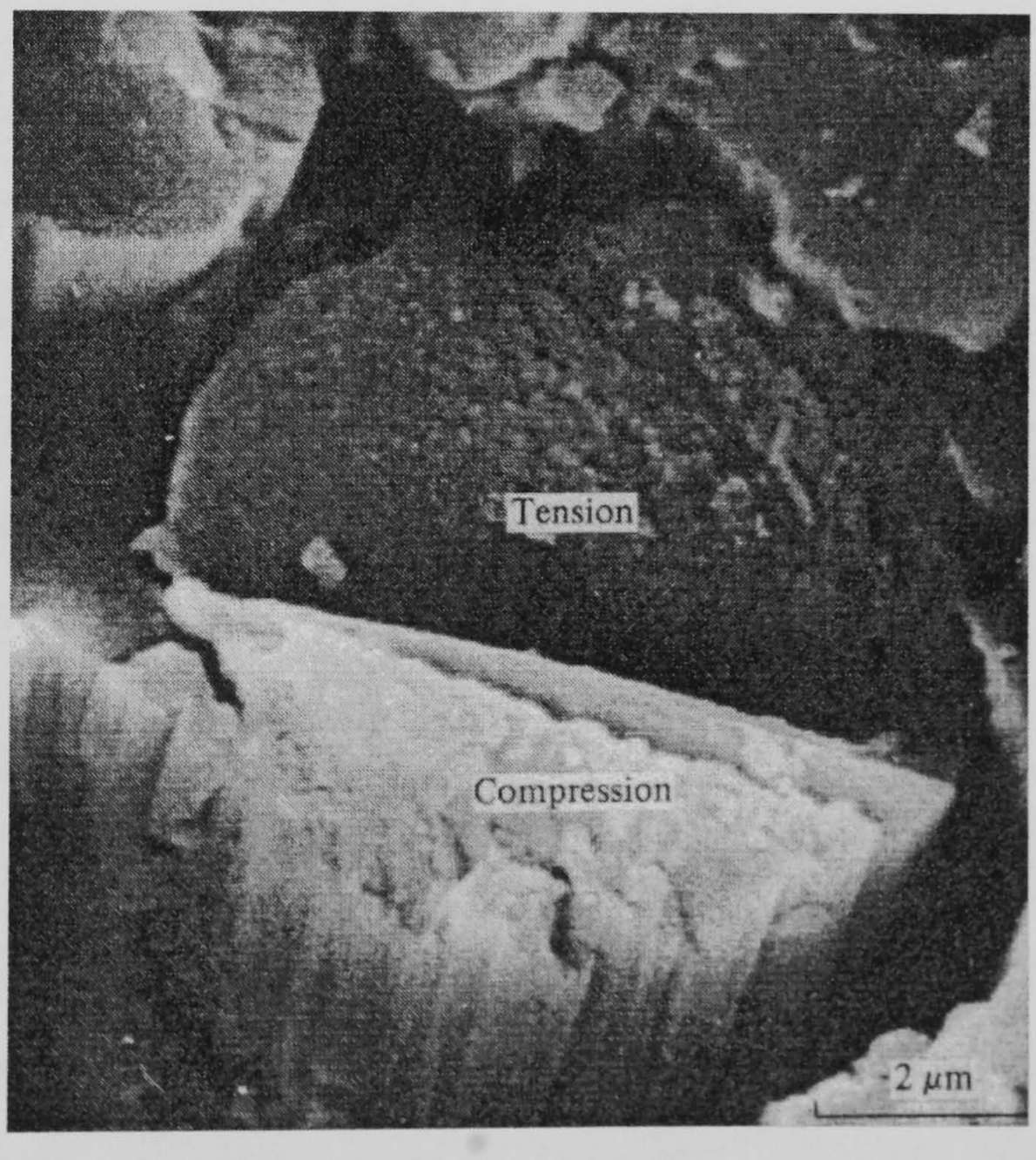

Plate 2.2. *High magnification scanning electron micrograph of the fracture surface of a single carbon fibre after microbuckling failure due to longitudinal compressive stress. [Ewins and Potter,1980]*

Work by Fleck and Budiansky [1990] indicates that the stress required to initiate the kink is greater than that needed to propagate the kink band. No exact measurements of the speed of kink propagation has been reported in the literature, as far as the author is aware, however it is reported [Klassen-Nekludova *et al*, 1961] that the speed of propagation of kink bands in single crystals is of the order of 1 m/s.

2.4.2. Multi-directional Laminates

In a multi-directional laminate plies of different orientations are used to improve the transverse properties of the composite. An estimation of failure strength can be gained by summing the contribution from each ply:

$$\sigma_{LAMINATE} = \sum_{i=1}^{n} \frac{A_i}{A_{total}} \sigma_c^{\theta_i} = \frac{\sigma_0}{A_{total} E_{\parallel}} \sum_{i=1}^{n} A_i E_x^{\theta_i}$$

where $\sigma_c^{\theta_i}$ is the compressive strength of the i-th unidirectional laminate at an angle θ to the loading direction, A_i is the cross-sectional area of the i-th ply and n is the number of laminae. $E_x^{\theta_i}$ is the longitudinal modulus for the i-th ply with fibres at an angle to loading of θ. This does not account for any interactions between plies and does not address the failure mechanism. The compressive modulus of each ply can be calculated using laminate theory (see Figure 2.3).

A consequence of changes in fibre direction from one ply to the next is that there are interlaminar regions of matrix material between plies. These regions allow extended planar crack growth known as delamination. If delaminations are present, due to a failure of the matrix between plies, this may allow some plies to buckle out and will reduce the strength and stiffness of the structure. It may also mean that the composite in the region of the delamination is no longer 'balanced'—if the laminate

does not have a symmetrical lay-up of plies then coupling forces are present in the laminate that can cause it to warp. The presence of matrix cracks and ply cracks can also be a point for initiation of delaminations. Adjacent plies support a lamina normal to plane (reduce bending out of plane) and in plane (reduce kink band formation). This support is transmitted via the matrix, and the presence of delaminations removes these constraints.

2.5. Concluding Remarks

The current work does not aim to produce a theory for the mechanism of failure of undamaged multi-directional laminates in compression—rather it aims to investigate how the introduction of damage due to low velocity impact affects the strength of the laminate and to determine if it is possible to predict the failure of the damaged specimen if the behaviour of the undamaged specimen is known. We assume that the micro-mechanical mechanisms of failure (i.e. on the scale of the fibre diameter) are similar in both cases.

Extensive work has been carried out in this field to determine the factors that affect the damage caused by impact. Much work has also been done to find the links between the residual strength after impact and composite material properties. Most of this work has investigated the relationship between post impact compressive strength and impact *energy*. What is required is an understanding of the mechanisms by which damage affects strength, such that one could predict the reduction in strength from measurement of the extent of damage and knowledge of the undamaged properties.

References

Bishop S.M.,Howard G.D. and Wood C.J.

"The Notch Sensitivity and Impact Performance of [0°,-45°,+45°] Carbon Fibre Reinforced PEEK."

RAE Technical Report 84066 June **1984** Vol. 26 pp. 1-15.

Cantwell W.J., Curtis P.J. and Morton J.

"An assessment of the impact performance of carbon fibre reinforced plastics with high strain carbon fibres."

Composites Science and Technology **1986** Vol. 25 pp. 133-148.

Cantwell W.J. and Morton J.

"The impact resistance of composite materials - a review."

Composites September **1991** Vol. 22 (5) pp. 347-62.

Cantwell W.J. and Morton J.

"Detection of Impact Damage in CFRP laminate."

Composite Structures **1985** Vol. 3 pp. 241-57.

Chaplin C. R.

"Compression fracture in unidirectional glass reinforced plastics."

Journal of Materials Science **1977** 12 pp. 347-52.

Choi H.Y. and Chang F.K.

"A Model for Predicting Damage in Graphite/Epoxy Laminated Composites Resulting from Low Velocity Impact Damage."

Journal of Composite Materials November **1992** Vol. 26(14) pp. 2134-69.

Curtis P.T., Gates J. and Molyneux C.G.

"An improved engineering test method for measurement of the compressive strength of unidirectional carbon fibre composites."

Composites September **1991** Vol. 22(5) pp. 363-7.

Davies G.A.O., Robinson P. and Freeman S.M.

"Predicting Failure by Debonding / Delamination."

American Society for Testing & Materials **1982** STP787 pp. 50-62.

Davies P., Cantwell W.J., Richard H. and Kausch H.H.

"Interlaminar fracture testing of carbon fibre/PEEK composites validity and applications."

Developments in the Science and Technology of Composite Materials. Proceedings ECCM3 Bordeaux **1989** pp.747-55.

Davis J. G.

"Compressive Strength of Fibre-Reinforced Composite Materials."

American Society for Testing & Materials STP580 **1975** pp.364-77.

Demuts E., Sandhu R.S.

"Barely Visible Damage Threshold in a BMI."

AGARD May **1992** CP-530 pp. 18.

Dorey G.

"Relationship between impact resistance and fracture toughness in advanced composite materials."

Effect of Service Environment on Composite materials. AGARD **1980** CP 288.

Dorey G.

"Damage tolerance and damage assessment in advanced composites."

Advanced Composites (Editor I.K. Partridge) *Chapter 11*.Elsevier Applied Science Publ. **1989**

Evans, A.G. and Adler, W.F.

"Kinking as a mode of structural degradation in carbon fibre composites."

Acta Metallurgica **1978** Vol. 26(5) pp. 725-38.

Fleck, N.A. and Budiansky, B.

"Proceedings of the IUTAM Symposium on Inelastic Deformation of Composite Materials." **1990**

Hahn, H.T.

"Compression failure mechanisms in unidirectional composites."

NASA **1986**;TM-85834.

Heida J.J., Beuker G., Verdegaal M.

"Manufacturing and inspection of artificial delaminations in composite materials."

National Aerospace Laboratory, TP 91085U Amsterdam February **1991** pp. 1-6.

Hiley M.J. and Curtis P.T.

"Mode II Damage Development in Carbon Fibre Reinforced Plastics."

AGARD 74th Structures and Materials Meeting, Patras, Greece. May **1992** CP-530 pp. 17.1-17-11

Hull D.

"An Introduction to Composite Materials."

(Cambridge Solid State Science Series). Cambridge University Press **1981** .

Hull D., and Yi Bing Shi.

"Damage mechanism characterisation in composite damage tolerance investigations".

Composite Structures **1993** Vol. 23 pp. 99-120.

Klassen-Nekludova, M.V., Chernysheva, M.A. and Tomilovskii, G.E.

Soviet Physics, Crystallography 1961 Vol. 5 pp. 617-621

Kumar P, Rai B

"Delaminations of Barely Visible Impact Damage in CFRP Laminates."

Composite Structures **1993** Vol.23(4) pp. 313-318

McGarry F.J., Mandell J.F. and Kawamoto J.

"Impact resistance of rubber modified carbon-fibre composite."

Advanced Composites (American Society of Metals) **1985** pp. 195-205.

Rogers K.F, Sidey G.R and Kingston-Lee D.M.

"Ballistic impact resistance of carbon-fibre laminates."

Composites **1971** Vol. 2 pp. 237-41.

Rosen, B.W.

"Mechanics of composites strengthening."

Fibre Composite Materials American Society of Metals October **1964**. pp 37-75

Srinivasan K., Jackson W.C.,Smith B.T. and Hinkley J.A.

"Characterisation of damage modes in impacted thermoset and thermoplastic composites."

Journal of Reinforced Plastics and Composites October **1992** Vol. 11 pp. 1111-26.

Strait L.H., Karasek M.L., Amateau M.F.

"Effects of Stacking Sequence on the Impact Resistance of Carbon Fibre Reinforced Thermoplastic Toughened Epoxy Laminates."

Journal of Composite Materials **1992** Vol. 26(12) pp. 1725-40.

Sinclair J.H. and Chamis C.C.

"Fracture modes in off-axis fibre composites"

Proceedings of the 34th SPI/RP Annual Technology Conference Paper 22A

Society of the Plastics Industry, New York **1979**.

Swanson S.R.

"Mechanics of transverse impact in fibre composite plates and cylinders."

Journal of Reinforced Plastics and Composites March **1993** Vol. 12 pp. 256-67.

Weaver C.W. and Williams, J.G.

"Deformation of carbon-epoxy composites under hydrostatic pressure."

Journal of Materials Science **1975** Vol. 10 pp. 1323-1333.

Wisnom M.R.

"The effect of fibre waviness on the relationship between compressive and flexural strengths of unidirectional composites.".

Journal of Composite Materials **1994** Vol. 28(1):66-76.

Wisnom, M.R.

"On the high compressive strains achieved in bending tests on unidirectional carbon-fibre epoxy."

Composites Science and Technology **1992** Vol. 43(3) pp. 229-35.

Wisnom M.R.

"Effect of shear stresses in indirect compression tests of unidirectional carbon-fibre epoxy."

AIAA **1991** Vol. 29(10) pp. 1692-1697.

CHAPTER 3.

ARTIFICIAL DAMAGE TECHNIQUES

3.1. Introduction

In studying the effects of impacts it would be useful to be able to work with coupons containing known amounts of damage. This can be achieved if damage is deliberately implanted during manufacture to simulate real damage. The main advantage gained by using artifical damage is that closer control over the level of damage in a specimen enables separation of the effects of delamination, fibre breakage and matrix cracks. It is then possible to investigate specimens that contain only delaminations, for example, when a real impact may contain all types of damage. Another advantage of artificial damage is that the position within the specimen can be controlled (for example the depth of a delamination) in a way that is not easily managed with real impacts.

The aim of this part of the work was to find effective ways of introducing artificially cracks and delaminations. This chapter looks at the requirements of artificial damage and methods that previous workers have used to implant damage. Next the candidate materials for inserts and methods used in this work are described. This is followed by the results of testing carried out to verify that the implanted damage replicated the

behaviour of real damage. The findings from this chapter were used in later work investigating post-impact behaviour.

3.2. The Requirements of Artificial Damage

Real impacts cause three types of damage: delaminations, matrix cracks and fibre breakage. In a laminate the definition of a delamination is taken to be a crack in the matrix material in the plane between adjacent plies. The term 'matrix crack' is used to describe other cracks in the matrix between fibres in a single ply (i.e. normal to delaminations). A fibre crack is defined here as where neighbouring fibres have broken in the same vicinity, and would usually be accompanied by a matrix crack through the gap between the broken ends. The position of the damage is usually towards the rear of the plate, away from the impact face [Clark, 1989] (For more detailed description of the damage incurred by impact see section 5.5). The actual configuration of the damage depends on the energy and velocity of impact as well as the geometry of the impact head, the constraints on the plate and its properties and thickness [Birch & Williams, 1978; Rhodes *et al*, 1979]. In studying real impact damage it soon becomes apparent that there is a certain amount of variability in damage produced by two impacts of the same energy, velocity and impact head. For this reason alone, building specimens that already contain delaminations and cracks, introduced artificially, can help by producing consistent levels of damage. All these variables, along with microstructural variations from specimen to specimen, mean that it is very difficult to produce consistent damage from actual impacts. In order to gain an understanding of the effect of different types of damage and their contribution to the ultimate failure of a material it is useful to be able to control the amount, type and position of the damage in a specimen. It was also found that the

type of damage caused by a given energy of impact was dependent on the material being damaged.

Artificially implanted delaminations must produce the same loss of adhesion between the two plies as occurs in a real delamination, without causing spurious effects because of the presence of the insert. Ideally, artificial ply cracks would be prevented from being sealed by the ingress of matrix. Matrix cracks are likely to be the hardest to replicate artificially because of their small size, the width possibly being of the order of a ply thickness.

3.3. Previous Work using Artificial Damage

The majority of early work using artificial damage concentrated on through-the-width geometries where the damage could be removed after curing of the composite. This was probably a result of the original use of inserts for starter cracks in double cantilever beam tests [Huang and Hull, 1989].

In these cases, where an initiation point for a crack is required, the effectiveness of the delamination was only assessed qualitatively—all that is required is that the crack appears in the correct position. Since this study is concerned with modelling an embedded delamination where buckling is expected, it was necessary to determine quantitatively the efficiency of the delaminant.

Polytetrafluoroethane (PTFE or Teflon) film has been the predominant choice for inserts, because of its non-stick properties. For a chemical reaction to occur between an adhesive and the PTFE the carbon-fluorine bond would have to broken, and they are very strong. [Peck and Springer, 1991; Cairns *et al*, 1994]. Aluminium foil has also been used [Davies *et al*, 1990]. In this particular case they also used it folded, presumably since the matrix might adhere to the aluminium, but if there were two

layers the aluminium would not adhere to itself and so would allow a crack to open. This automatically introduces another variable—the thickness of the delaminant, and this must be kept small.

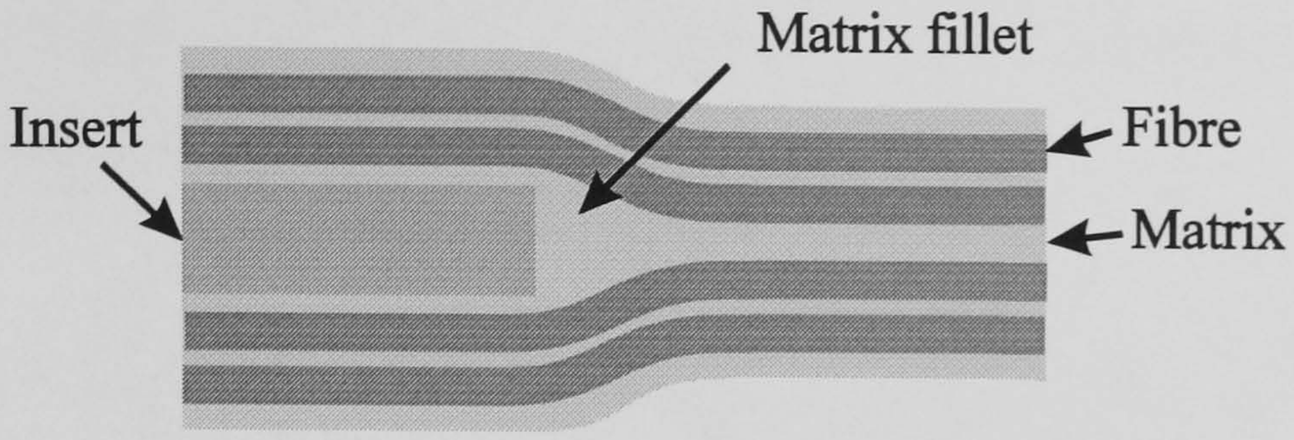

Figure 3.1 The effect of a thick delaminant on the surrounding fibres.

The presence of a thick insert in a fibrous composite is likely to result in a matrix rich region where the fibres cannot conform to the insert at its edge, as shown in Figure 3.1. This has the effect of increasing the initiation value for crack growth [Martin, 1988]. Hiley and Curtis [1992] also reported this effect in their work on mode II delamination growth using ENF specimens and kapton inserts. They measured the width of the matrix rich zone to be ~3-4 times the insert thickness (50-60μm). There is the added problem that the insert may distort the fibres, so they may be more prone to buckling or micro-buckling under compressive loading. (If the fibres followed the insert as closely as this resin rich region suggests it would indicate a radius of curvature on the fibres of ~1 mm, or a misalignment ~ 10°, compared to initial waviness of ~ 1 m. If this is compared to work done on fibre waviness and kink bands by Wisnom [1996a], where a kink with a wavelength of approximately 6mm resulted in a reduction in compressive strength of the order of 50%, it can be seen that this situation should be avoided if possible.)

Another study that looked at different thicknesses [Davies *et al,* 1989] folded a single sheet to get multiples of one thickness, but found that the insert moved during the manufacturing process. This particular study also used Kapton film. The general opinion has been to prefer thinner inserts, as mentioned in the report on a round-robin on DCB testing for interlaminar fracture toughness [O'Brien & Martin, 1993]. Their

work covered the use of several materials as inserts, some combined with release agents. The thinnest insert was a 7.5µm Upilex film. O'Brien notes that this did not give the lowest value for fracture toughness, and this may be due to the film being distorted by the fibres above and below and hence allowing 'meshing' of the fibres through the film, as shown in Figure 3.2.

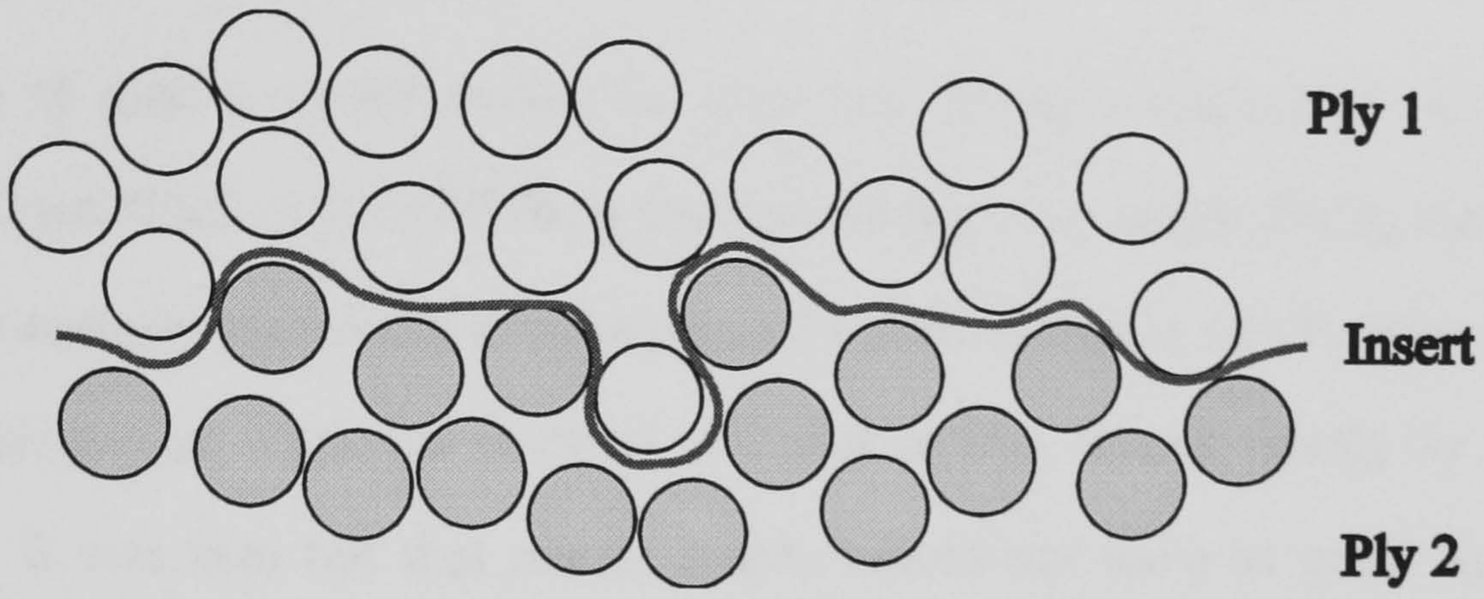

Figure 3.2. A possible result of using a very thin insert to cause a delamination, the film becomes wrapped around individual fibres during manufacture. (end on view of fibres surrounded by matrix)

Work on implanting artificial fibre cracks has generally used cuts in the plies prior to manufacture. In some cases this is to allow investigation of tapering plies while having constant thickness specimens [Cui *et al*, 1995], in others as an initiation point for delamination [Wisnom, 1992]. Fibre breakage has been simulated by cutting plies [Tian & Swanson, 1991]. Their study investigated the tensile properties of the laminate and found a reduction in strength in proportion to the loss of load carrying fibres. Delaminations occured, starting at the cuts, when the specimens were loaded. The dimensions of the delamination depended on the length of cut and the fibre orientation in adjacent plies.

3.4. Artificial Damage Techniques used in this work

This work investigates the effect of impact damage that is wholly contained within a plate, the probability of which is much higher for large plate like structures such as

wings and body panels. For this reason delaminations have been modelled by inserting a film of material (the delaminant) that has been left in place after manufacture; and cracks by making short cuts of the fibres across the pre-impregnated tape before lay-up. The artificial damage is wholly surrounded by undamaged composite.

Modelling of matrix cracks within the plies has not been attempted—a 0.125 mm wide by 10 μm thick strip of PTFE is unlikely to stay in position during manufacture. There was a greater variabilty in position and extent of matrix cracks from ply to ply, so the decision on where to position artificial matrix cracks would be somewhat arbitrary. It was also felt that matrix cracks would not have as great an effect on modelling post impact compressive strength as delaminations fibre cracks.

One possible way to insert artificial matrix cracks in the fibre direction would be to insert PTFE in filament or tube form between the fibres of a ply [Wisnom, 1996b]

3.4.1 Artificial delamination

Delaminations are extensive cracks in the matrix in the region between laminae. In real damage the delamination has two free surfaces, possibly with a gap between them. The usual approach is to insert a thin film of material to prevent adhesion between the two plies between which simulation of a delamination is required. Two layers can be used to ensure the two faces of the delamination can separate freely. This assumes that the adhesion between two surfaces of the insert is less than that between insert and matrix.. In reality this separation is not essential as long as the adhesion between the two laminae when the insert is present is no more than between two laminae after a real delamination has occurred (there may still be some adhesion between the two fresh surfaces of the delamination if the surfaces return into contact).

The criteria for choosing materials to test for use as inserts were therefore as follows.

The insert thickness compared to the ply thickness should be small; the thinner the insert the less that the fibres would be distorted and so the less the sample would be weakened at the edge of the delamination.

Low adhesion between the matrix and the insert is required; the less likely that the material would bond to the matrix the better, and the less likely that a double layer of insert would be necessary. In addition, if the use of release agents can be avoided it will reduce the risk of contamination of specimens during manufacture.

The insert material must have resistance to the curing regime; the material must survive the curing process, typically 180-260°C for a few hours (including post-cure). If release agents are used they must not migrate during manufacture.

Considering these criteria, the following candidate materials were chosen (see Table 3.1):

Insert material	Thickness (μm)
Gold foil[1]	3-6
Aluminium foil[2]	16
PTFE tape[3]	80
PTFE film[4]	10
Frekote 700NC™[5]	(Release agent)
Typical carbon fibre (for comparison)	8

Table 3.1. Possible candidates for use as delaminant.

[1]Source: Alfred Harris, Horfield Road, Bristol.
[2]Source: Goodfellow, The Science park, Cambridge. CB4 4DJ Catalogue Number Al000392
[3]Source: Goodfellow, The Science park, Cambridge. CB4 4DJ Catalogue Number FP301275
[4]Source: Goodfellow, The Science park, Cambridge. CB4 4DJ Catalogue Number FP301100
[5]Source: Dexter ASM Division, Stag Industrial Estate, Altrincham, Cheshire, WA14 5DW

Introducing an artificial delamination was achieved by inserting between two adjacent layers of composite two pieces of tape (25 mm x 25 mm) separated in some cases by a release agent. In these cases the insert was coated before insertion and left to dry, to ensure the release agent was confined to the surface of the delaminant and to avoid seeping of the release agent into the composite.

The first concern was to ensure that any artificial delaminations inserted into a sample would stay where they were during the curing process, when the resin matrix becomes mobile on heating before it cures. Checks were carried out to verify that no movement occured.

3.4.2 Ply Cracks

Cracks in the fibres were modelled artificially by cutting the fibres before curing. This was carried out using a surgical scalpel and steel rule, cutting through all affected plies after they had been layed up, but with the backing paper still in place. (I.e. if multiple plies were to be cut, the pre-impregnated plies were laid onto each other, but the outer backing paper was not removed. The position for the cuts were marked on the backing paper, and this paper used as a template when cutting specimens from the plate - up to 10 specimens were cut from each plate.)

Only breaks in the fibres in the 0° plies were considered to have a significant effect on the properties in tension and compression since these plies carry the majority of the load. In a real impact where fibres have broken there is always associated matrix cracking at the same point. In the artificial damage the gap where the fibres are cut will fill with matrix during curing, so steps were taken to counter this. Since for some specimens delaminations and cracks were modelled together, in some cases PTFE was used as the insert and to wrap around the cut ends of the fibres—see Figure 3.3.

3.5. Verification of Artificial Damage

It was felt to be an important part of this work to justify the use of particular methods and materials for modelling delamination and fibre cracks. Verification was necessary to be certain that using artificial damage is equivalent to real damage of the same type and size. There were two stages to this process. The first was to experiment with possible materials to find one that fulfilled the requirements. The second stage involved experimenting with actual size specimens with various configurations of artificial damage to see which produced the same effect as real damage.

Delaminations were simulated by using various materials in the form of a thin film inserted between plies during lay-up of the laminate. The effect of using release agents and doubled inserts was also investigated.

Ply cracks were made artificially by cutting 0° plies prior to curing the plate. Where the specimen included delaminations and ply cracks, experiments were carried out using inserts to prevent the matrix filling the gap.

3.5.1 Delaminations

Position of delamination

After curing, visual and X-ray inspection of the test specimens was carried out to ensure that the inserts had not moved during the curing process. A specimen was made from glass fibre so that visual comparison of pre-cure and post-cure specimens would be possible. A tracing of the sample before cure can be compared to the specimen after cure to see if the foil insert has moved. There was no observable movement of the artificial damage. The metal foil inserts showed up clearly in X-ray

pictures of the specimens. Penetrant enhanced pictures of delaminations caused by PTFE showed that no movement had occurred.

Two tests were done to determine the effectiveness of the materials as delaminants. The preliminary test was an interlaminar shear strength test, then an adapted double-cantilever beam test was used on a range of more suitable materials.

Modified inter-laminar shear test

For the inter-laminar shear strength test a plate (250 mm by 75 mm by 2 mm [16 layers]) of glass fibre/913c resin was laid up. Three materials were used as artificial delaminations: 30mm wide strips, spaced evenly along the centre line between the two centre laminae. No release agents were used at this stage. (For this test this interlaminar region containing the delamination is referred to as 0 and the interlaminar regions above as positive, those below as negative) .

Four test pieces were cut out (20 mm by 10 mm) and used in the test (volume fraction 0.6): each contained a delamination along the centre-line (the modification). The form of the specimens is shown in Figure 3.3, in the test fixture, a three point bend test. The test was carried out using a Nene with 30kN load cell, with a loading rate of 200N/s (failure in approximately 30 seconds).

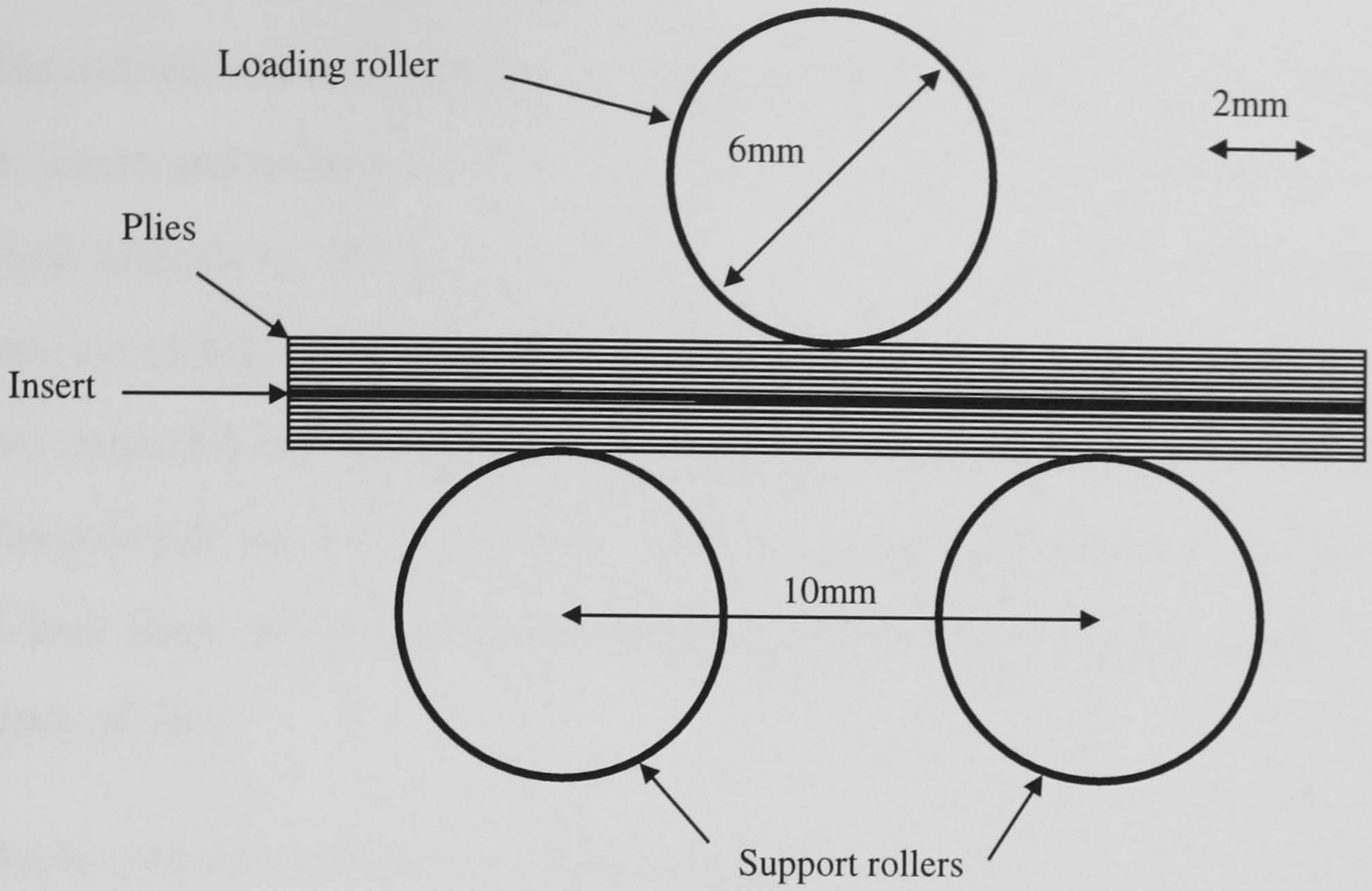

Figure 3.3 Specimen and test fixture for modified interlaminar shear strength test.

The results of the test were as follows:

Insert Material	Strength [MPa]	Position of delamination(s) (from centre)	Comments
Gold foil:	109.8	0,4	Delamination only along one edge of specimen, caused by matrix seepage through tears in the foil.
Aluminium foil:	106.7	0,2,-2	Delaminations covered full width of specimen.
PTFE tape:	104.4	-2,4	Only a partial delamination along interface containing insert.
None (control):	115.0	2,4	Lower bound for strength - fibres broke before the delamination reached the end of the specimen.

Table 3.2. Results of inter-laminar shear test on specimens with through the width delamination.

This test was not as informative as had been hoped, as the difference between results for inserts and no inserts was small compared to the actual results. It only indicates a small decrease in interlaminar shear strength, and the position of the delaminations does not match the position of the insert. For this reason another method was tried that measured the ease with which artificially delaminated faces were pulled apart. The gold foil was very fragile and prone to tear during manufacture, so was not used in later tests. In addition it was thought worth including release agents in the next series of tests.

Double cantilever beam test on delaminations

As a way of measuring the effectiveness of artificial delaminations in carbon fibre composites, samples containing sheets of delaminant between laminae were subjected to a modification of the double cantilever test. (See Figure 3.1.) This version of the test was not used to determine the value of the strain energy release rate, G_{Ic}, but the adhesion force due to the inserted film. For this reason, thin 8-ply unidirectional laminates (1mm thick) were chosen so that the contribution due to the artificial delamination would be large compared to that needed to bend the composite. Four specimens containing each insert were made from carbon fibre epoxy composite (T300/913c). Dimensions are shown in Figure 3.4. When petroleum jelly was used as the release agent it was applied to the touching faces of a double thickness insert, before inserting into the lay-up. The Frekote was applied to all surfaces of the inserts, and allowed to dry, before the inserts were added to the layup.

The delaminations extended across the full width of the specimen, so that the force needed to initiate the crack between the two sides would be zero for a perfect delamination. Once the delamination crack is initiated the force required to extend the crack would be non-zero even for a perfect delamination because of the force needed to bend the carbon fibre. By repeating the experiment on each specimen after

the crack had been opened once would enable the component due to the adhesive force of the delaminant to be calculated and accounted for.

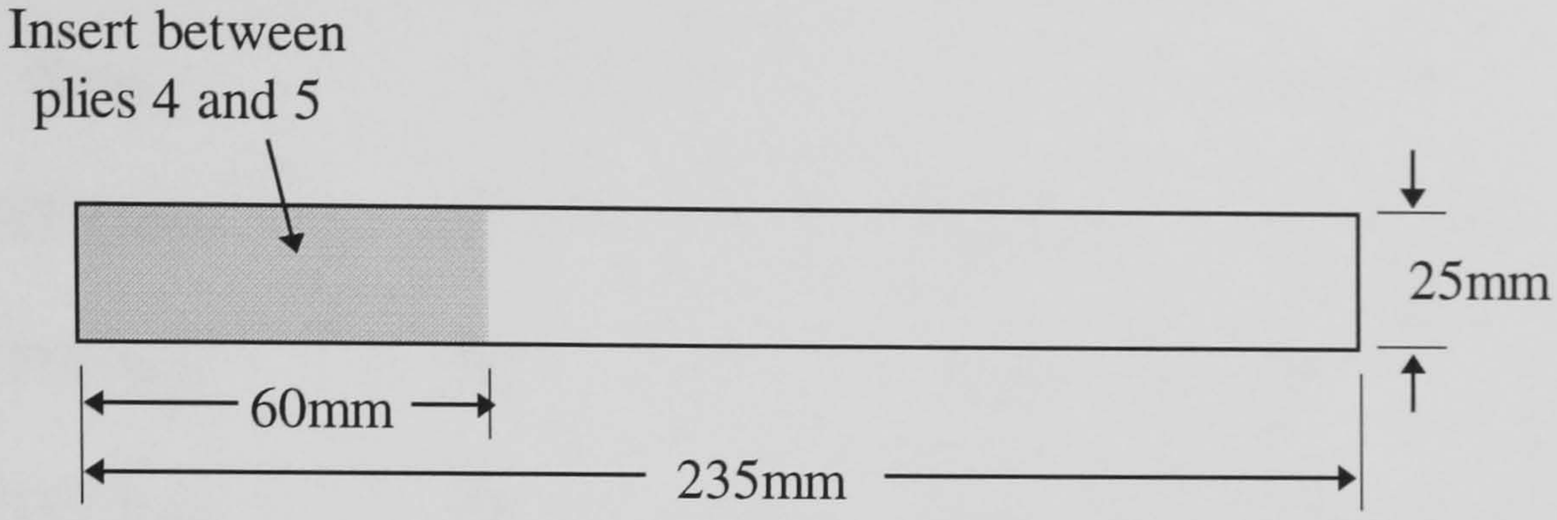

Figure 3.4. Dimensions of specimens for modified double cantilever bend test.

The edges of the coupons were abraded with successive grades of emery paper to ensure that they were smooth, as preliminary experiments showed that the cutting marks caused the laminae either side of the delaminant to become attached to each other. (Later specimens were cut on a diamond saw, which removed this problem.) Hinges were attached to the specimens as shown in Figure 3.5, using Araldite2001 epoxy. The results of the double cantilever bend test, carried out using a Nene test machine with a 100N(or 1kN, 30kN) load cell, are shown in Table 3.3.

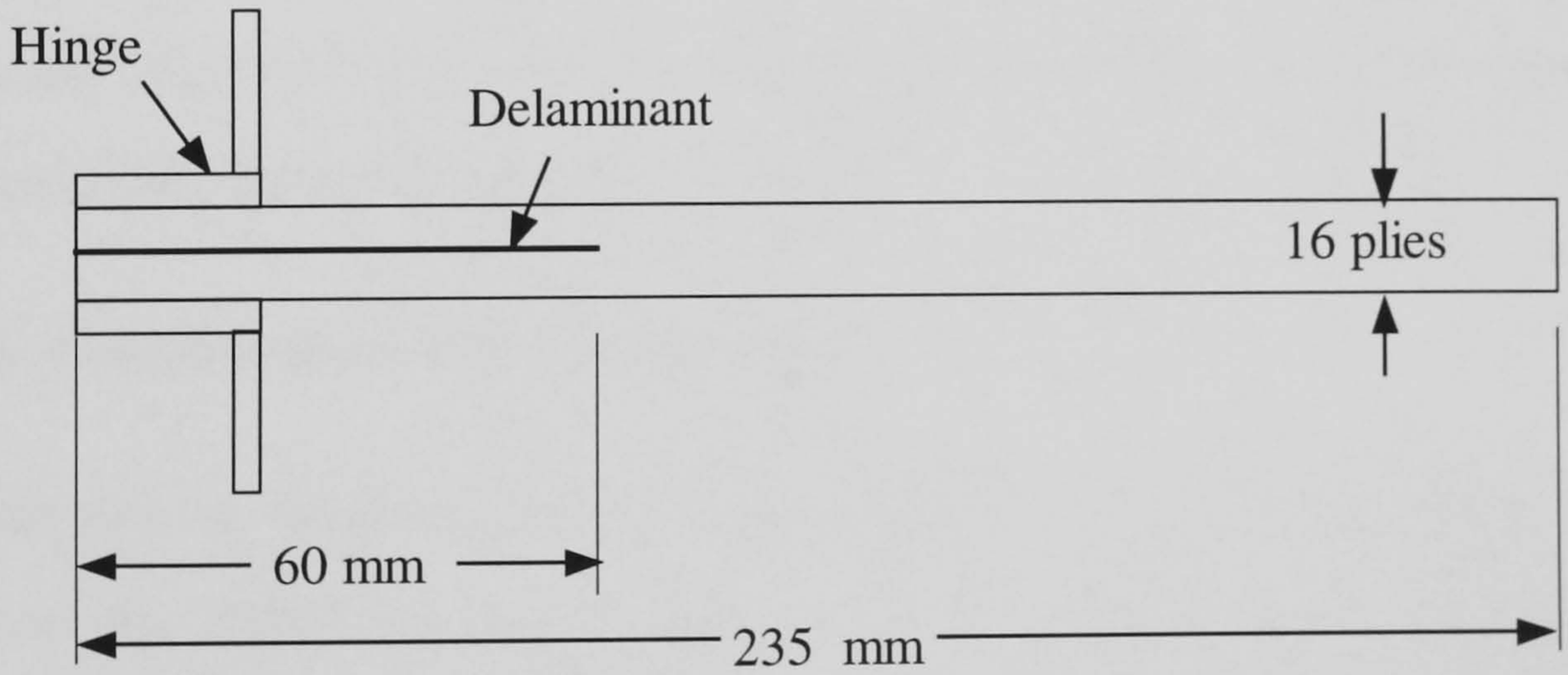

Figure 3.5 Double cantilever test for adhesive strength of delamination.

Delaminant	Thickness (μm)	N° of layers	Release agent	Breaking force (N)
None	-	-	-	> 2000
PTFE tape	80	2	None	450
PTFE tape	80	2	Frekote	34
PTFE film	10	2	none	0.3
PTFE film	10	1	none	0.3
Aluminium foil	16	2	Frekote	0.4
Aluminium foil	16	2	Petroleum jelly	25.0

Table 3.3. Force required in double cantilever beam test to open crack. (Average for four specimens)

The results demonstrate that the foil tended to adhere to the specimen but the two sheets came apart easily. The PTFE came away from the specimen but tended to stick to the other film when there were two films. The Frekote™ was a much more effective release agent than the petroleum jelly.

3.5.1.3. Conclusions on tests of delaminants

The inter-laminar shear tests show that the materials all cause a weak layer, but the results for the PTFE tape were surprisingly high. On inspection of the supplied material properties for the tape it was found to contain micro-pores. Presumably these allow resin to bridge the delamination and so bond the two adjacent layers together (though a weaker bond than with pure matrix).

The gold layer was so fragile that during manufacture it was impossible to avoid tearing the foil, but to compensate it is very ductile and so the leaves of foil could shear easily. The difficulty in handling it precluded its use in later experiments.

The aluminium foil was quite successful at preventing adhesion, and with a more careful application of the foil (i.e. smoother and with three layers of release agent) would be a good candidate for the purpose.

At this point PTFE tape was dropped as a possible candidate, as it was found to be the least successful and is also the one most likely to damage fibres by causing localised bending at the edge of the delamination. (The PTFE layer is >160 μm compared to a fibre diameter of 8 μm.) A source of non-porous PTFE film of 10 μm thickness was found as an alternative.

Overall, the test method was satisfactory for distinguishing good candidates from poor ones. Due to the small forces involved compared to those necessary to bend the specimen, the results for PTFE film and aluminium with Frekote™ can be considered to be on a par. For both of these materials repeating the tests on individual samples produced the same trace from the test machine. This indicates that there was no extra force (apart from that necessary to bend the sample) needed to pull the two halves of the sample apart.

From the double-cantilever test it can be seen that all delaminants have reduced adhesion between layers. Any of the materials used causes delamination to occur preferentially at the insert, but clearly the foil with release agent or PTFE film would come closest to representing a real delamination.

3.5.2 Fibre cracks

A ply crack is a crack through both the fibres of a ply and the matrix. When a ply crack occurs the fibres either side of the break are held in the cured matrix, so it is important that the broken ends of the fibres are kept from overlapping, either during laying up of the specimen or during curing (when the resin is mobile), and that the

fibres do not move apart during the cure. A real ply crack will also be the site of a matrix crack and (in compression loading) this may affect the behaviour of the damaged specimen. This matrix damage could be a point of initiaion for further damage, such as delamination, especially if the composite is loaded in tension.

In this study compressive loading is considered, in which case the affect of the cut on properties is not so intuitively obvious. In this case, if matrix has filled the gap it may not fail, as it is likely to do under tension.

An insert at the cut in the fibres to prevent ingress of matrix may help to model the crack, but at the same time it is desirable that the amount of inserted material is kept to a minimum. (If the cut fills with resin the fibres are bonded together, whereas in real fibre fracture there will be matrix damage at the point where the fibre is cracked. This means that in real damage there is a loss of support for the fibres at the break which is not being modelled by the artificial damage.)

Construction of artificial ply-cracks

The philosophy behind the construction of artificial ply cracks was to implant damage that produced a similar effect to real damage. If possible, this would be limited to cuts in 0° plies only. The aim was to relate the residual strength to the amount of initial damage, thus allowing damage to be inserted that matched the effect of real damage.

The ply-crack specimens were made by cutting a slot (0.5 mm by 25 mm) through 0° plies, using a scalpel and steel rule and cutting through the backing paper of the pre-preg, before they were included into the specimen during laying up. In some cases the crack was held in place during the curing process by inserting aluminium foil or PTFE tape as shown in Figure 3.6. Plate 3.1 shows a micrograph of a cross-section of the ply-crack after cure.

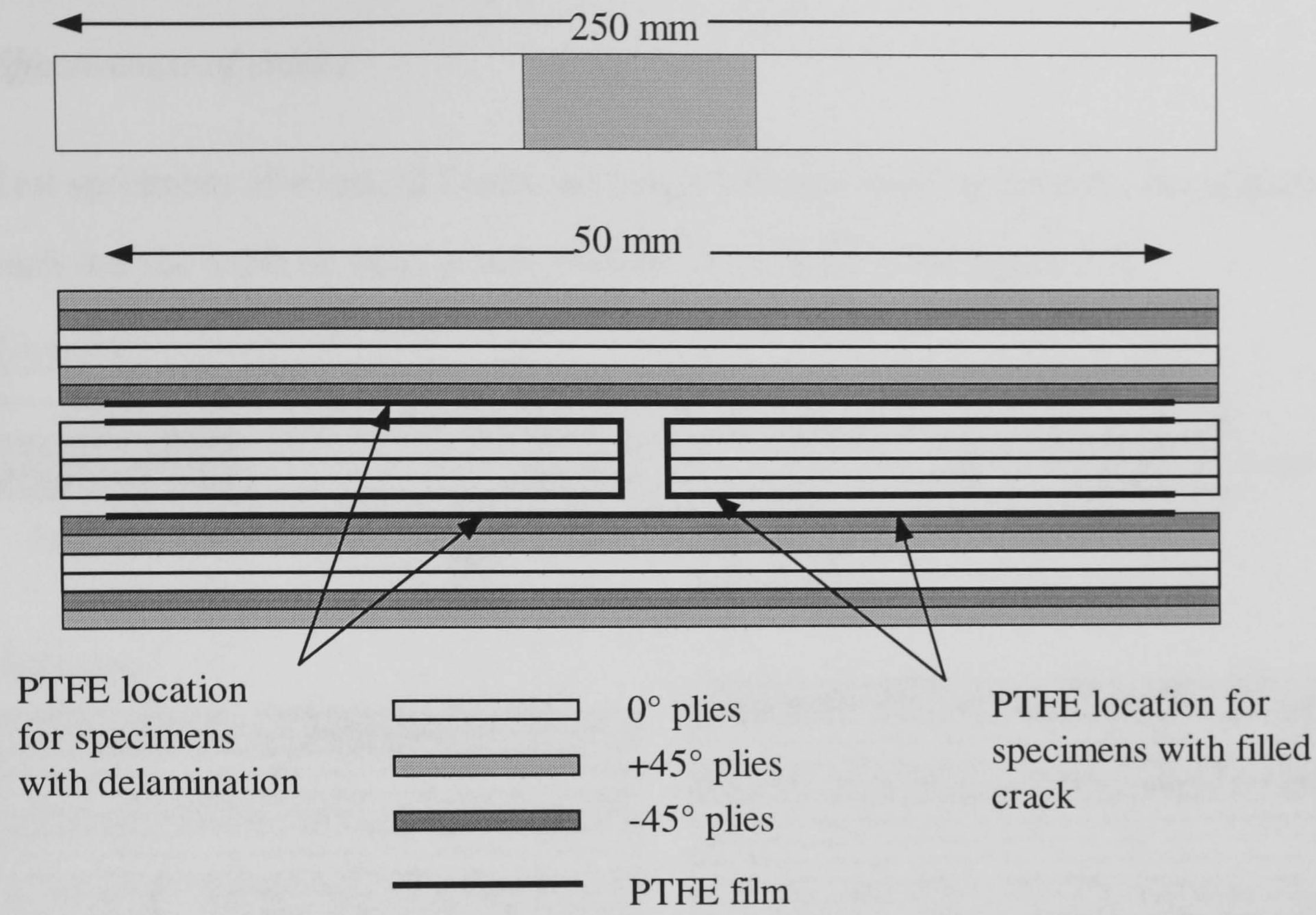

Figure 3.6 *Artificial delamination specimen and enlargement of damage zone. Artificial delamination and crack across four central plies during lay-up.*

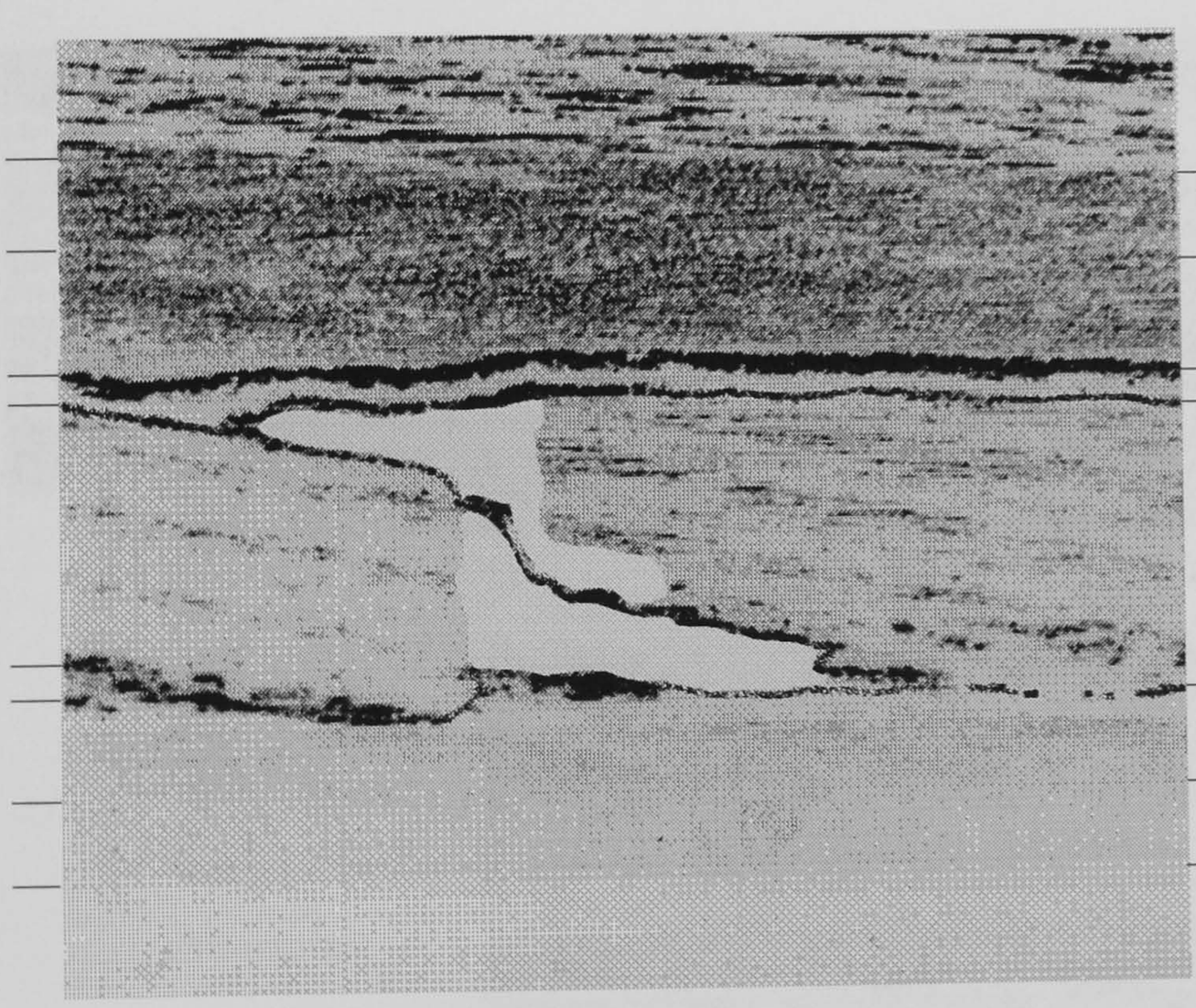

Plate 3.1. *Micrograph of the artificial delamination - cross-sectional view of gold foil insert (negative view) [Gold is used as PTFE is invisible against composite background.]*

Effectiveness of cracks

Test specimens of width 12.5 mm and length 250 mm were cut from the cured plates such that the artificial damage was positioned centrally. (See Figure 3.7)

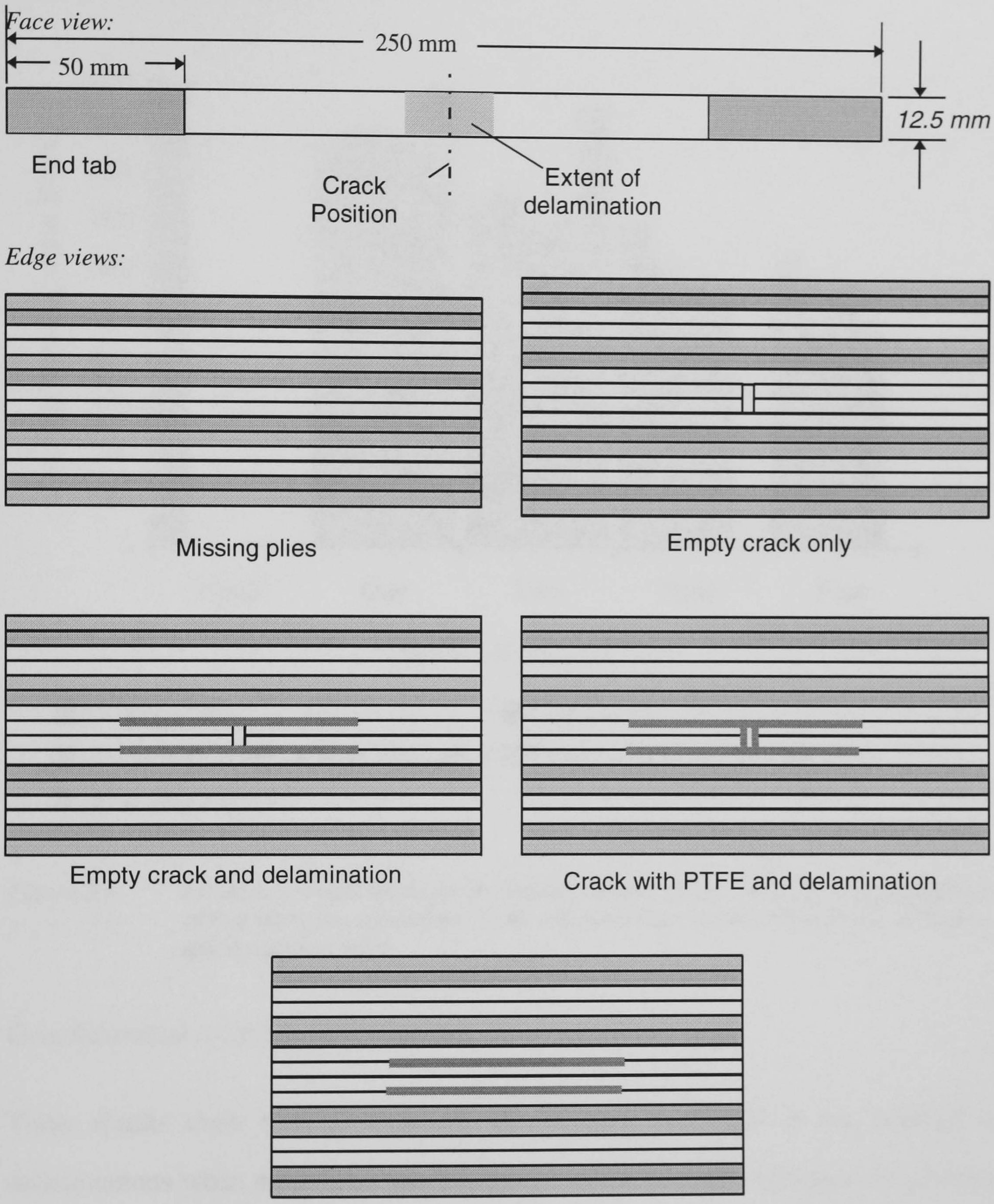

Figure 3.7. *Geometry for specimen to test ultimate tensile stress of artificial cracks. The damage shown is for two affected plies, as an edge view.*

The effectiveness of ply-cracks can be determined by measuring the ultimate tensile stress for samples with and without cracks. Since the load is mainly carried by the unbroken 0° plies, the strength of the specimens should be proportional to the number of uncracked plies.

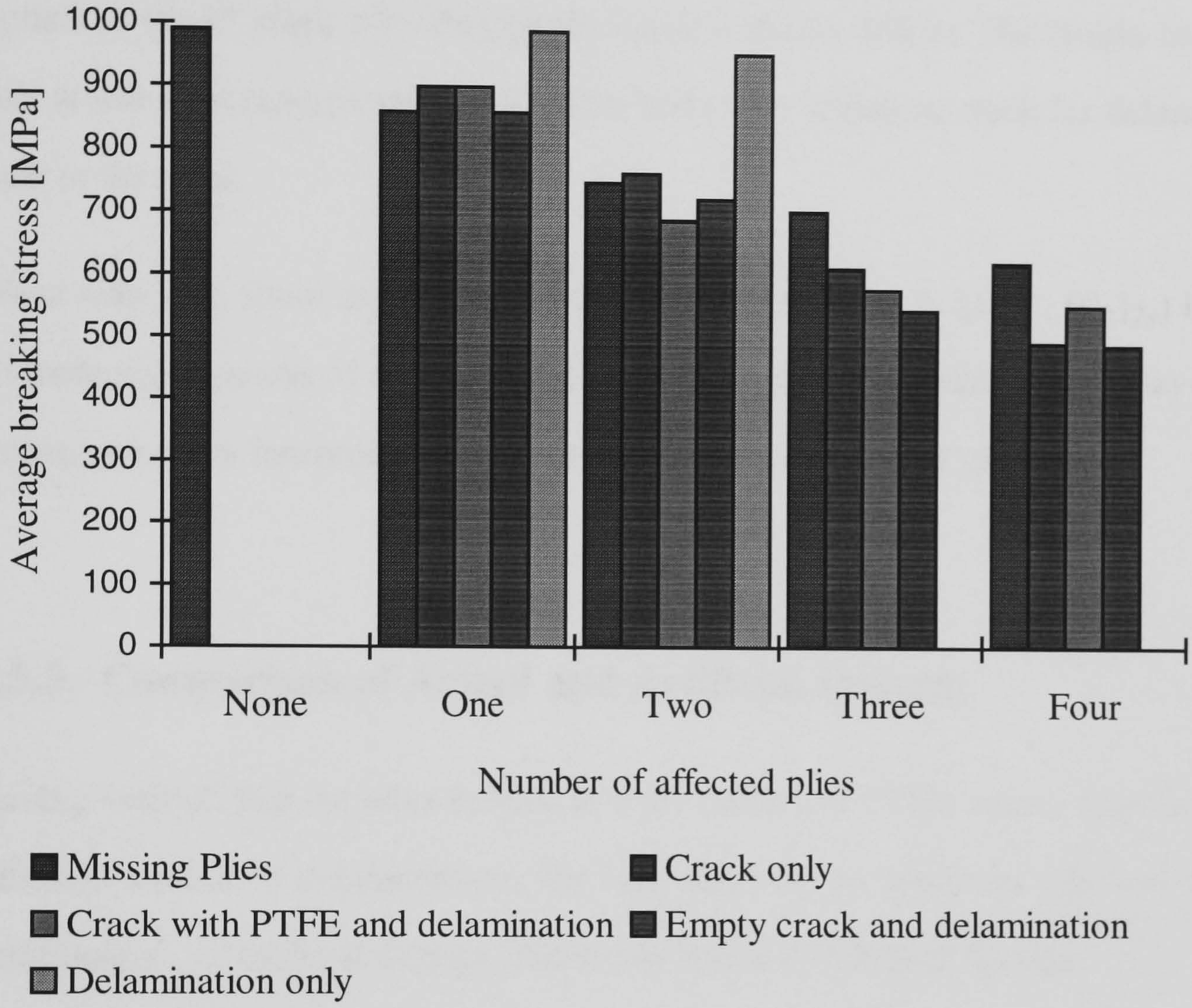

Figure 3.8. *Effect of artificial damage on ultimate tensile stress. Results are the average of five tests per specimen. Only one result for no affected plies as all cases are equivalent here.*

Conclusions on artificial delaminations

These results show that, as expected, the strength in tension is not affected by delaminations when there is no crack present. When a crack is present the presence of a delamination does not affect the residual tensile strength. The presence of a PTFE filler in the crack does not reduce the residual strength. Having a broken ply in a plate weakens the plate more than not having the ply at all, probably because the fibre break is a source for further damage.

The failure of the coupons usually involves a delamination running from the damaged zone back towards the grip. The stress at which the matrix in the crack failed and initiated the delamination was approximately 20 MPa

The drop off in strength with plies cut indicates that the cut is working effectively as a crack in the 0° plies, even though the crack is matrix filled. The matrix in the cut fails at low load (approximately 20 MPa) and is the initiating crack for delamination back to the grips.

These tests also show that the undamaged specimens (16-ply $[\pm 45°, 0°_2]_{2s}$) have an ultimate tensile stress of approximately 0.98 GPa which indicates that the lay-up and curing procedure has produced a reasonable quality of finished specimen.

3.5.3. Comparison of Actual and Artificial Damage

Having verified that cut plies behave as a ply crack and PTFE inserts cause a loss of adhesion similar to delaminations, the next task was to determine the amount, and combination, of artificial damage that would match real impact damage.

The difficulty with testing damaged specimens is that it is not easy to measure the extent of the damage (without destroying the specimen in the process), nor can one introduce consistent damage from one specimen to the next. Compressive tests are notoriously variable as it is. If we can replace real damage with artificial damage, then the damage position, size and quality can be carefully controlled.

There is a compromise between making specimens that contain an accurate representation of real damage, which are complex and time-consuming to construct, (and also to analyse) and making specimens with simple artificial damage that does not closely resemble the results of real impacts. The aim will always be to keep the inserted damage as simple as possible, in order to separate the effects of the different

components of damage, and to reduce the possible interactions between the types of damage.

Later chapters cover the process of analysing actual damage using X-ray and deply techniques. By mapping the damage caused by impact, it is possible to insert a representative amount of damage artificially. By comparing the results for these specimens with those for actual damage specimens, estimations can be made about the closeness to reality of the different artificial damage configuration. The simpler the model can be the easier it will be to determine the contributions made by ply cracks and delaminations. In addition, the easier it will be to perform a finite element analysis of the configuration, because of the simpler geometry and boundary conditions.

For these reasons the initial configurations of implanted damage that would be compared to actual damage were constructed of simple cuts and implanted delaminations. Specimens were made with a close matching of actual damage in terms of areas and layers affected, but with simple shapes for the delaminations and straight cuts for ply-cracks. In reality the delaminations are often dumbbell shaped with edges following smooth curves, with lobes following the direction of the 45° plies. While the cracks are usually jagged, the asymmetric nature of the delaminations about the impact point was included by positioning delaminations asymmetrically. It was hoped that the complexity of the artificial damage could be reduced and that as testing of the specimens continued the results would indicate at what point the simplification is producing an artificial damage that no longer represents real damage. The crucial point is that the artificial damage should give failure mechanisms similar to that in the real impact.

Since the main thrust of this study is to investigate the effect of low velocity impact damage on compressive strength, the next step was to test artificial damage against real damage under compression. In these tests the specimens used were 50 mm by

250 mm, to allow for embedded damage, and were constructed of 18 ply T300/913c (2,25 nominal thickness) (see Figure 3.5). This is the same format for specimens that would be used in the main study. Where a ply cut is included, a matrix crack at the cut was created by pre-stressing the specimen in tension (from observations made during the tests on ply cracks) until the matrix was heard to crack—typically at a load of about 2 kN.

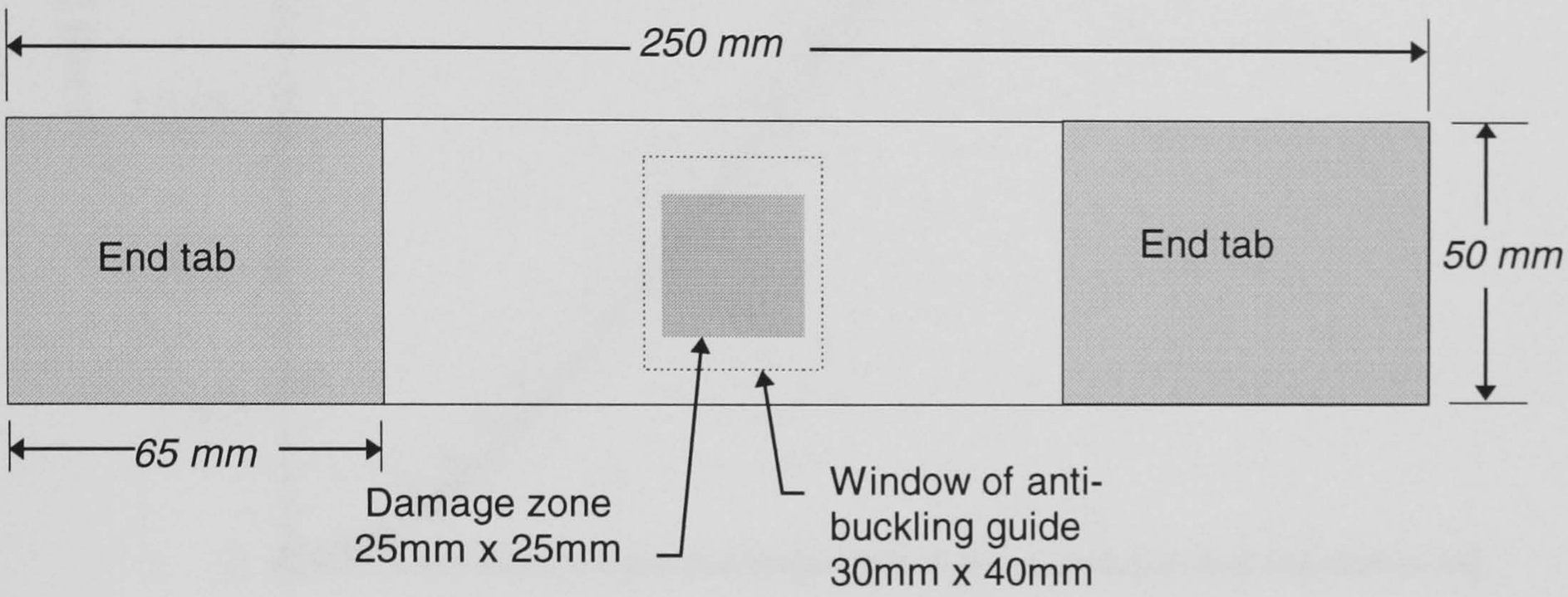

Figure 3.9. Geometry of specimens with embedded damage.

The end tabs for these tests were 2mm thick soft aluminium, attached to the specimen with Araldite2001, a room temperature curing adhesive. The specimens were put into a jig to ensure that the end tabs were attached squarely, and after setting the edges milled to ensure they were perpendicular to the loading direction.

Sample results of the compressive tests are shown in Figure 3.6. The test was conducted using a Zwick 1478 test machine with 100kN load cell. and a cross head displacement rate of 1mm/min. The test finished when the machine detected a drop in the load of 20%. Clamping plates were fixed over the end tabs of the specimens and these clamps fitted into a fixture on the platens that ensured the specimen stayed in line with the load. The clamping plate included the tongue that fitted into the anti-buckling guide. The tests, on four specimens of each damage configuration, produced plots with consistent slope and peak load and strain.

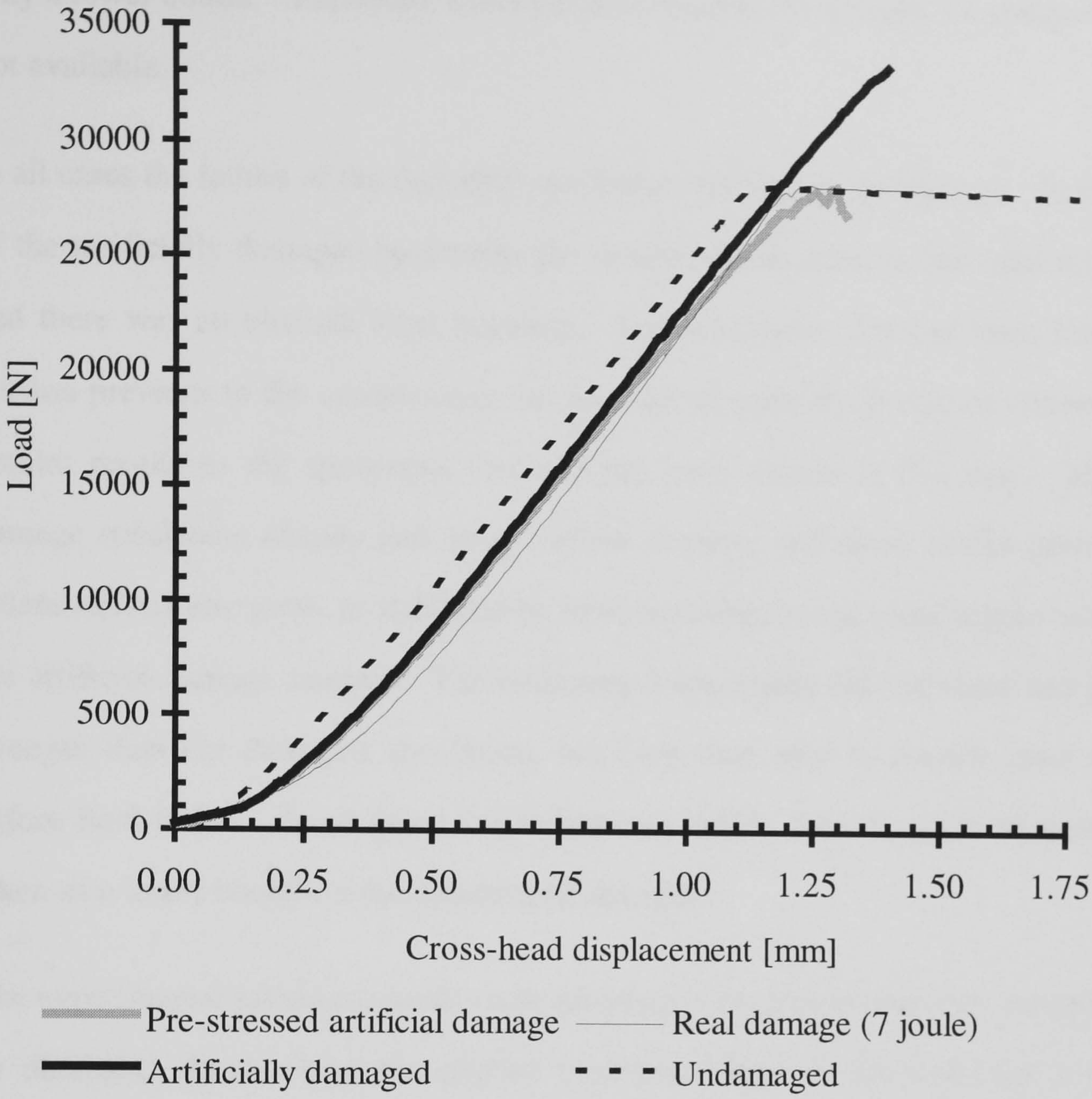

Figure 3.10. Comparison of stress displacement curves for real and artificial damage. Sample curves from sets of four specimens - each set had a similar form.

The actual damage was a 7 Joule impact, and the artificial damage replicated this amount of damage. (Further tests were carried out later using different configurations of implanted damage, and these are described in chapters 4 and 5). Artificially damaged specimens buckled smoothly until failure. When pre-stressed (in order to produce a crack in the matrix-rich region between the cut ends of the fibre) the specimens partially failed at a slightly lower load, which they carried to a similar strain before failing catastrophically. This plateau on the load-displacement curve was similar to real damage, except that specimens with real impact damage failed at a greater strain and the buckle was not so smooth. Tests were made on undamaged specimens, but all failed within the tab zone and so their strengths are

only a lower bound. Therefore, a recognised compressive strength for comparison is not available.

In all cases the failure of the damaged specimens initiated at the damage. In the case of the artificially damaged specimens the delaminations grew as the load increased and there was an obvious local buckling. The specimens that had been loaded in tension previous to the compression test in order to open the ply-crack showed very similar results to the specimens that had not been treated in this way. The real damage specimens already had some surface damage, and these cracks grew. The delaminations also grew, as indicated by local buckling, but in a less regular way than the artificial damage samples. The undamaged specimens did not show any greater strength than the damaged specimens, but they were able to absorb more energy before final failure. In all cases this failure was within the tab, so these results are taken as a lower bound for the undamaged strength.

The experimental technique needs some adapting if the true undamaged strength is to be obtained. In this case the applied transverse force on the end tabs is due to mechanical clamps (with hand-tightened bolts - clamping pressure of the order of 3 MPa). The clamps are fixed to the specimen, over the end tabs, and then the clamps were fitted into the antibuckling guide (see Appendix A). This ensures alignment of the specimen during loading as well as preventing gross buckling of the coupon. The transverse clamping force is therefore constant during the test, unlike the forces when a wedge-type compressive grip is used.

Work carried out by Camponeschi *et al*, [1993] on the compressive failure of thick composite laminates showed that the drop in strength with thickness of coupons could be accounted for by through-thickness fixture induced effects. The restraint on the Poisson expansion provided by the end clamps causes a through thickness fibre misalignment close to the clamp, and this is sufficient to cause a loss in strength. The effect would be reduced for thinner composite plates, but would still exist.

The tabs are flush with the specimen so the load applied to the specimen is partly compressive (by direct loading) and partly shear (from the aluminium alloy end tabs). The end tabs came apart from some specimens as they failed—suggesting that improvements to the bonding were required. For the later tests a different adhesive was used, Redux 403. The debonding may have been due to the local transverse movement of the specimen as the ends were crushed at the large strains. As far as modelling the real damage is concerned this configuration is not far from a realistic amount of damage. Reductions can probably be made in the amount of delamination, to produce a simpler artifical damage, as the specimens underwent local buckling very easily compared to the real damage. A more realistic amount of ply-cracking may be necessary.

3.6. Conclusions

It is possible to produce the effects of cracks and delaminations artificially, and to achieve the same failure load for artificial and real damage. For the following work, therefore, it was decided to reproduce delaminations artificially using a single film of PTFE (10μm thick). This prevents adhesion of the two laminae and there is evidence that the film is thin enough not to produce a substantial resin rich region at the edges of the insert and shouldn't cause a stress concentration. The insert is chemically inert and does not require a release agent, simplifying the manufacturing procedures. A disadvantage is that it does not show up on the X-ray, but since the delamination is expected to grow a penetrant to reveal the extent of the damage will have to be used anyway.

To simulate ply cracks, the fibres can be cut during the layup stage. The ingress of resin into the cut region does not affect the tensile strength - either to strengthen the coupon or weaken it. For compression tests it is necessary to apply a tensile pre-load

to the coupon to produce a crack in the resin at the point where the plies are cut. (Obviously, in real damage there is always a crack in the matrix at the point where the fibres have broken.) During manufacture the cut fibre ends do not move significantly so the resin rich region in the crack is not too extensive.

References

Birch M.W. and Williams J.G.

"The effect of rate on the impact fracture toughness of polymers."

International Journal of Fracture Vol. 14(1) February **1978** pp. 69-84.

Cairns D.S., Minguet P.J. and Abdallah M.G.

"Theoretical and Experimental Response of Composite Laminates with Delaminations Loaded in Compression.".

Composite Structures Vol. 27(4) **1994** pp.431-7.

Camponeschi E.T.Jr, Gillespie J.W.Jr. and Wilkins D.J.

"Kink-band failure analysis of thick composites in compression."

Journal of Composite Materials **1993** Vol. 27(5) pp.471-90.

Clark G.

"Modelling of Impact Damage in Composite Laminates."

Composites Vol. 20(3) May **1989** pp. 209-14.

Cui, W.C., Wisnom, M.R. and Jones, M.I.

"New model to predict static strength of tapered laminates."

Composites Vol. 26(1) **1995** pp. 25-32.

Davies P., Cantwell D. and Kausch H.H.

"Initiation values of GIc in IM6/PEEK Composites."

Composites Science and Technology Vol. 35(3) **1989** pp. 301-13.

Davies P., Moulin C., Kausch H.H. and Fischer M.

"Measurement of GIc and GIIc in Carbon/Epoxy Composites."

Composites Science and Technology Vol. 39(3) **1990** pp. 193-205.

Hiley M.J. and Curtis P.T.

"Mode II Damage Development in Carbon Fibre Reinforced Plastics."

74th Structures and Materials Meeting, Patras, Greece. AGARD CP-530 May **1992** pp. 17.1-17.11

Kutlu Z. and Chang F.K.

"Modelling Compression Failure of Laminated Composites Containing Multiple Through-the Width Delaminations."

Journal of Composite Materials Mar **1992** Vol. 26(3) pp. 350-87.

O'Brien T.K. and Martin R.H.

"Round robin testing for Mode I interlaminar fracture toughness of composite materials."

Journal of Composites Technology and Research Vol. 15(4)

Winter **1993** pp.269-81.

Peck S.O. and Springer G.S.

"The Behaviour of Delaminations in Composite Plates—Analytical and Experimental Results."

Journal of Composite Materials Vol. 25(7) **1991** pp. 907-29.

Rhodes M.D., Williams J.G. and Starnes J.H.Jr.

"Low Velocity Impact Damage in Graphite Fibre Reinforced Epoxy Laminates".

34th Annual Conference on Reinforced Plastics - Composites Institute

Jan **1979** New Orleans, Louisiana.

Tian Z. and Swanson S.R.

"The fracture behaviour of carbon/epoxy laminates containing internal cut fibres."

Journal of Composite Materials Vol. 25 November **1991** pp. 1427-35.

Wisnom, M.R.

"On the increase in fracture energy with thickness in delamination of unidirectional glass fibre epoxy with cut central plies."

Journal of Reinforced Plastics and Composites Vol. 11(8) **1992** pp. 897-907.

Wisnom, M.R. and Atkinson, J.W.

"Compressive failure due to shear instability - experimental investigation of waviness and correlation with analysis."

Journal of Reinforced Plastics and Composites Vol. 15(4) **1996** pp. 420-39.

Wisnom, M.R.

"Modelling the effect of cracks on interlaminar shear strength."

Composites Part A- Applied Science and Manufacturing Vol. 27(1) **1996** pp. 17-24.

CHAPTER 4.

EXPERIMENTAL METHODS FOR STATIC TESTS

4.1. Introduction

Work by previous workers has been done in testing composite materials after damage has been inflicted [Williams and Rhodes, 1982; Evans and Masters, 1987]. In these cases the work has been attempting to relate post impact compressive strength to the material properties of the composites' components or impact energy. In the work described here the aim is to determine the relationship between the actual damage and the residual strength. This damage can be from real impacts, artificially implanted damage or from holes or notches. Reliability of test results for compression is a particular problem, because of the sensitivity of measured values to factors such as test method, quality of specimens and loading of specimens [Sims, 1991].

The aim here is to describe the methods used to measure the static residual strength of our specimens after damage has been inflicted. Here the load is monotonically increasing; later chapters deal with cyclic loading. Similar techniques were therefore used as those employed for measuring notched strength of composites [Soutis, 1989].

In choosing a suitable material and specimen configuration for this investigation into impact damage, three factors were taken into account. Firstly, the material used should be likely to be used in practice so that if the results obtained were material specific they would be useful. Secondly, it is helpful if the material has been used in

other studies so that comparison of results is possible. Thirdly, the lay-up of the plies needs to be similar to those used in structures that are designed to tolerate impact [Jang *et al*, 1989; Choi *et al*, 1992; Strait, 1992; Cantwell and Morton, 1991].

This chapter describes the techniques and materials used in the manufacture of specimens, including the implanting of artificial damage. Also covered are the impact procedures: how impact damage is caused, inspection methods for detecting damage from impact and for measuring the extent and position of damage, the test method for determining residual strength and for incremental testing to follow damage growth. A shadow Moiré fringe technique used to measure the magnitude of the out-plane-displacement of the delamination buckle is also described. Some results are included to demonstrate methods.

4.2. Description of Specimens

The coupons used for the post-impact residual strength tests were cut from 18-ply multi-directional laminate plates. The thickness was a nominal 2.25 mm, as the pre-impregnated tape is 0.125 mm thick. The specimens were 250 mm long and 50 mm wide, as CRAG specifies [Curtis P.T. (editor), 1988]. This allows the specimen to contain fully any impact damage or artificially implanted damage, at least for the energies considered here. Implants of damage took the form of 25 mm x 25 mm squares of PTFE film, 10 μm thick, which cause a delamination; and cuts in the 0° plies to simulate cracks. More details can be found in chapter 3). For measuring the extent and type of damage from actual impacts, energies of 3, 5, 7, 9 and 12 Joules were used, but only specimens subjected to 7 Joule impacts were tested for residual strength and delamination growth. The choice was made on the basis of the extent of the damage, which had to be contained within one coupon.

A range of damage levels was used, as shown in Table 4.1, with the damage map from the real damage being used as a guide for the implantation of artificial damage (in terms of size and position of the implanted damage). The delamination area inserted artificially was chosen to match the total area of delamination as determined from impact experiments, but situated at the interface(s) with the largest individual delamination.

Coupon description	Plies cracked	Delaminations
Control	None	None
Top delamination	0° plies - 14,15,16	25mm x 25mm between plies 16 and 17
Bottom delamination	0° plies - 14,15,16	25mm x 25mm between plies 13 and 14
Double delamination	0° plies - 14,15,16	25mm x 25mm between plies 16 and 17 and 25mm x 25mm between plies 13 and 14 (see Figure 4.2)
Crack only	0° plies - 14,15,16	None
Delamination only	None	25mm x 25mm between plies 13 and 14
Realistic damage	0° plies - 14,15,16 = 75mm of cuts	Total of 2500 mm^2 distributed as per Figure 4.1
Actual damage	T800 - none T300 - approximately 150mm see Figure 4.3	Approximate 2500 mm^2 distributed as per Figure 4.3

Table 4.1 *Specimen configurations used in study. Plies are numbered from the impact surface - numbering is shown in Figure 4.4.*

The specimen containing realistic artificial damage only attempted to match the roughly the area and position of delaminations produced by actual impact. not the shape. Cuts to the fibres in the 45° plies were not attempted, since these are generally very short. The cracks in the 0° plies were only modelled for the back plies, the aim

was to have an artificially damaged specimen that was not totally dissimilar to the artificially damaged specimens that would be modelled with finite elements.

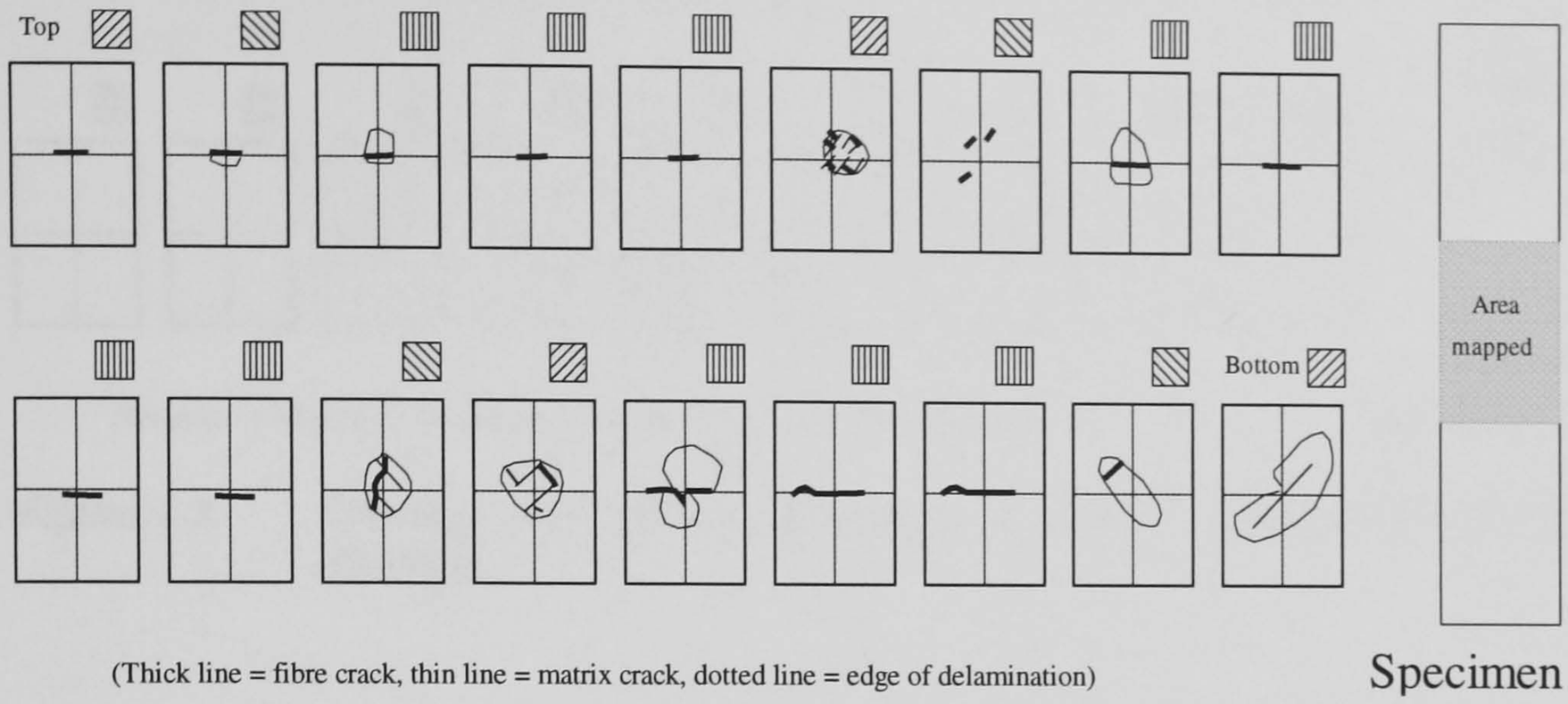

Figure 4.1. Damage map from deply of a specimen after a 7 Joule impact

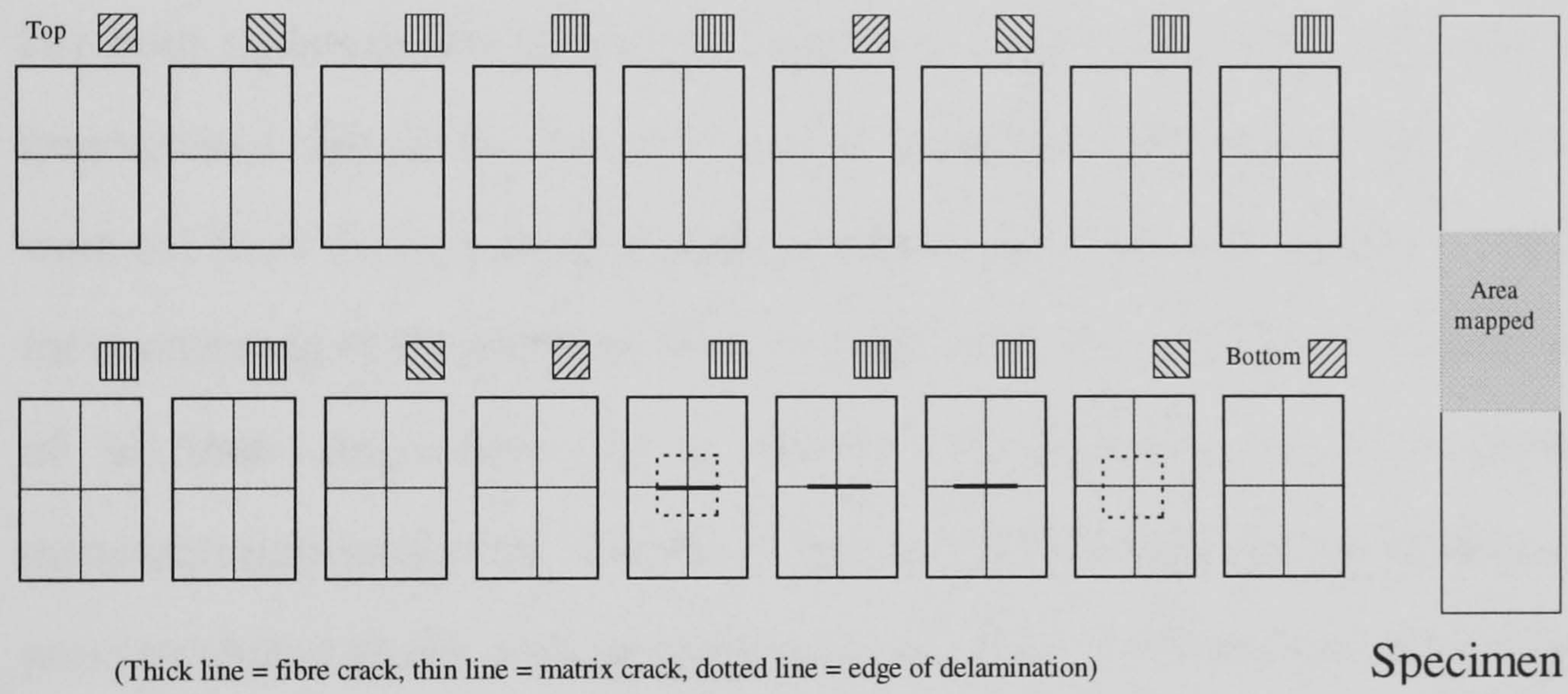

Figure 4.2. Damage map of inserted damage - double delamination and crack (A simple representation of 7 Joule damage.)

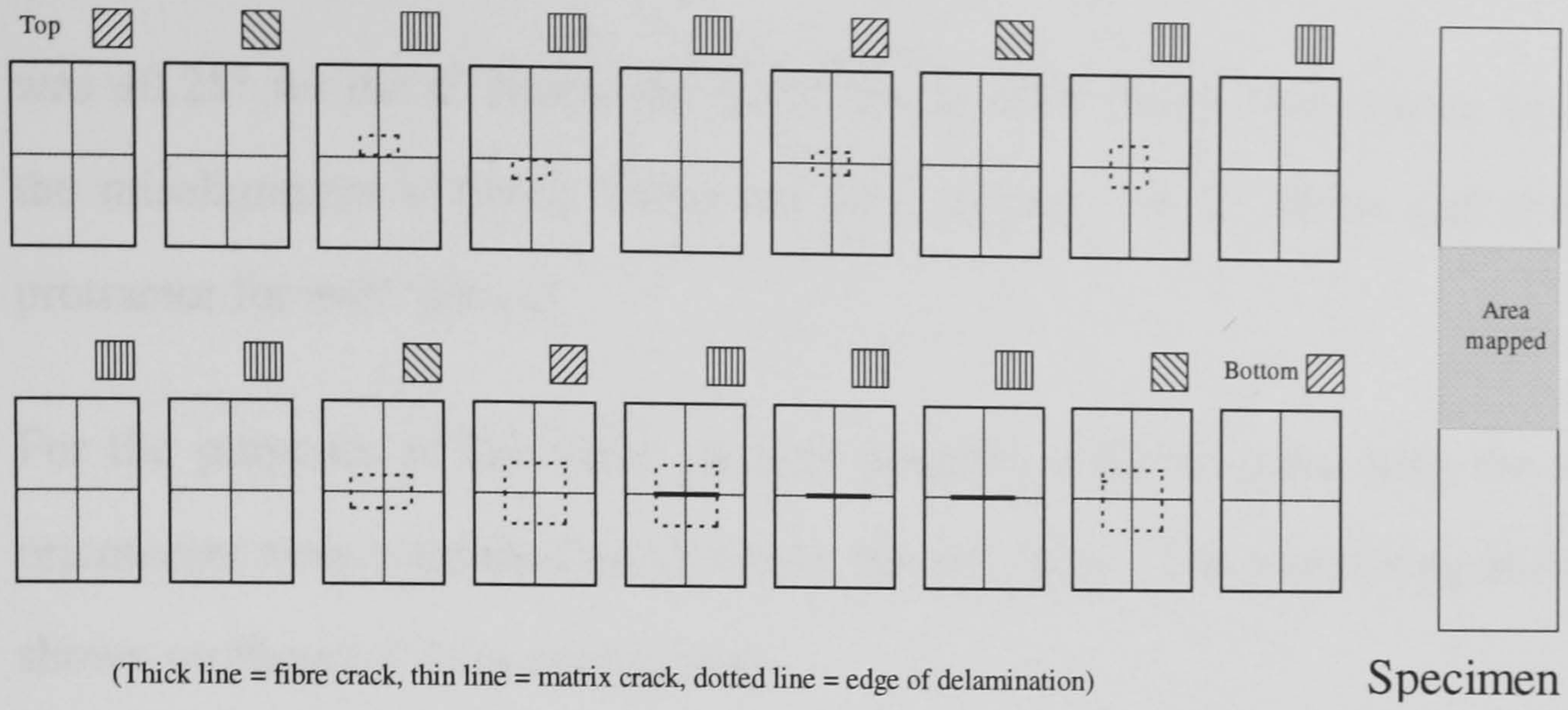

Figure 4.3. Damage map of inserted damage - a realistic representation of 7 Joule damage.

4.3. Manufacture of Specimens

For both materials the plates were made by hand lay-up using the edge of the pre-impregnated tape as the datum to ensure accuracy of ply orientations. The 45° plies were cut from the tape using a guide to ensure the angles were correct. Measurements for positioning of the artificial damage were made from the datum edge to an accuracy of ±0.5mm (equivalent to a possible misalignment of 0.1° introduced by manufacturing methods). Details of the curing schedules are given below. The hot press produced plates with an accurate edge (final plates had the same dimensions as the pre-cured plates), so measurements were made from the edge when cutting out specimens. The auto-claved plates spread a little during curing, so a C-scan was used as guide to cutting test coupons from the plate.

4.3.1 Stacking sequence

The stacking sequence used was $[\pm 45°, 0°_3, \pm 45°, 0°_2]_s$. This leads to an 18-ply composite plate that is nominally 2.25 mm thick. (see Figure 4.1). The plates were layed up by hand, and were of dimensions 254 mm x 254 mm (for hot press) and 300 or 600 mm x 300 mm (for the autoclave). The alignment of the fibres before curing

was ±0.25° for the 0° fibres and ±0.5° for the ±45° fibres. (calculated by measuring the misalignment of fibres along the edge of plate for 0° fibres and using a large protractor for ±45° fibres).

For the purposes of the finite element program adjacent plies with the same fibre orientation were combined into a single, thicker, layer. The numbering of these is also shown on Figure 4.4 for comparison.

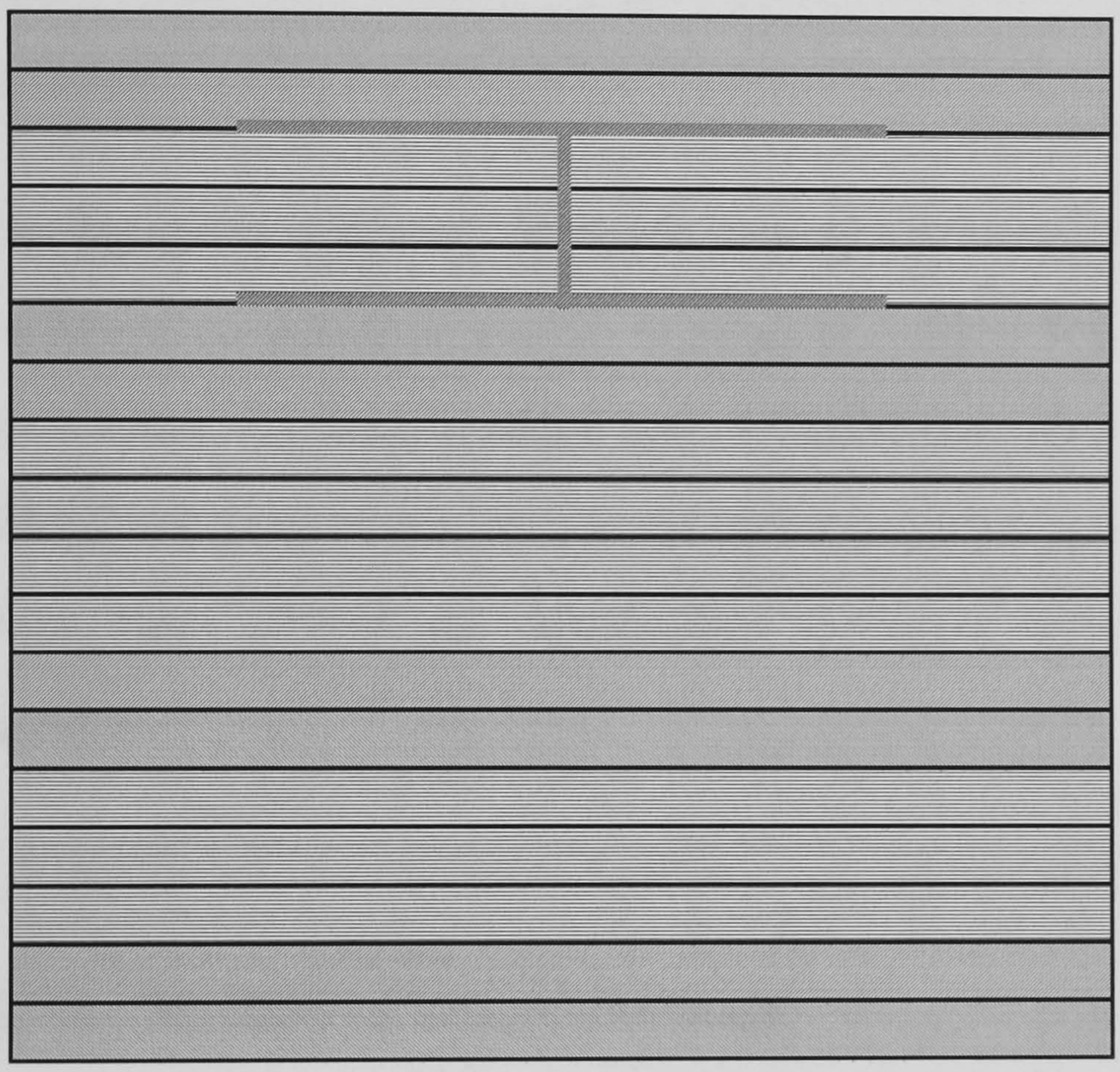

Figure 4.4. Lay up of composite panels showing numbering and position of artificial damage.

4.3.2. Material used: curing cycles

T300/913c is a medium performance high tensile fibre in the form of a tape, 0.125 mm thick, made of unidirectional Toray 300 fibres pre-impregnated with Ciba-Geigy 913c modified epoxy resin, for low temperature cure and high environmental resistance.

Curing cycle: 120°C for 1 hour at 160kPa in a pre-heated hot press; cool to 60°C @2°C per minute. Frekote ™ release agent is sprayed onto the heated mould and allowed to dry before inserting the layed-up laminate. The mould tolerances allow some leakage to allow air to escape

T800/5245c is a high performance fibre in the form of a tape, 0.125 mm thick, made of unidirectional Toray 800 fibres pre-impregnated with Narmco 5245c modified bismaleimide resin, which has good impact strength/toughness and hot/wet strength retention.

Curing cycle: Vacuum bag plate. Heat at 2°C/minute to180°C, hold for 2 hours at 680kPa in an autoclave; cool to room temperature at 3°C/minute. Post cure at 210°C for 4 hours. (A small breather hole is drilled through to the delamination from the thicker side prior to post cure, as the higher temperature and lower external pressure in some cases allowed the delamination to buckle outward before any loads were applied).

4.3.3. Method of impact damage

An impact test rig was used that conformed to CRAG specification [Curtis, ed. 1988]. This consists of two metal rings of inner diameter 100mm and outer diameter 180mm which clamp the plate securely, as shown in Figure 4.5. The impactor is dropped from a height of 1m to strike the plate at the centre of the clamped area, and caught after rebound to prevent multiple strikes to the plate. When more than one impact was carried out on a plate, each one was on an undamaged area at least 100mm from any previous impact and also the plate was positioned so that the clamping rings were not in contact with previous damage. The energy of impact was controlled by varying the mass of impactor used, which had a spherical tip, radius 5mm.

The extent of impact damage was assessed by de-ply and X-ray techniques, and specimens cut from the plate such that the point of impact was central to the coupon.

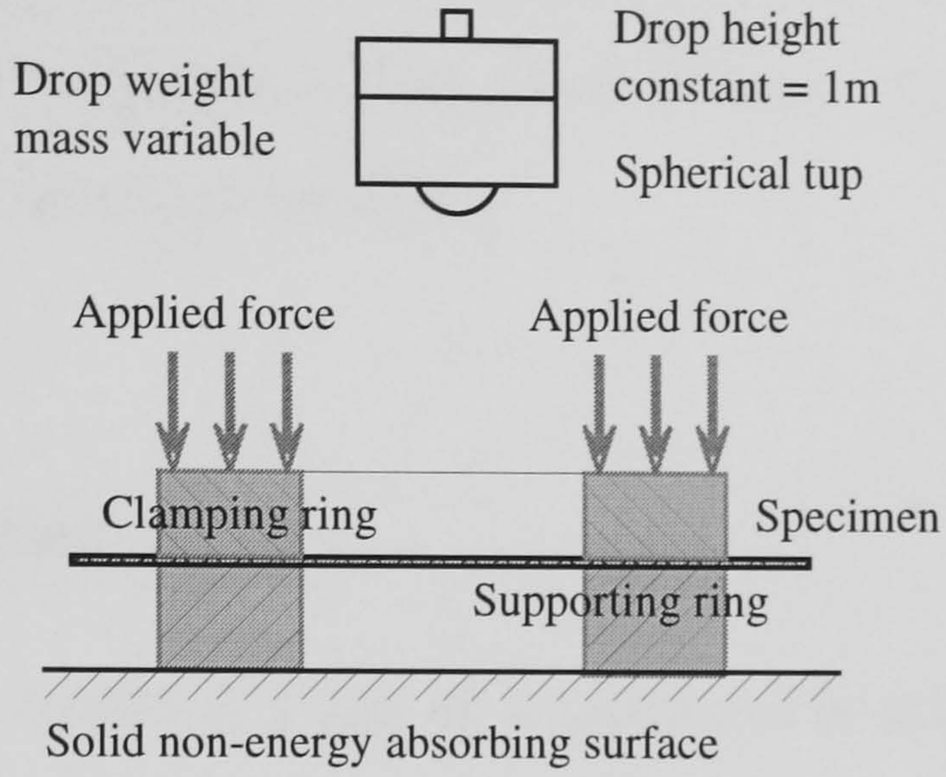

Figure 4.5 *Schematic of impact rig. Internal diameter of support ring = 100 mm, external diameter = 140 mm.*

4.4. Test Procedures

The specimens were tested in compression and tension to determine residual strength after damage. In all cases the results are for specimens that broke within the central section. In compressive tests an anti-buckling guide was used which had a window above the implanted damage, to allow local buckling above the delamination. (See Appendix A). The coupons were end-tabbed with 2mm soft aluminium bonded on with Redux 403 adhesive[1]. Particular care was taken in the case of the compressive specimens to ensure that the end tabs were square at the loading edge so that the load applied to the specimen was even. Therefore, oversized end-tabs were used, and after the end-tabs had been fixed to the specimen they were milled to size ensuring that the

---

[1] From Ciba-Geigy, supplied by B&K Resins, Bromley

edges were flush with the specimen and parallel to the long axis. The ends were milled so the loading surfaces were square (in both directions). An end fixture for the testing machine was built that ensured that the loading on the specimen was through the centre-line of the specimen and did not allow off axis loads or macro-buckling of the coupon (localised buckling is expected, and allowed, at the damage zone). See Appendix A for fuller details of end fixture.

4.4.1. Tensile testing

The specimens were loaded at a rate of 4mm/minute to achieve failure within 90 seconds (following CRAG specifications, [Curtis, 1988]), using a Zwick 1478 test machine. The jaws used were of a wedge grip type. A reduction in load of 20% was used as the criterion for triggering the end of the test.

In all cases the failure was sudden and catastrophic with no indication of the onset of failure apart from increased acoustic emission (audible creaks and cracks, generally interspersed with periods of quiet, but no quantitative measurements were made). In some cases individual fibres broke and peeled away from the edges. Where the coupon contained an artificial crack, and there was enough of the specimen left after failure to observe the area, it was clear that the specimen had failed at that point. Further description of failure is given in chapter 5.

4.4.2. Compressive testing

The specimens were loaded at 2mm/minute to achieve failure between 30 and 90 seconds, using a Zwick 1478 with endplates and anti-buckling guide (see Appendix A). Failure was defined as a reduction in load of 20%, at which time the testing

machine stopped, allowing inspection of the specimen immediately after failure. The load was removed before the specimen could be removed from the test machine, at which time buckled out delaminations sometimes returned to their original flat state.

Final failure of the specimen was preceded by delamination growth in all specimens, except the control coupons. Where initial delaminations were present, they had grown across the width of the specimen to within approximately 5mm of the edge of the specimen before failure of the external plies. The delamination appeared at various loads and in some cases appeared gradually, in others suddenly. In most cases there was some indication that some of the inner plies had buckled, in the form of a slight ridge along the centre of the local delamination. The load at which there was evidence of internal buckling was as low as 3kN.

For the specimens containing only a ply crack (no delaminations before loading), the failure was similar to an undamaged specimen, but with some indication after failure of a small local delamination above the crack. In those specimens with no initial cracks (delaminations only) the load for initiation of local buckling was considerably higher. Just prior to failure it was common for a matrix crack to appear in the surface layers from the corner of the (extended) delamination to the edge of the coupon in the direction away from the centre of the delamination.

4.4.3 Stepped Compression Testing

Since the delaminations will have a greater effect on strength in compression, by allowing local buckling, measurements of the growth of damage with loading were attempted - the size of the buckle might control the failure load of the 0° plies below the surface. Stepped loading tests were therefore carried out in compression, with penetrant enhanced radiography between loading stages to investigate the growth of

the delamination under load, for specimens with artificial damage. In order to open the damage to allow the zinc iodide to penetrate, the specimen was loaded in tension first. (After manufacture the artificial crack is filled with matrix: the aim was to produce a crack in the matrix.) The load used for this was determined from the results of the tensile tests. A load of 2.5% of the ultimate tensile load was sufficient to cause matrix failure in the region of the cut plies without growth of the delamination beyond the edge of the artificially damaged area.

The loading steps in compression were determined by loading the specimen until the onset of acoustic emission indicated an increase in the damage in the specimen (at each subsequent loading the previous peak load was reached without any clearly audible acoustic emission), or a sudden growth in the local delamination was observed. The specimen was removed from load, injected with the penetrant and x-rayed. The film was developed immediately and, if the X-ray exposure was successful, the specimen then replaced in the test machine for further loading. Five to seven stages were usually necessary before the specimen failed, with each stage taking 15 to 20 minutes.

Settings for stepped loading

The loading rate was 1mm/min to allow time to observe the growth of the delamination, which could clearly be seen. This tended to happen in steps rather than gradually, so after each increment of growth load was removed and measurements taken.

Description of failure under stepped loading

The first specimen tested was removed at set intervals in addition to those mentioned earlier, and the results indicate that delaminations grew in steps. The direction of growth was related to the geometry of the original implanted damage. The steps of load were based on acoustic emission - as the coupon was loaded significant acoustic emission was taken as indicating an increase in damage and the load removed for inspection. Matrix cracks were observed to grow as the load increased. In one case when the load was one step before the final load the ply crack was observed to have grown. As with static loading, the delamination grew toward the edge of the specimen as it approached the failure load. After failure it was not possible to determine the position of individual plies immediately prior to failure (i.e. out of plane or not) because of the catastrophic nature of failure, and the post failure damage. It is not possible to use the post failure specimen to determine which plies had buckled in the local damage and which had remained in plane. An X-ray of the specimen after failure was too complex to give useful information.

4.5. Investigative Techniques

The aim of X-radiographic and de-ply investigations was to produce a sequence of damage maps so that the area of delamination produced at various layers, and the cracks across the plies could be recorded and a realistic artificial damage manufactured. X-ray photographs are used to provide a view of the total damage and some indication of the extent of fibre cracks and matrix cracking. More detailed information about the positioning of damage through the thickness was obtained from deplying the specimen. Further information about which plies were buckling out during loading was gained by a novel resin injection technique.

In order to help confirm the results from the finite element analysis of the artificially damaged specimens a shadow Moiré fringe measurement of the out-of-plane displacement of the specimen surface was carried out.

4.5.1. X-ray

Radiography of graphite/epoxy composites is of limited usefulness unless the contrast is enhanced by using liquids such as tetrabromoethane (TBE) or diiodobutane (DIB) as penetrants to improve the visualisation of delaminations and cracks. These particular penetrants are useful because of their penetrating properties and because of their opaqueness to the low energy X-rays used in radiography of composites [Rummel *et al*, 1980; Sendeckjy, 1980]. However their use is undesirable because TBE is toxic and DIB is an irritant.

An alternative is to use zinc-iodide (a dense material) dissolved in equal volumes of water (a polar solvent) and isopropyl alcohol (a non-polar solvent) with a small amount (<1%) of wetting agent (a linear alcohol alkoxylate) which reduces the surface tension of the solution. An advantage of this particular mixture is that it has been shown to have no detrimental effect on the properties of the specimens of graphite/epoxy either at room temperature or at elevated temperatures [Ratwani, 1980]. This is helpful in studying delamination growth as the penetrant may stay in the specimen for some time as experiments continue: gradually increasing the load or the number of fatigue cycles.

X-ray settings

After preliminary tests (starting from values quoted by Soutis, 1989) it was found that the best contrast and exposure for X-ray radiography of our specimens were achieved

by using a tube voltage of 32 kV at a current of 4 mA, with the exposure time set at 200 seconds. Agfa Structurix D4 film was used in grainless plastic folders with no backing behind the film (to reduce graininess from the film envelope). For maximum resolution the film was placed at the greatest possible distance from the X-ray source (60cm) in a Torrex 150D cabinet.

It is interesting to note that below 27 kV the composite was capable of absorbing the X-rays almost completely, so that the film was hardly exposed irrespective of exposure time or intensity of the beam. This means that the lowest possible energy necessary to penetrate the composite and envelope was used, so the penetrant was quite opaque at this energy level. Consequently, even a very thin layer of penetrant was sufficient to produce an image on the film. To enable comparison of the X-ray picture with the deply mapping technique's results the x-ray was printed using low-contrast paper (to show the variation in image intensity to the best advantage) and also enlarged to enable the detail to be seen. An example of an X-radiograph produced using this technique is shown in Plate 4.1)

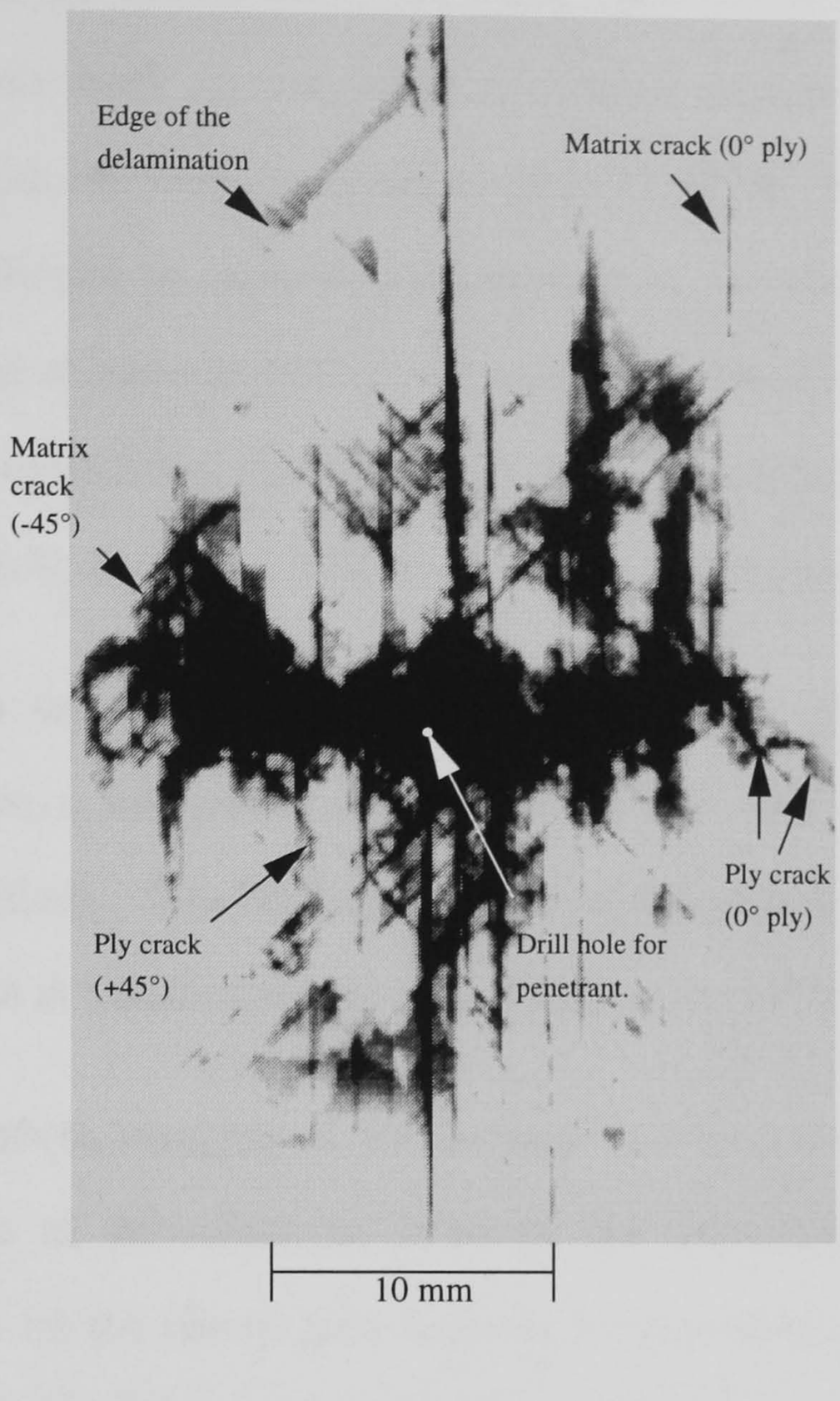

Plate 4.1. *X-ray of actual damage to T300/913c (7 Joules), Zinc iodide penetrant enhanced.*
(note: the resolution and contrast of the original is significantly better than can be reproduced in print at this scale)

4.5.2. Deply

One of the potentially most informative methods of evaluating damage in a specimen is a simple destructive examination technique that involves pyrolysing the matrix resin so that the plies of the laminate can be unstacked. Combining this technique with the use of a penetrant such as those used in the X-radiography of specimens means it is possible to reveal the extent of delamination between two plies.

Harris reports on the work that he has carried out on the materials T300/5208 and AS4/3502. In his work he was using a stacking sequence that did not have any adjacent plies with the same orientation: [0°/±45°/90°]. This meant that there was only a slight difficulty in separating adjacent plies. In other work [Freeman, 1982] there is no record of multiple plies of the same orientation being separated from each other during the unstacking. This should be very difficult anyway, if the specimen has been made properly, as there should be no obvious matrix layer between similar plies.

Obviously, each material will need a different regime of heating and cooling to pyrolyse the matrix sufficiently to allow separation of the plies without causing damage to the fibres. The heating must be carried out in an inert atmosphere and precautions taken in handling the noxious fumes produced by the process.

This method enables mapping of the damage to fibres in individual layers and the pattern and size of delaminations between the successive plies of the laminate. Freeman reports on the use of gold-chloride for revealing the delaminated area, but other authors have found that this is not always necessary.

Preparation of specimens for deply

The specimens were cut down to a size that included all the damage so that the exhaust of noxious fumes from the furnace would be minimised. The top right hand corner (when viewed from above) was trimmed so that there would be no problem with orienting the specimen after deplying. The furnace was filled with argon and pre-heated to 420 °C.

A penetrant was used that would fill the delaminations and leave a residue after pyrolysis of the matrix. The specimens were prepared for the penetrant by drilling a

small (1.0 mm) hole through the centre of the impact dent. This had two aims: firstly to allow full penetration of the solution to those delaminations connected to the impact zone, and secondly to allow accurate positioning of the delaminations in relation to the impact, after the plies had been separated. Additional holes of diameter 0.3mm were drilled near the edges of the delamination to allow trapped air to escape, ensuring the penetrant reached the edges of the delamination.

Deply penetrants

Deply involves burning away the interlaminar resin so that the plies can be separated. This allows the damage in each layer to be seen (unlike the x-ray which is a shadow picture of all layers). The positions of the cracks are easily seen, but the extent of delamination is harder to ascertain. There is a small difference in the surface texture where there has been a delamination, but to improve the contrast a penetrant can be used which will stain the delaminated area. Gold chloride is generally used for this purpose. The gold chloride decomposes to leave a fine layer of gold that is clearly visible.

The suggested concentration of 9.2% [Harris] was found to be unsatisfactory, hence the use of a 20% solution. In addition, the solution used is not stable (the gold starts to precipitate out after about a day, so reducing the concentration). This does mean that the deply mapping technique would be quite expensive and so various other materials were tried as alternatives.

The need is for a salt that is readily soluble in water, or alternatively an organic solvent with lower viscosity, which will survive the deply temperature and leave a clearly visible stain against the black background of the composite. The solvent must have evaporated at the temperatures used, so the flammability of the solvent must also be considered. One solution would be to use a fluorescent material as the mark could be made to show up under ultra-violet light, but unfortunately none could be found

that did not decompose below 420°C. The penetrants tried were zinc iodide (the X-ray penetrant), sodium sulphate (Na_2SO_4), potassium (IV) chromate (K_2CrO_4), calcium oxide (CaO), magnesium sulphate ($MgSO_4$) and gold-chloride (as chloroauric acid $HAuCl_4.xH_2O$).

All penetrants left a deposit, but for some it was a loose powder that was easily dislodged, for example the sodium sulphate. The most effective alternative to gold chloride was the calcium oxide, though the deposit was dark yellow rather than white. The zinc iodide left a very dark residue and this was not easily visible against the (black) carbon fibres. (The mark on the fibres is in the form of a dulling of the surface finish, which is clearly visible in the right lighting conditions, but difficult to record on film or to trace.) Overall, gold chloride is by far the best in terms of performance, but expensive, and was the choice for deply of the impacted specimens.

The gold-chloride solution was made by dissolving 20% by weight of chloroauric acid (containing 51% gold by weight) into diethyl ether. A proprietary wetting agent was added, which had the (unexpected) added benefit of improving the stability of the solution. The solvent has a very low viscosity which aids penetration.

The penetrant was introduced into the delamination using a fine syringe to reduce wastage. The solution seeps into the specimen and more is added until no more solution is absorbed. The process is repeated from the other side, since all the impacts produced sufficient damage to the specimens to break the rear surface. At least half an hour was allowed for the liquid to penetrate before the surface residue was wiped away. During this period the specimen was warmed to help evaporate excess solvent, in order to prevent gas bubble formation during pyrolysis which could drive the penetrant out of the delamination.

The specimen was X-rayed and then put into the pre-heated furnace, supported on pins to allow ventilation of all sides. At this point the furnace was again flushed with argon and the exhaust system turned on. Since the material produces an appreciable amount of vapour as it pyrolyses it was not felt necessary to pump argon through the furnace as air was unlikely to enter. No problems were encountered with this decision.

After 1 hour in the furnace the heater was switched off and the specimen allowed to cool in the furnace until the specimen holder could be removed from the oven. Since the specimen was now in a fragile state it was thought best not to move it unnecessarily.

The unstacking process was achieved without too much difficulty by laying a sheet of colourless adhesive-backed plastic film onto the specimen. Lifting the film was usually enough to separate the lamina from those below; occasionally judicious use of a scalpel was needed to complete the separation.

The individual 0° plies in a stack would not separate at all and were re-heated to see if the remaining resin could be removed. Even though there was some evidence of separation of the fibres at the end of the specimen, this separation did not coincide with the ply boundaries, as would be hoped if the specimen had originally been manufactured properly.

Fibre cracks visible from one side of a stack of 0° plies were essentially identical to those on the other side, although some of the stacks had minor delaminations within them. The unstacked plies were protected from damage by applying another layer of colourless plastic to the back, which enabled close examination and recording of the damage, as well as facilitating storage. The results for one such mapping are shown

in Figure 4.6. Since delaminations occur between two faces, they are shown on the surface below the delamination.

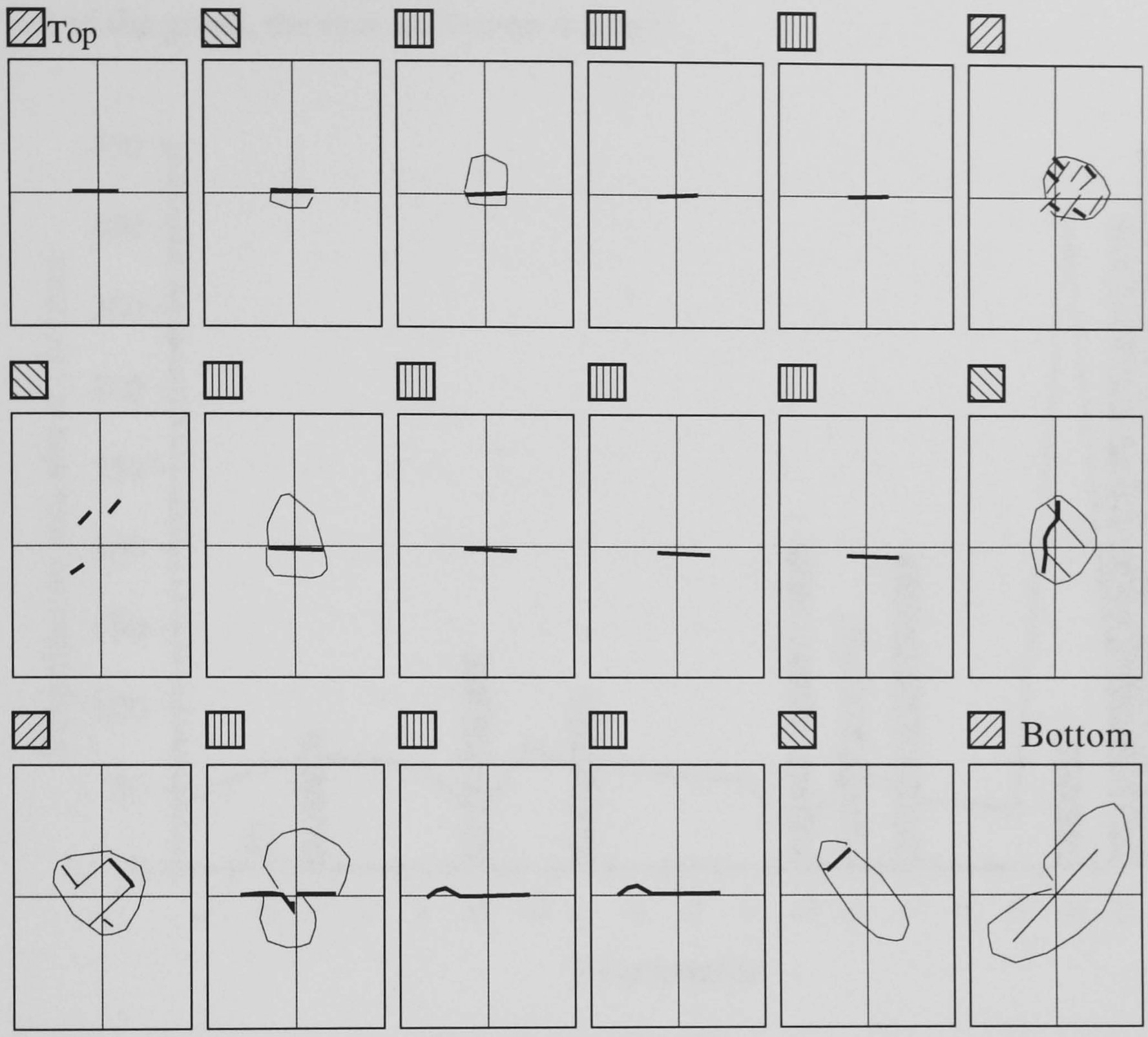

Figure 4.6. Impact damage from a 7 Joule impact, T300/913c.

The gold-chloride was quite effective at revealing the extent of delamination between the first few laminae, but at layers more distant from the surface the delamination could be perceived due to a slight dulling of the fibre surfaces and not always because of a layer of deposited gold. It is at least possible to use the results to check that the method does work by comparing the deply mapping with the picture from radiography as the gold-chloride is quite efficient as an X-ray penetrant. Graphical representations of the extent of damage through the thickness of the laminate for various energies are

shown in chapter 5. A sample is shown in Figure 4.7. The delamination area between two plies is shown as a bar on the ply that it is above. The impact surface is on the left of the graph, the rear surface on the right.

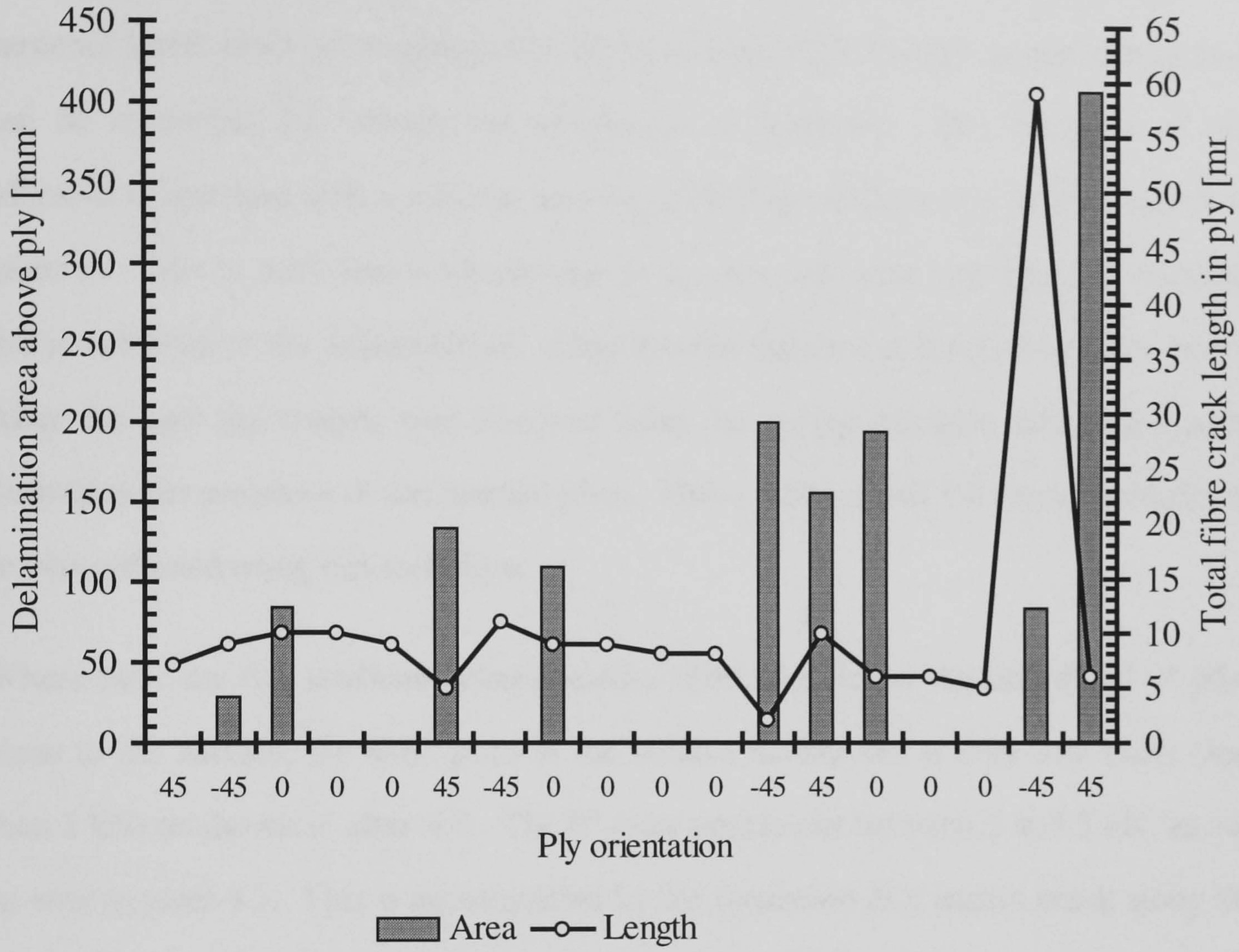

Figure 4.7. Damage versus position for 7 Joule impact, for T300/913c.

4.5.3. Resin injection

A novel technique was developed to allow the positions of the internal plies to be ascertained when the delamination had buckled out of plane. This is only necessary when twin artificial delaminations are inserted, as there are then two sets of sub-laminates that can buckle out during loading in compression. When the load is removed from the specimen the buckle disappears. The method described here allows

the buckled plies to be held in place when the load is removed. This involves loading the coupon until the delamination had buckled out and then holding the displacement while a quick setting adhesive is injected into the specimen. A compromise had to be found between viscosity and setting time. The adhesive used was LMB4555 with hardener LMB 4930 (an experimental adhesive from Ciba Geigy), as the setting time can be controlled by varying the proportion of hardener. The viscosity of this adhesive is low, and with a suitable amount of hardener will remain so for about 5-10 minutes. This is sufficient working time to mix the adhesive and inject it, allowing full penetration of the delamination. After this the full cure is reached in a few hours. After the cure the coupon was removed from the testing machine and sectioned to determine the positions of the internal plies. Plates 4.2, 4.3 and 4.4 show examples of results obtained using this technique.

Where there are two artificial delaminations, above and below the first set of 0° plies close to the surface, the ±45° plies at the surface buckle out at very low loads (less than 1 kN) as shown in plate 4.2. The 0° plies buckle out between 2 and 3 kN, as can be seen in plate 4.3. This is accompanied by the formation of a matrix crack along the edges of the delamination (plate 4.4). The lines along which the resin injected damage was sectioned is shown in Figure 4.8.

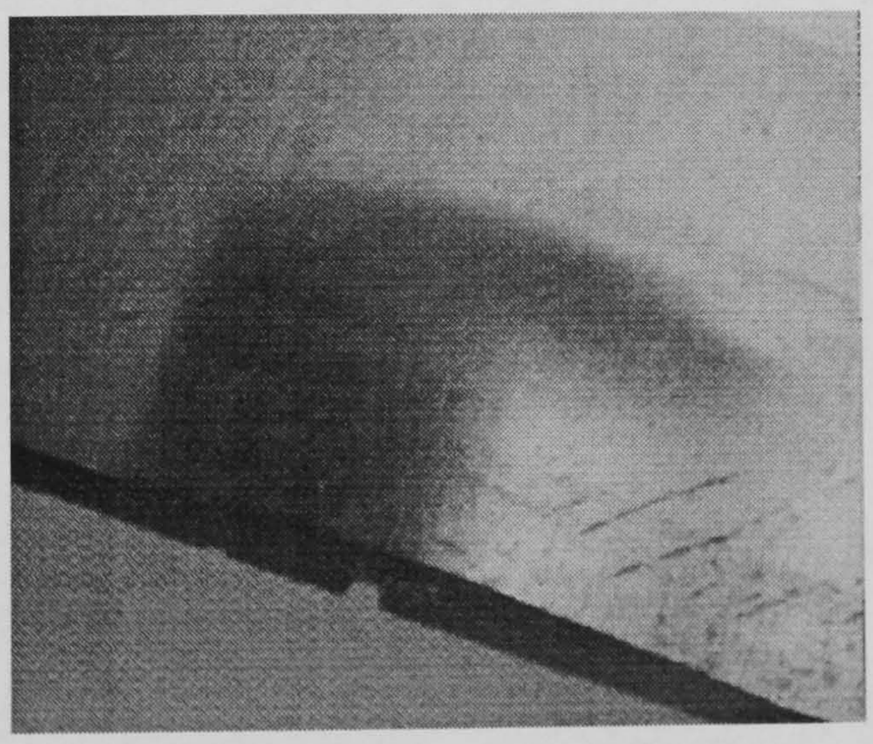

Plate 4.2 *Buckled delamination - external view, after sectioning, loading axis left to right.*

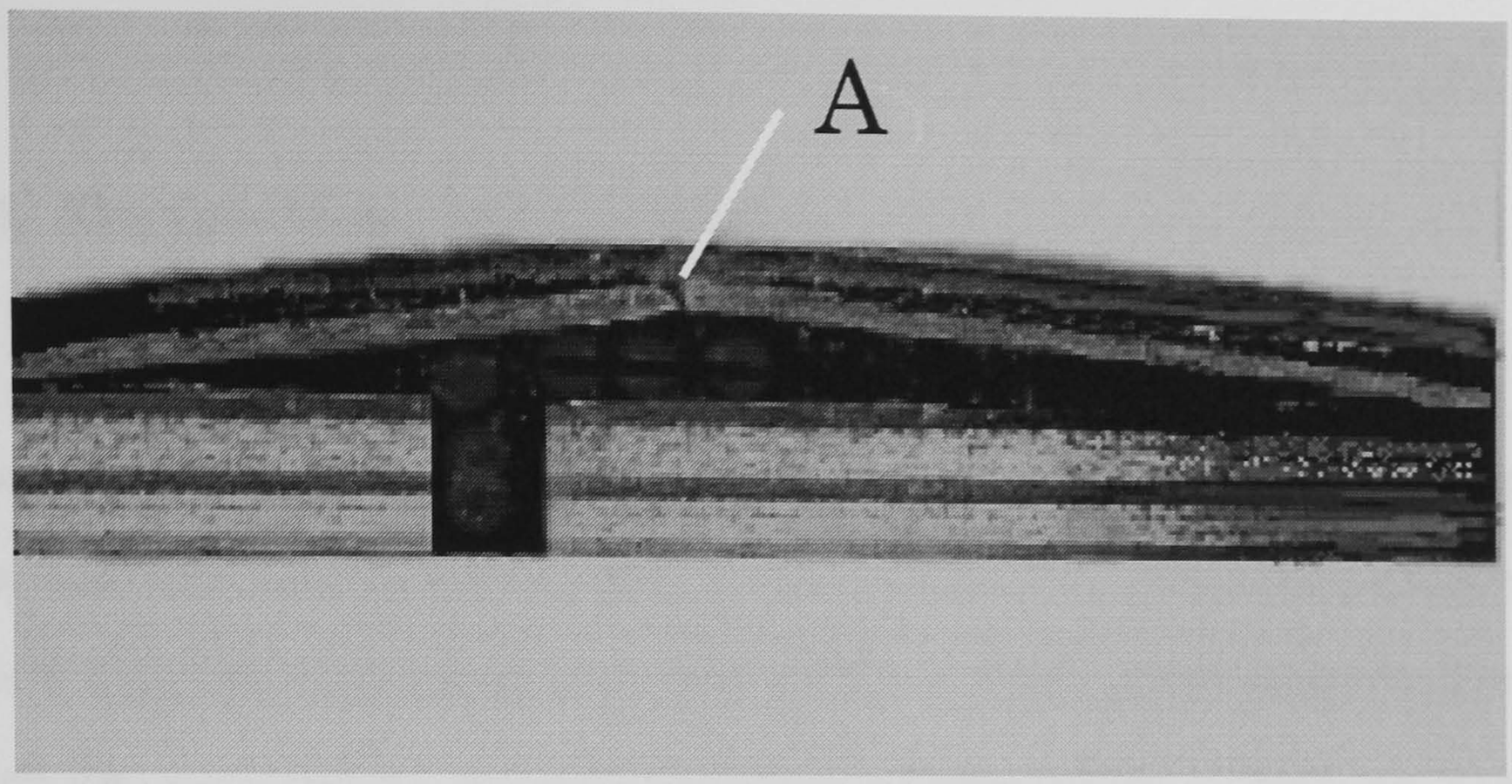

Plate 4.3. *Sectioned coupon after resin injection, loading axis left to right in compression. Crack in 0° plies indicated at* **A**, *showing the plies have buckled.*

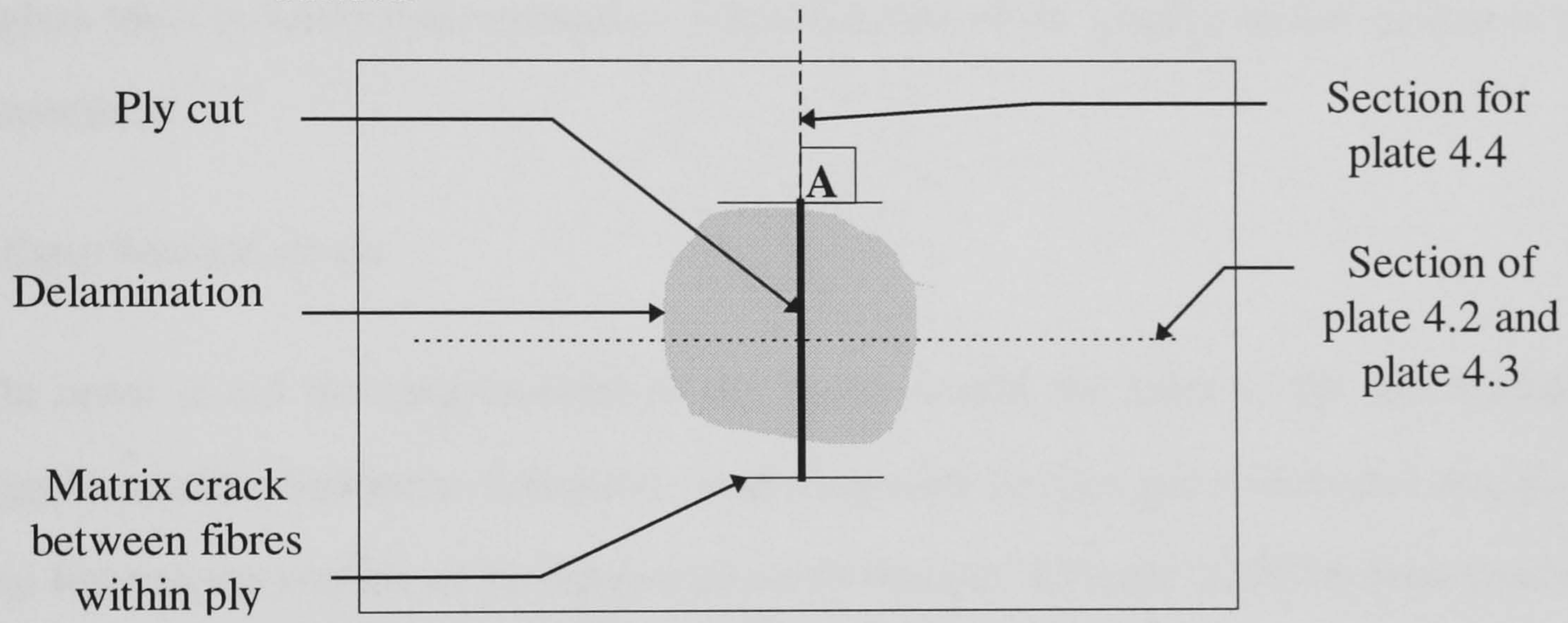

Figure 4.8. *Position of cuts to expose buckled plies*

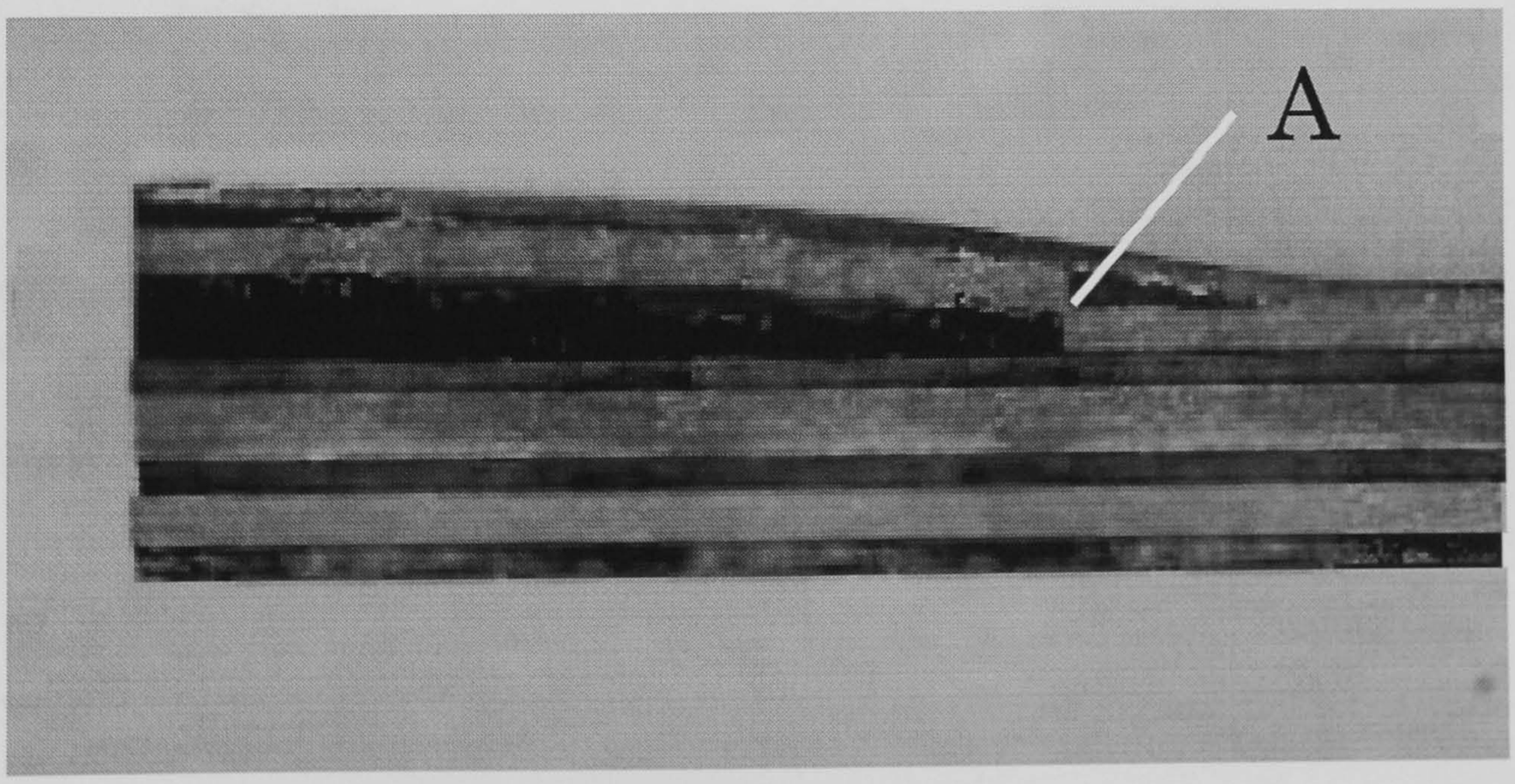

Plate 4.4. *Sectioned coupon after resin injection, loading axis normal to page, in compression, matrix crack seen end on at* **A**

4.5.4. Shadow Moiré Interferometry

It is possible to use Moiré methods to determine both in-plane and out-of-plane displacements [Basehore, 1980], however these require complicated surface treatment of the specimen (depositing a grating on the surface) or expensive equipment (e.g. lasers or computer-linked scanners). In this study a simple out-of-plane displacement was all that was required, so a straightforward shadow Moiré method was used. In essence the fringe is the result of interference between a grating on an optically flat glass sheet in front of the specimen and the shadow of the grating on the surface of the specimen.

Experimental set-up

In order to aid the measurement of the buckle height the sides of the anti-buckling guide window had been chamfered. A grating with 10 lines per millimetre[2] was fixed in front to the surface of the coupon to cover the area with the artificial delamination. The grating was attached by bonding four ball bearings to the corners, in order to make the grating parallel to the surface. See Figures 4.9 and 4.10.

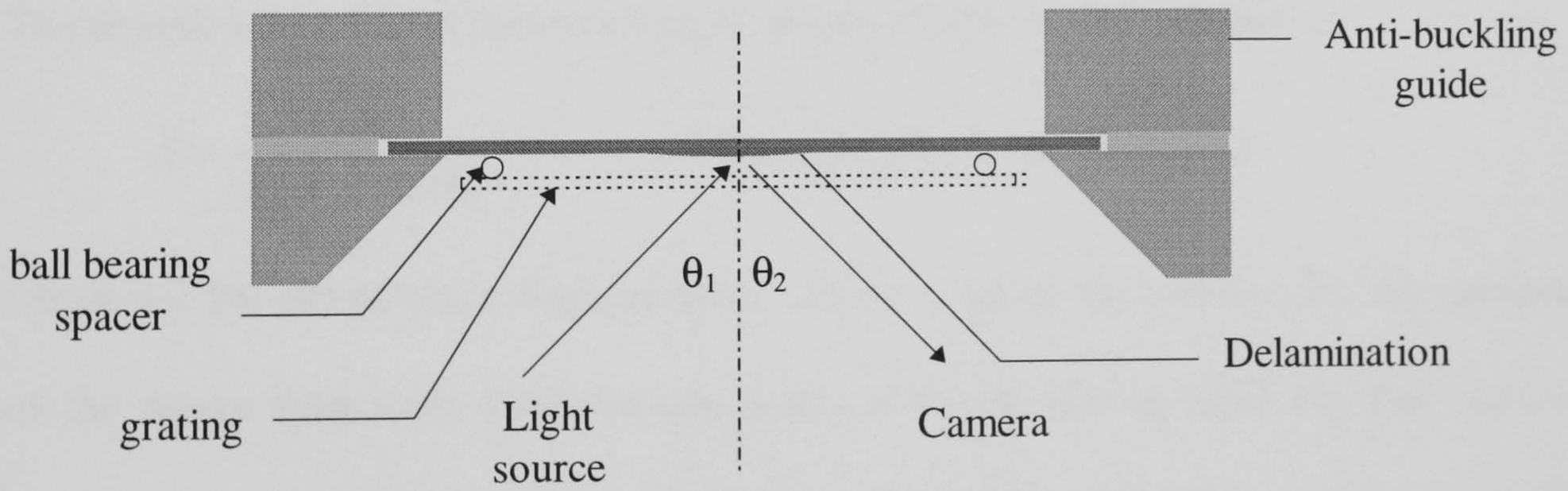

[2] Supplied by GRATICULES Ltd, Morley Road, Tunbridge Kent TN9 1RN

Figure 4.9. Arrangement of apparatus for shadow moiré fringe interferometry. (Top view)

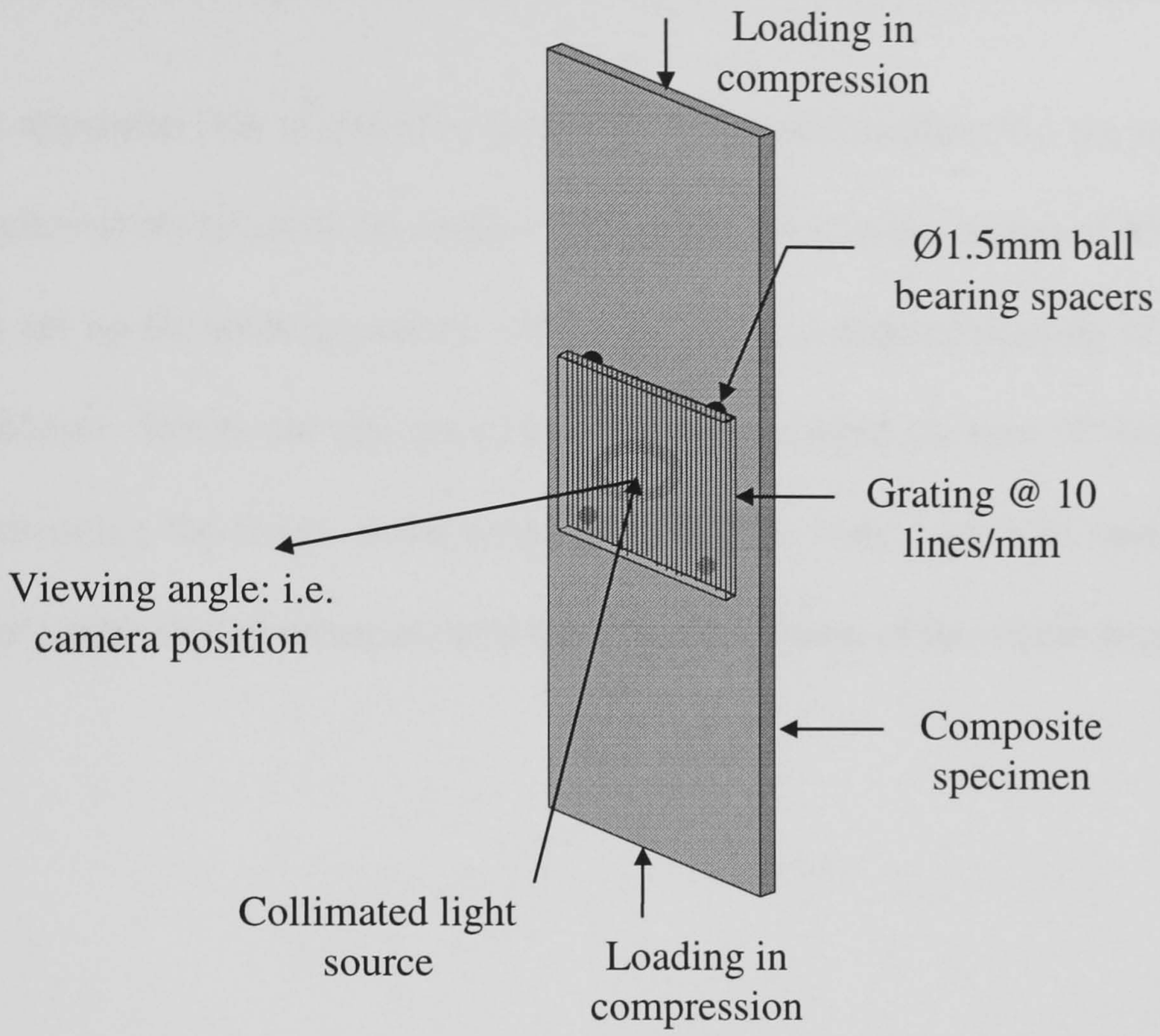

Figure 4.10. Arrangement of apparatus for shadow moiré fringe interferometry. Anti-buckling guide not shown for clarity.

The equation that relates the out-of plane displacements to the contours is:

$$d = \frac{np}{\tan\theta_1 + \tan\theta_2} \qquad \text{(see Appendix B for derivation)}$$

where d is the out-of-plane displacement, n is the order of the contour (i.e. the number of the fringe from zero displacement zone), p is the grating pitch (in this case = 0.1mm, 10 lines/mm), θ_1 is the angle between the normal to the plate and the incident light and θ_2 is the angle between the normal to the plate and the incident light.

In theory, greater precision can be achieved by increasing the projection and viewing angles, but in practise the contrast between the fringes reduces above a certain angle (as the effective width of the lines decreases diffraction effects increase).

The apparatus was arranged to ensure the maximum contrast for the fringes and then measurements taken of the angles. The angles were in the region of 30° (varying as it was set up for each specimen), which equates to a contour spacing of approximately 0.085mm. Errors are introduced into the measurement because of the imprecision in determining the fringe at the peak of the buckle—one cannot be sure without using more sophisticated measurements the exact brightness of the centre fringe.

References

Cantwell W.J. and Morton J.

"The Impact Resistance of Composite Materials - a review."

Composites Vol. 22(5) **1991** pp. 347-62.

Curtis P.T. (editor)

"CRAG Test Methods for the Measurement of the Engineering Properties of Fibre Reinforced Plastics."

RAE Technical Report 88012 **1988** pp. 1-108

Evans R.E. and Masters J.E.

"A New Generation of Epoxy Composites for Primary Structural Applications: Materials and Mechanics"

Toughened Composites ASTM STP 937 **1987** pp. 413-436

Freeman S.M..

"Characterisation of Laminae and Interlaminar Damage in Graphite/ Epoxy Composites by Deply Technique."

American Society for Testing & Materials STP787 **1982** pp. 50-62.

Harris C.E.

"Damage Evaluation by Laminate Deply." pp.147-9.

Jang B.Z., Chen L.C., Wang C.Z., Lin H.T. and Zee R.H.

"Impact Resistance and Energy Absorption Mechanisms in Hybrid Composites,"

Composites Science and Technology Vol. 34(4) **1989**; pp. 305-35.

Ratwani M.M.

"Influence of penetrants used in X-ray radiography on compression fatigue life of graphite/epoxy laminates."

Composites Technology Review Vol. 2(2) **1980** pp. 10-12

Sendeckjy G.P.

"The effect of tetrabromoethane-enhanced X-ray inspection on the fatigue life of resin-matrix composites."

Composites Technology Review Vol. 2(1) **1980** pp. 9-10.

Sims G.D.

"Development of Standards for Advanced Polymer-Matrix Composites."

Composites Vol. 22(4) **1991** pp. 267-74.

Soutis C.

"Compressive Failure of Notched Carbon Fibre-Epoxy Panels."

PhD. Thesis, Jesus College, Cambridge. Oct. **1989**

Strait L.H., Karasek M.L. and Amateau M.F.

"Effects of Stacking Sequence on the Impact Resistance of Carbon Fibre Reinforced Thermoplastic Toughened Epoxy Laminates."

Journal of Composite Materials Vol. 26(12) **1992** pp. 1725-40.

Williams, J.G. and Rhodes, M.D.

"Effect of Resin on Impact Tolerance of Graphite/Epoxy Laminates"

Composite Materials: Testing and Design (Sixth Conference) ASTM STP 787 **1982** pp. 450-480

CHAPTER 5.

EXPERIMENTAL RESULTS

5.1. Introduction

The results for all static tests are shown in this chapter. Fatigue test results are included in the chapter on fatigue testing. The experimental results consist of residual ultimate strength in tension and compression strength for both materials (T300/913c and T800/5245c) for the range of damage tested. The stepped loading tests have results in the form of extent of damage plotted against load. Some preliminary comment is made on the significance of these results, with further comment in later chapters.

The results from the impact testing investigations are described at the end of the chapter.

5.2. Residual Tensile Strength

The geometry and manufacture of the specimens used for these tests are described in chapter 4. Figure 4.2 shows the position of inserted damage for the specimen with a

crack and two delaminations. Where less damage is inserted, the crack was in the same place, and the single delamination one of the two positions shown.

5.2.1. T300/913c

The results for tensile testing of T300/913c are shown in Table 5.1 and Figure 5.1. There are no results for the realistic artificial damage in tension due to a shortage of material for making specimens.

Treatment of coupon	Failure Load [kN]
Undamaged	93.60
Crack [3 plies , 25mm]	83.20
Crack[3 plies, 25mm] + delamination far from surface	80.00
Crack[3 plies, 25mm] + double delaminations	90.32
Real damage [7 Joule impact]	65.20

Table 5.1. Residual tensile strength of T300/913c after impact or insertion of artificial damage. Values from one specimen, except for undamaged - average.

From these results it can be seen that in tension the residual strength is dependent on the amount of undamaged 0° plies. The presence of delaminations does not have a significant effect on the strength, as is shown by comparison of the artificially cracked specimens with varying delamination damage.

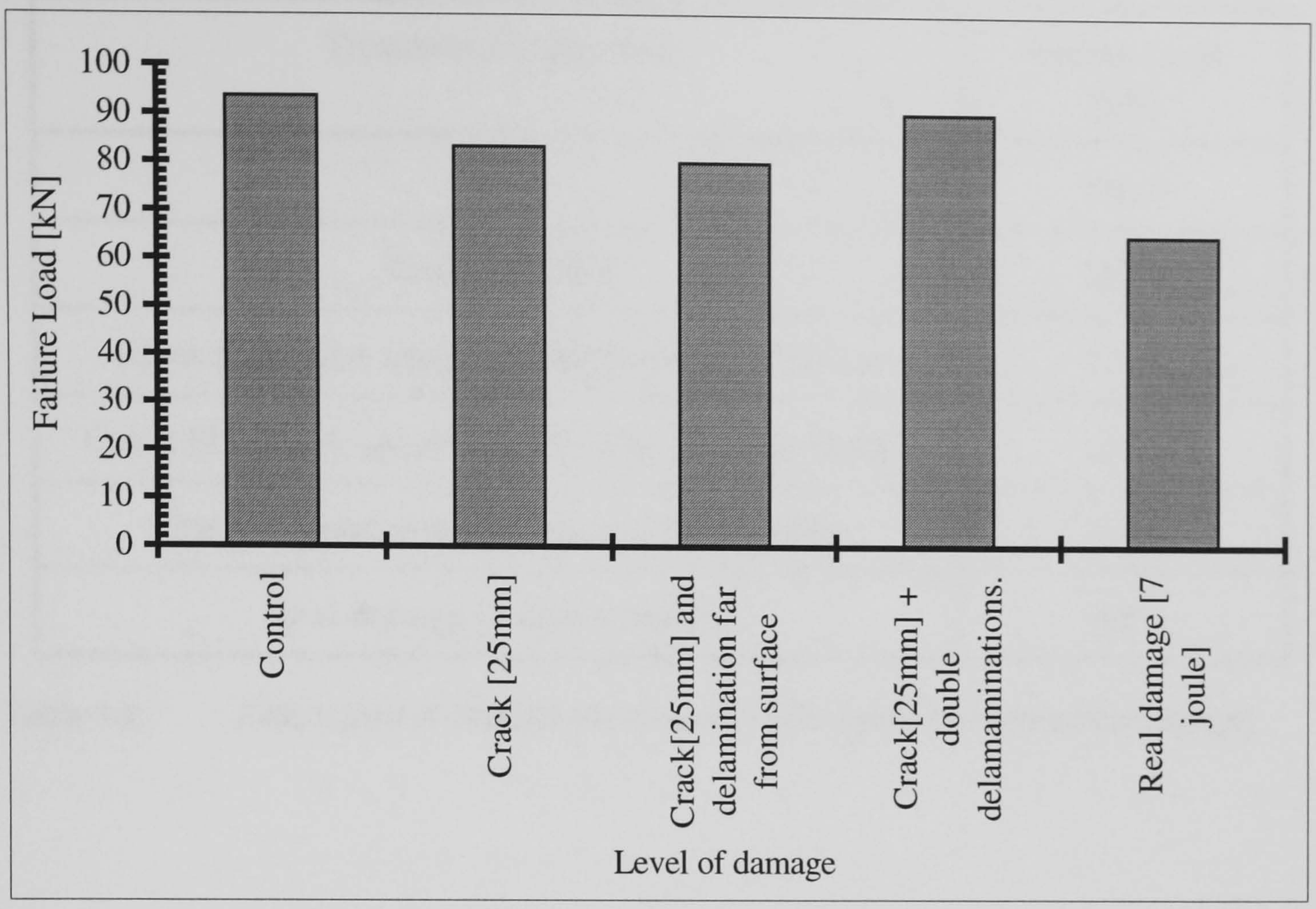

Figure 5.1. Ultimate strength of T300/913c specimens in tension.

5.2.2 T800/5245c

The results for tensile testing of T800/5245c are shown in Table 5.2 and Figure 5.2. There are no results for the realistic artificial damage in tension due to a shortage of material for making specimens. These tests were carried out on a Denison 500kN hydraulic test machine, as the Zwick 1478 could not produce the loads required. The loading rate was identical to that used on the Zwick, 4mm/minute, and the grips were of a similar wedge type. The coupons all failed in the test section.

Treatment of specimen	Failure Load [kN]
None	190.9
Crack [25mm]	163.1
Crack [25mm] + square delamination near surface	179.4
Crack [25mm] + square delamination far from surface	155.2
Crack [25mm] + double square delamination	170.6
Real damage [7 Joules impact]	199.2

Table 5.2. Failure load of T800/5245c in tension after actual and implanted damage.

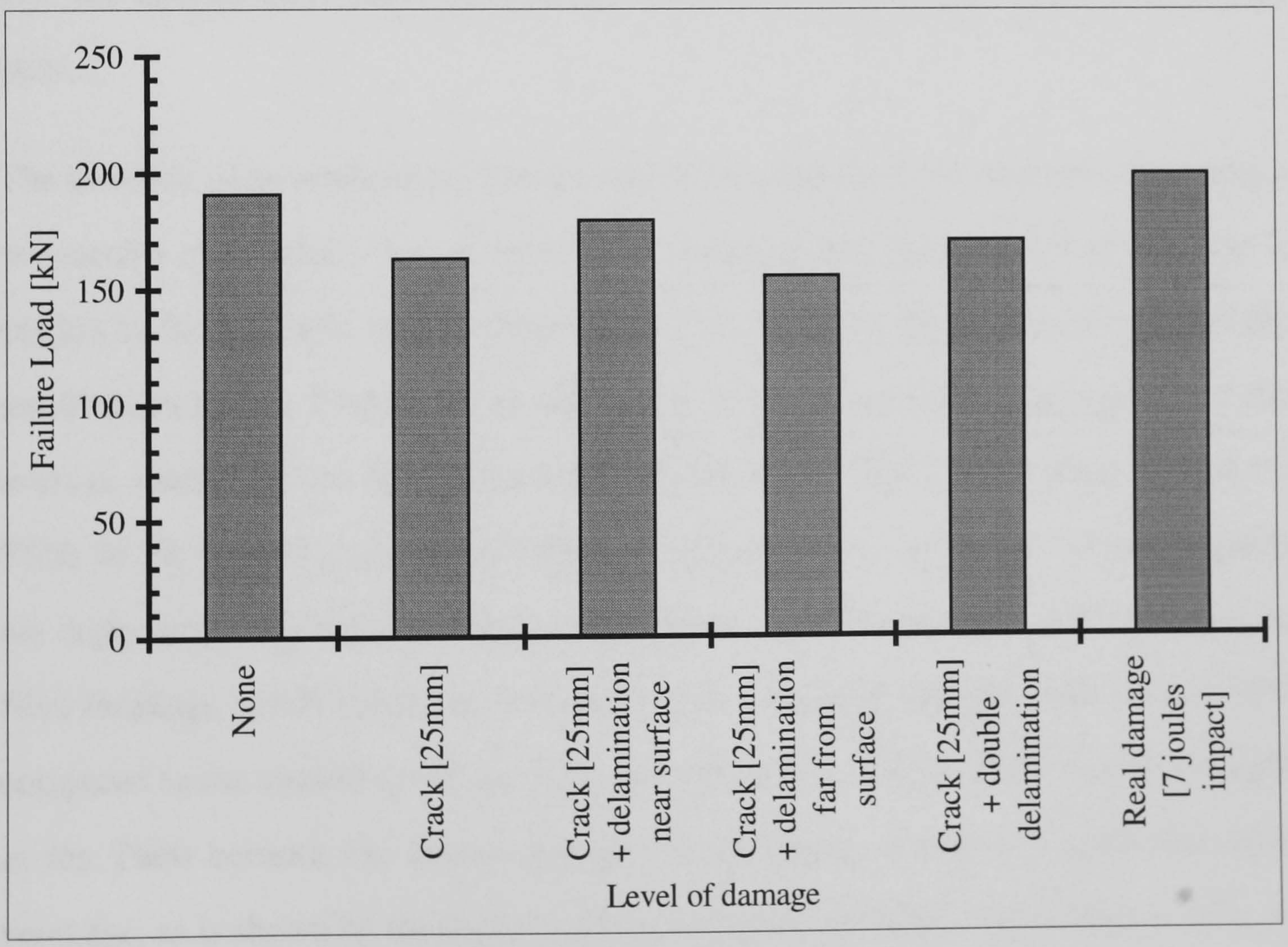

Figure 5.2. Comparison of tensile strength of T800/5245 with varying levels of damage.

5.2.3. Preliminary discussion of results

From Figure 5.2 it is clear that delaminations do not reduce the residual tensile strength of T300 or T800. This is to be expected as the effect of tensile loading is to close, rather than open, the delamination.

Inspection of the failed tensile test coupons indicated that in all specimens without delaminations at the start a delamination had been initiated at the crack in the 0° plies (where a delamination is not already present). In all cases the delamination has grown toward the grips. The failure of the specimen, however, occurs when the remaining 0° fibres fail. In earlier tests of specimens with though-the-width damage, when testing the effectiveness of ply cuts, (section 3.5.2), a similar failure occurred; and in this case also the delamination could be observed to start at the crack and grow towards the grips.

The insertion of an artificial ply crack reduces the strength of the coupon in line with a net-section of 0° fibres rule, in which it is assumed that the majority of the load is carried by the 0° fibres. In both materials 15% of the fibres have been cut (3 out of the ten 0° plies have a 25 mm cut in the centre of the 50 mm wide specimen) and the average strength of the damaged coupons is, for T300, 89% (11% reduction) and for T800 84.3% (15.3% reduction) of the maximum strength. In the case of real impacts the deply map for T300 (see Figure 4.1) indicates a 29% reduction in 0° plies due to fibre breakage which compares favourably with a residual strength reduction of 31% compared to the control specimen. The real impact does not affect the tensile strength in the T800 because the impact energy is insufficient to produce significant fibre breakage, as is shown by the deply mapping (comparing Figure 4.6 and Figure 5.3). A more detailed analysis is included in Section 5.8.

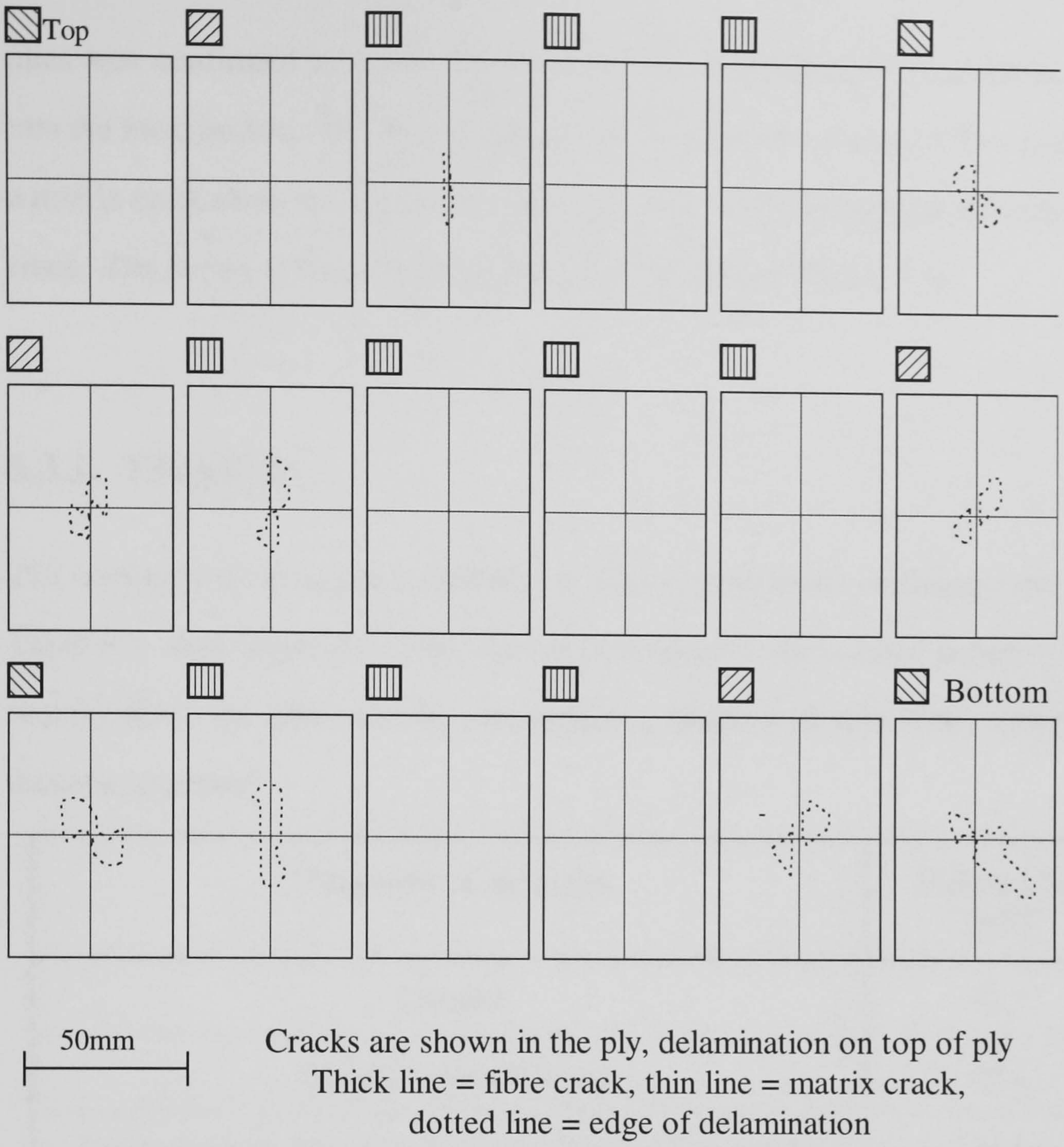

Figure 5.3. Deply of impact damage, 7 Joule impact on T800/5245c.

5.3. Residual Compressive Strength

Before presenting the values for the strengths of different specimens comments will be made on some observations during testing. In all cases where an initial delamination was present local buckling of the ±45° outer plies occurred at relatively low load. The 0° plies below also buckled out at relatively low loads as could be inferred by the presence of a ridge on the buckle. The exact position of these hidden

plies was confirmed as previously described by the technique of inserting adhesive into the local buckle. The micrographs show that the plies buckle at the crack and that a matrix crack along the edges of the delamination is formed starting at the ends of the ply crack. The X-rays of the stepped loading clearly show this. (Figure 5.6)

5.3.1. T300/913c

The compressive strengths of T300/913c with various levels of damage are shown in Table 5.3. and Figure 5.4. The amount of damage in the coupon generally increases moving down the table, and the corresponding failure load approaches that of the real damage specimen.

Treatment of specimen	Failure Load [kN]
Control	72.1
Crack (3 plies, 25mm)	72.2
Crack (3 plies, 25mm) + delamination close to surface	57.5
Crack (3 plies, 25mm) + double delamination.	35.7
Realistic artificial (see Figure 4.3)	28.31
Real 7 Joule	28.26

Table 5.3. *Residual compressive strength of T300/913c after impact damage - real and artificial. Maximum values.*

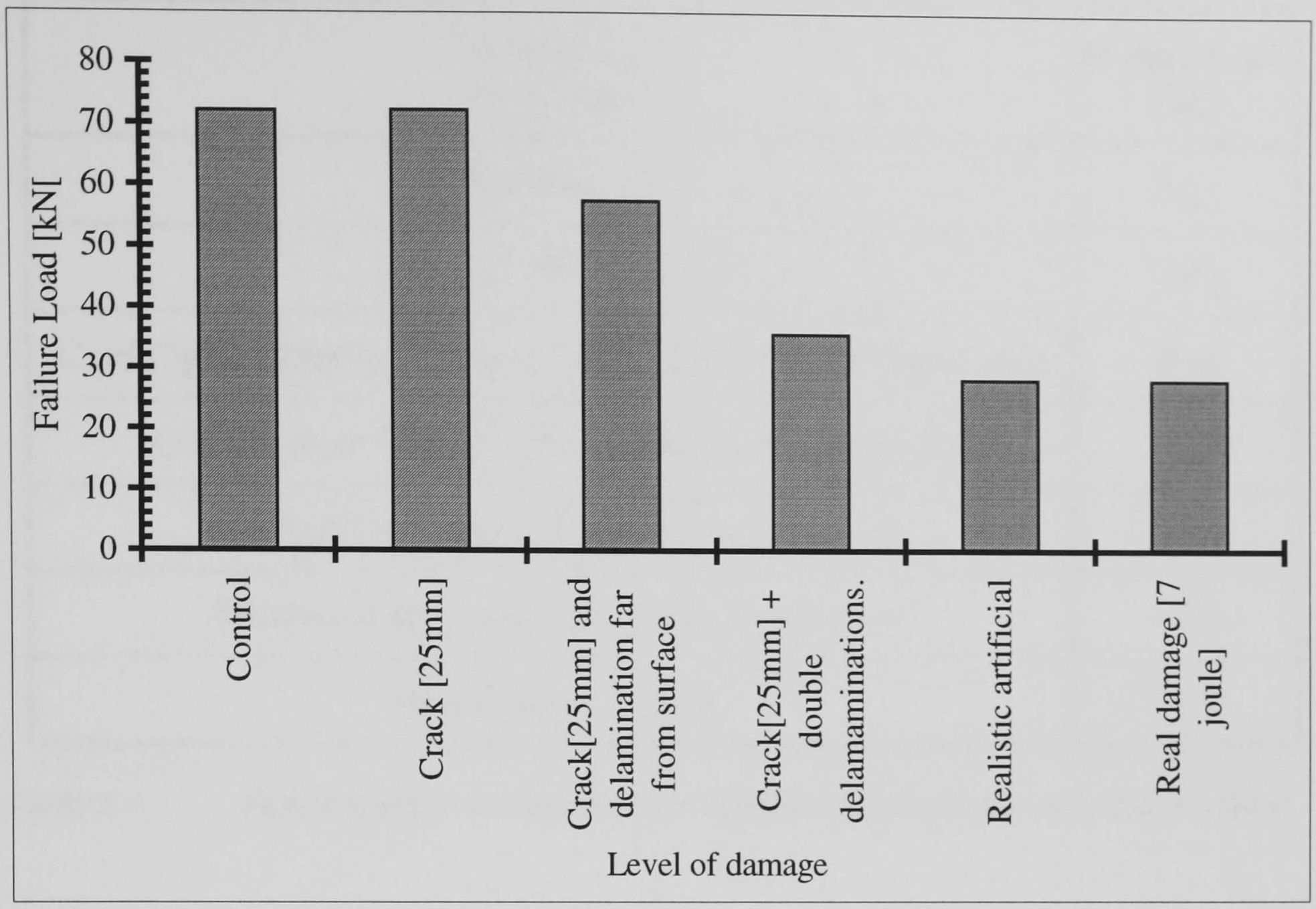

Figure 5.4. Ultimate compressive strength of T300/913c with increasing amounts of damage.

5.3.2 T800/5245c

The compressive strengths of T800/5245c with various levels of damage are shown in Table 5.4. and Figure 5.3 The amount of damage increases moving down the Table.

Treatment of specimen	Failure Load [kN]
Undamaged	68.1
Crack (3 plies, 25mm)	54.9
Crack(3plies, 25mm) + Delamination (nearer surface than crack)	53.8
Crack(3 plies, 25mm) + Delamination (below crack)	52.3
Crack(3plies, 25mm) + double delamination	51.6
Realistic artificial damage (as per Figure 4.3)	35.6
Real damage, 7 Joule	35.0

Table 5.4. Failure loads in compression for T800/5245c specimens. Maximum values

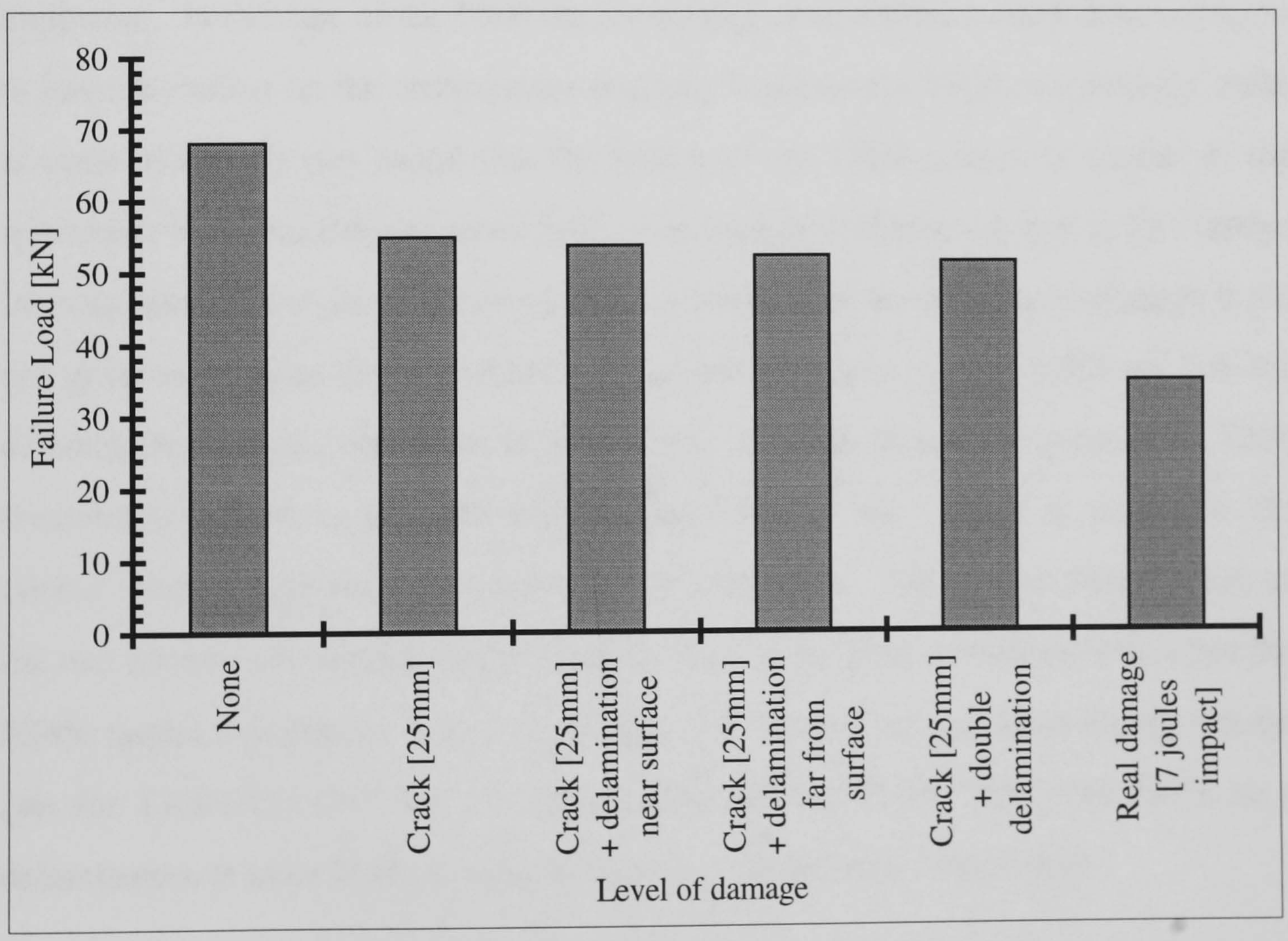

Figure 5.5. Residual compressive strength of T800/5245c with increasing damage.

5.3.3. Discussion of results

The first point to note is that a realistic amount of artificial damage produces a reduction in strength that is very close to that from real damage. However, this amount of damage is impractical to implant into all coupons because of the complexity involved, and does not ease the separation of effects due to delamination and ply cracks. It would also make mathematical modelling of the artificial damage very difficult.

A more useful amount of damage, as far as modelling is concerned, is a ply crack and two delaminations, which comes reasonably close to real damage in terms of the effect on residual strength, particularly in the case of the T300/913c.

A point of interest is the difference between the two materials when only a crack is implanted. In the case of the T300 the implanting of an artificial crack does not seem to have any effect on the compressive strength, however for T800, surprisingly, there is some effect. It was found that the failure of the T800 coupon is similar to the specimens that have delaminations before the loading commenced, and in fact further investigation showed that a delamination was initiated at the crack, and although it did not grow as large as the pre-existing delaminations there is the likelihood that the delamination affected the failure of the coupon. That this does not happen in the T300 is probably related to the difference in properties of the matrix, in particular the critical strain energy release rates for the two materials. The relative failure loads of the two composites (mainly due to the difference in the fibre properties) mean that the 5245c matrix experiences a greater loading. The mode 1 critical strain energy release rate for T300/913c (255 Jm^{-2}) is greater than that for T800/5245c (180 Jm^{-2}), so a delamination is more likely to open from a crack in the case of the T800.

The amount of delamination in the T300/913c seems to be related to the strength reduction, whereas in the T800/5245c the insertion of an extra artificial delamination

does not contribute to a reduction in strength. This is possibly because one delamination dominates in the failure process. If a delamination closer to the centre of the coupon buckles out then the tendency for a delamination closer to the surface to open up is reduced. The growth of delaminations under loading in compression will make a big difference to the final failure load so these results need to be considered in conjunction with those from the stepped loading.

5.4. Stepped Compression

This section deals with the results from testing of specimens described in section 4.4.3. The aim was to follow the growth of delamination and crack damage by interrupting the loading and using penetrant enhanced X-radiography to reveal the extent of damage.

The specimens tested are shown in Table 5.5.

Specimen	Description (All specimens 18-ply T800)
2D+C	Double delamination [25mmx25mm], plus crack [3 plies, 25mm] (as per Figure 4.1)
DB+C	Delamination [25mmx25mm], far from surface, plus crack [3 plies, 25mm]
DT+C	Delamination [25mmx25mm], close to surface, plus crack [3 plies, 25mm]
ND+C	No delamination, crack [3 plies, 25mm]

Table 5.5. Description of specimens used for stepped compression loading.

The growth of delaminations can be seen from the tracings of the X-ray photographs. As can be seen from the initial pictures, the penetrant has not reached the full extent of the artificial delamination, which indicates that PTFE is a good choice for an insert (aluminium foil would have masked this area on the X-radiograph). It is probably due to the delamination closing up when the load is removed and so making it more difficult for the zinc iodide to penetrate. Once the buckle grows beyond the range of the initial insert the penetrant seems to reach to the edge of the delamination as a comparison of the x-ray and the ultra-sonic scans of the delamination shows. (The specimen was also marked on the outside using a pen while under load to show the extent of the buckle. This matched well with the x-ray and deply results.)

It is possible to inject the x-ray penetrant during loading, while the buckle is out, ensuring that the penetrant reaches to the full extent of the buckle [Clarke and Pavier, 1992a], but this results in corrosive penetrant seeping out when the load is removed causing damage to the compression grips and anti-buckling guide.

In all cases failure was preceded by growth of delamination. Even in the case where there was no implanted delamination, one was initiated at the ply crack and grew during loading.

A tracing of delamination growth for one particular case (DB+C) is shown in Figure 5.6. The growth of delamination area with load is recorded in Figure 5.7. This delamination growth is typical, but in one specimen we also recorded a crack growing, as indicated in the diagram.

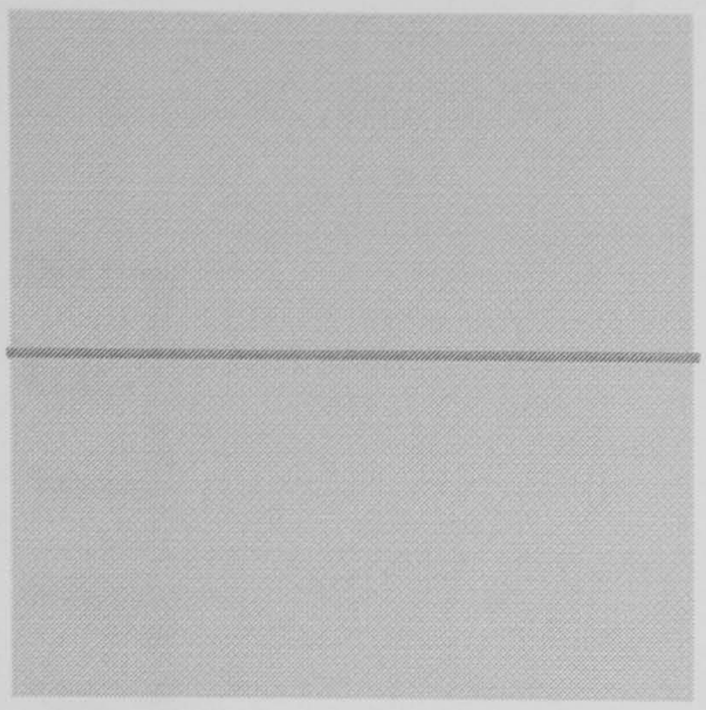

Figure 5.6. *Growth of damage with loading for a delamination 2 plies from the surface. Loading is vertical, crack and artificial insert shown in grey. (T800/5245c) Delamination growth is typical of all combinations of damage in stepped compression, crack growth only occurred in* DT+C *specimen. Loading is perpendicular to initial ply crack.*

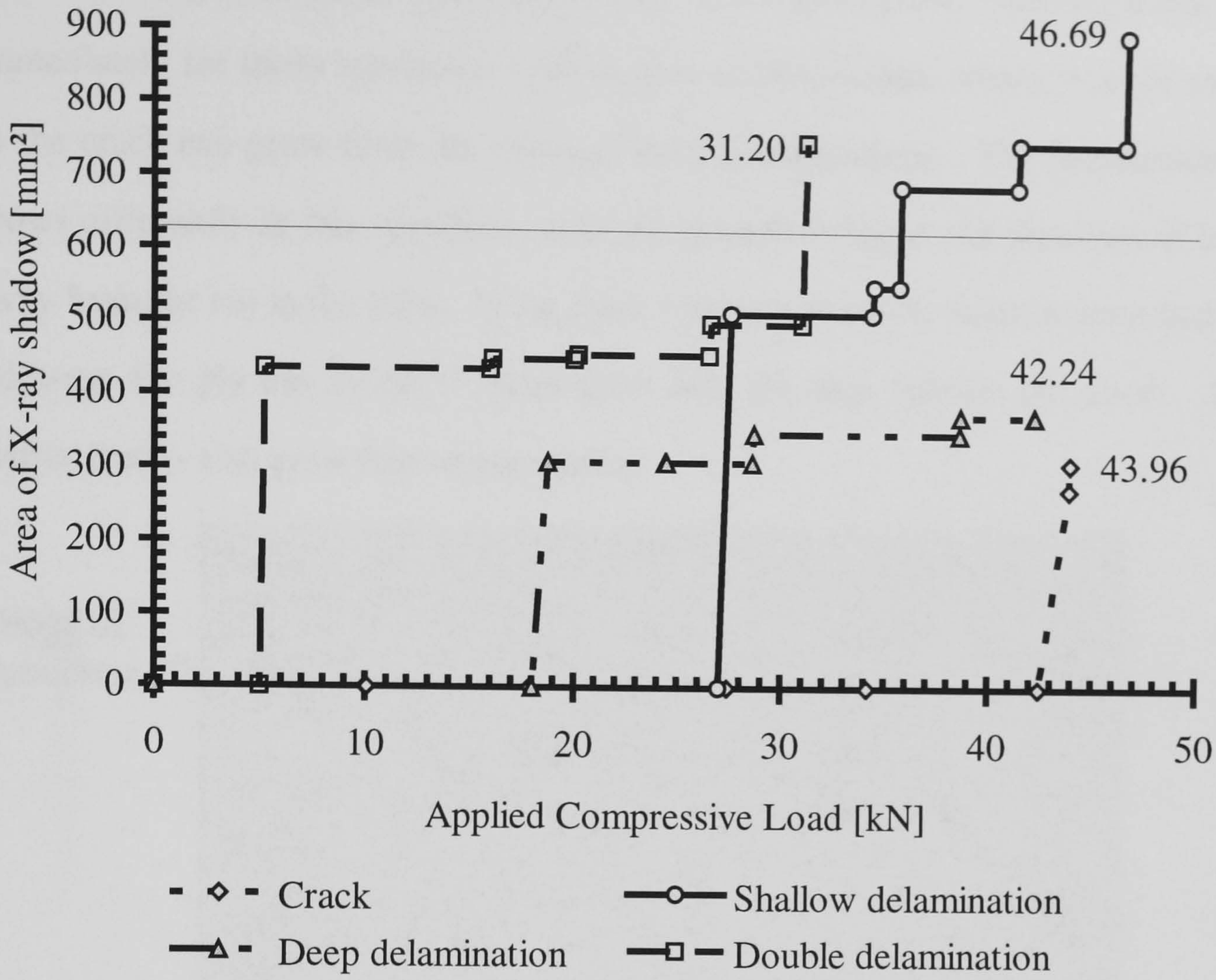

Figure 5.7. *Growth of delamination with loading in T800/5245c. Horizontal line shows the initial insert size (except for the specimen with only a crack)*

As can be seen from the Figure 5.7, the rate of delamination growth (inferred from X-ray shadow measurements) with applied load is greatest in those specimens which have the lowest stiffness for the material above the delamination.

The measured delamination may not be as great as expected as the material above the delamination can recover after the load is removed and prevent penetrant from revealing the damage. Only when permanent out-of-plane deformations have occurred will the X-radiography indicate delamination growth. It was not possible to carry out the X-radiography without removing the specimen.

In all cases the ply cut crack was revealed by the penetrant from low load, and matrix cracks running from the ends of the cut were observed to grow. They appeared almost immediately for those specimens with double delaminations, which is to be expected as the crack can grow from the edges of both delaminations. The delamination also grows differently in this specimen, with the growth being in the direction of loading, away from the cut in the plies. In the other coupons, once the delamination had grown sideways the ply cut in the 0° plies grew into the area outside the insert. Further matrix cracks also grew from these cracks.

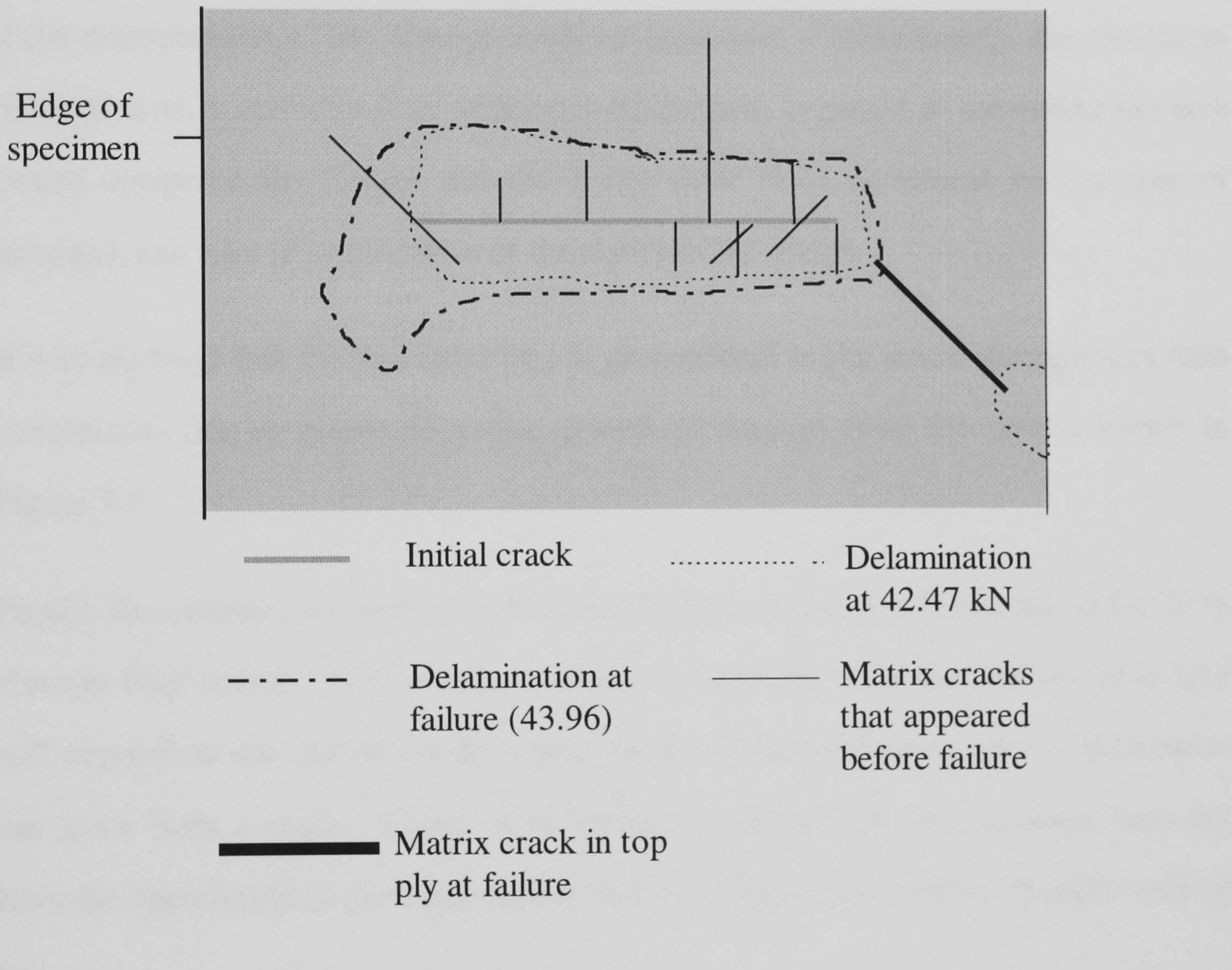

Figure 5.8. Growth of delamination with loading in T800/5245c - specimen containing only a crack. Loading is perpendicular to initial ply crack.

Of particular interest is the failure of the coupon that did not contain a delamination at the start. The crack was the starting point for the growth of a delamination, which was slightly wider than the crack but only about 10mm in the loading direction.

5.4.2. Discussion of results

Since the nominal area for the delamination is 25 mm by 25 mm (625 mm²), it is clear that the X-ray technique does not reveal the full extent of the damage. This is probably due to the penetrant failing to register on the film close to the edge of the delamination as the film of penetrant would be thinnest at this point. It is clear from many of the x-rays that there are more than one delamination in some specimens although it is difficult to ascertain if they both grow, due to the nature of the X-ray. It was decided to do some tests using both ultrasonic scanning and X-radiography to see if the measurement of the damage could be improved. Unfortunately, the resolution of the C-scan is such that little additional information is gained in measuring the area (when compared the C-scan and the X-ray show close agreement on the area of damage), and a lot is lost in terms of the clarity of the image.

If it is assumed that the measured area is proportional to the actual damage area then conclusions can be drawn about the growth of damage from the results shown in Figure 5.7.

Firstly, the coupon with only a crack did not buckle until a very high load, in fact very close to final failure. This is as we would expect in the sense that the buckling load will depend on the size of the delamination, but it also indicates that a delamination can grow from a crack. Under these loading conditions the delamination does not have the opportunity to grow any further, but in a fatigue environment it might well do so.

Secondly, the greater the amount of delamination the lower the load at which the delamination growth initiates. The plies above the delamination have less support and are more prone to buckle.

The depth of the damage affects how quickly the delamination grows. The specimen with the delamination closer to the surface, and therefore with a thinner layer (2 plies) to buckle, grows more quickly than the specimens where there are 5 plies to buckle out. In the case of the double delamination the two sets of plies, the ±45° and the 0° plies must move as one so the delamination nearest to the surface does not reduce the stiffness once the 0° plies have buckled. The low load for initiation of the buckle could be explained if the ±45° plies buckle first, followed by the 0° plies which are no longer restrained.

The direction of significant growth of the delamination is perpendicular to the loading direction. This has been observed in other studies [Greenhalgh, 1989]. The stress conditions vary around the circumference of the delamination; in the loading direction there are compressive forces on the crack tip from the main laminate and the sub-laminate/delamination. Perpendicular to the loading direction the forces from the main laminate (i.e. the undamaged laminate beyond the delamination) are tensile relative to the delamination (due to the Poisson's ratio expansion). Greenhalgh suggests that the mode of delamination growth is dominated by mode I transverse to the loading direction and mode II parallel to the loading direction.

5.5. Measurement of out-of-plane displacements

The presentation of the results for the measurement of out-of-plane displacements will mainly be covered in the section on finite element analysis (chapter 7) as the object of using this technique was to verify the validity of the results from numerical analysis. A summary of the results, however, is shown in Figure 5.9.

The measurements were taken during a stepped loading in compression of the coupon. with a loading rate of 0.5mm/minute. The loading was continuous except for the pauses necessary to photograph the fringes. Although the fringes are clearly visible to the naked eye, recording the fringe on film for future reference and measurement required low ambient light and long exposure to ensure the best contrast between light and dark contours in the final image. Sample pictures are shown in Figure 5.10 to illustrate the results (these are for specimens with a 15mm by 15mm insert below the first set of 0° plies, used here as they give the best reproduction in print).

This loading regime was used to allow the delamination to grow slowly enough to allow interruption to make measurements.

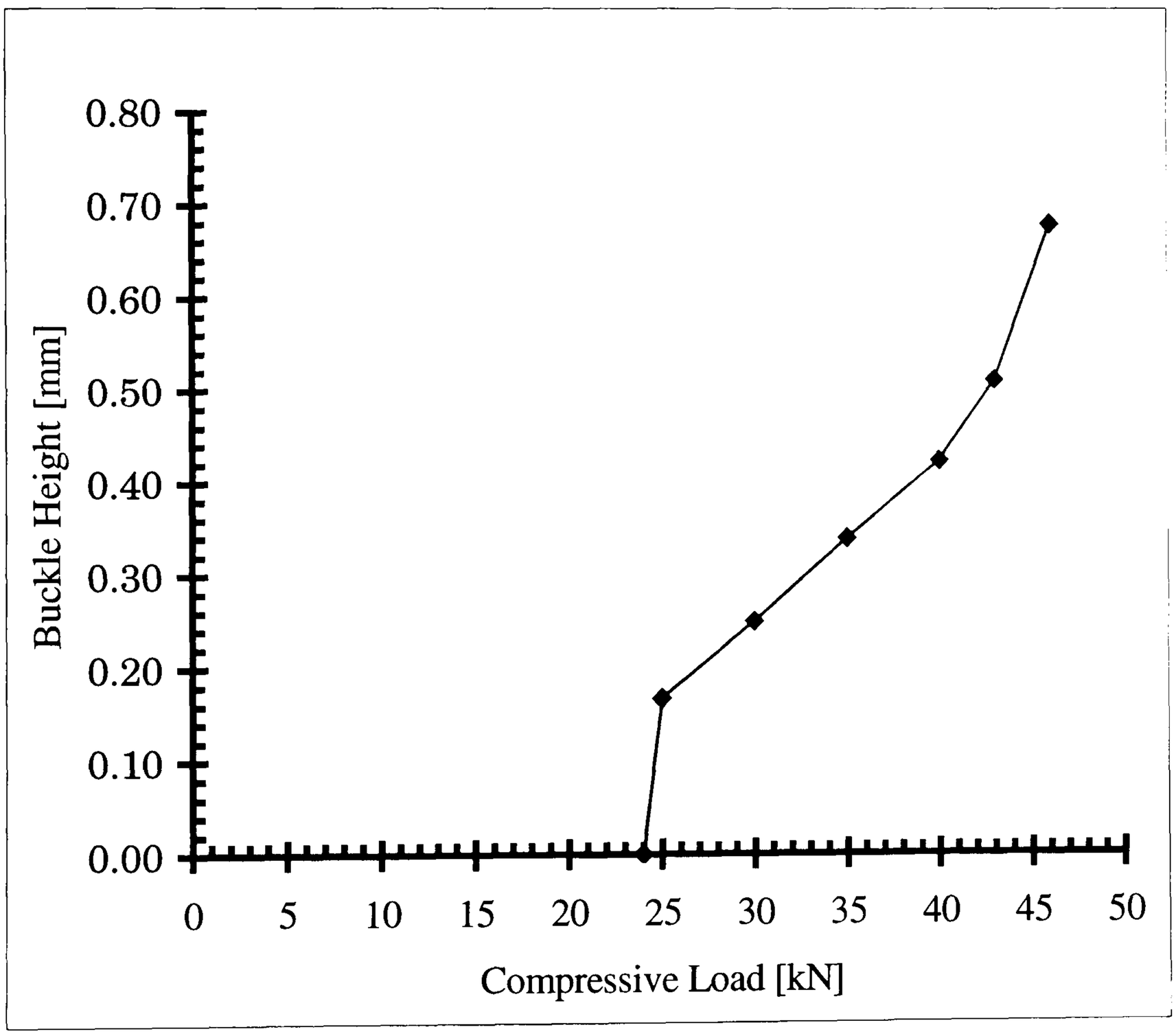

Figure 5.9. *The height of the local buckle plotted against compressive load for a T300 specimen containing a 25mm by 25mm PTFE insert 5 plies in from the surface.*

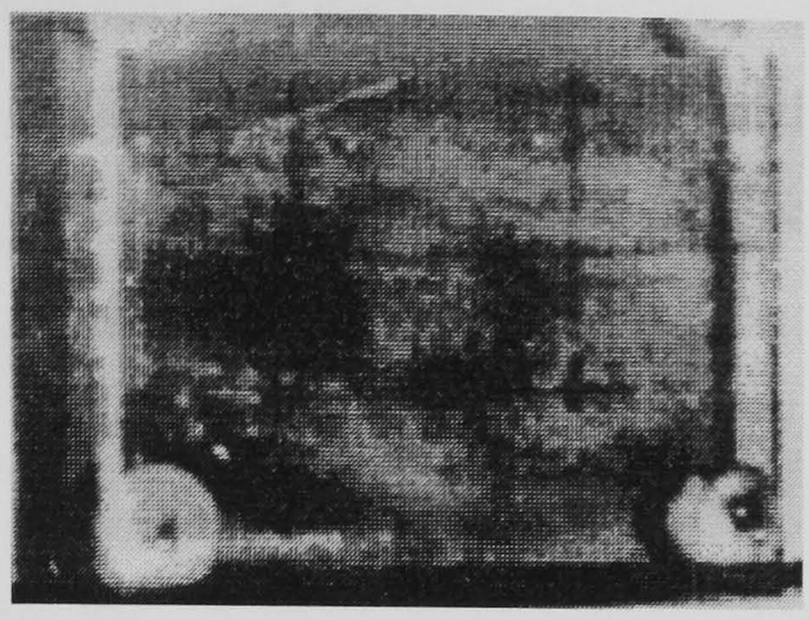

35 kN, 2 contours

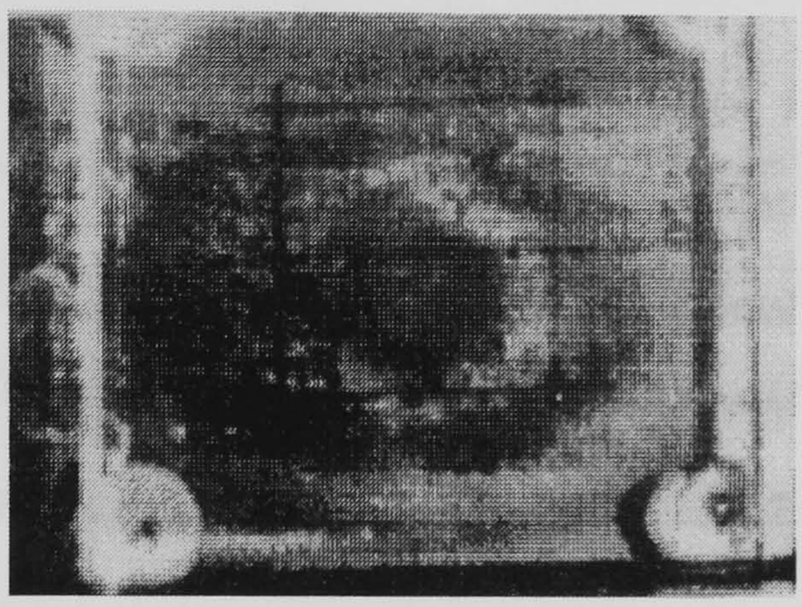

40 kN, 3 contours

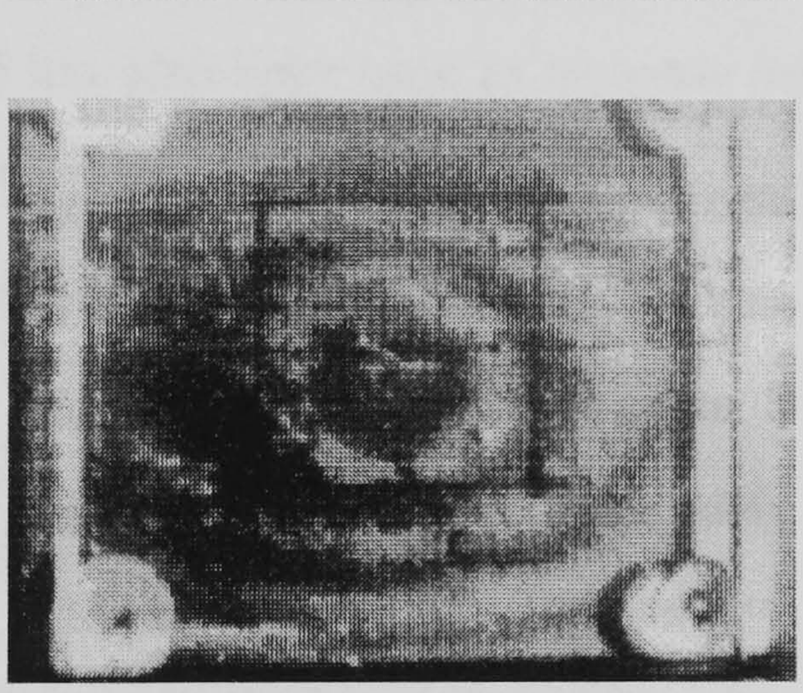

43 kN, 4 contours

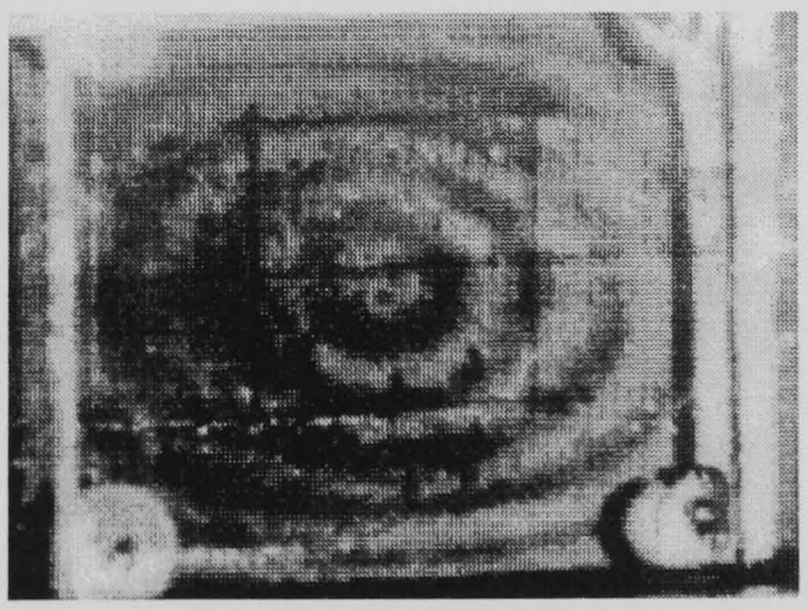

44 kN, 5 contours

Figure 5.10. *Photographs of the shadow Moiré fringes during compressive loading, for a specimen containing a 15mm square PTFE insert 5 plies deep. In this test each contour represents an out-of-plane displacement of 85μm*

5.6. Comparison with previous data

The residual strengths that we have recorded for the composite plates tested in both static tension and compression are comparable with the results from other work in terms of percentage reduction for the given impact energy [Bishop *et al*, 1984; Cairns *et al*, 1994; Prichard and Hogg, 1990]. cf. Figure 2.7.

The behaviour of the delamination under stepped loading was studied using X-radiography to determine the growth of the delamination with load. At the same time shadow Moiré fringe measurements were used to determine the extent and height of the delamination. These results followed closely the out-of-plane displacements predicted by the finite element method for various sizes of delamination [Lowe, 1994]

Shadow moiré has also been used to measure the damage growth [Greenhalgh, 1993; Cairns *et al*, 1994] and a similar mode for growth of the delamination, perpendicular to the loading direction, has been found.

5.7. Impact damage investigations

The aim of predicting strength loss due to impact damage requires first that detailed information on the types of damage that are caused by low velocity impacts is obtained. The tests that we carried out involved using a range of impact energies at a constant velocity, and on two different materials. The intention was to ensure that the level of damage chosen could be fully contained within a specimen while also containing enough damage to make a significant difference to the residual strength.

After impact (details are in section 3.3.4) the plates were cut into sections such that each impact was contained within one plate. X-ray investigation was carried out on some specimens using zinc-iodide as a penetrant, and on some specimens the deply techniques were also applied. The damage in the majority of specimens was evaluated using deply with gold-chloride as the indicator.

5.7.1. X-ray investigation of damage

The X-ray images were of a high enough resolution to indicate clearly the presence of ply and matrix cracks. The full extent of the delamination was not always as clear, because the penetrant at the edge of a delamination is a thin layer and is thus less opaque to X-rays—so contrast is low. Since the cracks extend through at least one layer (125 μm minimum) their x-ray image has a high contrast. (Unfortunately, the resolution of the original photographic images cannot be reproduced here.) An example of the result of a 7 Joule impact can be seen in Plate 5.1.

The limitation on using X-ray images to evaluate damage is similar to that for ultra-sonic C-scans - they give only two dimensional information of the damage: there is insufficient information to determine the through thickness position of the damage. However, it is possible to see on an X-ray image that there are two or more areas of delamination, and the delaminations do not obscure the ply and matrix cracks.

In the fatigue work, which is described in greater detail in chapter 8, X-rays and C-scans were taken of the same damage. This showed that the extent of the damage as revealed by the C-scans was the same as that shown by the X-ray picture, although the edge of the delamination was much clearer in the C-scan.

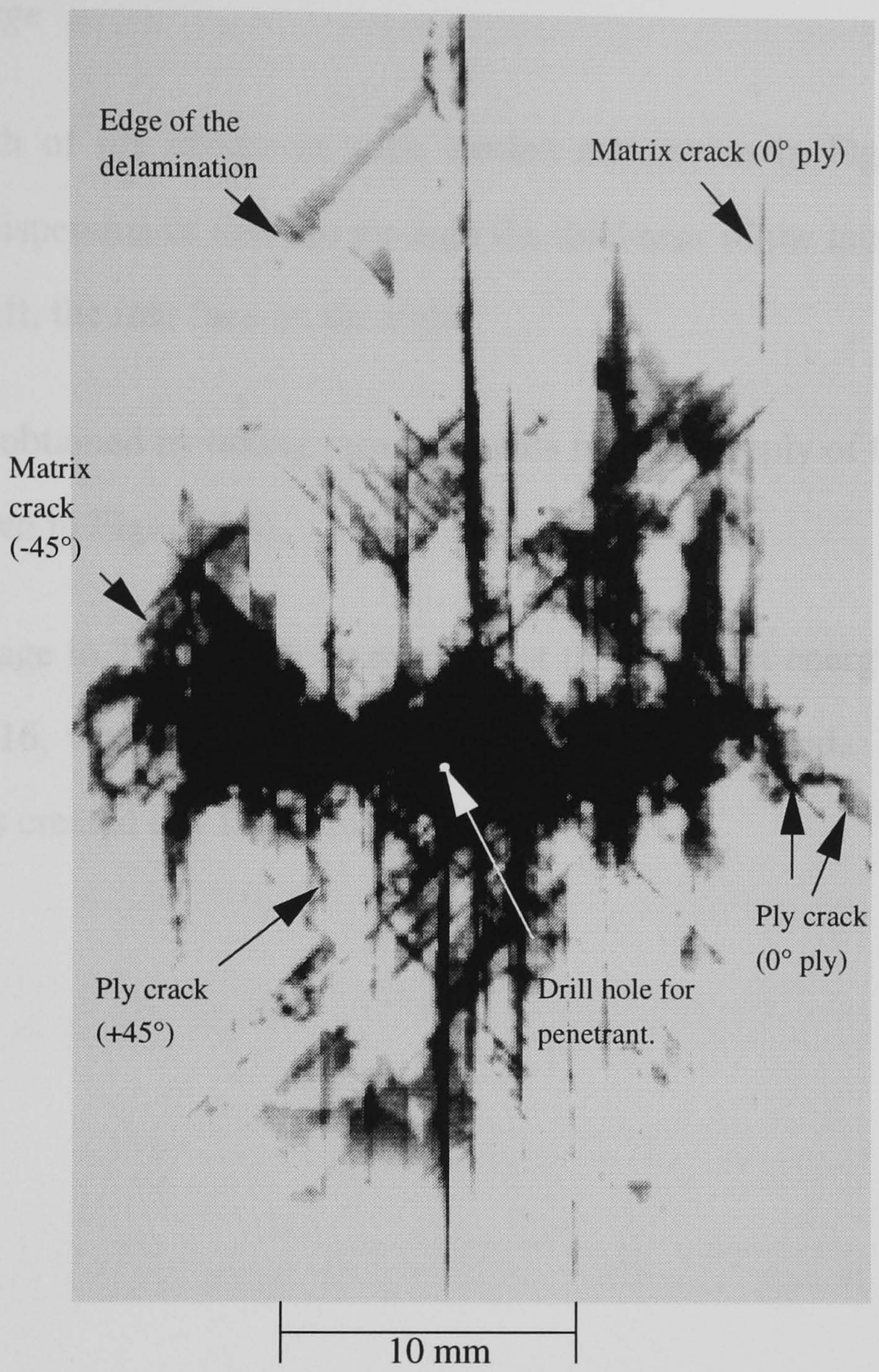

Plate 5.1. X-ray of actual damage from 7 Joule impact (zinc iodide penetrant as contrast enhancer)

5.7.2. Deply evaluation of damage

The results of the deply investigation are recorded here. In order to allow comparison of different energies of impact and different materials used in the composite the crack length and delamination areas for each lamina were measured and plotted against ply position. As far as using this information for creating artificial replicas of impact damage is concerned, it was not necessary to measure the matrix cracks.

Ply crack damage

The total length of ply cracks in each lamina are shown in Figures 5.11 to 5.16, indicating the dispersion of damage through the thickness of the laminate. The impact face is on the left, the rear face on the right.

The results are obtained by taking measurements from the deply of the specimens after impact (as shown in Figure 4.6).

The crack damage in T800/5245c is minimal at these impact energies, as can be seen from Figure 5.16, which is for the greatest impact energy used. None of the other impact energies created any fibre cracks at all.

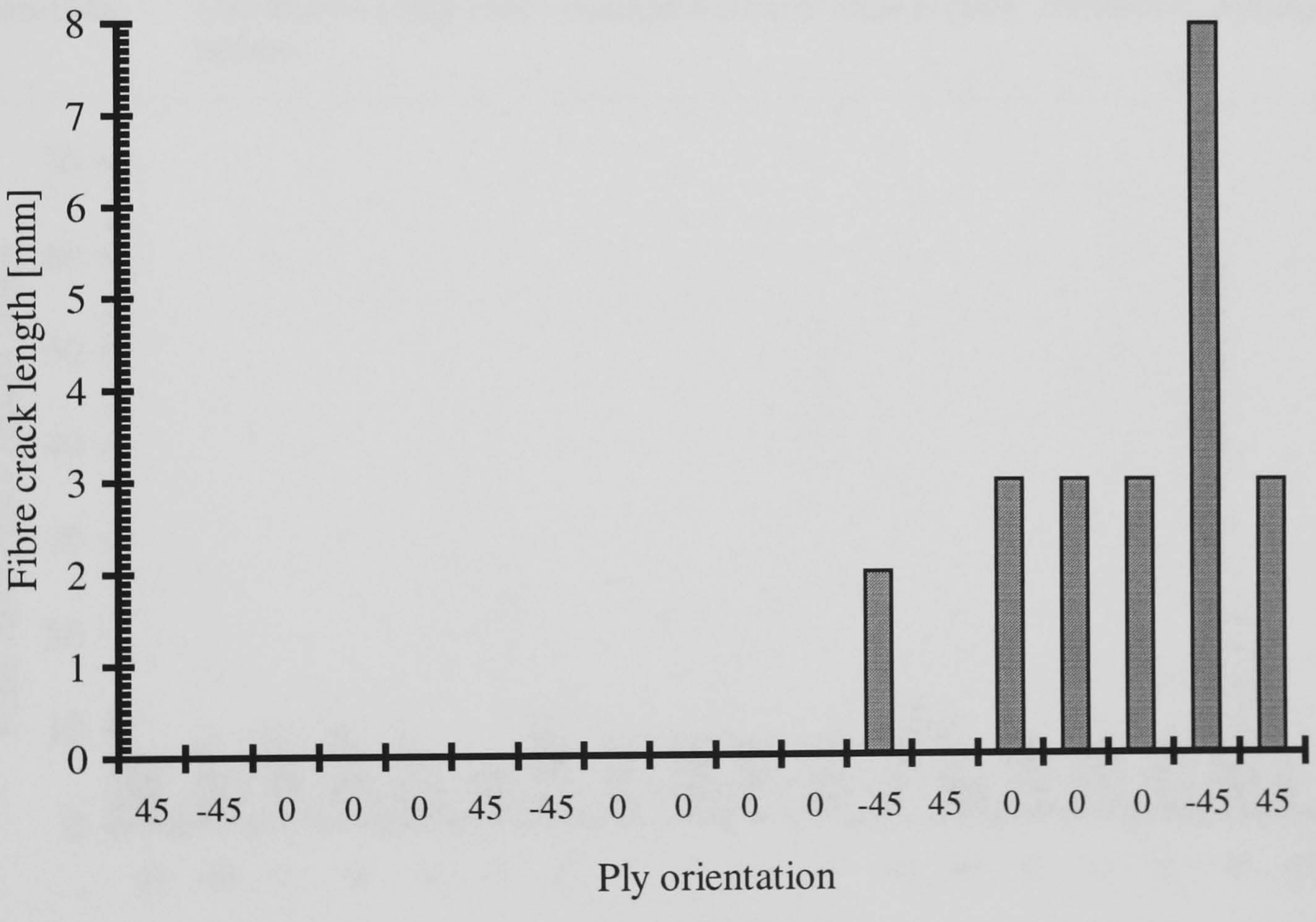

Figure 5.11. *Distribution of ply-crack damage from a 3 Joule impact, T300/913c, average values.*

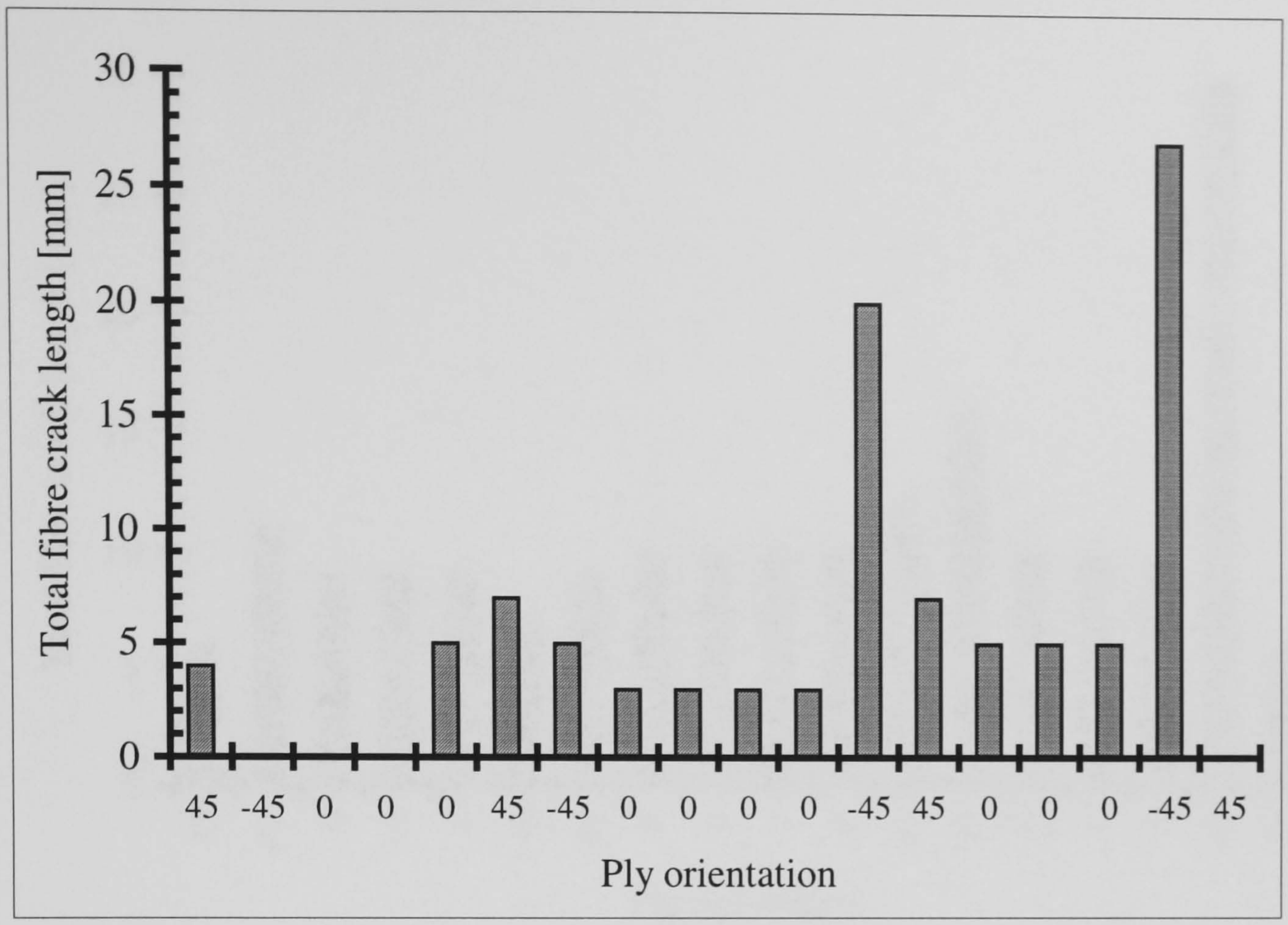

Figure 5.12. *Distribution of ply-crack damage from a 5 Joule impact, T300/913c, average values.*

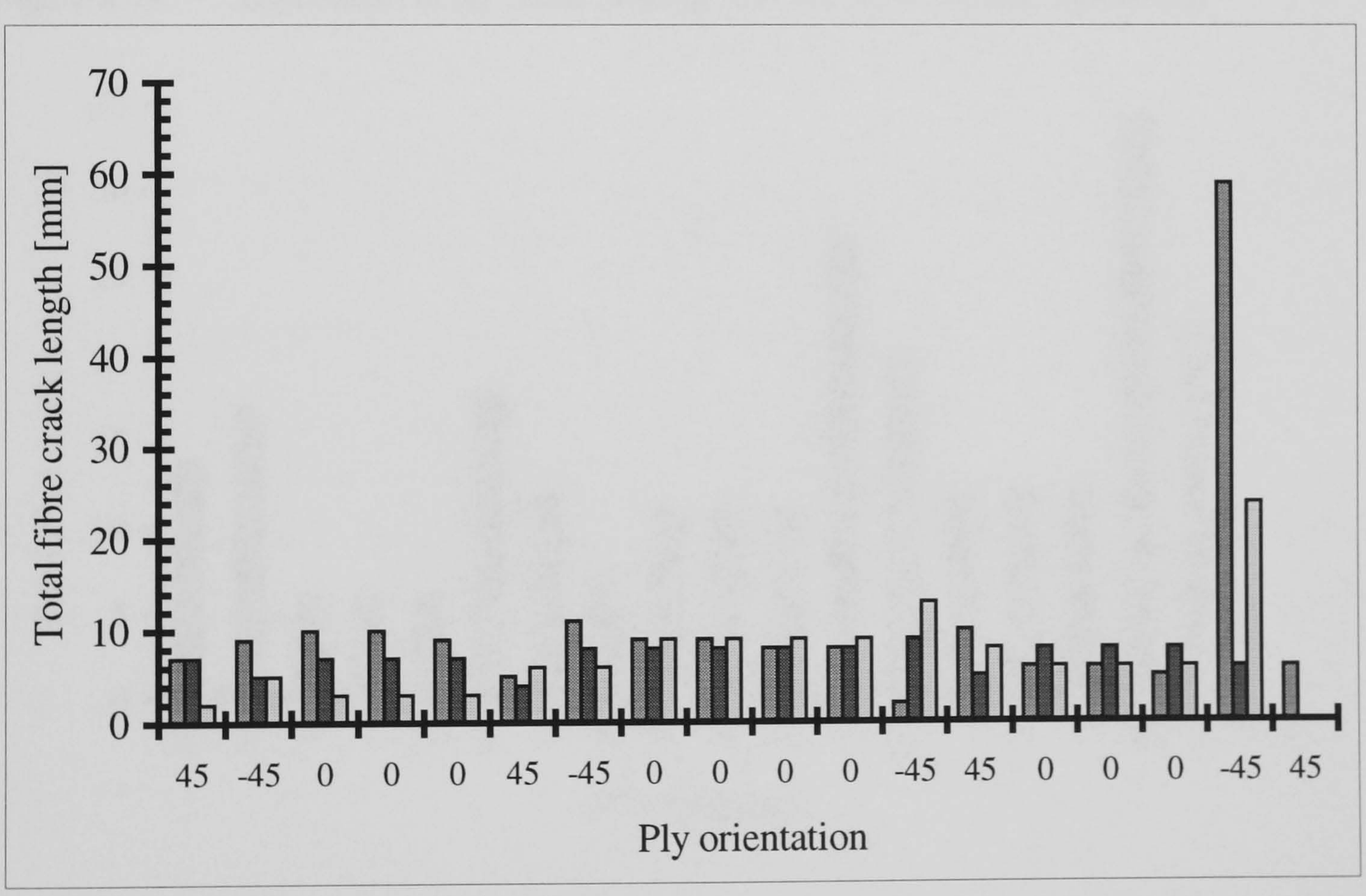

Figure 5.13. *Distribution of ply-crack damage from a 7 Joule impact, T300/913c, showing variability of damage between specimens.*

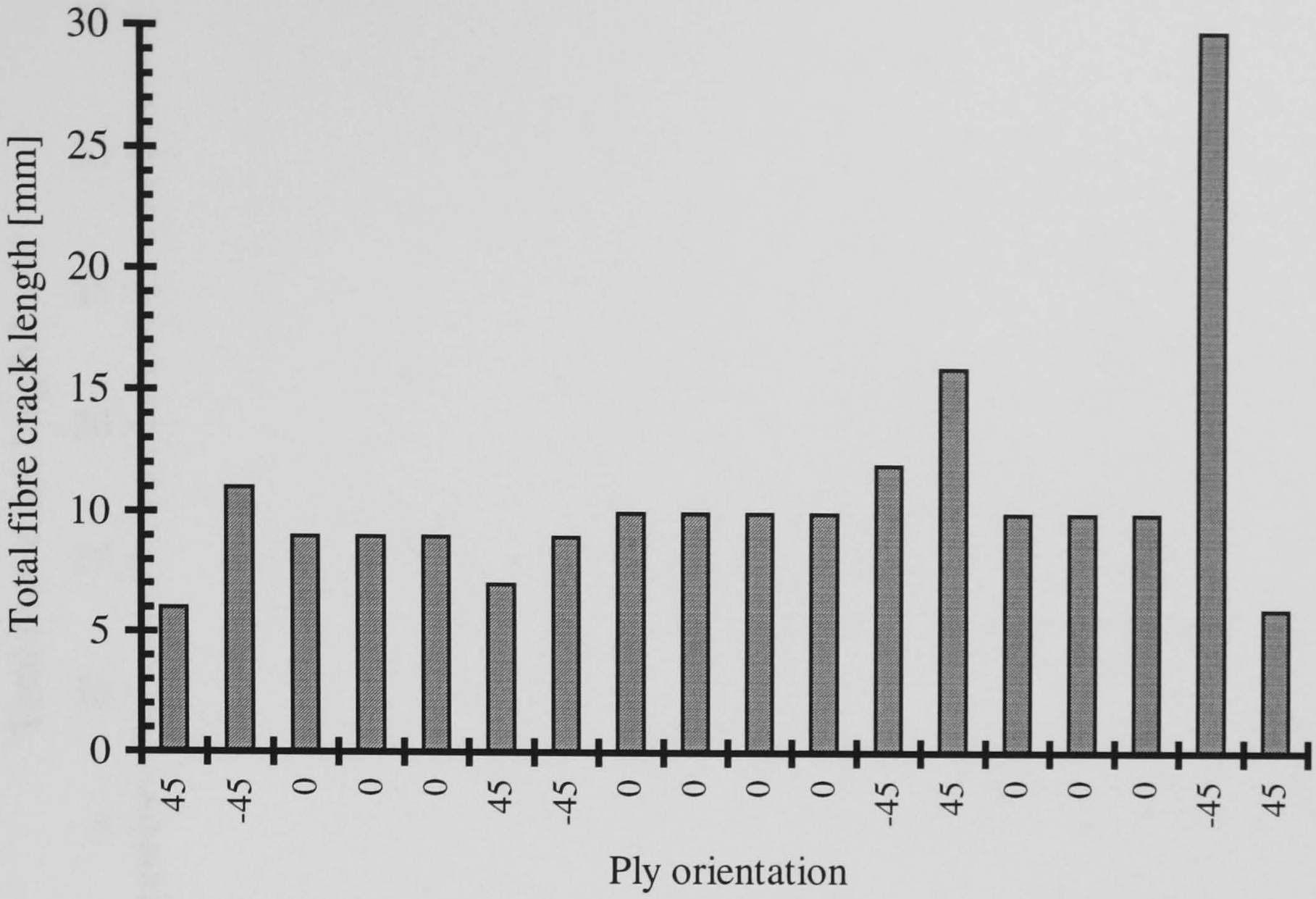

Figure 5.14. Distribution of ply-crack damage from a 9 Joule impact, T300/913c

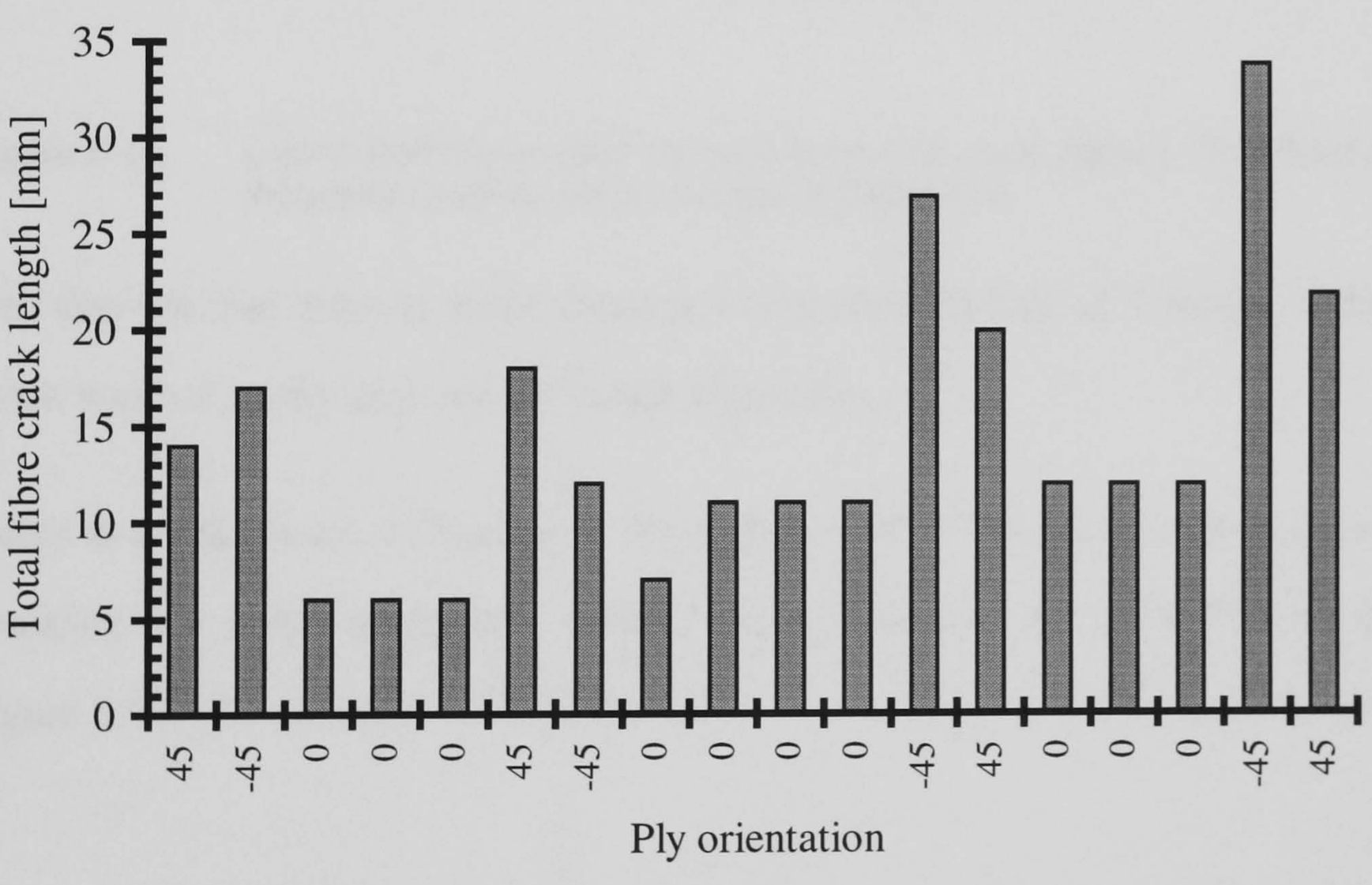

Figure 5.15. Distribution of ply-crack damage from a 12 Joule impact, T300/913c

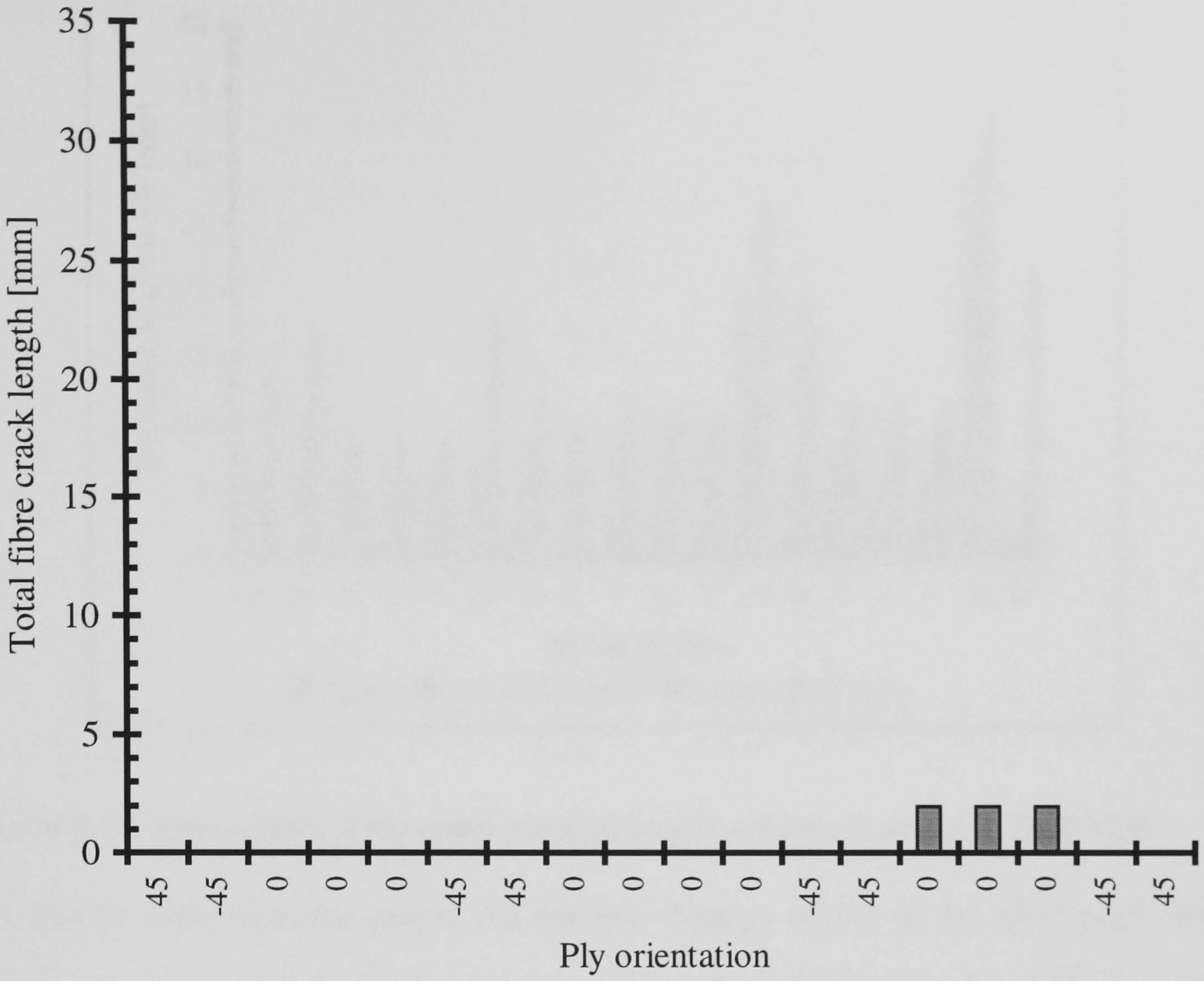

Figure 5.16. Distribution of ply-crack damage from a 12 Joule impact, T800/5245c, using the same scale as similar impact in T300/913c

One can see that there is some damage to the front surface at 7 Joules, although the crack was not easily detected by visual inspection.

There is a significant difference in the response of the two materials in terms of ply-cracking. A graph comparing various impact energies for T300/913c is shown in Figure 5.17.

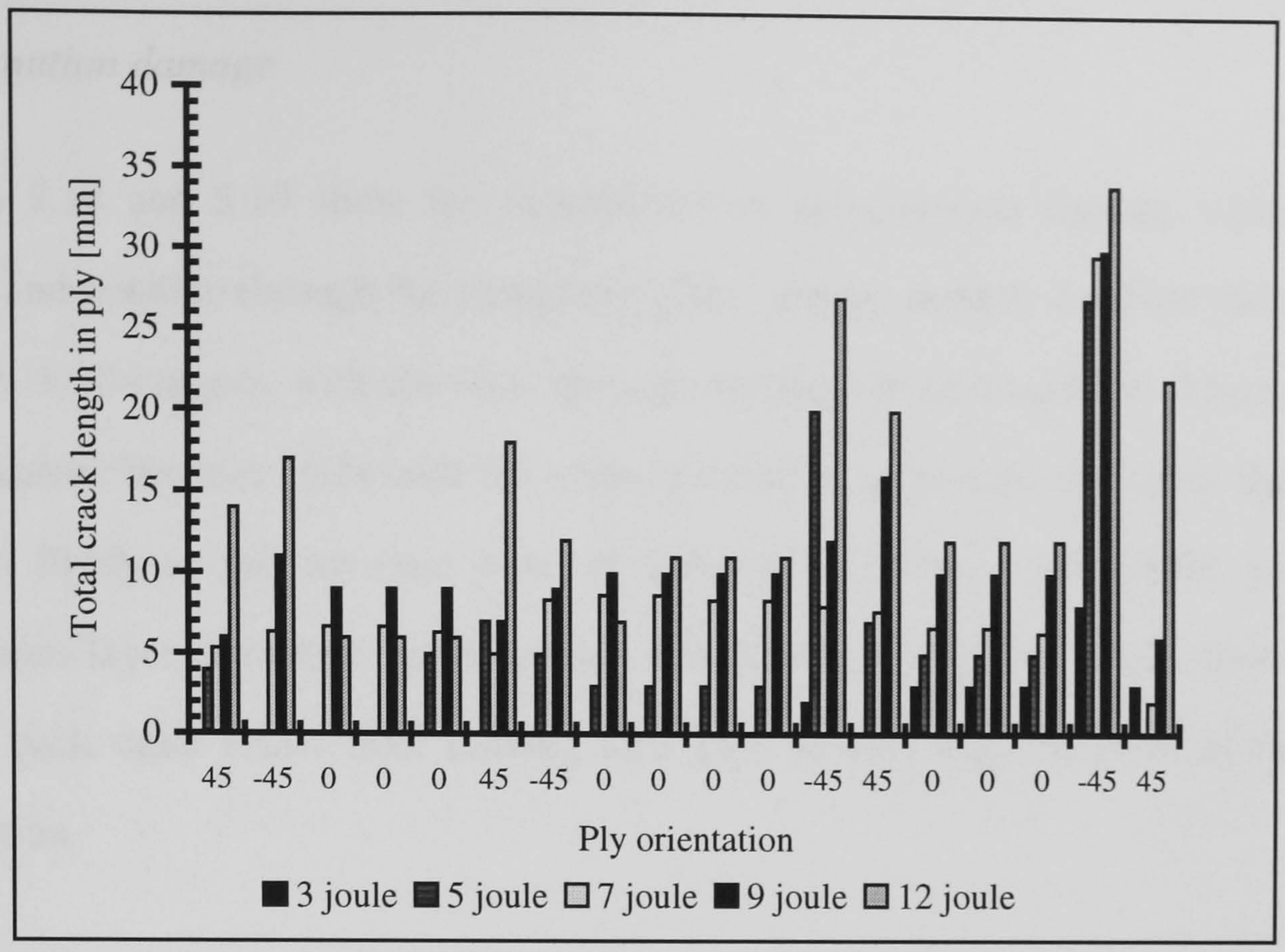

*Figure 5.17. Comparison of **ply-crack** damage for different impact energies. T300/913c*

As can be seen from the graph, the greatest damage occurs in the ±45° plies, with greater damage towards the rear surface. The crack damage in the ±45° plies was generally made up of many short cracks connected by matrix cracks. No attempt has been made to model the cracking of the ±45° plies with artificial damage because of this distribution of the damage. Additionally, the majority of the load is carried by the 0° plies (more than 90%), so damage in the ±45° fibres is not expected to have a large effect on the strength of the specimens.

The values recorded in the graph do not include the matrix cracks as these are possibly an artefact of the deply method, but were recorded on the deply maps [Clarke *et al*, 1992b].

The T800/5245c contained very little fibre breakage after impact. In fact there was no damage except at 12 Joule—a two mm crack in the 0°plies closest to the rear surface.

Delamination damage

Figures 5.18 and 5.19 show the distribution of delamination damage with impact energy and position through the composite plate. Again, there is a similar distribution through the thickness, with the most damage towards the rear surface. There is little delamination between plies with the same orientation, as is expected since the matrix is most likely to fail between plies of differing stiffness. Also there will be a continuous layer of matrix between plies at angles to each other, as the fibres lie on top of each other rather than moving into gaps as they can in plies of the same orientation.

A comparison of the two materials reveals that the T300/913c has, in terms of total delamination area, a greater resistance to impact damage, (the same is not true in terms of fibre breakage) but a poorer performance in terms of compression after impact. The greater fibre damage in T300 may contribute to its relatively poor performance, in comparison to T800, for CAI, as the cracks provide additional initiation points for delamination. The distribution of damage through the thickness was also different, in that the greatest damage in the T300/913c is closest to the rear surface, whereas the T800/5245c has a peak of damage in the interface between the rear 0° plies and the ±45° next to the central plies.

The T800/5245c has a much more even distribution of damage through the thickness, and the threshold for delamination damage is lower than the T300/913c.

As would be expected, the effect of increasing the impact energy is to increase the amount of damage. This means that for greater energy impacts the delamination is larger with a consequent loss of out-of-plane support for the main sub-laminate, and thus a greater reduction in residual compressive strength would be expected.

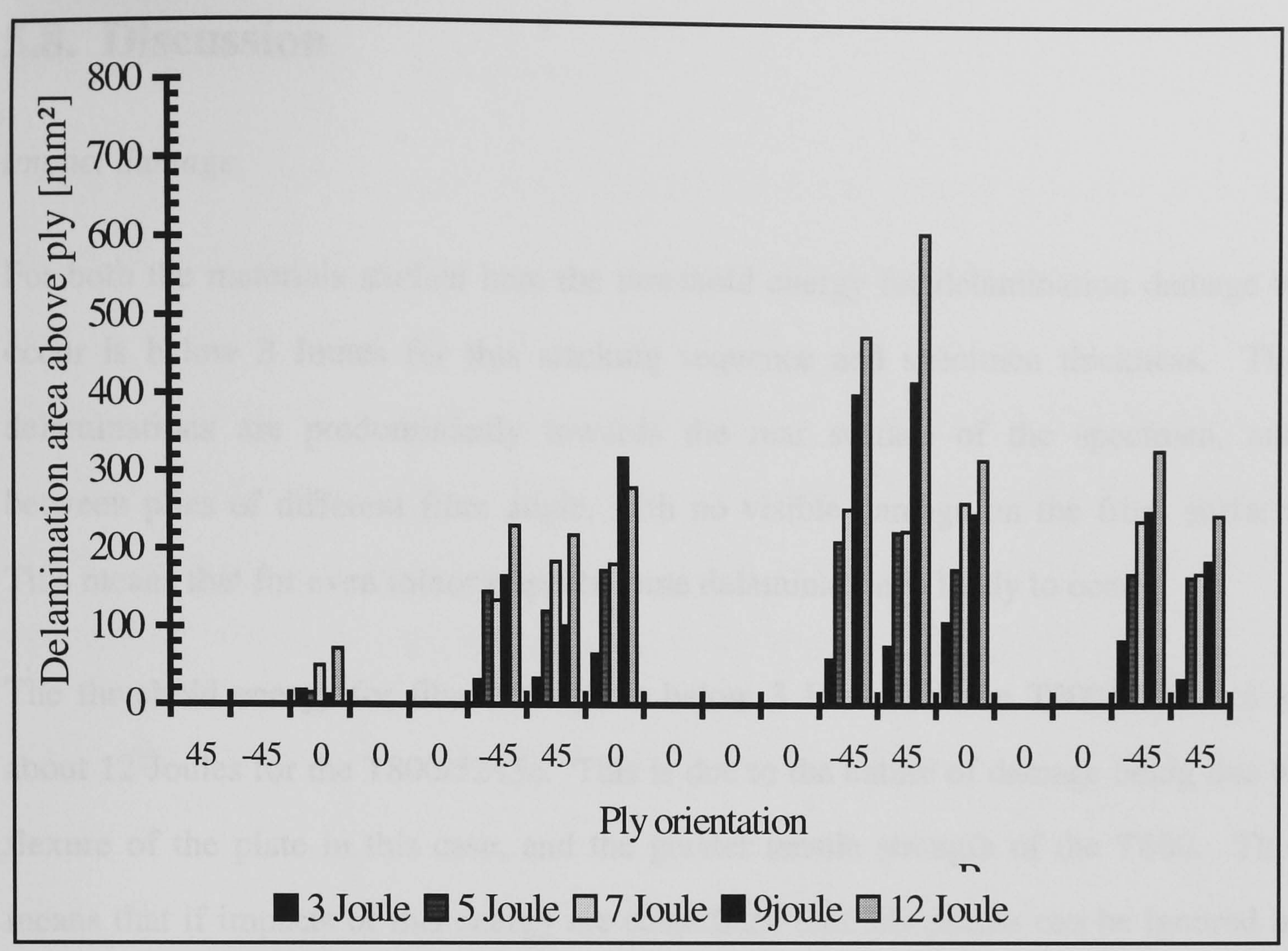

Figure 5.18 Delamination damage to T300/913c with varying impact energy.

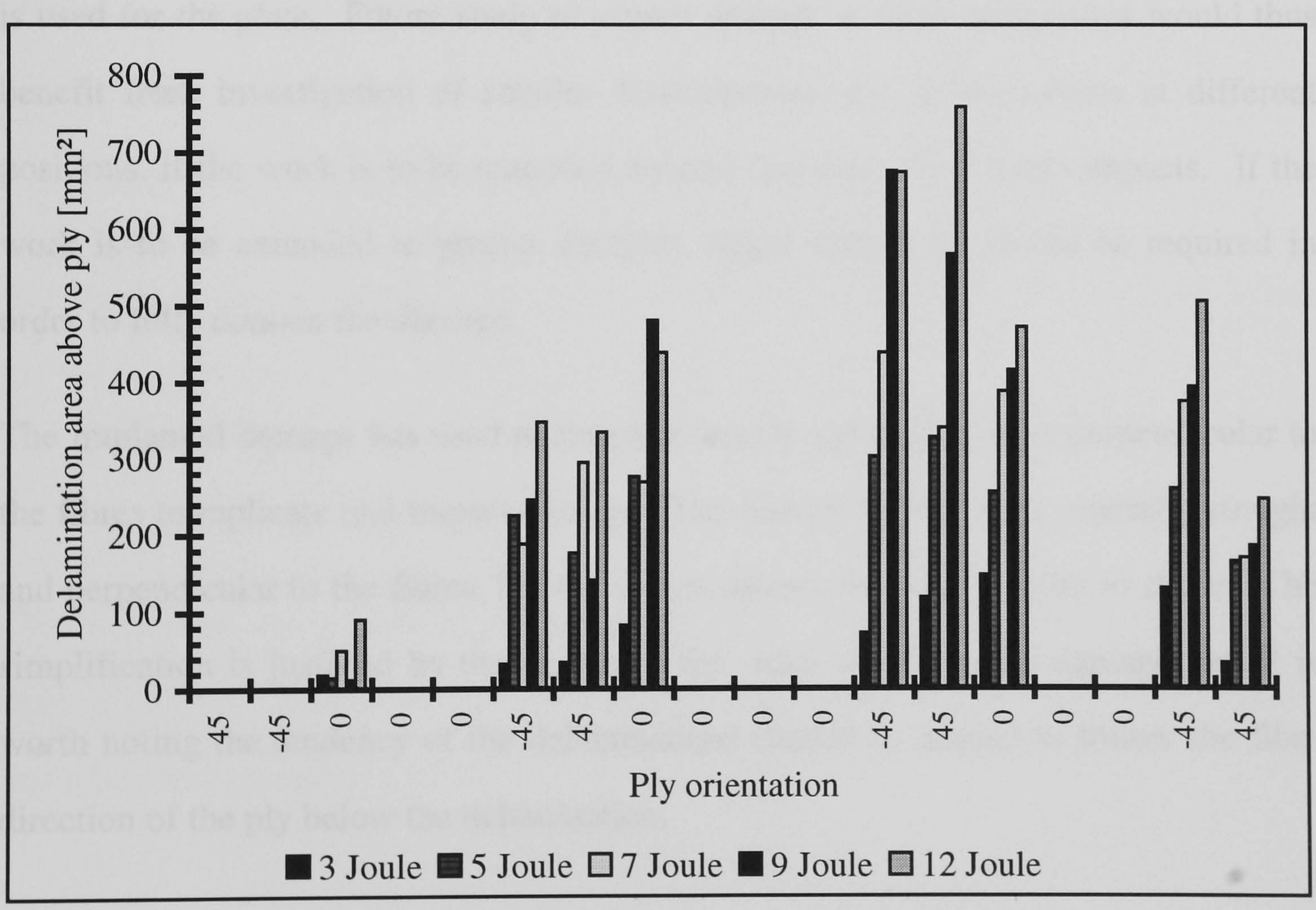

Figure 5.19 Delamination damage to 18 ply T800/9245c with varying impact energy.

5.8. Discussion

Impact damage

For both the materials studied here the threshold energy for delamination damage to occur is below 3 Joules for this stacking sequence and specimen thickness. The delaminations are predominantly towards the rear surface of the specimen, and between plies of different fibre angle, with no visible damage on the front surface. This means that for even minor impacts some delamination is likely to occur.

The threshold energy for fibre damage is below 3 Joules for the T300/913c and at about 12 Joules for the T800/5245c. This is due to the nature of damage being due to flexure of the plate in this case, and the greater tensile strength of the T800. This means that if impacts of this energy are considered then ply cracks can be ignored in T800/5245c if the same stacking sequence is used, and the same thickness or thicker is used for the plate. Future study of impact damage in these composites would thus benefit from investigation of smaller delaminations and delaminations at different positions, if the work is to be extended beyond that done for 7 Joule impacts. If the work is to be extended to greater energies, larger specimens would be required in order to fully contain the damage.

The implanted damage has used rectangular inserts and straight cuts perpendicular to the fibres to replicate real impact damage. The real ply cracks were generally straight and perpendicular to the fibres, but the delaminations were not regular in shape. The simplification is justified by the results of the tests on implanted damage, but it is worth noting the tendency of the delaminations caused by impact to follow the fibre direction of the ply below the delamination.

Strength reduction due to impact damage

As has already been stated previously, the residual tensile strength is related to the net section of unbroken 0° fibres. Here a simplified model of delamination damage is used to show the effect on compressive strength. The reduction in compressive strength is assumed to result from superimposed compression and bending as delaminated plies buckle out of plane, hence unbalancing the remaining sub-laminate. If the delamination is assumed to extend across a proportion r of the width of the laminate the following simplified treatment of the problem is possible. .

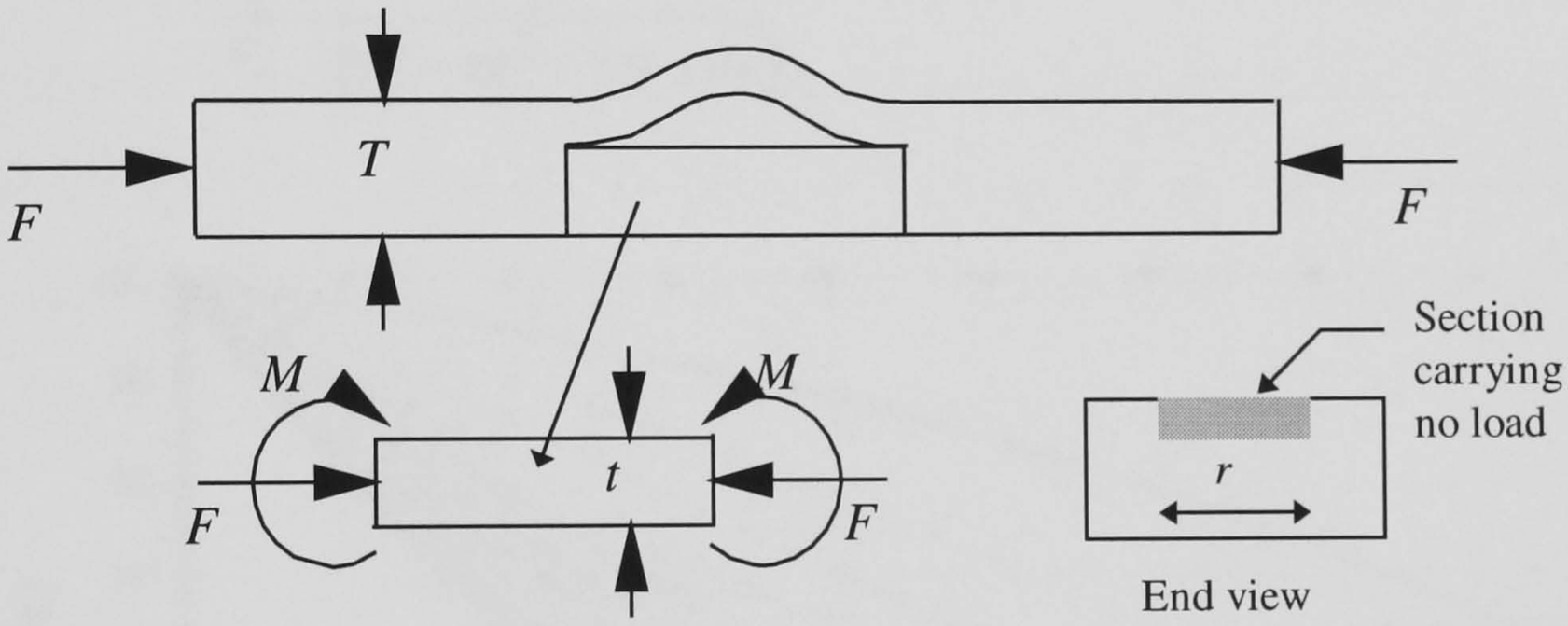

Figure 5.20 Forces on the main sub-laminate in a specimen with a delamination

The delamination is initially analysed using the isotropic strip in Figure 5.20. When the strip is undamaged the stress (assuming unit width) is

$$\sigma = \frac{F_u}{T} \tag{1}$$

With damage, the portion above the delamination has buckled and is supposed to carry little load. The remainder of the strip is carrying an axial compressive load F_d and a bending moment M where

$$M = \frac{F_d r(T - t)}{2} \tag{2}$$

T is the thickness of the undelaminated strip and t the part thickness of the strip below

the delamination, and r is the fraction of the width that is delaminated. This calculation assumes that the undelaminated part of the strip is sufficiently flexible so as not to resist bending of the delaminated part. Simple bending theory can be used to calculate the maximum compressive stress in the part of the strip below the delamination:

$$\sigma = \frac{rF_d}{t} + \frac{(1-r)F_d}{T} + \frac{3rF_d(T-t)}{t^2} \tag{3}$$

combining equations (1) and (3) and using $t/T = p$, gives a strength reduction of:

$$\frac{F_d}{F_u} - \frac{p^2}{\left(p^2 - rp^2 - 2rp + 3r\right)} \tag{4}$$

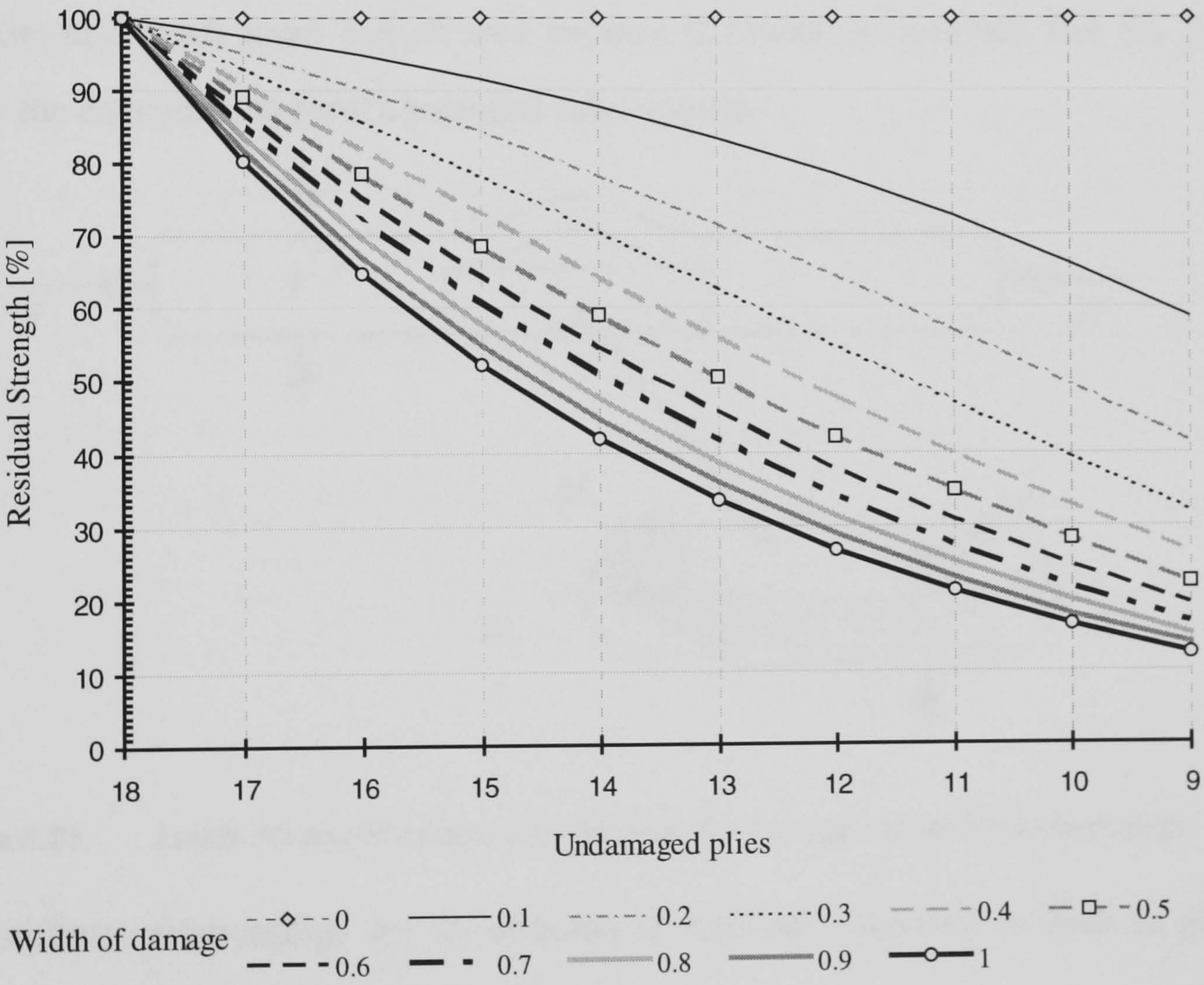

Figure 5.22 *Residual strength predictions from model with loss of load carrying above delamination.*

For the case of the artificially damaged $(\pm 45°, 0°_3, \pm 45°, 0°_2)_s$ 18 ply laminate with one ply crack and a delamination across half the width below the outermost 0° plies, (i.e. a delamination 5 plies from the surface) $t / T = 13 / 18$ giving a predicted residual strength of 51% compared to the experimental value of 77%. (T800).

The model could also be applied to the specimen with a double delamination—we are assuming that the delaminated plies do not resist bending. In this case the experimental results are 76% (T800) and 50% (T300)

The composite is not, of course, isotropic, but the above analysis can be extended in a simpler form to a layered orthotropic strip, as shown in Figure 5.21. In this case the damage is assumed to extend across the full width of the specimen. The calculations now become much more complicated because it cannot be assumed that the plies below the delamination form a balanced sub-laminate.

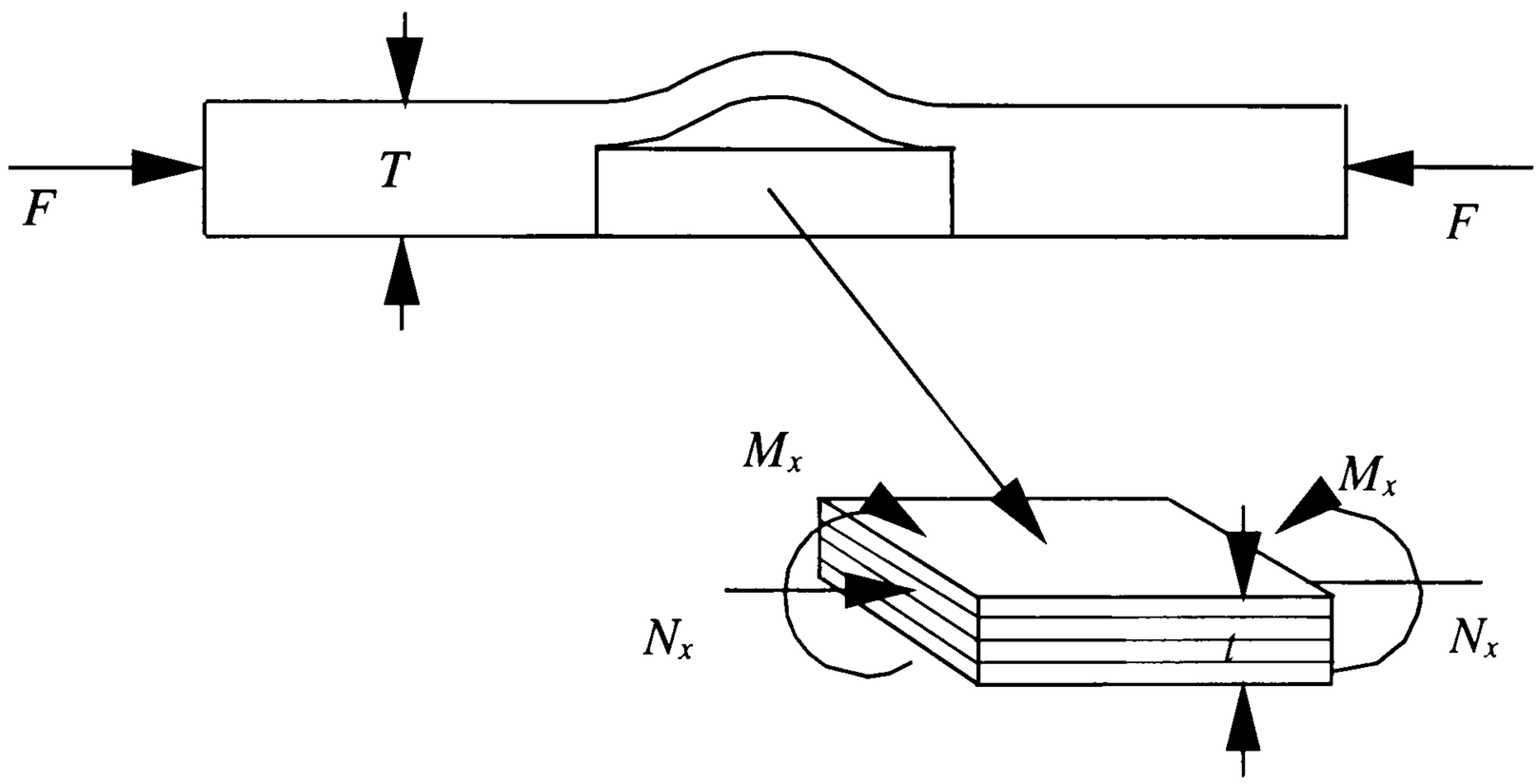

Figure 5.21. Loads on an orthotropic sub-laminate for through-the-width delamination

The stiffness relationships for an orthotropic laminate subjected to both in plane forces and moments may be expressed by

$$\begin{bmatrix} N_x \\ N_y \\ N_{xy} \\ \hline M_x \\ M_y \\ M_{xy} \end{bmatrix} = \left[\begin{array}{ccc|ccc} A_{11} & A_{12} & A_{16} & B_{11} & B_{12} & B_{16} \\ A_{12} & A_{22} & A_{26} & B_{12} & B_{22} & B_{26} \\ A_{16} & A_{26} & A_{66} & B_{16} & B_{26} & B_{66} \\ \hline B_{11} & B_{12} & B_{16} & D_{11} & D_{12} & D_{16} \\ B_{12} & B_{22} & B_{26} & D_{12} & D_{22} & D_{26} \\ B_{16} & B_{26} & B_{66} & D_{16} & D_{26} & D_{66} \end{array}\right] \begin{bmatrix} \varepsilon_x^o \\ \varepsilon_y^o \\ \gamma_{xy}^o \\ \hline \kappa_x \\ \kappa_y \\ \kappa_{xy} \end{bmatrix} \tag{4}$$

where N_x, N_y and N_{xy} are in-plane forces per unit length, M_x, M_y and M_{xy} are bending moments per unit length, A_{ij}, B_{ij} and D_{ij} are the extensional, coupling and bending stiffnesses, calculated in the normal way, ε_x^o, ε_y^o and γ_{xy}^o are the mid-plane strains and κ_x, κ_y and κ_{xy} are the curvatures. For the case of the sub-laminate below the delamination in Figure 5.21 it is assumed that $N_y = N_{xy} = 0$, $M_y = M_{xy} = 0$ and

$$M_x = \frac{N_x(T-t)}{2} \tag{5}$$

The mid-surface strains and curvatures, which can be found by solving Equation 4, may then be used to calculate ply strains and hence stresses. Maximum compressive stresses in the fibre direction of the 0° plies may then be found and compared with those for the undamaged case. Following this procedure for the artificially damaged T300/913C laminate with one ply crack and two delaminations (i.e. assume that 5 plies are damaged) gives a predicted strength reduction of 67% compared to the isotropic case of 64%. The predicted strength reduction is now slightly higher than that assuming isotropic properties.

References

Bishop S.M., Howard G.D. and Wood C.J.

"The Notch Sensitivity and Impact Performance of [0,-45,+45] Carbon Fibre Reinforced PEEK.".

RAE Technical Report TR84066 June **1984** pp. 1-15.

Cairns D.S., Minguet P.J. and Abdallah M.G.

"Theoretical and Experimental Response of Composite Laminates with Delaminations Loaded in Compression."

Composite Structures Vol. 27(4) **1994** pp.431-7.

Clarke M.P. and Pavier M.J.

"Artificial Damage techniques for Low Velocity Impact in Carbon-Fibre Composites."

Composite Structures Vol. 25(3) July **1993** pp.113-20.

Clarke M.P., Pavier M.J. and Kemp M.

"Modelling of Artificial Damage in Carbon-Fibre Composites."

Proceedings ICCM Vol. 9 July **1993** pp. 250-7.

Greenhalgh, E.S.

"On defect growth and failure in carbon-fibre composite structures."

RAE Technical Report TR89045 September **1989** pp. 1-17.

Lowe A.T.

"The Effect of Single Embedded Delaminations on the Compressive Strength of CFRP."

Undergraduate Project Report 94/2 Bristol University June **1994** pp.1-45.

Prichard J.C. and Hogg P.J.

"The Role of Impact Damage in Post Impact Compression Testing."

Composites Vol. 21 **1990** pp503-511

CHAPTER 6.

DEVELOPMENT OF FINITE ELEMENT TECHNIQUES FOR ANALYSIS OF POST IMPACT STRENGTH.

6.1. Introduction

Finite element analysis is a tool that has become increasingly useful in recent years, because of the rapidly increasing availability of computing power. There are many problems that are not easy to solve using classical mathematical analysis. For many of these the technique of breaking the problem up into many simpler parts can provide a way of reaching an answer. In structural mechanics this means defining the properties of a material for a small geometrically simple shape (the finite element) and then combining many of these to build the structure. The computational power required to solve the resulting set of simultaneous equations is related to the number of degrees of freedom in the problem, (between a second and a third power relationship, depending on the geometry of the problem) and thus to the number of finite elements. The problem considered here, the post buckling behaviour of an anisotropic material, is sufficiently complicated to make direct mathematical modelling to calculate stresses and strains throughout the model for a given loading impractical, so numerical analysis is used.

This chapter describes the formulation of the specialised finite element used in the investigations described in chapter 7 and discusses the reasons for the use of such an element formulation.

If the finite element analysis of impacts is to produce useful results it is essential that the methods used model reality as accurately as possible, and where simplifications are made these are accounted for when evaluating the results of analysis.

As has already been shown in the experimental sections of this work, the result of low-velocity impacts on carbon fibre composites is the introduction of matrix cracks, fibre cracks and delaminations between plies. These are the features that the model needs to replicate. The first stage in the finite element analysis is to predict the likely behaviour of the damaged zone so that a suitable model can be created. The model must not be constrained from behaving as the real specimen does under load, for example, out of plane displacements must be allowed in the damage zone, but not in the anti-buckling guide area.

Low velocity damage reduces the compressive strength of the structure because the mode of failure, buckling of the delamination, is sensitive to the loss of bending stiffness of the delaminated laminate. Failure, however, is not controlled by the buckling load of the delamination, there is some post-buckling strength. To model this using the finite element method requires that the regions both above and below the delamination are meshed, and that the finite element model allows large out of plane displacements of the elements.

6.2

6.1.1. Previous work

Initial finite element modelling of damage in carbon fibre reinforced plastics was limited to through-thickness delaminations, as shown in Figure 6.1, since it is possible to approximate this geometry to a two dimensional analysis [Kutlu & Chang, 1992; Whitcomb, 1981,1982,1986].

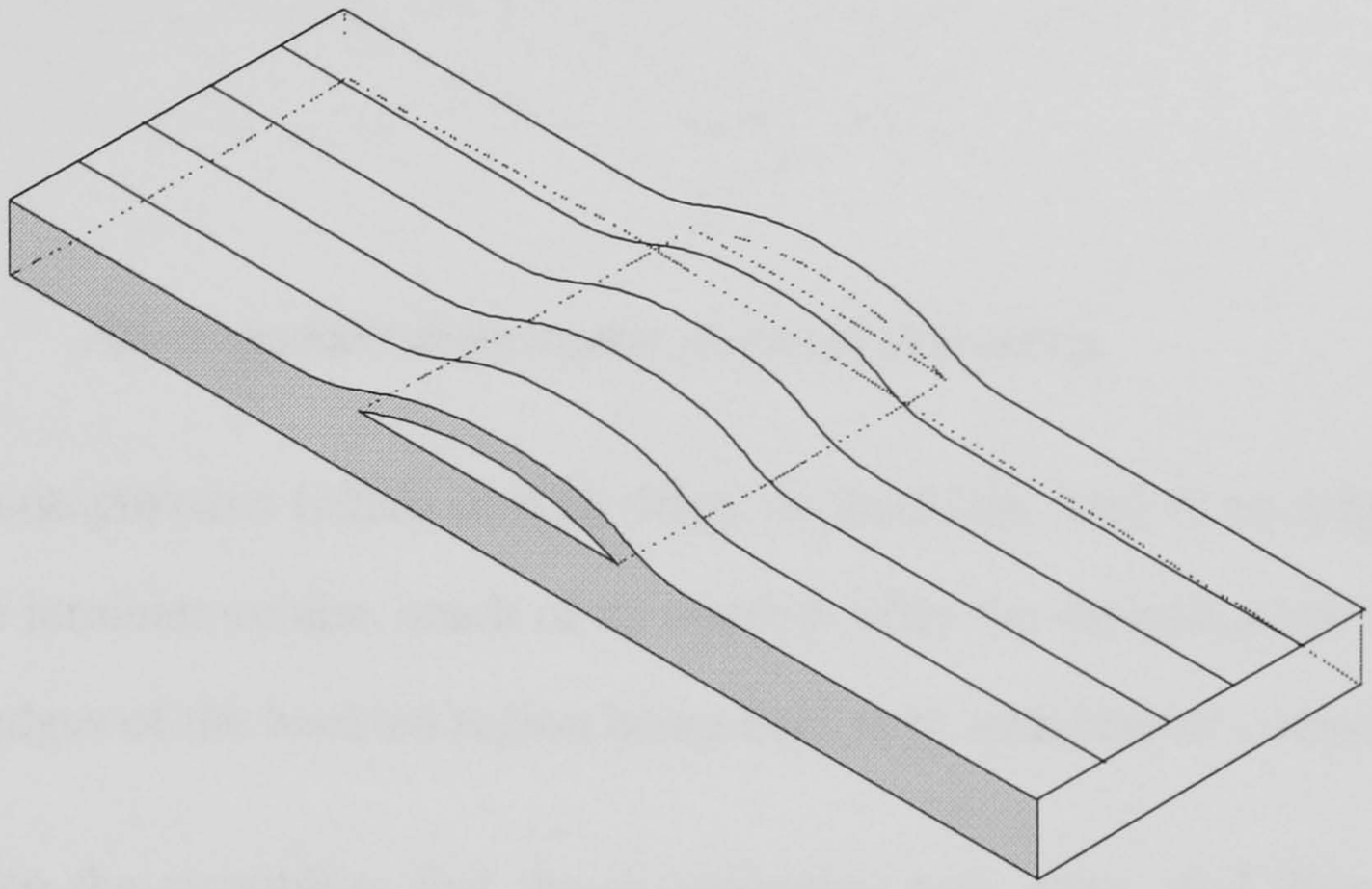

Figure 6.1. Through-the-width delamination—the shaded area can be analysed using two dimensional elements.

The failure load in the two-dimensional case can be estimated fairly accurately as the buckling load can be predicted easily and there is little post-buckling strength. The buckle is unstable, and therefore the buckling load is also the failure load[1]. In addition, delamination growth can be predicted using a strain energy release criterion, as the delamination can only grow at the two ends (which are usually equivalent due to symmetry), so the crack growth can be modelled simply in the finite element mesh.

More recent work [Whitcomb, 1989, 1992] has extended the investigation to embedded delaminations, as in Figure 6.2. Here finite element methods have been used exclusively because of the requirement for a full three-dimensional analysis.

---

[1] In this case the buckling load is that of the strongest sublaminate, not the few plies above the delamination, as shown by Kutlu and Chang, [1992].

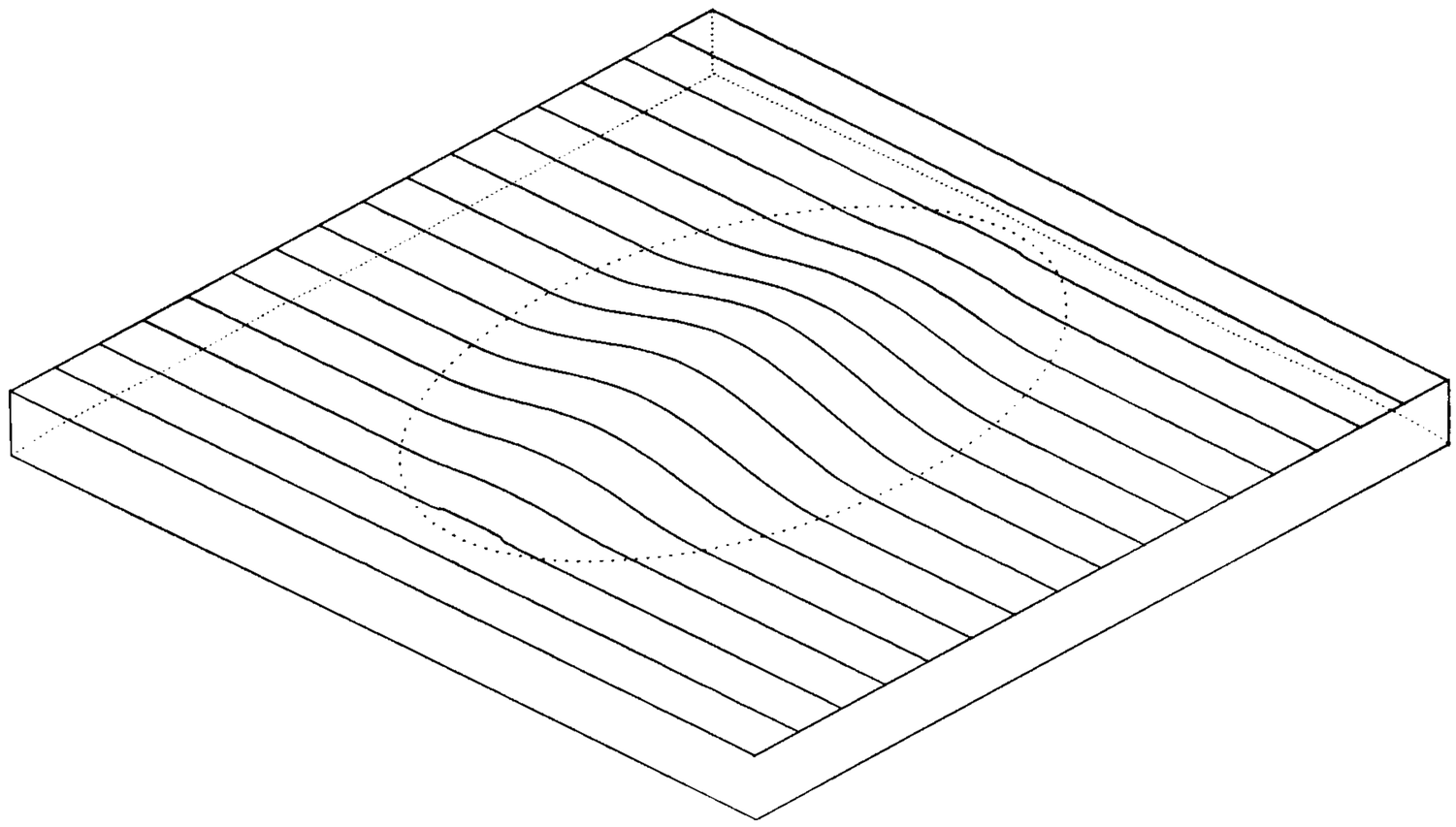

Figure 6.2. An embedded delamination, shown post-buckling.

Predicting compressive failure directly from the buckling load is no longer possible because the laminate retains much of its strength after the delamination has buckled, due to the edges of the buckled region being built in to undamaged composite.

There is also the possibility that the delamination may grow, and there have been some analyses of buckling delaminations that predict delamination growth [Pavier and Chester, 1990]. Finite element analysis can be used to predict failure if a failure criterion is introduced, for example based on degradation of properties of delaminated plies [Kutlu & Chang, 1992]. When using the method to predict delamination growth there is now the added difficulty that the point of initiation of growth cannot be determined beforehand and must be calculated by some means (for example calculating the strain energy release rate for all possible initiation points).

The geometry of the problem now precludes the use of two-dimensional analysis. The problem has been tackled using solid elements [Whitcomb, 1989; Jones *et al.* 1984], but the main difficult here is containing the size of the problem while using elements with reasonable aspect ratio. Typical composite structures constructed using laminates have a large size to thickness ratio, so if the ratio of solid element in-plane size to thickness is to be kept low a large number of elements will be required.

The problem is exacerbated when studying delaminations as the area above the delamination has a smaller thickness still, requiring smaller elements. This adds to the difficulty of setting up the model, as matching the delaminated ply to the rest of the model requires either consistent element size throughout the model (precluded due to computation time for a large problem), mesh transitioning at the interface (time consuming for any but the simplest geometry of delamination) or complicated constraint relationships (those these can be automated).

6.1.2. Alternative approach with plate elements

The problem of excessive computational time for analysis of embedded delaminations has been addressed by using plate elements [Noor and Mathers, 1977; Chaudhuri and Seide, 1987]. The work by Pavier and Clarke [1996], for example, reduces a solid element problem with 2085 nodes [Whitcomb, 1989] to a plate element model with 451 nodes. Although the aspect ratio is no longer an issue, there is some loss of accuracy. The obstacle now is in connecting the plates used for the delamination and the rest of the model. Figure 6.3 shows a typical cross section at the edge of a delamination, modelled using plate elements.

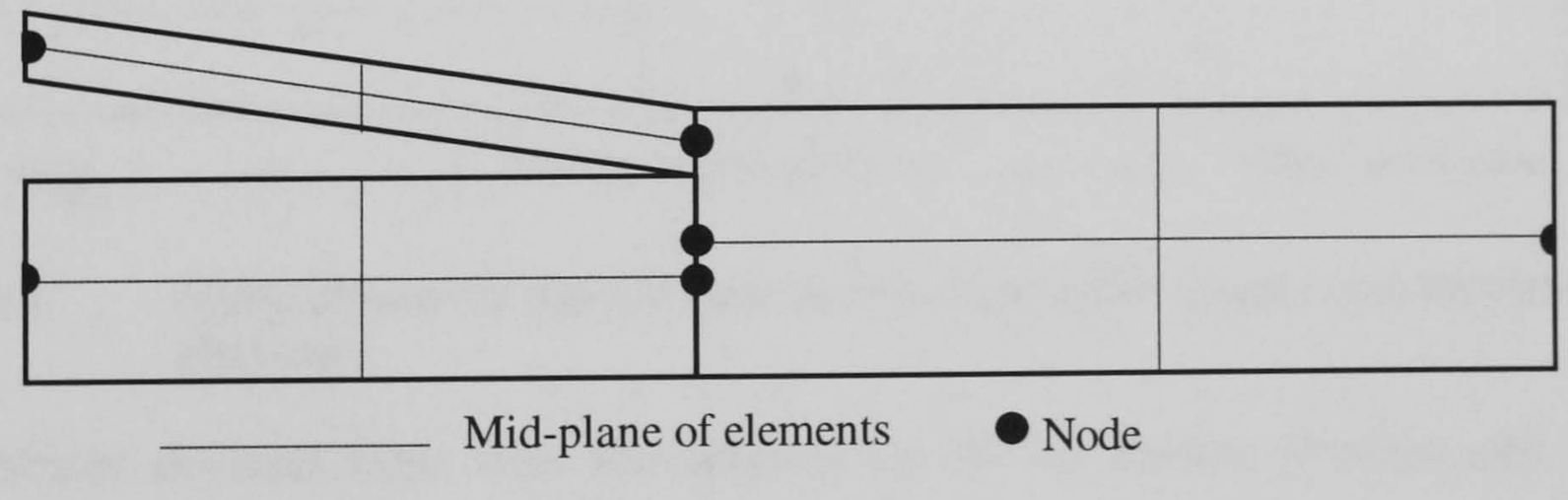

Figure 6.3. Cross section of a delamination modelled using standard plate elements.

Plate elements have degrees of freedom for the displacements and rotations of the mid-plane of the element. This means that to use plate elements as indicated in

Figure 6.3 requires them to be constrained so that the plane sections match at the junction of the plates—where the three nodes meet at the edge of the delamination. This needs constraint equations to be defined, including the in-plane displacements and rotations of the nodes at the delamination tip, taking into account the vertical offset of the nodes.

6.2. Description of the new element

The solution provided by this new element is to have degrees of freedom that represent displacements in a plane **parallel** to the mid-plane, but offset by an arbitrary distance. This allows plate elements with different thicknesses to be connected together without the need of additional constraint relationships, as shown in Figure 6.4. In addition, the initiation of buckling is handled more easily by the provision for small initial out-of-plane displacements in the element's formulation. The plate allows for layered composite properties.

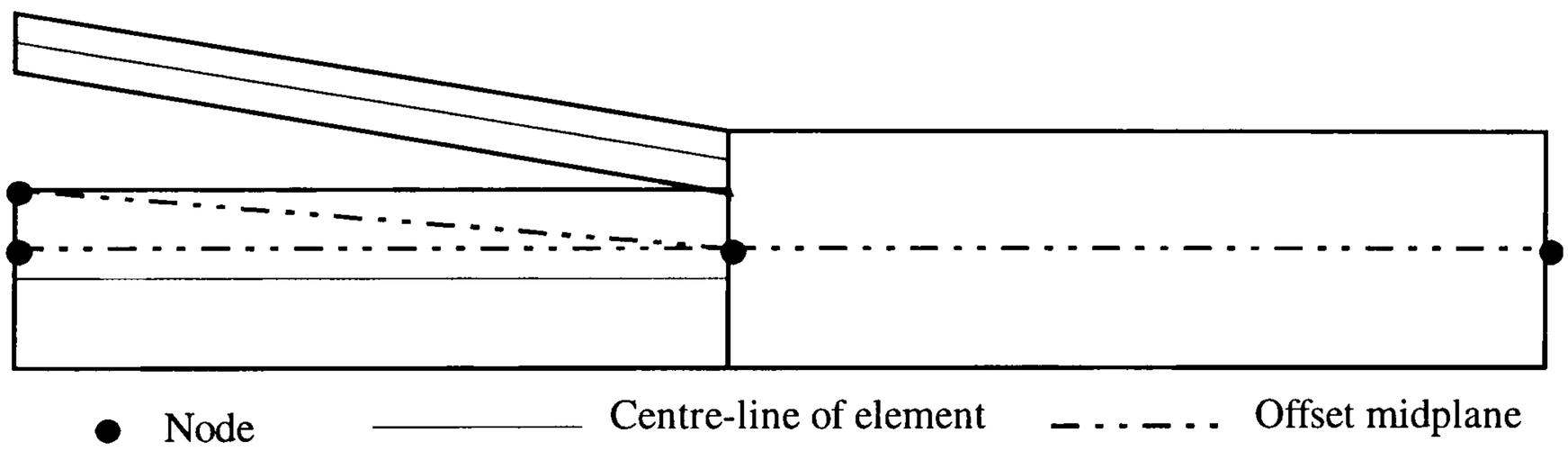

Figure 6.4. Using offsets for the element mid-plane to allow simpler connection of elements.

The element derived here was formulated by Dr M Pavier [Pavier and Chester, 1990], and has been implemented in the finite element program STYX [Pavier, 1993], developed specifically for the analysis of delamination behaviour. A standard Newton-Raphson iteration is used to achieve convergence at each load step in an incremental solution [Zienkiewicz & Taylor, 1991].

6.3. Theory

The specialised composite plate element is based on a large displacement 8 node serendipity plate element, as shown in Figure 6.5.

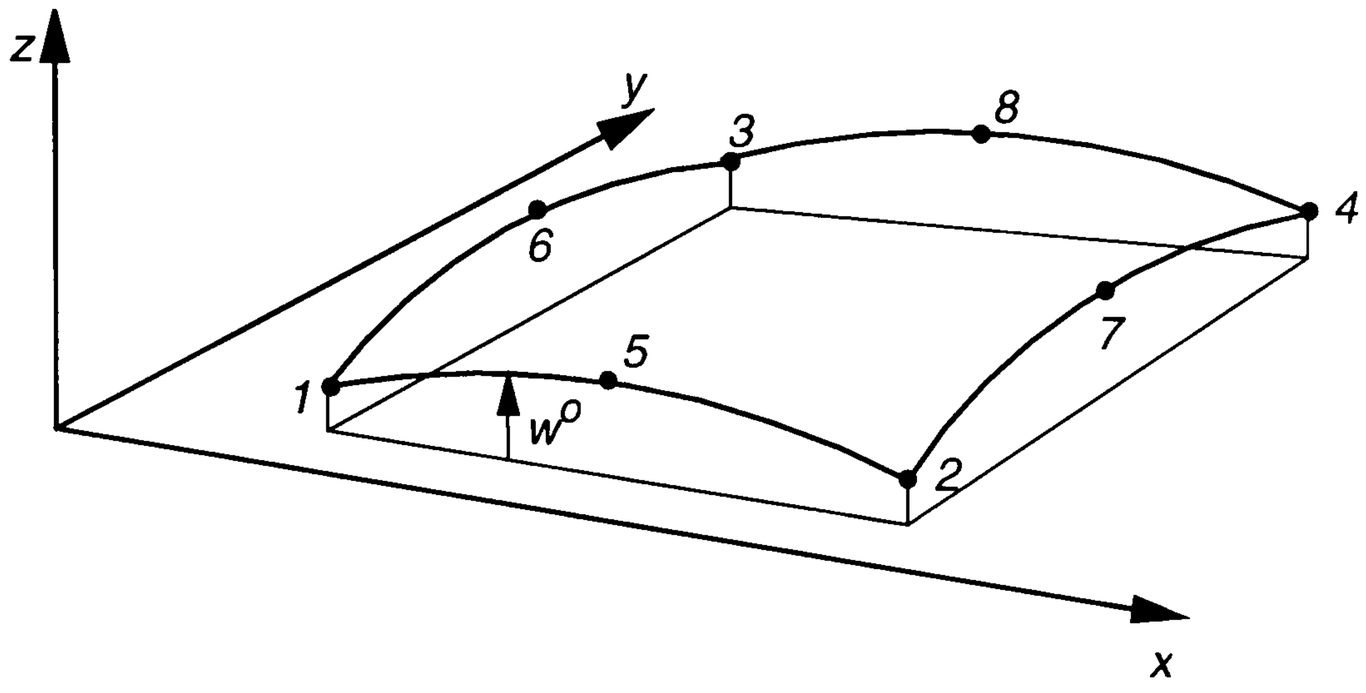

Figure 6.5 Initial out-of-plane displacement of the element.

The element lies approximately in the xy plane, but an initial out-of-plane displacement of the mid-plane is allowed, denoted by w^0, where

$$w^0 = w^0(x,y) \qquad [1]$$

This initial out-of-plane displacement prevents numerical difficulties in transition from small to large out-of-plane displacement (with no initial out-of-plane displacement the out-of-plane displacement when buckling occurs is sudden and large, and the numerical solution cannot be obtained). The value of the displacement should be small relative to the thickness of the element. (As is shown in Figure 6.8, the finite element results converge to the analytical solution as the initial out of plane displacement is reduced.)

Alternative methods for obtaining numerical solutions are to use a small normal load to cause out-of-plane displacement or use a full composite shell formulation [Chang and Sawamiphakdi, 1981; Chao and Reddy, 1984].

Standard thick plate relationships are used to describe displacements of points in the element:

$$\begin{aligned} u(x,y,z) &= u_{mp}(x,y,z) + z\theta^{x}(x,y) \\ v(x,y,z) &= v_{mp}(x,y,z) + z\theta^{y}(x,y) \\ w(x,y,z) &= w_{mp}(x,y) \end{aligned} \qquad [2]$$

where u_{mp}, v_{mp}, and w_{mp} are displacements of points in the mid-plane of the element and θ^{x} and θ^{y} are rotations of the mid-plane normal about the x and y axes. A total Lagrangian approach is used, where a point is described in terms of its co-ordinates in the initial, undeformed state.

The composite capabilities of the element are incorporated using lamina by lamina integration of the tangential stiffness matrix equation:

$$\mathbf{K}_T = \int_V \mathbf{B}^{\mathbf{T}}\mathbf{D}\mathbf{B}\,dV + \int_V \mathbf{G}^{\mathbf{T}}\mathbf{M}\mathbf{G}\,dV \qquad [3]$$

where the matrix **B** relates incremental strains to incremental displacements by

$$\delta\varepsilon = \mathbf{B}\delta\mathbf{u} \qquad [4]$$

Details of matrices are given in Appendix F.

Matrices **G** and **M** depend on the element shape function derivatives and current stress while matrix **D** relates the stresses to the strains by

$$\sigma = \mathbf{D}\varepsilon \qquad [5]$$

As already stated, the integration in equation [3] is carried out lamina by lamina, therefore the matrix **D** is recalculated for each lamina according to

$$\mathbf{D} = \mathbf{T}\mathbf{Q}\mathbf{T}^{\mathbf{T}}$$

where **T** is a transformation matrix depending on the orientation of the lamina and **Q** is a matrix containing the elastic properties in the principal material directions of the lamina. There are two integration points through the thickness for each ply. An alternative method for calculating properties for composite plate elements is to use an analytical integration of the through-thickness properties [Barbero and Reddy, 1991; Reddy, 1993]. Here the more general numerical integration is retained to allow more flexibility; for example in an analysis to degrade the properties of individual plies. In any case proportionally little computer time is saved by an analytical integration except for very small problems.

The integration order used in the plane for the element is 2 by 2. The positions of the integration points are as follows: the through-the-thickness integration points are placed at a distance of ±(thickness of ply/2√3) from the mid-plane of the ply; the in-plane Gauss point co-ordinates are set so as to position the points at a distance of ±(dimension of element/2√3) from the centre line of the element, as shown in Figure 6.6.

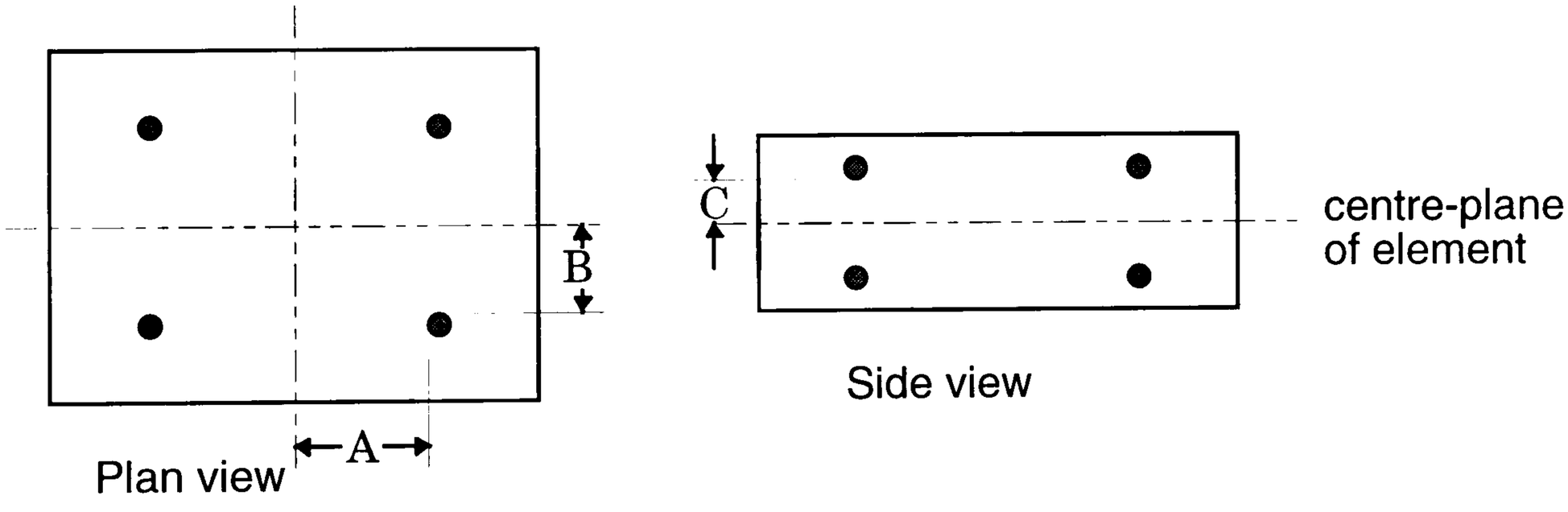

$$A = \frac{\text{length}}{2\sqrt{3}}, \qquad B = \frac{\text{width}}{2\sqrt{3}}, \qquad C = \frac{\text{thickness}}{2\sqrt{3}}$$

Figure 6.6. Position of Gauss points within element.

The composite element consists of a stack of *n* orthotropic laminae with direction of principal axes of θ . The position of each lamina relative to the element mid-plane are specified by z_{i-1} and z_i, the distances of the bottom and top surfaces of the *i*'th laminae from the initial element mid-plane.

The co-ordinates of through thickness integration points are denoted by z and are calculated using the distances of the bottom and top surfaces of the laminae from the element mid-plane. Therefore for the *i*'th lamina the through thickness positions of the two gauss points $z = z_1$ and $z = z_2$ are

$$z_1 = z_{i-1} + \frac{z_i - z_{i-1}}{2}(1+\xi_1)$$
$$z_2 = z_{i-1} + \frac{z_i - z_{i-1}}{2}(1+\xi_2) \qquad [7]$$

where $\xi_1 = -1/\sqrt{3}$ and $\xi_2 = 1/\sqrt{3}$ (the integration point positions.)

6.4. Numerical Experiments

To ascertain that the element functions correctly, it was used in three experiments designed to test the element formulation. Also included is a comparison made between using these elements and using three dimensional elements for a model of an embedded delamination [Whitcomb, 1989].

Fuller details of these verification tests can be found in reference [Pavier and Clarke, 1996]. Brief details of the test are included here. Isotropic properties were used in these experiments: each element had only one ply with orthotropic material properties:

$$E_{11} = E_{22} = E, \quad \nu_{12} = \nu_{21} = \nu, \text{ and } G_{23} = G_{12} = \frac{E}{2(1+\nu)}$$

The first test verifies the formulation of the terms for the initial out-of-plane displacement: an analysis of the post-buckling behaviour of a simply supported square plate.

The second test verified the correct functioning of the elements when the laminae and element mid-planes do not coincide: tensile loading of a delaminated strip.

The final verification was the large displacement bending of a rhombic plate due to normal forces applied at its corners.

6.4.1. The post-buckling behaviour of a simply supported plate

There is an approximate analytical solution for the central deflection of a simply supported isotropic square plate, where there is an in-plane (compressive) displacement in one direction. To model this situation a quarter model is used with symmetry conditions applied at the edges $x = 0$ and $y = 0$. The outer edges ($x = a$, $y = a$) are allowed to rotate, but restrained from out-of-plane displacement. The lateral displacement for the edge $x = a$ in the x direction is zero and a constant displacement in the y direction is applied to edge $y = a$. The plate and the constraints applied to it are shown in Figure 6.7.

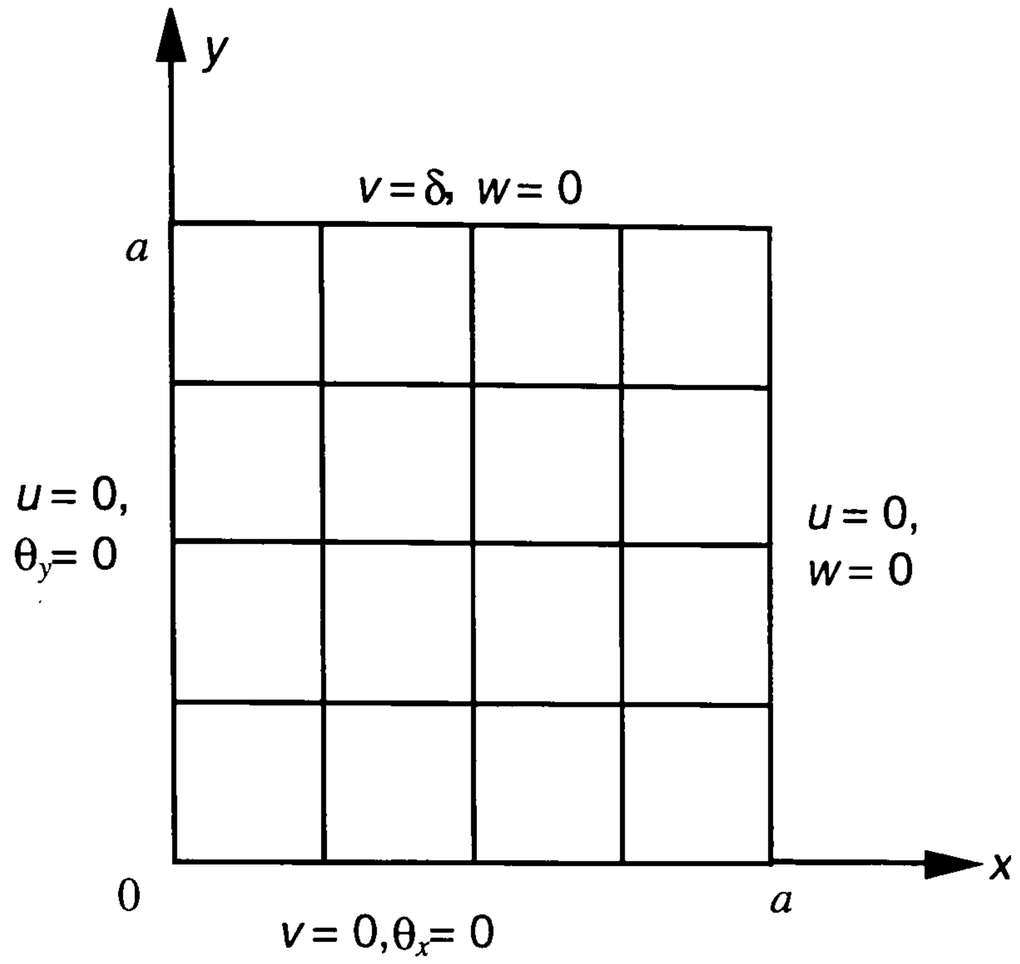

Figure 6.7. *Constraints on finite element model of isotropic square plate. All other displacements are free.*

Dimensions and material property values used were:

$$a = 2 \text{ m},\ t = 0.01 \text{ m},\ E = 1 \text{ GN / m}^2 \text{ and } \nu = 0.3$$

where t is the plate thickness and the initial out of plane displacement of the plate centre given by $\dfrac{w^o}{t} = 0.1,\ 0.01 \text{ and } 0.001$

A parabolic variation in initial out-of-plane displacement is used, from zero at the edges $x = a$ and $y = a$ to the set value at the plate centre.

Comparison of the results with the approximate analytic solution [Timoshenko & Gere, 1963] show the finite element results converge on the analytical solution as w^0 is reduced, see Figure 6.8.

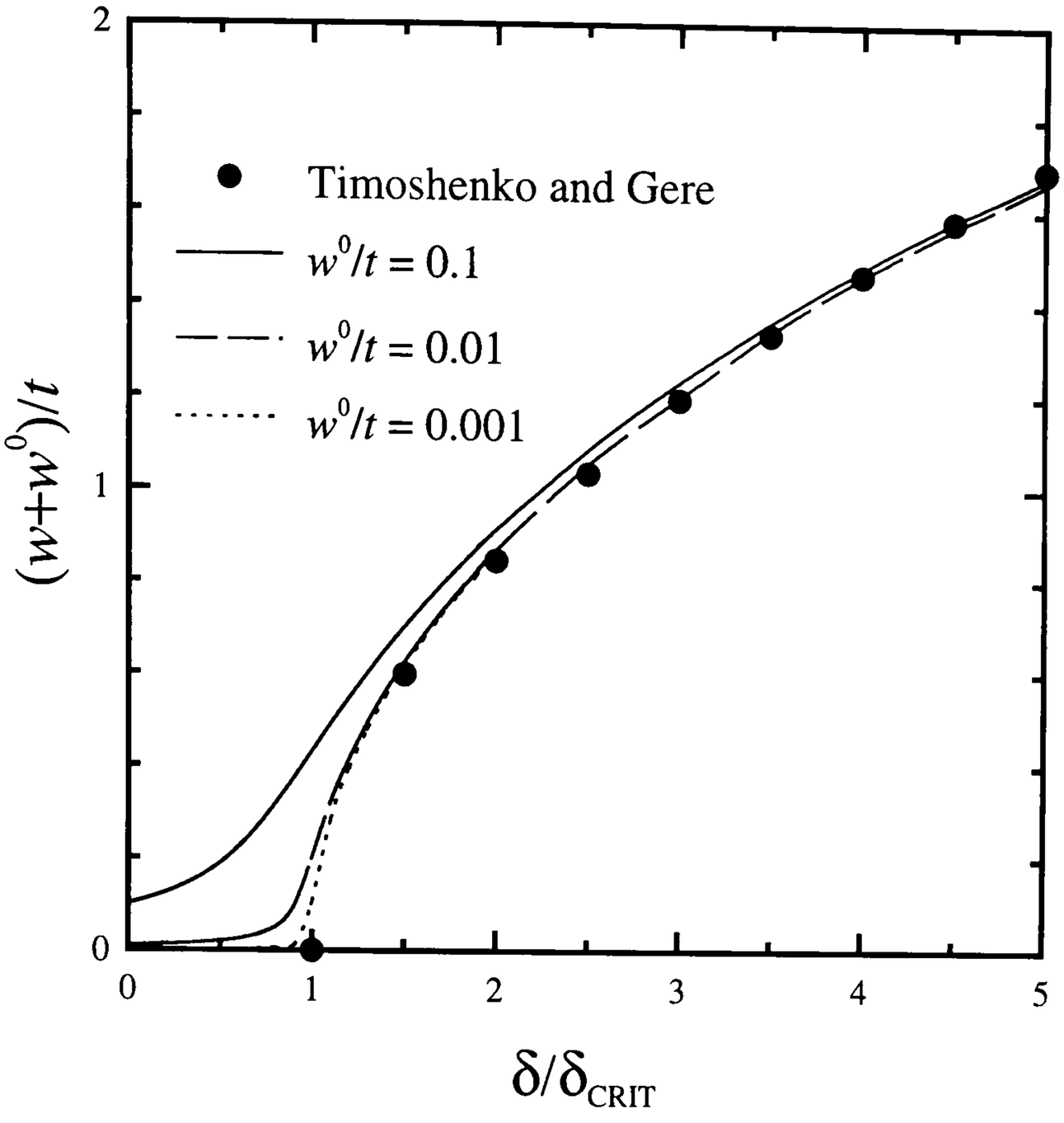

Figure 6.8. *Out-of-plane* vs. *applied lateral displacement (normalised against buckling displacement) for a simply supported plate*

The compressive displacement of the plate, δ, is normalised with the buckling displacement, δ_{CRIT}, calculated using the analytical solution. No difficulty was found with convergence of the solution, even for the smallest initial displacement.

In this test example, the solution is sensitive to the location of the mid-plane of the element relative to the mid-plane of the laminate, because the in-plane applied load at the edge causes, in addition, a moment to be applied. If the plate is clamped at the external edges, then the results should be insensitive to the mid-plane location. This was verified by additional analysis, in which the additional constraints $\theta^x = \theta^y = 0$ were applied to edges $x = a$ and $y = a$ (refer to Figure 6.7).

6.4.2. The tensile loading of a delaminated isotropic strip

To model a delaminated strip, three sets of elements are used. One represents the undamaged section of the strip, the other two are superimposed (share the same mid-plane) and represent the laminates either side of the delamination. The arrangement is shown in Figure 6.9, with sets 2 and 3 offset for clarity: the *laminate* mid-plane is as shown in the top diagram, the *element* mid-planes all coincide.

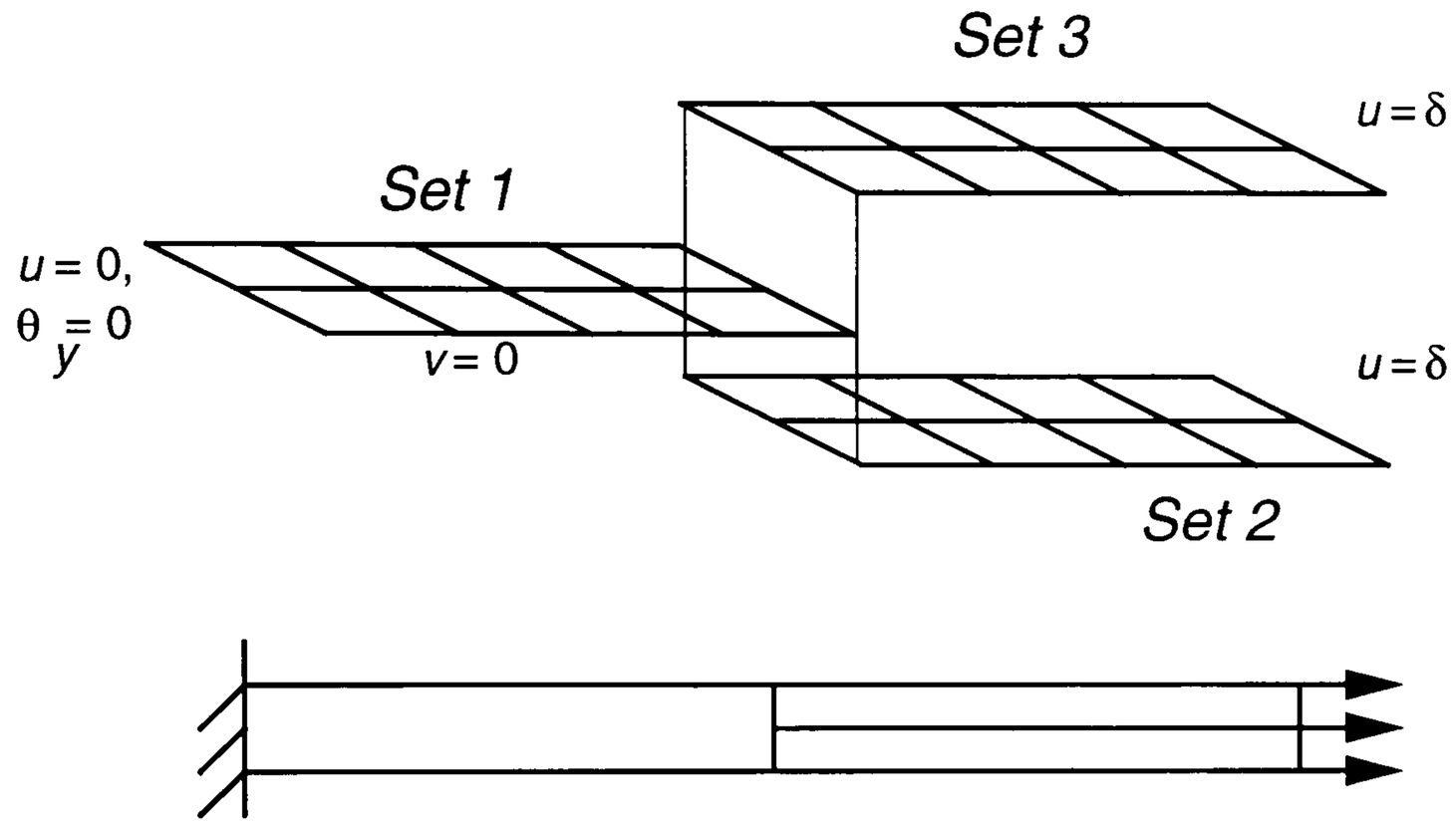

Figure 6.9. Finite element model of a delaminated strip.

Two tests are carried out. In the first, all sets are present and there should be no out-of-plane displacement as the bending moment on set 1 from sets 2 and 3 should balance. In the second, set 3 is removed, in which case a net bending moment is applied by set 2 on set 1 and out of-plane-displacements should occur.

Identical displacements in the x direction were applied to the right hand end of sets 2 and 3, while the left hand end of set 1 was fixed. The finite element results verify that no out-of-plane displacements occurred. When set 3 is removed, the finite element model shows out-of-plane displacements.

6.4.3. The bending of a rhombic plate under corner forces

The final verification uses a large displacement bending of a diagonally supported rhombic plate. Again, symmetry constraints allow the use of a quarter model. Figure 6.10 shows the constraint applied to the plate to model to model a plate supported by a rigid bar along $x = 0$ and symmetry condition along $y = 0$.

Dimensions of the plate and material properties used were:

$$a = 5 \text{ m},\ t = 0.01 \text{ m},\ \theta = \tan^{-1} 3/4,\ E = 10.92 \text{ MN/m}^2 \text{ and } \nu = 0.3$$

Prescribed out-of-plane displacements were applied to the corner node (at $x = a$) and the corresponding reaction P recorded.

Figure 6.11 shows the normalised reaction versus the out of plane displacement of the corner node w normalised by the plate thickness t compared to simple theory and the hybrid plate element of Allman [1982].

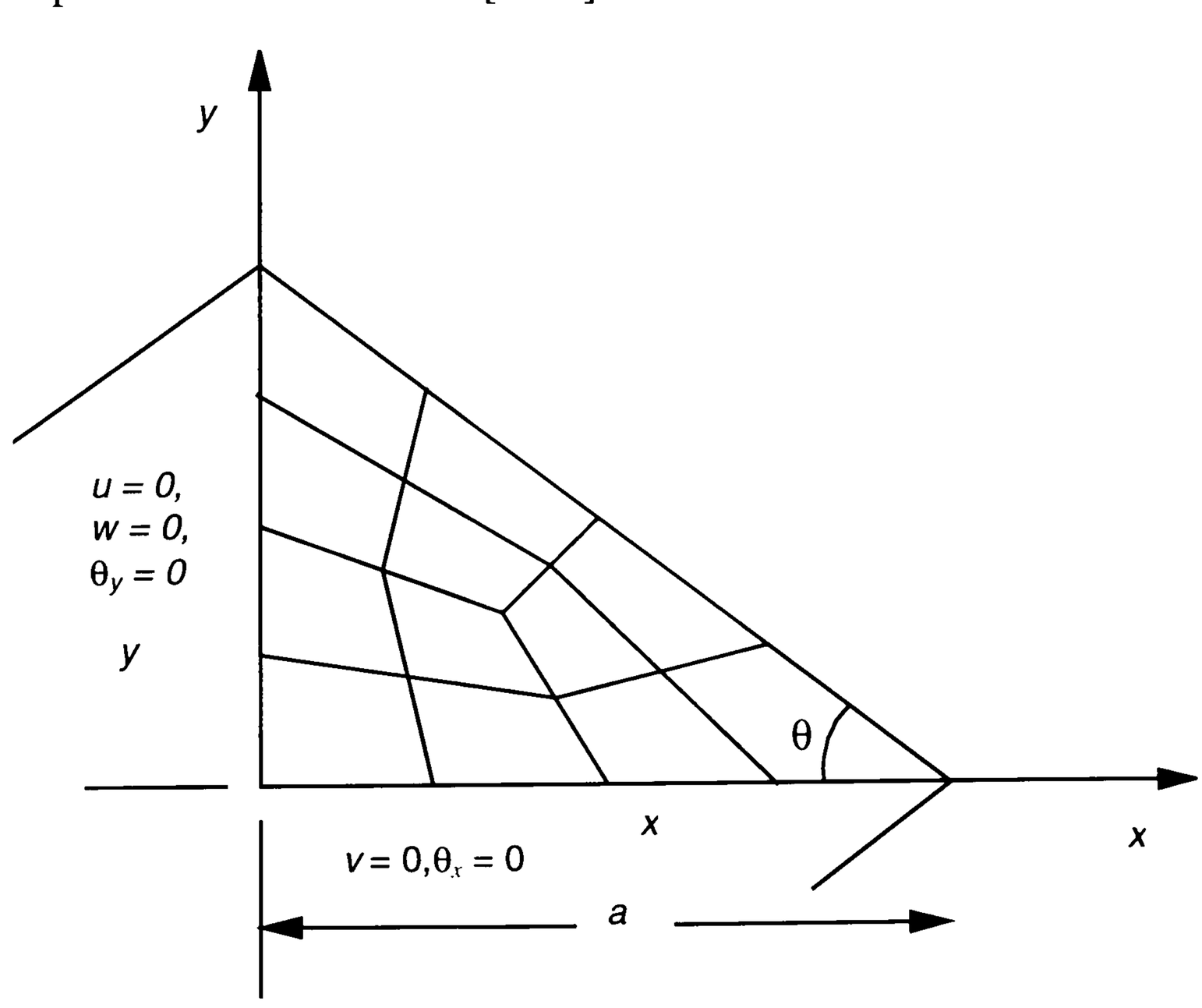

Figure 6.10. Constraints on the quarter model of a rhombic plate.

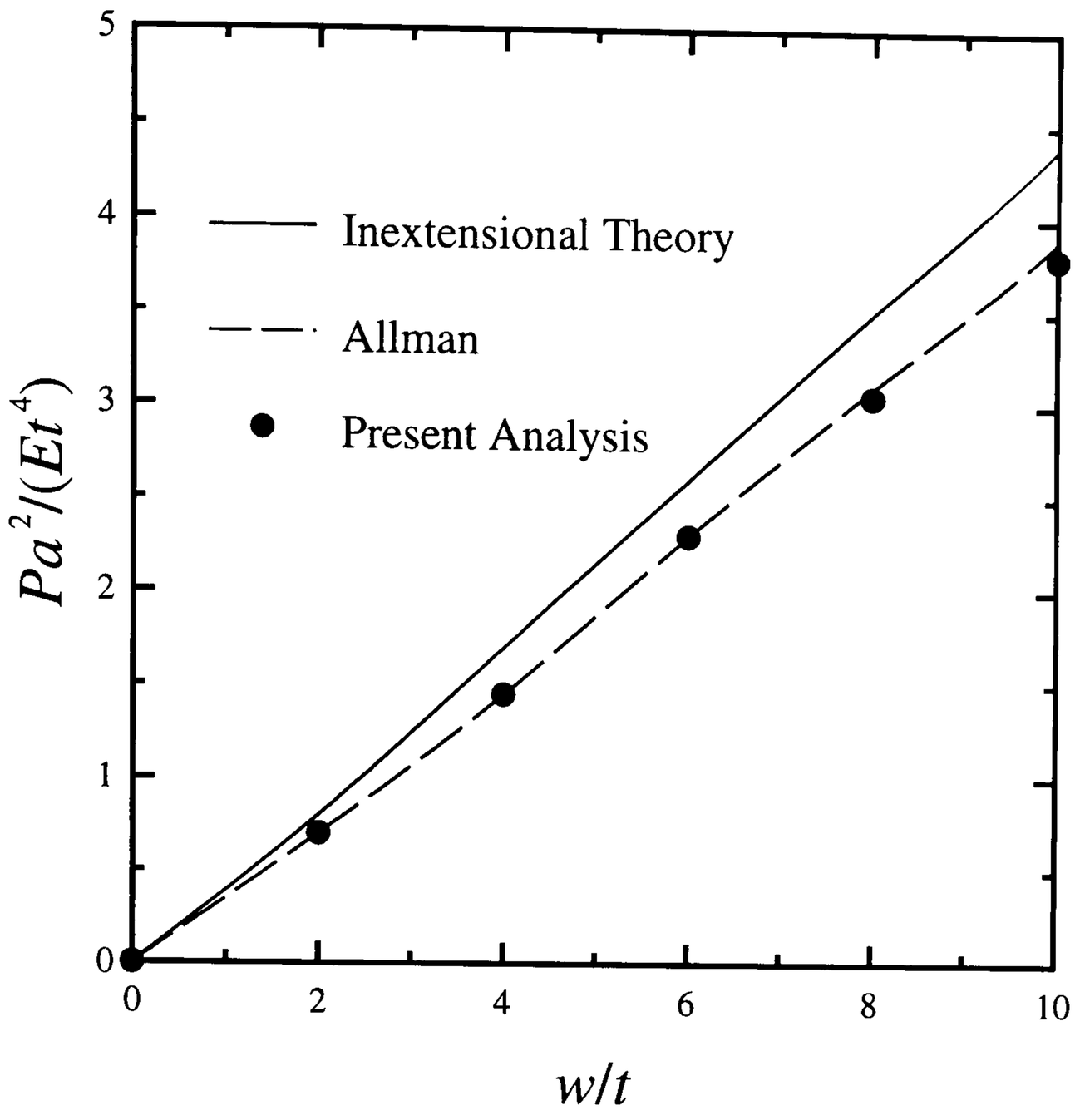

Figure 6.11. Normalised reaction force vs. normalised out-of-plane displacement.

6.4.4. Comparison with a three dimensional element model

The element formulated here was used to calculate strain energy release rates around a circular embedded delamination using the three dimensional element results of Whitcomb [1989]. Here a comparison will only be made of the out-of-plane displacement of the buckle with applied compressive strain. (More detail on the energy release rate study is contained in Pavier and Clarke [1996].)

Whitcomb's analysis was of a square plate, edge 100 mm and thickness 4.4 mm, with a circular delamination at the centre, 30 mm in diameter and 0.4 mm deep. He used three layers of elements, of differing thicknesses. The top layer, used for the delamination, was 0.4 mm thick, the remaining two layers that represent the

undelaminated laminae have total thickness of 4.0 mm. Details of the mesh used are shown in Figures 6.12 and 6.13

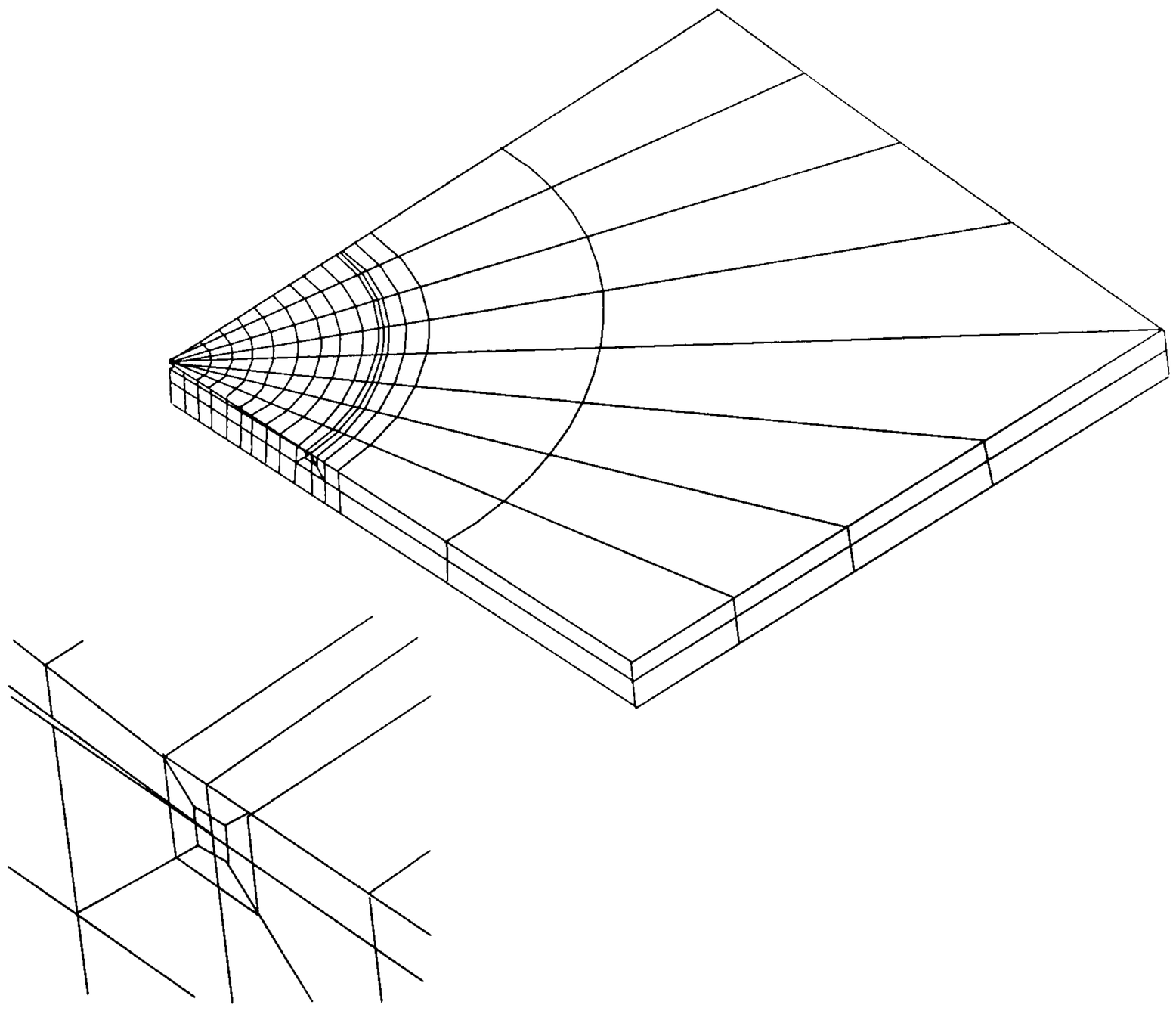

Figure 6.12. Three-dimensional finite element mesh used by Whitcomb for analysis of a circular delamination, with detail of mesh refinement at delamination edge.

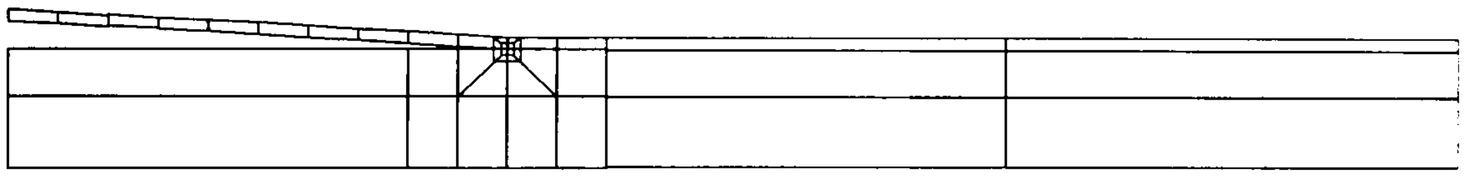

Figure 6.13. Cross section of mesh showing mesh refinement at crack tip, and delamination enlarged.

The lay-up for the composite was $(\pm 45°, 0°, 90°)_s$, though Whitcomb used constant element properties for all layers through the thickness, based on the average properties for this stacking sequence. Similar properties where used for the elements in the two dimensional element model using the element described here. The model was meshed using plate elements as shown in Figure 6.14.

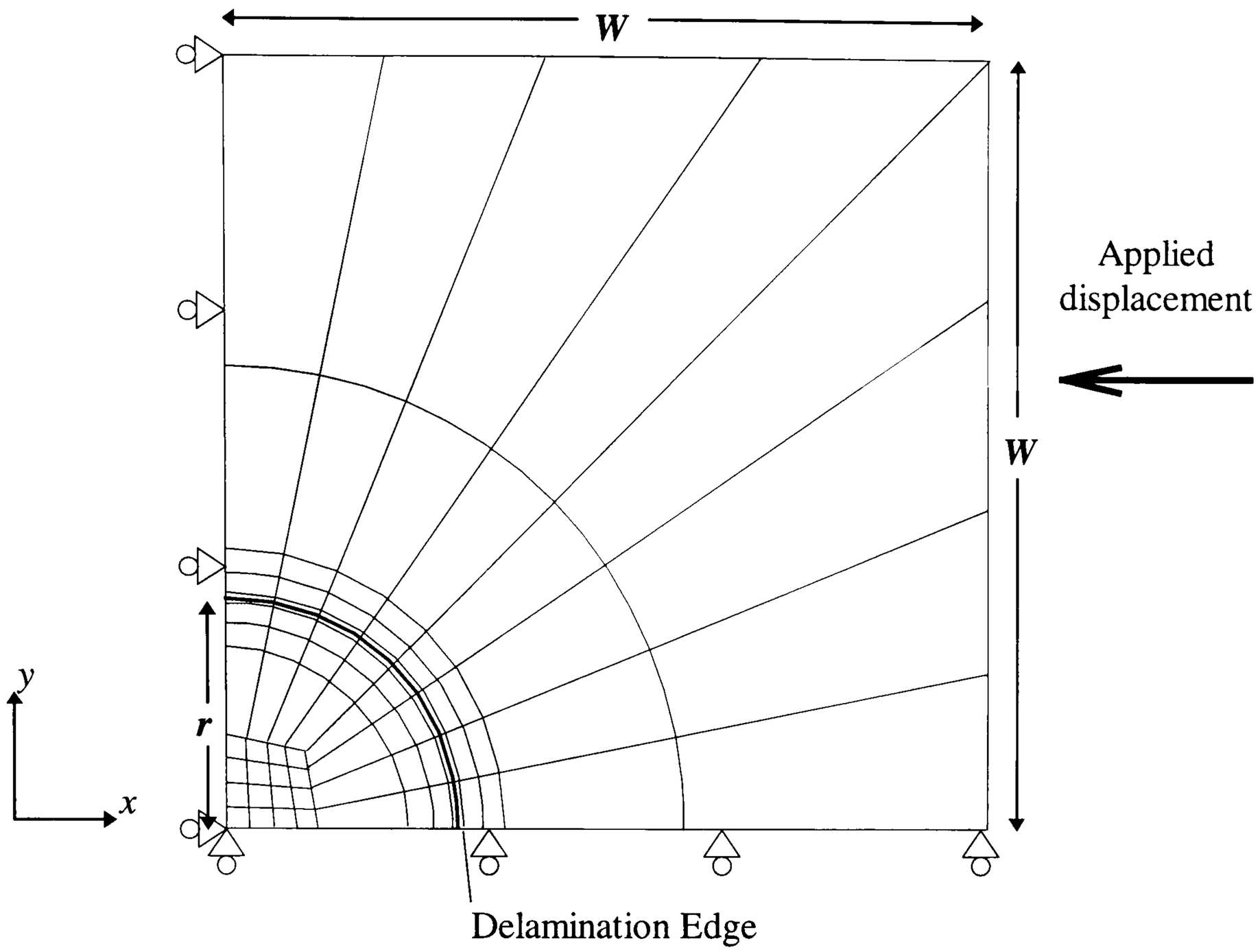

Figure 6.14. Finite element mesh for analysis using plate elements.

Loading is applied as fixed displacements to the edged x=*W* corresponding to applied strains of ε_x=0 to -0.005., while allowing free movement in the *y* direction. Symmetry constraints are applied to the edges x=0 and y=0. In addition the edge y=*W* is free to move in both *x* and *y* directions. The centre node, at x=0 and y=0, is given an initial out of plane displacement of 0.01 mm.

The out-of-plane displacement of the central node is plotted against applied compressive strain in Figure 6.15.

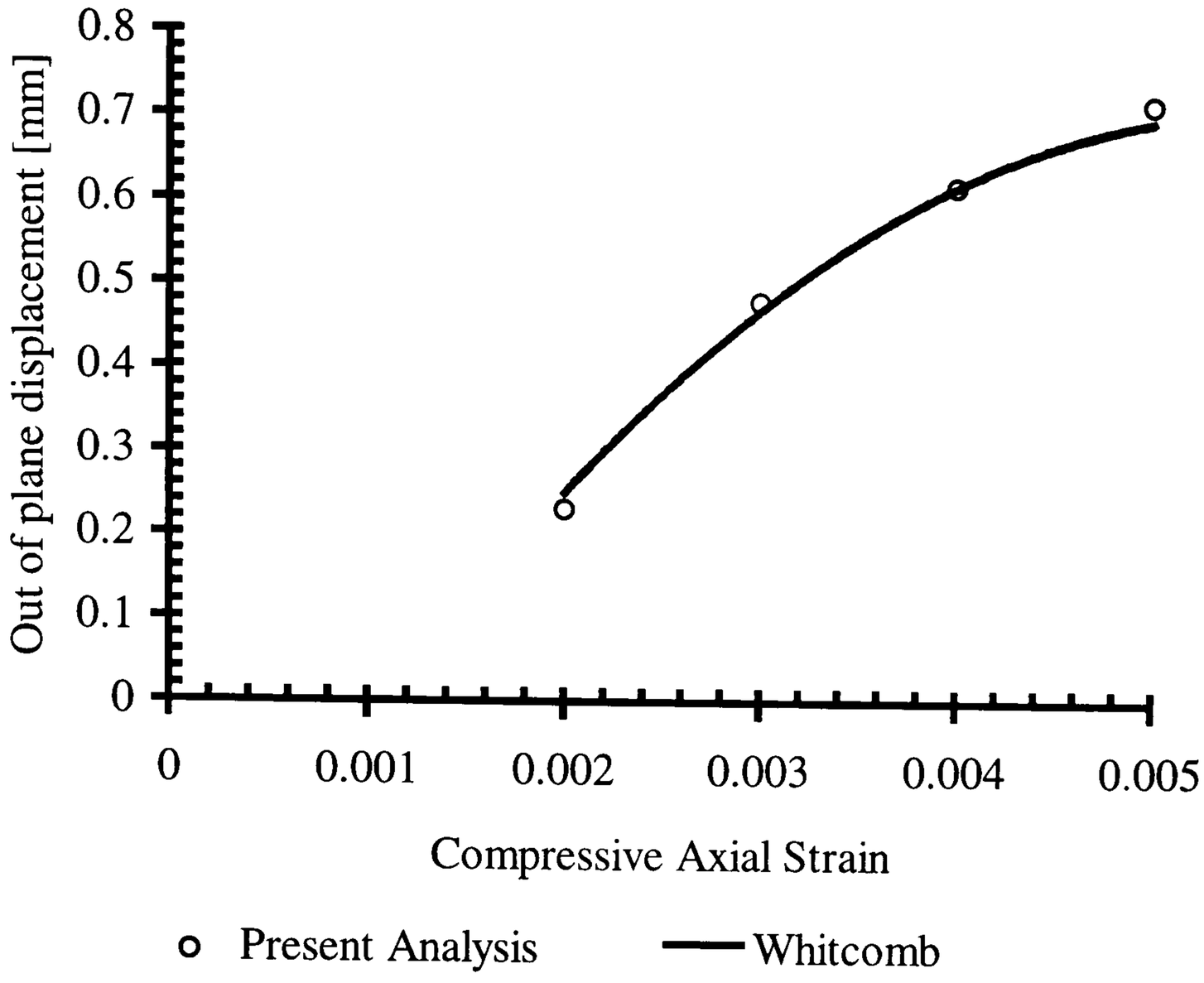

Figure 6.15. *Results of analysis of a circular delamination, showing the out-of-plane displacement of the central node.*

6.5. Concluding Remarks

The element described here has been shown to function correctly, using simple test cases, and that it is capable of matching the results from analyses using solid elements. In the comparison with Whitcomb's work, an analysis using 144 plate elements and 451 nodes has produced results in good agreement with an analysis using 336 solid elements and 2085 nodes. The solid element model has elements that have extreme aspect ratios and poor edge angle[2] (respectively, up to 100 and approximately 45°), even for a model with but one delamination. These are problems that are much less likely to occur with the plate elements.

---

[2] Aspect ratio is length of longest side divided by length of shortest side. Face angle is the smallest internal angle between adjacent faces.

The element is particularly useful for analyses that require laminae of varying thickness to be connected simply, and thus allows modelling of multiple overlapping delaminations without the complications that would arise if either solid elements or standard plate elements were used.

The element includes the ability to apply small initial out-of-plane displacements that simplify the modelling of buckling behaviour as there is no need for small normal loads.

The plate element as described here, has the ability to incorporate multiple layers within the element, which has some advantages. Firstly, it reduces the need to model each ply with a separate element. Secondly, it allows a larger aspect ratio to be used (in this case the aspect ratio is the ratio of in-plane dimensions to thickness) when composite properties are used. This is due to the lower shear stiffness of composite plates relative to isotropic properties.

References

Allman, D.J.

"Improved Finite Element Models for the Large Displacement Bending and Post buckling Analysis of Thin Plates."

Int. Journal of Solids and Structures Vol. 18 **1982** pp. 737-62.

Atkin, R.J. and Fox, N

"An introduction to the theory of elasticity."

Longman **1980**.

Barbero, E. and Reddy, J.

"Modelling of Delaminations in Composite Laminates using a Layer-wise Plate Theory.".

International Journal of Solids and Structures Vol. 28 **1991** pp. 378-88.

Chang, T.Y. and Sawamiphakdi, K.

"Large Deformation Analysis of Laminated Shells by Finite Element Method."

Computers and Structures Vol. 13 **1981** pp. 331-40.

Chao, W.C. and Reddy. J.N.

"Analysis of Laminated Composite Shells using a Degenerated 3-D Element."

Int. Journal of Numerical Methods Eng. Vol. 20 **1984** pp. 1991-2007.

Chaudhuri, R.A. and Seide, P.

"Triangular Finite Element for Analysis of Thick Laminated Plates."

Int. Journal of Numerical Methods Eng. Vol. 24 **1987** pp. 1203-24.

Kutlu Z. and Chang F.K.

"Modelling of Compression Failure of Laminated Composites Containing Multiple Through-the-Width Delaminations."

Journal of Composite Materials Vol. 26(3) **1992** pp. 350-387.

Jones, R., Callinan, R., Teh, K. K. and Brown, K.C.

"Analysis of Multi-Layer Laminates using Three-Dimensional Super-Elements."

Int. Journal of Numerical Methods Eng. Vol. 20 **1984** pp. 583-7.

Nilsson K.F. and Storåkers B

"On Interface Crack Growth in Composite Plates."

Journal of Applied Mechanics Sept. Vol. 59 **1992** pp. 530-8.

Nilsson K.F., Thesken J.C., Sindelar P., Giannakopoulos A.E. and Storåkers B

"A Theoretical and Experimental Investigation of Buckling Induced Delamination Growth."

Journal Mech. Phys. Solids Vol. 41(4) **1993** pp.749-82.

Noor, A.K. and Mathers, M.D.

"Finite Element Analysis of Anisotropic Plates."

Int. Journal of Numerical Methods Eng. Vol. 11 **1977** pp. 289-307.

Pavier M.J. and Chester W.T.

"Compression Failure of Carbon Fibre-Reinforced Coupons Containing Central Delaminations."

Composites Vol. 21(1) January **1990** pp. 23-31.

Pavier, M.J.

"STYX Users Guide."

Department of Mechanical Engineering. University of Bristol **1993**.

Pavier, M.J. and Clarke, M.P.

"A Specialised Composite Plate Element for Problems of Delamination

Buckling and Growth."

Submitted for publication **1996**.

Reddy J. N.

"An Evaluation of Equivalent-Single-Layer and Layerwise Theories of Composite Laminates."

Composite Structures Vol. 25 Jul. 16 **1993** pp. pp. 21-35.

Timoshenko, S.P. and Gere, J.M.

"Theory of elastic stability." 2nd Edition

McGraw-Hill **1963**

Whitcomb J.D

"Finite Element Analysis of Instability Related Delamination Growth."

Journal of Composite Materials Sept. Vol. 15 **1981** pp. 403-26.

Whitcomb J.D

"Approximate Analysis of Post-buckled Through Width Delaminations."

Composites Technology Review Vol. 4(3) Sept. **1982** pp.71-7.

Whitcomb J.D

"Strain Energy Release Rate Analysis of Cyclic Delamination Growth in Compressively Loaded Laminates."

American Society for Testing & Materials STP836 **1984** pp. 175-93.

Whitcomb J.D

"Parametric Analytical Study of Instability Related Delamination Growth."

Composites Science and Technology Vol. 25 Sept. **1986** pp. 19-48.

Whitcomb J.D

"Three-Dimensional Analysis of a Post-buckled Embedded Delamination."

Journal of Composite Materials Vol. 23 September **1989** pp. 862-89.

Whitcomb J.D

"Analysis of a Laminate with a Post-buckled Embedded Delamination, including Contact Effects."

Journal of Composite Materials Vol. 26 Sept. **1992** pp. 1523-35.

Whitney, J.M.

"Shear Correction Factors for Orthotropic Laminates under Static Load."

Journal of Applied Mechanics Vol. 40 **1973** pp. 302-4.

Zienkiewicz, O.C. and taylor, R.L.

"The Finite Element Method" Vol. 2: "Solid and Fluid Mechanics, Dynamics and Non-Linearity."

MacGraw Hill, **1991**

CHAPTER 6. DEVELOPMENT OF FINITE ELEMENT TECHNIQUES FOR ANALYSIS OF POST IMPACT STRENGTH.....1

CHAPTER 7.

NUMERICAL MODELLING

7.1. Previous Work

Given the range of possible failure mechanisms in composite materials there are a correspondingly large number of finite element techniques in use. Numerical methods can be used to calculate stresses and strains in specimen under load, the loads at which plies buckle [Kutlu & Chang, 1992], the strain energy released when cracks and delaminations grow, the force-time history during impacts [Choi & Chang, 1992], pre- and post-buckling behaviour and many other characteristics of composites under in-service conditions. Of particular interested here is the behaviour of damaged specimens under compression, so this is where the work is concentrated.

Finite element analysis has increased in sophistication as new techniques have been developed, and as the required computational power has become available. Early numerical analysis of the effect of damage looked at the behaviour of through the width delaminations. This reduces the computational load because of the possibility of using a two-dimensional analysis. The buckling sub-laminate problem requires a non-linear analysis, because of the relatively large magnitude (compared to the thickness of the specimen) of the displacement. One way of circumventing the

problem that this causes in terms of computation size is to have a mixed linear–non-linear analysis where only the delamination region is treated in a non-linear fashion [Whitcomb 1981, Whitcomb 1982].

In these, and other papers [Whitcomb 1986] the aim was to predict the load at which delamination was initiated. The technique used was to calculate the strain energy release rate near the tip of the crack (end of the delamination) and compare this to the experimental value for the critical strain energy release rate.

The simple geometry in these analyses allow for the analysis of G_{Ic} and G_{IIc} separately and hence their contributions to crack growth. The effect of crack length on the values of G_{Ic} and G_{IIc} was also investigated.

Two simplifications were made in Whitcomb's models (and later 3-dimensional ones [Whitcomb 1988, 1992]). Firstly, that the main laminate below the delamination remains flat. This requires that the delamination is very thin in comparison to the laminate. In the investigations described in the work here, the sub-laminate is a significant proportion of the total thickness. Delaminations occur preferentially between plies with different fibre orientation, so the minimum sub-laminate containing load bearing 0°plies will be (with the lay up used here) five plies out of 18, or approximately 28% of the laminate. Secondly, constant material properties were used throughout the thickness. The use of homogeneous quasi-isotropic material properties removes any effects due to stacking sequence and possibly unbalanced delaminated plies.

Later work has included the introduction of interface elements between the delamination and the laminate which have either modelled the properties of the matrix interface [El-Senussi & Webber, 1986; Allix & Ladeveze, 1992] or have been used to constrain the mesh to prevent interpenetration of the sub-laminate and the

laminate, while allowing the sub-laminate to buckle outwards. [Whitcomb, 1992; Nilsson *et al*, 1993].

Some work has been done on the actual growth of the delamination, as opposed to the initiation of growth [Pavier and Chester, 1990]. In this case the effect of incremental release of nodes to simulate growth of the delamination is used. The maximum value of strain energy release rate around the perimeter of the original delamination indicates the point at which the delamination grows. This process is repeated and becomes quite time consuming. A simplified rectangular geometry was used for the delamination and a relatively coarse mesh, but results were consistent with the growth of delaminations. More recent work [Nilsson and Storåkers, 1992] has used automatic mesh generation to follow the growth of the delamination.

A further refinement of the finite element model is to include the behaviour of the main laminate (not the delaminated plies). Experiment has shown that the buckling of the delamination does not imply immediate failure of the specimen, therefore the failure may be linked to the behaviour of the main sub-laminate. This requires a model that is able to model the behaviour of multiple plies through the thickness, without artificially constraining plies to remain in plane. The influence of the post-buckled delamination on the failure of the load carrying main laminate can then be investigated.

A two-dimensional analysis of the buckling (and post-buckling) behaviour of composites containing multiple delaminations has been carried out by Kutlu & Chang, [1992]. In their work, which allowed growth of delamination, there were no in-plane constraints, so the buckling of the main laminate was incorporated. The analysis also contained a failure analysis using property degradation rules. It is of interest that the experimental study accompanying this work showed that the collapse of the specimen was usually associated with the macro-buckling of the main block of laminates.

The next step in improving the finite element model is to extend this approach to structures with contained damage, requiring a 3-dimensional model. The behaviour of a delamination which is constrained on all four edges will be different to one modelled using a 2-dimensional analysis.

As the computer power needed for more complex analyses has become available many of the studies mentioned so far have been repeated with refinements—for example inclusion of full isotropic layered properties and linear–non-linear analysis in the same study [Guedra-Degeorges *et al*, 1991].

7.2. Description of STYX Finite Element Program

In this finite element work the STYX program was used, written specifically for analysing large displacement problems with composite laminates. The program is run in increments, with the far field displacement or force being increased at each step. Between increments the data may be modified to change the initial constraints (in order, for example, to allow a crack to grow). Each increment creates a link file which contains the necessary information for subsequent increments. Full details of the capabilities and use of the program can be found in the STYX User Guide [Pavier, 1993]

In order to access the data produced by the program there are four utilities:

- LOOK allows viewing of the numerical results on screen;

- VIEW produces a graphical display of the displacements of the mesh; and

- PRNT produces a printable file of the displacements and/or stresses and/or loads on blocks, elements or nodes produced by the loading/displacements applied to the mesh.

- XYZP produces a data file of stresses and associated co-ordinates within the model for input to contouring packages such as the Silicon Graphics™ program Explorer.

The program has been compiled to run on a VAX VMS system, Silicon Graphics and Sun work-stations and on IBM PC compatibles. (The size of problem is quite limited on PCs.)

The mesh is built up of blocks of elements. This simplifies the construction of large meshes considerably, as the program calculates the positions of the majority of the nodes and numbers nodes and elements. The number of elements along the side of a block is a user definable variable.

There are a selection of block types available that allow meshing of both two and three dimensional objects, as well as mesh refinement.

There are six types of element available, covering plane elements, plate elements and three dimensional wedge and cubic elements.

The properties of composites are included in the model by calculating the properties of each element based on the material properties of the composite and the ply orientations and thicknesses of plies. The element formulation allows the stresses in individual plies to be calculated.

An annotated input file to the STYX program is included in Appendix C, illustrating the methods by which the information necessary to define the model is passed to the STYX program. Full details of the properties used in each analysis are contained in Appendix D, which lists the input files for the finite element analysis.

7.3. Finite Element Models used in this work

7.3.1. The basic model

Choice of elements

In this study the finite element analysis needs to model thin plates which may undergo buckling. For this reason the elements used in this work are eight noded quadrilateral plate elements, as plane elements cannot allow for out of plane displacements. Three dimensional elements would require many more nodes, with the additional problem in this case of a thin plate geometry. This is because the limit of accuracy with the aspect ratio of the elements (which occurs because of deformation of the elements and would therefore be most noticeable around areas of interest) would necessitate more elements than the model with plate elements and a commensurate increase in computing power or solution time.

The through thickness properties are handled by modelling undamaged laminate with a single element through the thickness. This element models all the plies, and information on the thickness, fibre angle and material properties for each ply are input to the program. In the regions were a delamination is present two elements are used through the thickness.

The preceding chapter goes into greater detail about the element formulation of the element used. In this section the use of the elements is dealt with.

Choice of boundary constraints

The aim is to choose constraints on the finite element model that match the actual conditions that applied in the experiments described in chapter 4. Since a quarter-model is used for the majority of the analyses, constraints have been chosen along the edges of the model that follow the centre-lines of the specimen that take account of

the symmetry. Figure 7.4 shows these constraints and the area of the experimental specimen that was modelled using finite element analysis.

To summarise, the longitudinal edge (centre-line of specimen) is constrained so that it cannot move in the plane of the specimen transverse to the loading direction, or rotate around the longitudinal axis. The transverse edge (centre-line of specimen) is constrained so that it cannot move in the plane of the specimen in the loading direction, or rotate around the transverse axis, except where a crack is present. The free edges are constrained in the out of plane direction and are prevented from rotating around the edge (to model the presence of the anti-buckling guide).

The load is applied in the form of *displacements* of the edge furthest from the delamination. This is better because of the instability present in the specimen. If *forces* were applied to the end of the model the changes in stiffness of the model as it buckles would cause problems in obtaining convergence. This means that the strain is specified for each increment in order to calculate deformations and stresses at a nominal load. The values of strain used are calculated using laminate theory. The precise load applied to the specimen can be found from the model.

Verification of the actual applied load in the FE model, as compared to the expected load from the applied displacement, was carried out for various models including the FE model of the control coupon. The far field load in the FE model (at the edge furthest from the damage) was less than the nominal load because the implanted damage reduces the stiffness of the coupon and the displacements are based on the behaviour of undamaged material. However, this is not a problem as the actual values can be used in any comparison with experimental results.

For the control specimen (which has no damage) the agreement between nominal and calculated loads in the FE model was very good, of the order of 1 to 5 percent (the variation is due to the change in stiffness as the coupon undergoes macro-buckling).

The window in the anti-buckling guide (see Appendix A) allows local buckling of the centre of the plate, and this is modelled by the edge constraints on the FE model. As the displacement applied to the end of the plate is increased the load increases, but the peak load increases more than expected because of buckling of the coupon. The compressive load distribution across the plate is uneven because of the component due to bending.

7.3.2. Modelling delaminations using a layered model

When modelling delaminations it would appear that a three dimensional model would be necessary as the coupon has two separate parts in the direction normal to its surface, whereas standard plate elements are all attached to each other within a single surface. It is here that the use of superimposed blocks avoids the need to move to three-dimensional elements.

The delamination is modelled by having two blocks occupying the same space and both attached to the surrounding blocks. The properties of the elements within each block, however, are calculated on the basis of each only containing some of the plies - in this example the bottom block contains the main sub-laminate and the other block contains the top three 0° plies and the surface ±45° plies. The two blocks combined model the whole thickness of the plate (see Figure 7.1), but the delamination is free to move independently of the sub-laminate (and vice versa). Taking the delamination as an example, the properties of an element in the delamination are based on the material properties of the composite for the top five plies and reduced properties (by a factor of 10^6) for the remaining plies. Since the loading on the elements is in the mid-plane the element will have a greater tendency to buckle outward, as would be expected of a delamination in compression.

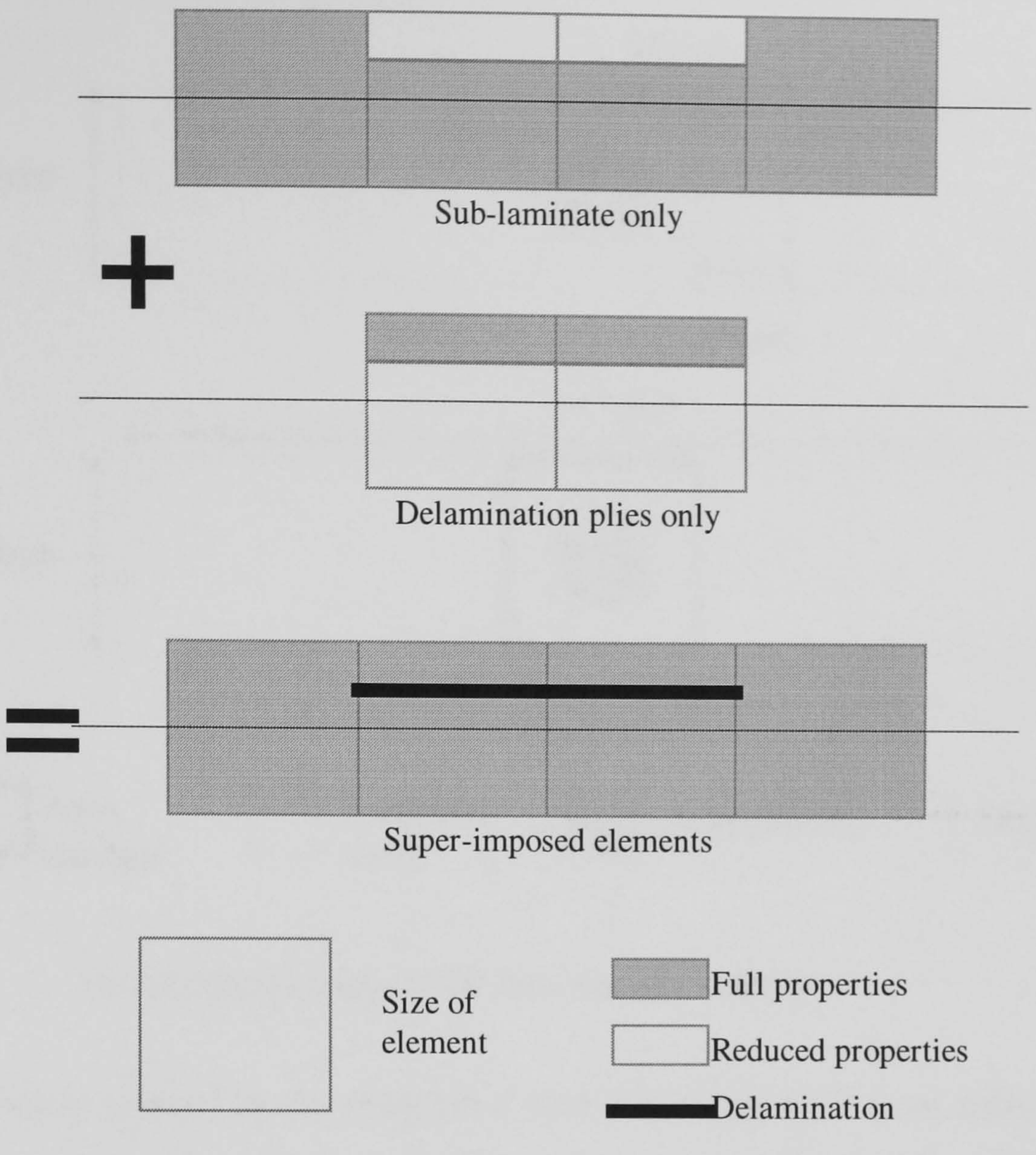

Figure 7.1. Modelling of layers using two-dimensional plate elements

7.3.3. Modelling cracks

In order to model cracks a break must be included in the mesh. If a quarter model is used the ply crack is coincident with the edge of the model and so an appropriate choice of constraints is used to model the behaviour of a crack. A full model is simpler to fit constraints to as there are no symmetries to be taken into account . Figure 7.2 shows the part of the coupon that was modelled.

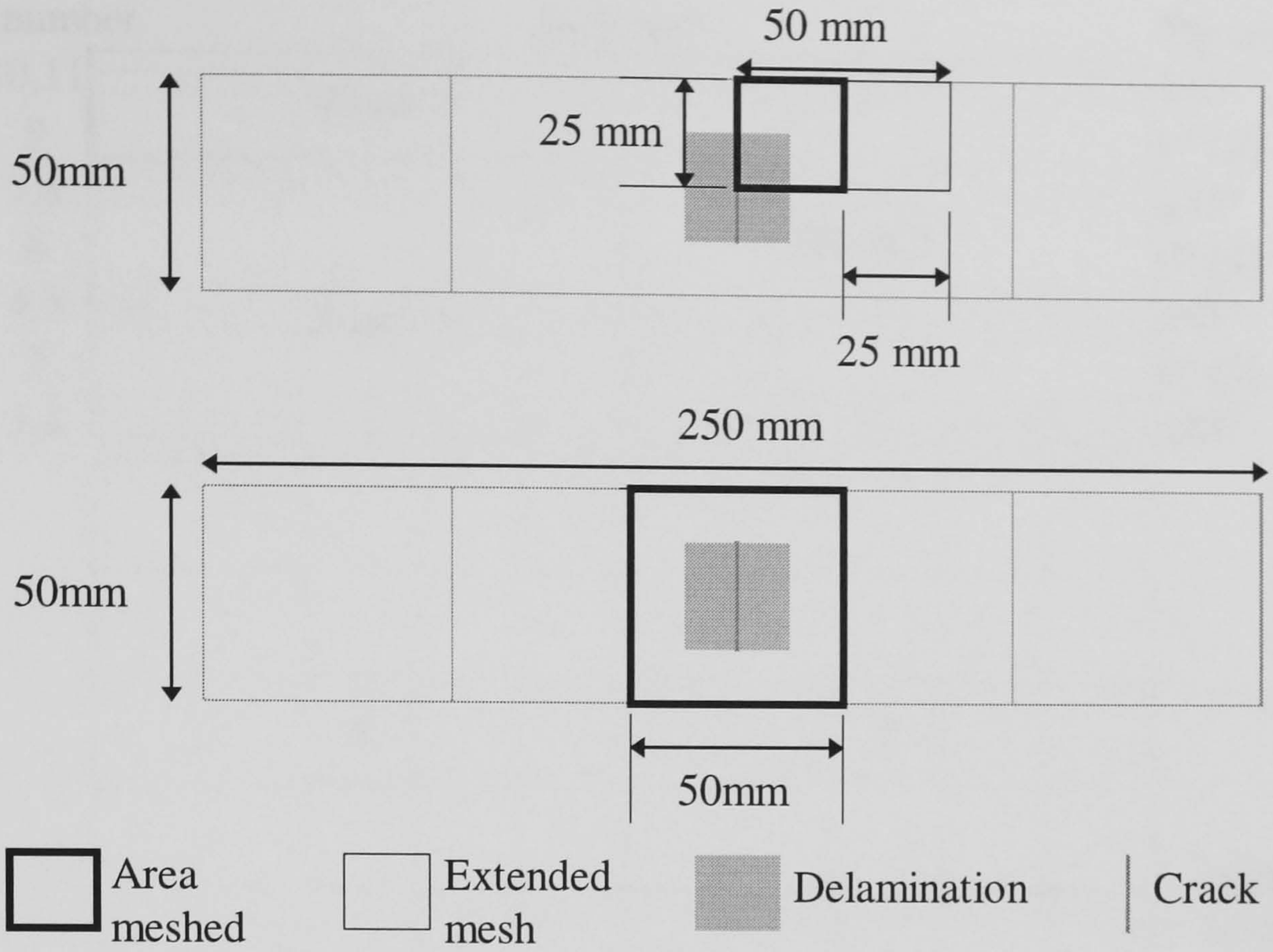

Figure 7.2. Part of coupon analysed by finite element method.

Nodes are equivalenced by the program if they are within 10^{-10} m of each other, so a crack can be made having as small a gap as desired. Each block is meshed separately creating elements as shown in Figure 7.3. Elements created within a block use the same nodes at common edges and corners. Where the blocks meet, adjoining elements do not have common nodes. The process of equivalencing joins adjacent elements by finding nodes that have the same co-ordinates (within the tolerance). One node is deleted and the other is used to replace it, so that neighbouring elements now share a node, and so are connected.

In the full model the crack was simulated by adjusting the position of the nodes along the edges of the blocks (areas of the model with identical properties) either side of the crack so that the nodes do not equivalence. This also prevents any of the nodes along the delamination interface being equivalenced, so the two blocks can behave independently.

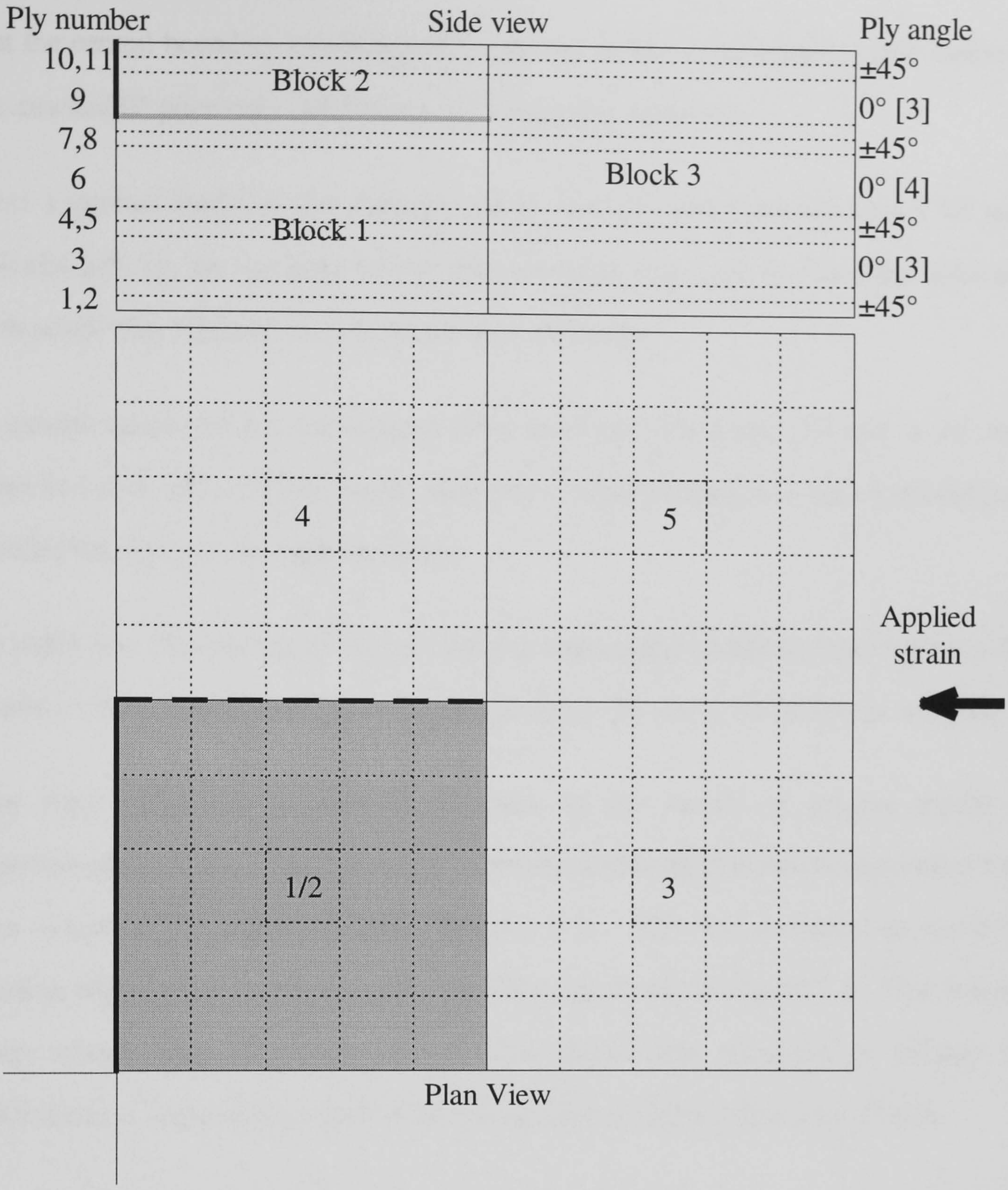

Figure 7.3. *Basic mesh showing the blocking relative to the ply lay-up, quarter model, symmetry about left and bottom edges*

The finite element analysis was undertaken in stages, gradually introducing more realism to the model, and including verification tests. The process of modelling the impact damage took the following form.

A quarter model of the cracked 0° plies above the delamination only (12.5 mm x 12.5 mm) [Block 2] was used to validate the buckling load for the delamination. To check

that the central boundary conditions of the quarter model were correct, a full model of the cracked 0° plies only (12.5 mm x 12.5 mm) was analysed.

Next a quarter model of the damaged plies built into specimen (25 mm x 25 mm) [Blocks 2-5, i.e. no laminate below delamination] was used to check the behaviour with actual edge boundary conditions for the local buckle.

A quarter model of the undamaged plies built into specimen (25 mm x 25 mm) [Blocks 1, 3-5, i.e. no delamination plies above delamination] was used to model post-buckled behaviour of the main laminate.

To check that the unbalanced plies do not give asymmetric results for local buckle a full model of the undamaged plies built into specimen (50 mm x 50 mm) was analysed.

The final stage was to include all parts of the model—a quarter model of superimposed blocks of both damaged plies and undamaged main laminate plies built into specimen (25 mm x 25 mm) [Blocks 1-5]. This was extended to move the loading edge further from the zone of interest, as shown in Figure 7.2. This was the main model used in investigations. The model was modified to enlarge the delamination, making the width of the delamination 30mm rather than 25mm.

In addition a single superimposed block full model of both damaged plies and undamaged main laminate plies built into specimen (50 mm x 50 mm) was analysed, to verify that there were no effects from the modelling of an unbalanced laminate above and below the delamination.

In the quarter model the constraints are chosen so that the edges that follow the centre-lines of the coupon are free to move in the z-direction but are not free to rotate around the centre-line. These constraints are shown on Figure 7.4.

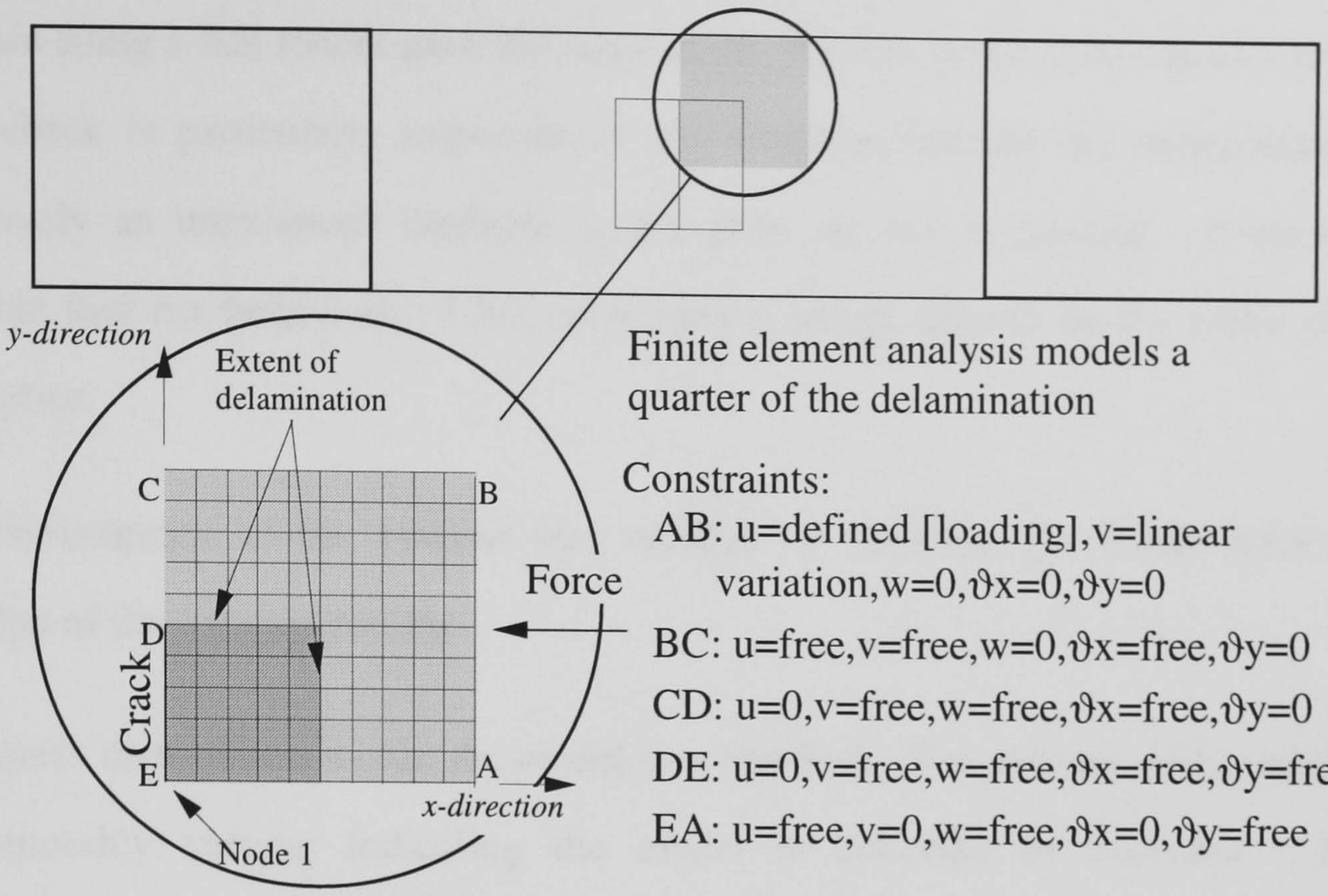

Figure 7.4. *Use of constraints to simulate a crack. Similar constraints are applied to the longer quarter model used in later modelling.*

7.3.4. Validation of finite element model

The model of the delamination caused by an insert has been validated in the following ways.

The finite element code has been checked against closed form solution benchmarks.

The mesh refinement was varied: repetition of the analysis with finer meshes has revealed that increasing the mesh refinement beyond 8 by 8 elements for the quarter model does not change the results achieved (within a tolerance of0.1%). (10 x 10 elements were used in later analyses so that growth of the delamination could be simulated in smaller steps.)

Asymmetry of the quarter models due to the stacking sequence—as the top 45° ply could have the fibres aligned towards the corner with the centre nodes, or

perpendicular to this direction—was checked using a full-model. Repeating the analysis using a full model gave the same nodal displacements as the quarter model. This check is particularly important in this situation because the delamination is effectively an unbalanced laminate as the plies are not symmetric. It could be possible that the behaviour of the delamination might depend on the order of the ±45° plies.

The convergence of the analysis was verified by checking the results after each iteration of the solution routine.

The stress distribution within the model was checked. The stresses within each ply are smoothly varying indicating the model is behaving as expected. More importantly the results match qualitatively with those expected for the model, with peak compressive stresses in those regions whose deformation indicated a superposition of axial and bending compression.

The initial deformation on the mesh which simulates loading should produce a uniform stress field. If it does not there is the possibility of interaction between the loading points and the area of interest. The models shown in Figures 7.3, 7.4 and 7.6 were extended to ensure this was the case, as shown in Figure 7.2. The meshing in the extended region is similar to the area shown.

7.4. Finite Element Results

The finite element analysis described here can be checked against the behaviour of actual specimens that have implanted damage of a similar geometry. The experimental results give a few areas in which to compare results: the load for initial buckling of the delamination; the failure load of the specimen; the point of failure of

the specimen; the effect of varying damage size and position and the out-of-plane displacement.

7.4.1. Buckling of delaminated plies

Experiments showed that if the 0° plies close to the surface were cut to simulate a ply-crack, they buckled after the ±45° plies at the surface (if there was a delamination present) at low loads. The buckling was visible as a ridge on the otherwise smooth bulge of the ±45° plies. If no ply-crack was present the initial buckling of the delamination occurred at a much higher load. The finite element model of only these plies (on the basis that a delamination on each side of the broken plies will mean that they are effectively independent of the rest of the coupon) gives a figure for a buckling load of approximately 2.00 kN, as is shown in Figure 7.5. The experimental results give a similar value. As can be seen the ply shows a classic Euler buckling behaviour as the initial out-of-plane displacement is reduced.

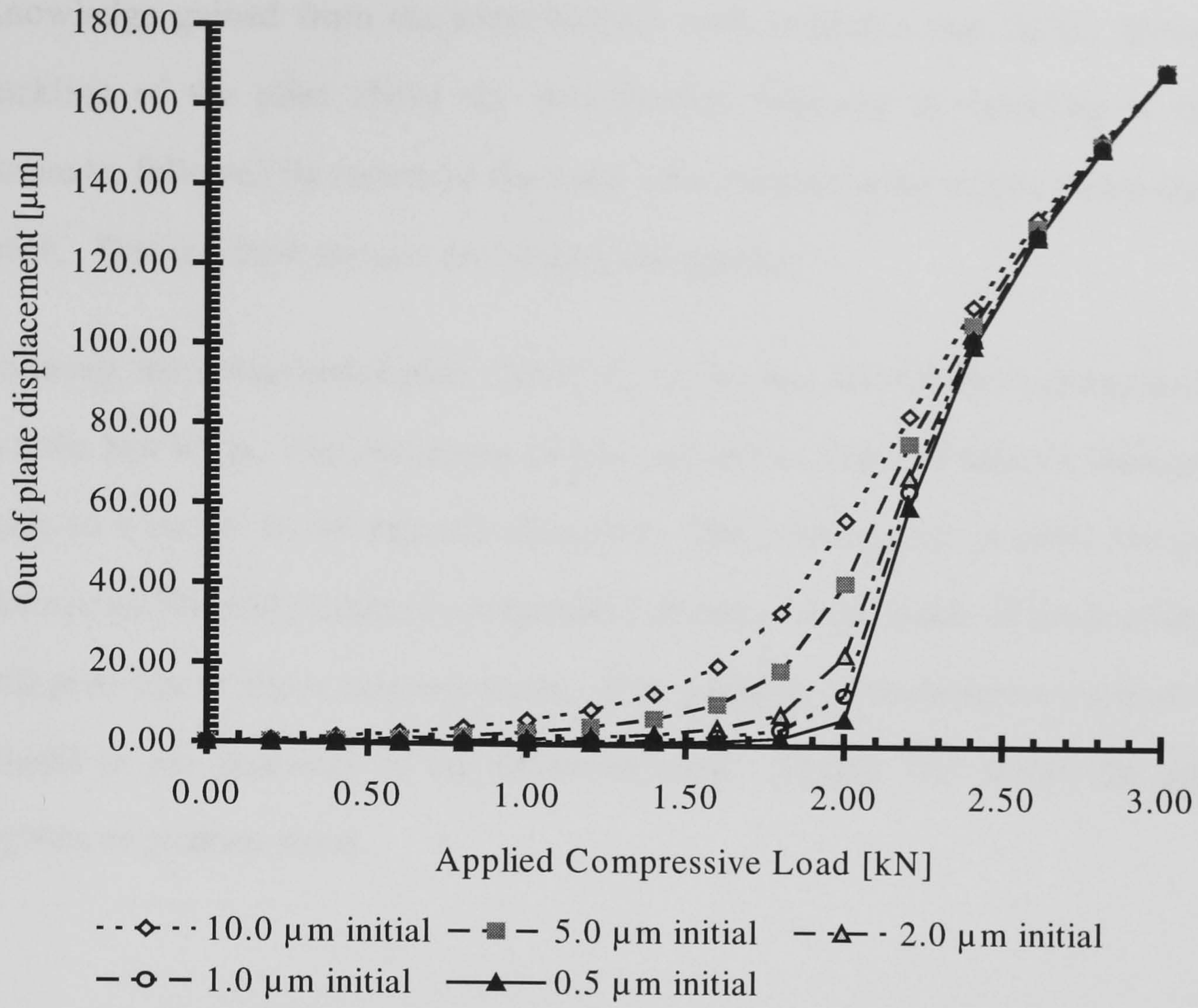

Figure 7.5. Buckling of 3 broken 0° plies (only) between two delaminations of 25 mm by 25 mm. Various initial displacements of central node are shown. T300/913c properties used.

The reason for this classic Euler buckling behavior is that this model considers only the 0° plies between the matrix cracks, so there are no side constraints.

7.4.2. Distribution of stresses within the model

The finite element model allows calculation of the stresses within the model for each increment of far field displacement. The component of the stress field that are of most interest are σ_{xx}, since the theory proposed on the basis of experimental results is that failure of the specimen will be linked to the failure in compression of the 0° fibres. It may be the case that ply cracking and delamination growth could occur, and these are likely to affect the stress distribution, but the specimen is still expected to fail when 0° fibres break because of the sudden and large loss of load carrying by those fibres and the transfer of that load to the rest of the specimen.

Knowledge gained from the experimental work indicates that failure proceeds by buckling of the plies above the delamination followed by buckling of the sub-laminate, followed by failure of the main sub-laminate in the region below the initial crack. This is where stresses are likely to be greatest.

To recap, the delaminated plies (,±45°,$0°_3$ on the rear side of the coupon) buckle out at quite low loads. The remaining 13 plies are left in an out of balance loading which leads to a buckle in the opposite direction. The combination of direct compressive stresses and bending-induced compressive stresses on the inside of the bending plies, will give rise to stress concentrations. The positions of these stress maxima will be related to the geometry of the deformed mesh. Figure 7.6 shows the predicted regions of greatest stress.

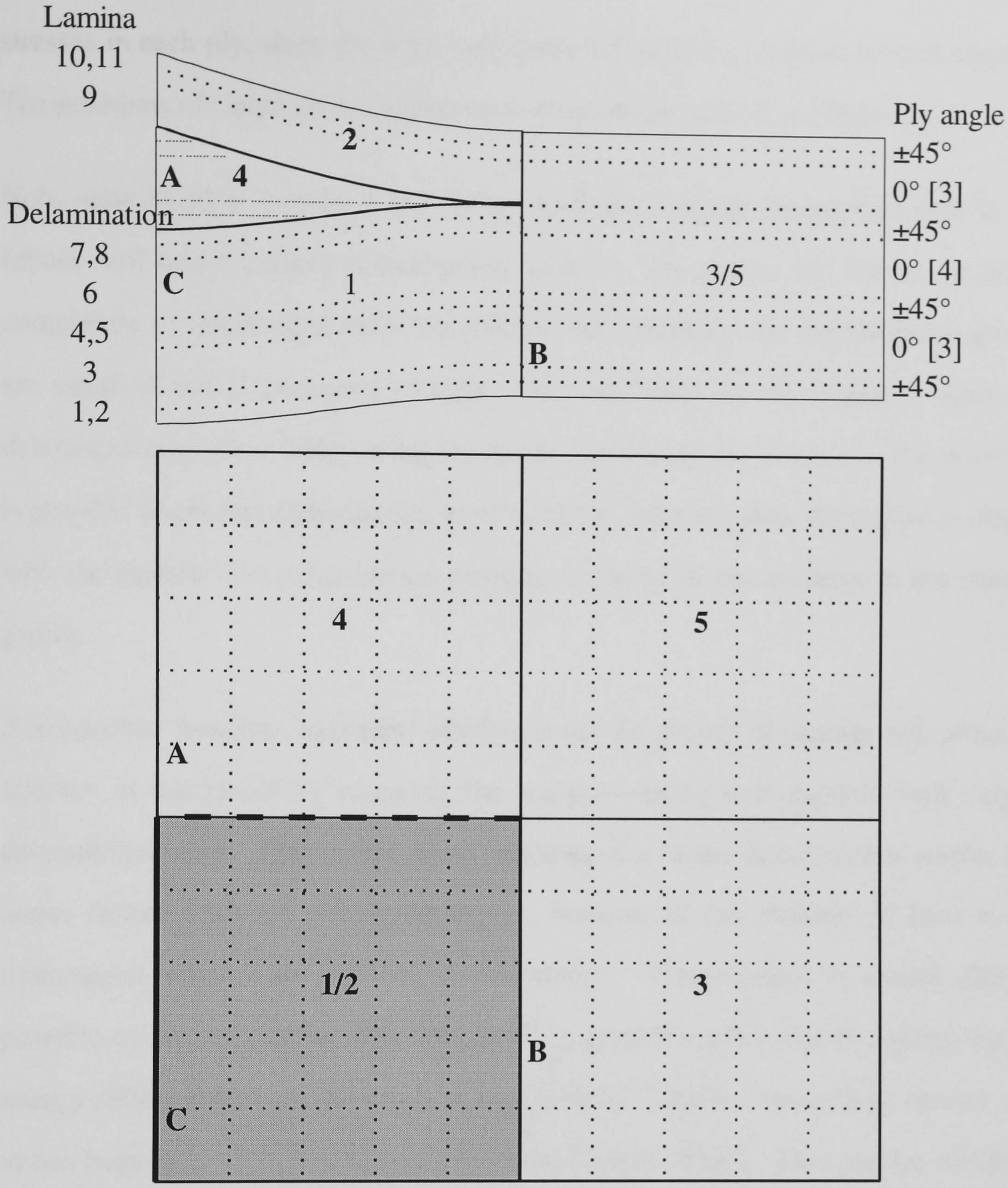

Figure 7.6. *Predicted locations (A,B and C) of stress concentration due to bending-induced compressive stresses, the deformed state of mesh is shown. See Figure 7.3 for key.*

Since the far field displacement is calculated from the behaviour of an undamaged coupon the stresses in the coupon can be related to the load applied to the coupon. This means that the failure of the specimen can be predicted from the load at which the stress, at the point in the specimen where it is greatest, reaches the failure stress for the material. Failure is predicted on the grounds of the greatest compressive stress in the loading direction in the 0° plies. The model allows evaluation of the

stresses in each ply, since these are calculated for each Gauss point in each element. The positions of Gauss points within each element are defined in chapter 6.

Note, delamination growth is not being predicted, and the assumption here is that failure will occur without delamination growth. The reason for this is the added complexity of checking at each increment if the conditions for delamination growth are satisfied and if necessary changing the constraints on the model to allow the delamination to grow, while at the same time calculating the stresses in the model. It is possible to predict delamination growth, but in order to allow the model to change with the growth of a delamination requires a change in the meshing as the damage grows.

It is possible, however, to predict whether or not the growth of damage will affect the stresses in the model by repeating the analysis—using twin models with varying delamination size. This would allow checking if a larger delamination results in a lower failure load (as we would expect, because of the shifting of load to the undamaged regions around the delamination). Theoretically, it would also be possible to predict whether this delamination growth could occur by comparing the energy release rate from the crack growth with the critical strain energy release rate, as has been done in previous work [Pavier & Chester, 1990]. This may be combined with the stress analysis approach described here. Such a combined analysis would, however, be very complex and therefore was not attempted.

7.5. Results

As predicted, the actual load applied to the model by applying a far-field displacement was less than that calculated using classical laminate theory. The theory does not account for the damage or the out of plane displacement of the

coupon—it only uses the effective stiffness of the material. Figure 7.7 shows the calibration curve used for converting nominal loads to actual loads. For clarity only the curves for the undamaged coupon and the 25mm and 30mm delaminations with ply and matrix crack are shown.

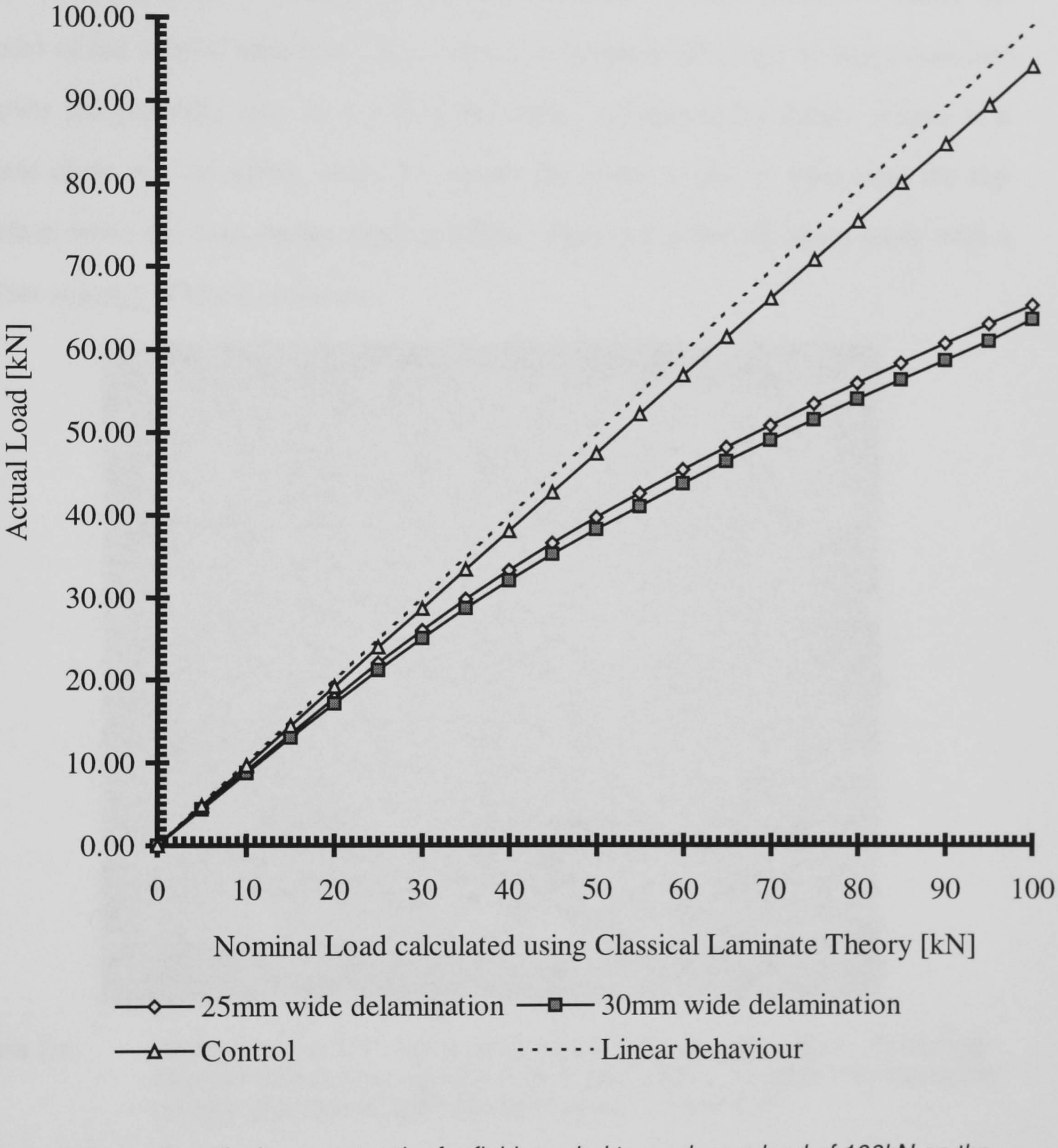

Figure 7.7. *The displacement at the far field needed to produce a load of 100kN on the specimen was calculated using classical laminate theory. Increments of this displacement were applied and the resultant forces on the mesh measured.*

The control (undamaged specimen) follows the nominal load quite closely, and is asymptotic to linear behaviour at low loads, but the error increases with load due to the slight out-of-plane deformation of the mesh. The error in the other models is

PAGE NUMBERING AS ORIGINAL

greater due to a greater reduction in stiffness of the model as the delamination buckles out.

7.5.1. Stress distributions within the models.

The following plates[1] show the compressive stresses in the x-direction within the model of the control specimen. For ease of comparison the range of stress contours shown are generally zero to 1.1 GPa full scale. (Compressive failure occurs at a stress close to 1.05 GPa) Plate 7.1 shows the stress in the 0° plies near the top surface when the load on the mesh is 72kN. Plate 7.2 is for the same mesh with a closer spacing of stress contours.

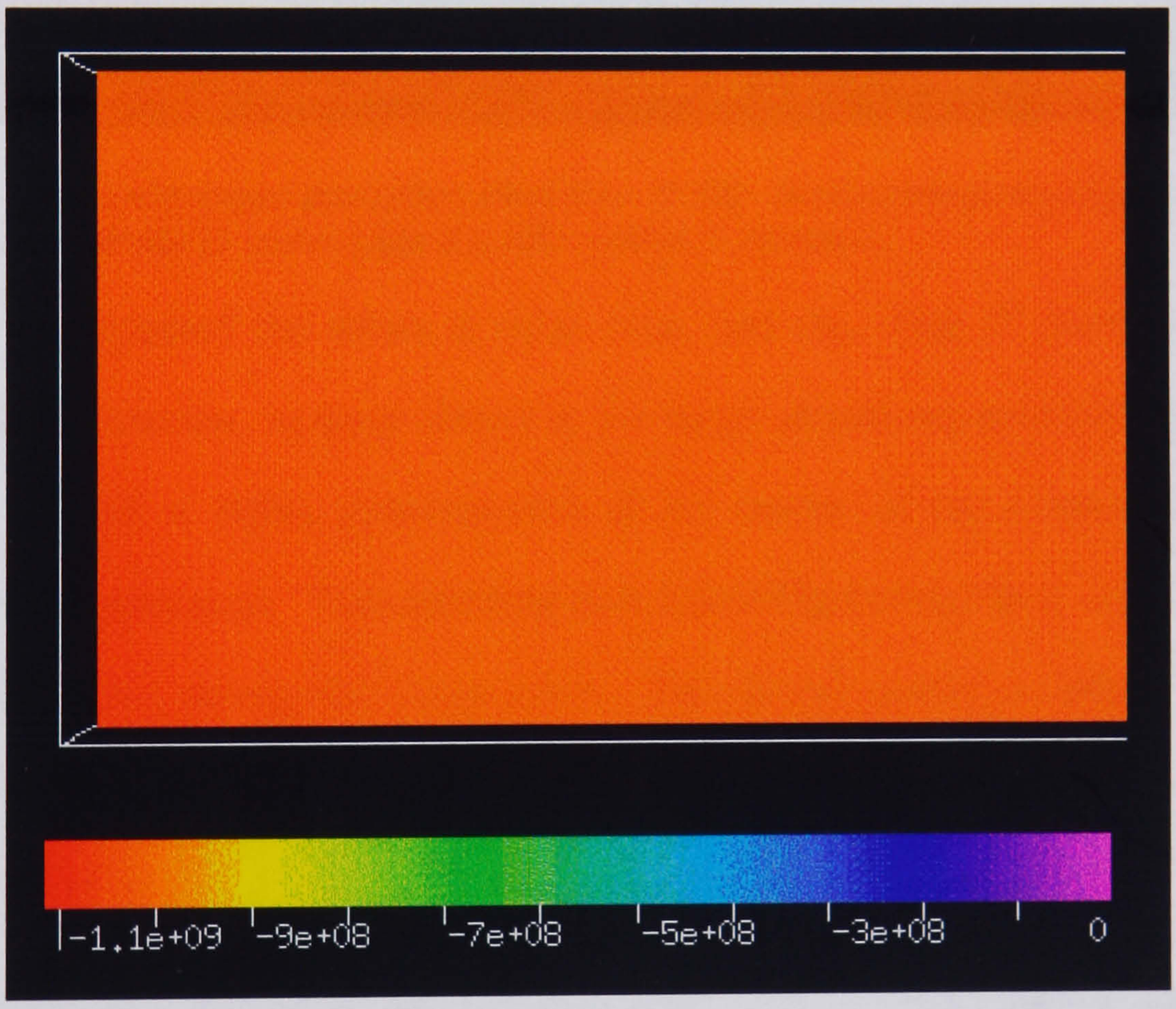

Plate 7.1. *Stress distribution in the top 0° plies of an undamaged coupon. Full range. Quarter model with centre-lines at left and bottom. Loading is compressive on right edge (similarly for all plates except 7.3 and 7.4)*

---

[1] In plates 7.1 to 7.8 the white box around the fringe plot shows the boundary of the specimen, which is scaled by a factor of 10 in the thickness direction for clarity.

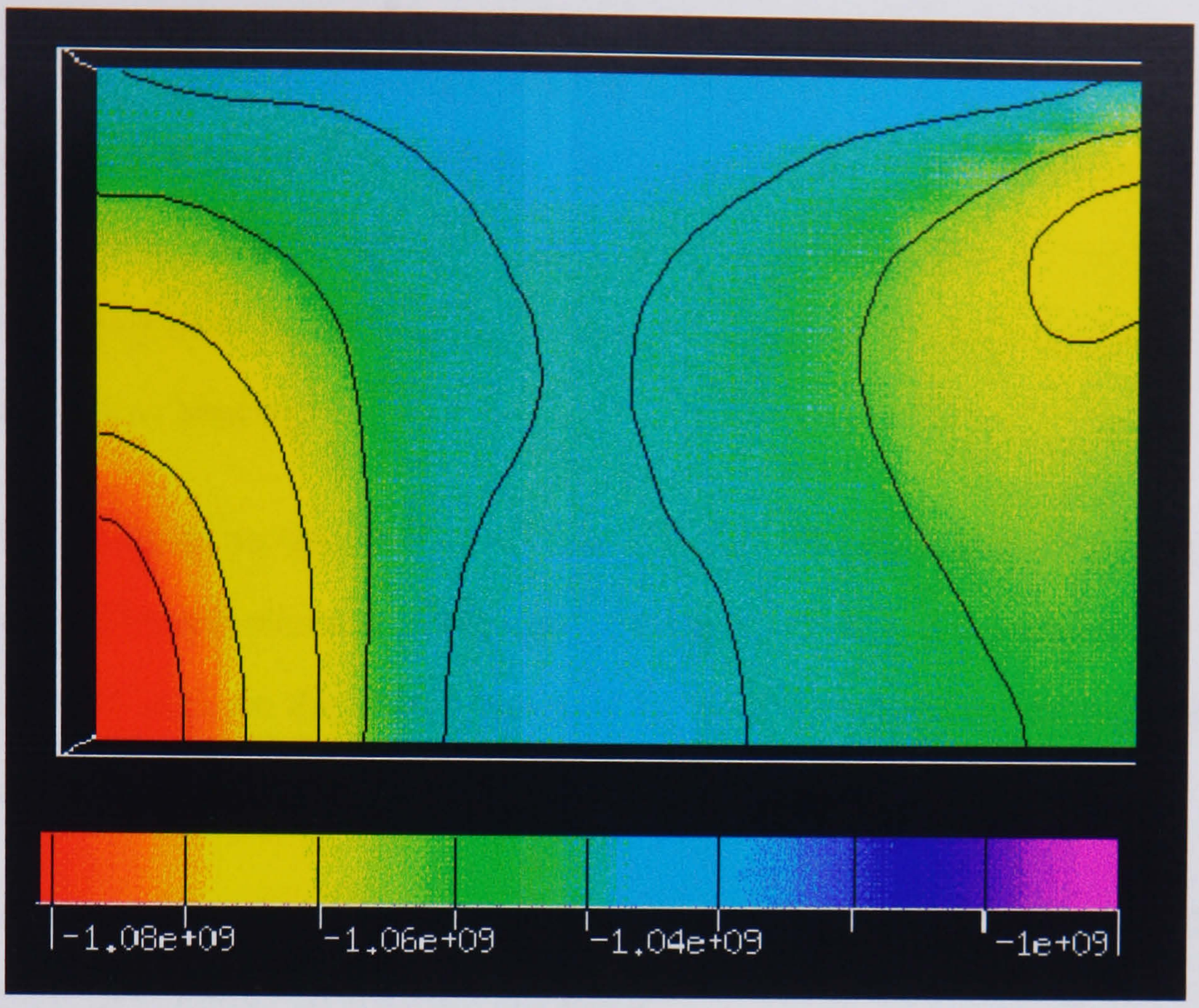

Plate 7.2 *Undamaged specimen loaded to 72 kN. Scale shows stresses close to peak stress to accentuate the differences in stresses.*

As would be expected the stress is quite even, and the other 0° plies show a very similar result. However, looking closely at the range of stresses near the failure stress, Plate 7.2, reveals a stress concentration at the centre of the coupon due to the buckling of the specimen. This superimposes a bending compressive stress on the in-plane compressive stress, for these plies. The actual specimen failed across the specimen at this point (the failure is sudden and it was not possible to observe the point of initiation).

Plates 7.3 through 7.7 show the stresses in a coupon containing a delamination between laminae 8 and 9, and a ply and matrix crack (see Figure 7.3), when loaded to 35kN (calculated). Plates 7.3 and 7.4 show stresses through the thickness of the coupon (z-dimension exaggerated for ease of viewing) Plate 7.3 is a cross section along the length of a specimen with a 25mm delamination, following the matrix crack, and shows how the load is carried primarily by the 0° plies, and also shows how the presence of the delamination causes a stress concentration in the 0° plies above the

delamination. There is also a slight increase in stress in the central 0° plies below the delamination, due to the main laminate buckling downward. The compressive stress in the bottom 0° plies is reduced because of the superposition of bending-tensile stresses. Away from the delamination zone in the bottom 0° plies the stress is again increased due to bending.

Plate 7.4 is a cross section of the mesh taken at the left edge (sectioned through the ply crack). The delamination in this case is 6 elements wide and is above the central plies and ±45° plies on the right of the picture. This indicates that the stresses in the delaminated plies are low and that effectively they carry no load.

The remaining plates show the mesh viewed from above, with the delamination in the bottom left hand corner (it is a quarter model).

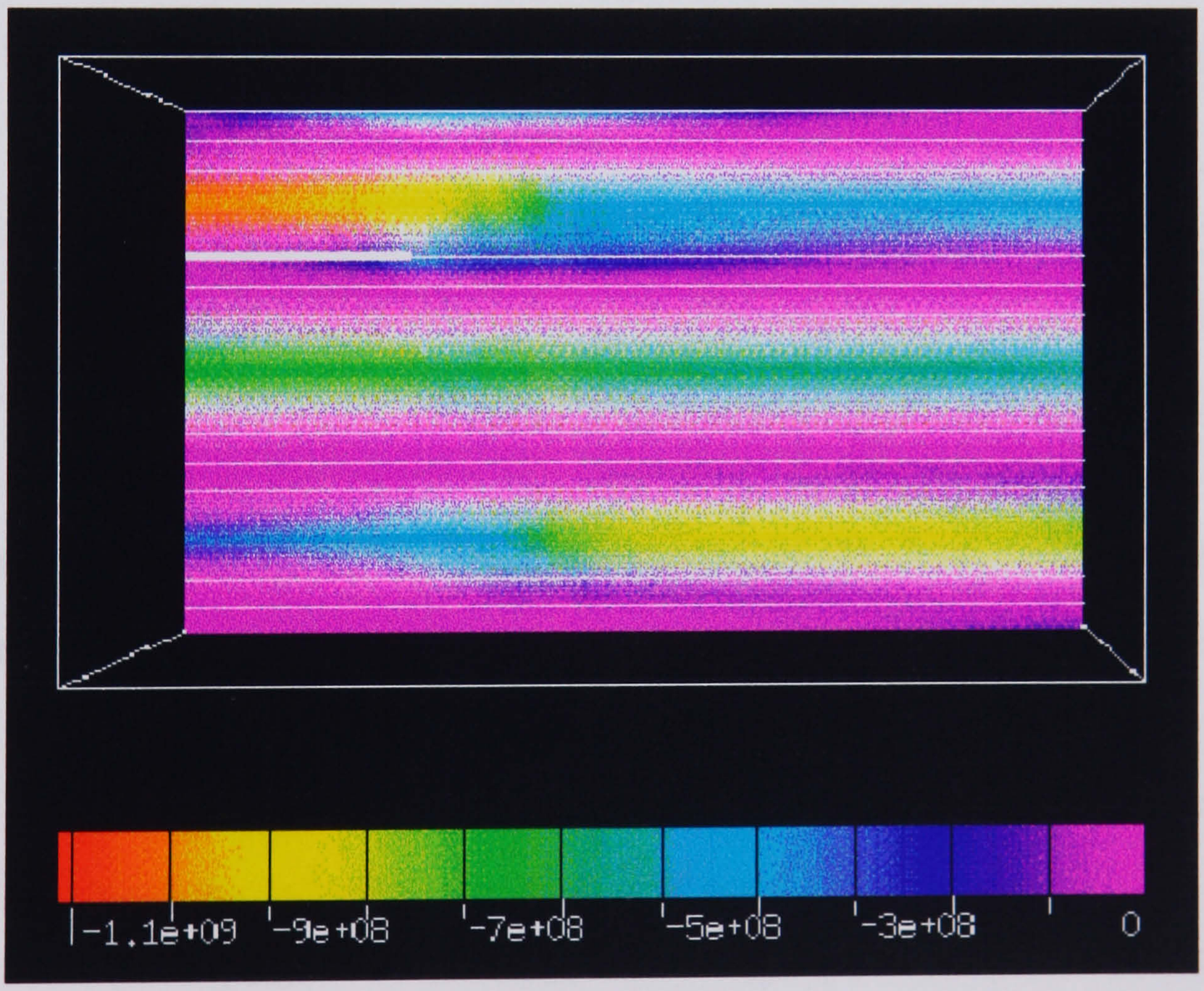

Plate 7.3. *A section along the length of the specimen at the mid-plane of the FE mesh; i.e. along the edge of the delamination, but through the undamaged region. See Plate 7.7 for position of cross section. The delamination, shown for reference only, at top left, is a thick white line. Ply bundaries shown in white*

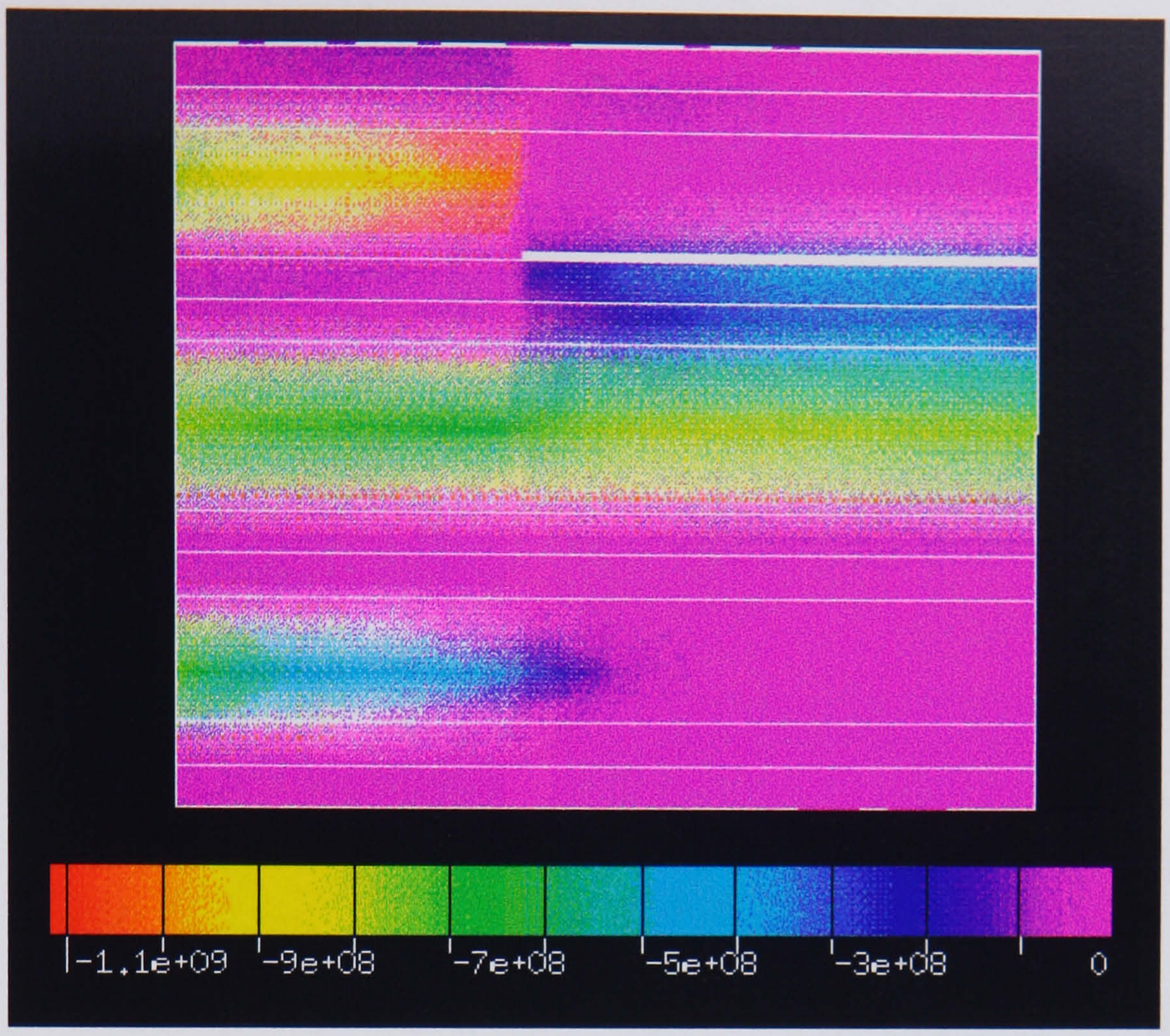

Plate 7.4. *A section across the specimen (the left edge of plates 7.8), which contains a wide delamination (shown as thick white line), in the plane of the crack. Ply boundaries shown in white*

Plates 7.5 - 7.7 compare the stresses in the 0° plies. The greatest stresses are clearly in the 0° ply above the delamination, the one containing the crack, in the region just beyond the end of the crack in the undamaged region. It must be emphasised that this is not an artefact of the presence of a singularity, because of the inclusion of the matrix crack in the model. Were it not for the matrix crack, there would be a continuous mesh across the width of the coupon in the top plies, but the loading would stop abruptly at the tip of the ply crack, due to the boundary conditions applied there. This can produce anomalous stresses from the numerical analysis, due to a numerical singularity, at a point of particular interest.

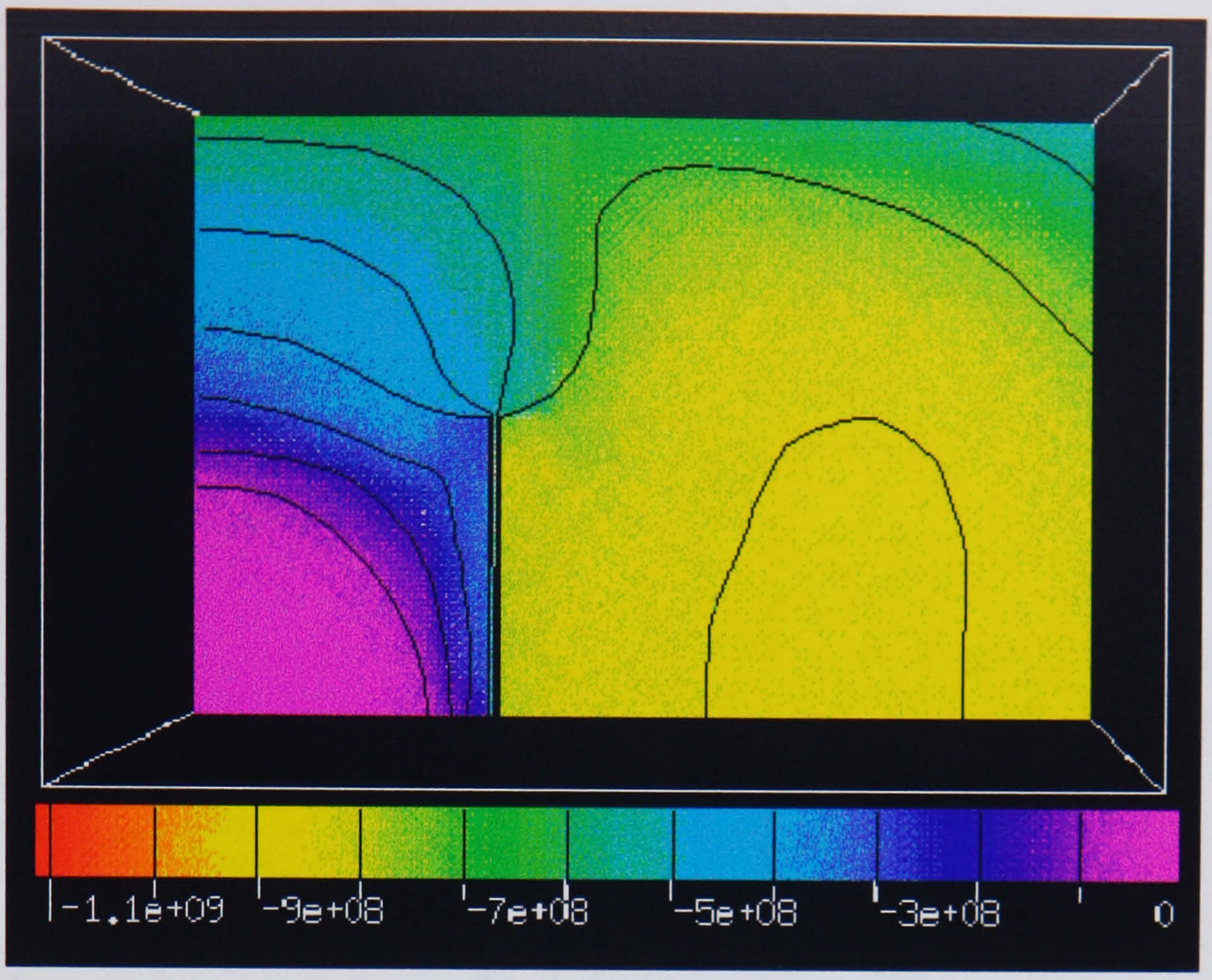

Plate 7.5. *Standard model—square delamination half the width of model in bottom left corner, with ply crack along left edge and matrix crack along top edge. Compressive stresses (xx) in ply 3 (bottom 0° plies, near impact face).*

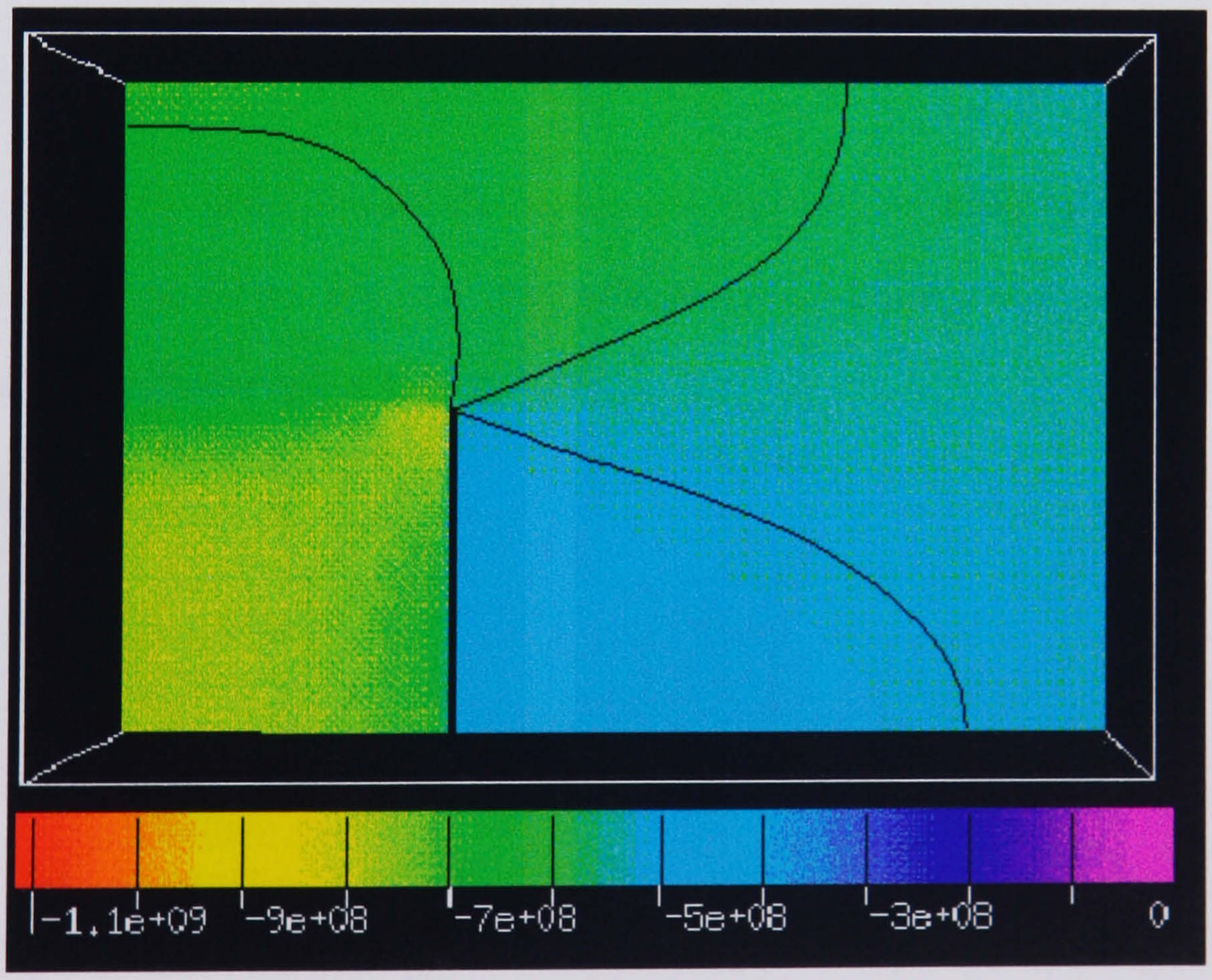

Plate 7.6. *Standard model—square delamination half the width of model in bottom left corner, with ply crack along left edge and matrix crack along top edge. Compressive stresses (xx) in ply 6 (central 0° plies).*

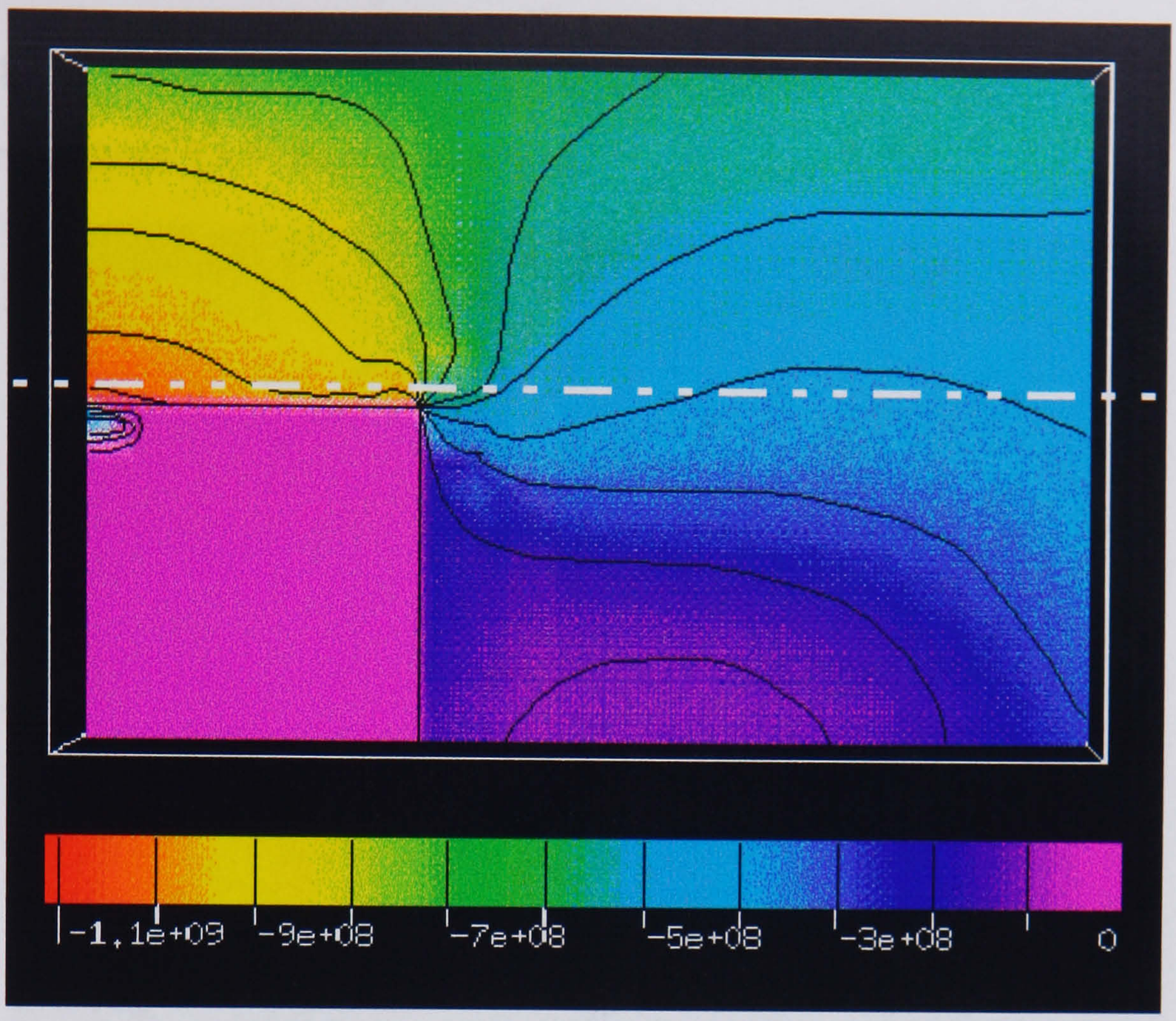

Plate 7.7. *Standard model—square delamination half the width of model in bottom left corner, with ply crack along left edge and matrix crack along top edge. Compressive stresses (xx) in ply 9 top 0° plies, far from impact face). Dashed line = section for plate 7.3*

The growth of the delamination during loading was also considered during the F.E. study. Figure 7.8 shows how the delamination area was increased. Attempts were not made to keep the original matrix crack.

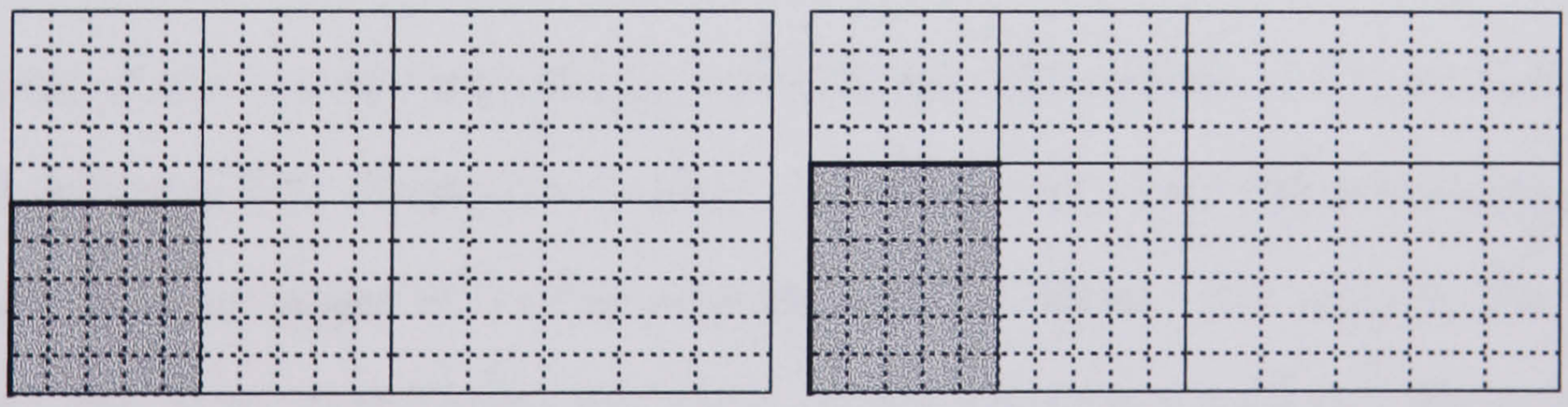

Standard model:
ply and matrix cracks plus
delamination (25mm x 25mm)

Wide model:
ply and matrix cracks plus
delamination (30mm x 25mm)

Figure 7.8. *Extension of delamination to model damage growth. Identical mesh density is used, different blocking prevents a larger area from being equivalenced.*

Plate 7.8 shows the growth of the delamination towards the edge of the specimen. (An increase from 5 x 5 elements to 5 x 6).

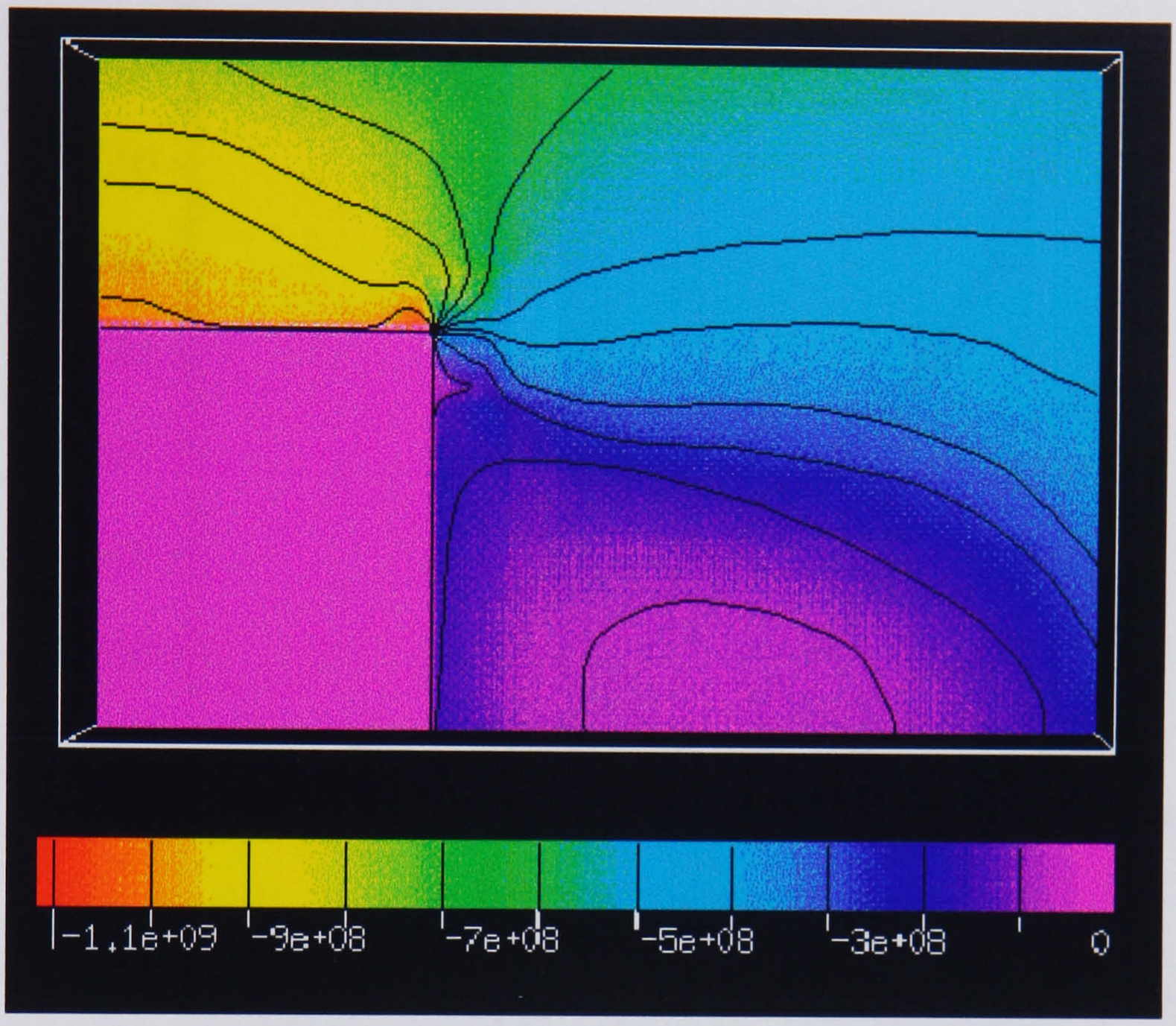

Plate 7.8. *Wide delamination model—rectangular delamination in bottom left corner, with ply crack along left edge and matrix crack along top edge. Compressive stresses (xx) in ply 9 (top 0° plies, far from impact face).*

7.5.2. Out of plane displacement

The form of the out-of-plane displacement of the delamination and main laminate is shown in Figure 7.9. There is not a sharp buckling point, since the delaminating plies are built in at the edges providing support, unlike a beam. The scale of the buckle matches that from experiment, and other work has shown a close correspondence using shadow Moiré fringe techniques [Lowe, 1994]. The finite element results are a good fit in the post-buckled region, but the prediction of buckling initiation is not good. This may be due to the simplifications made in the model (initial matrix crack, and ply crack through all plies above delamination) and possibly due to material imperfections.

PAGE NUMBERING AS ORIGINAL

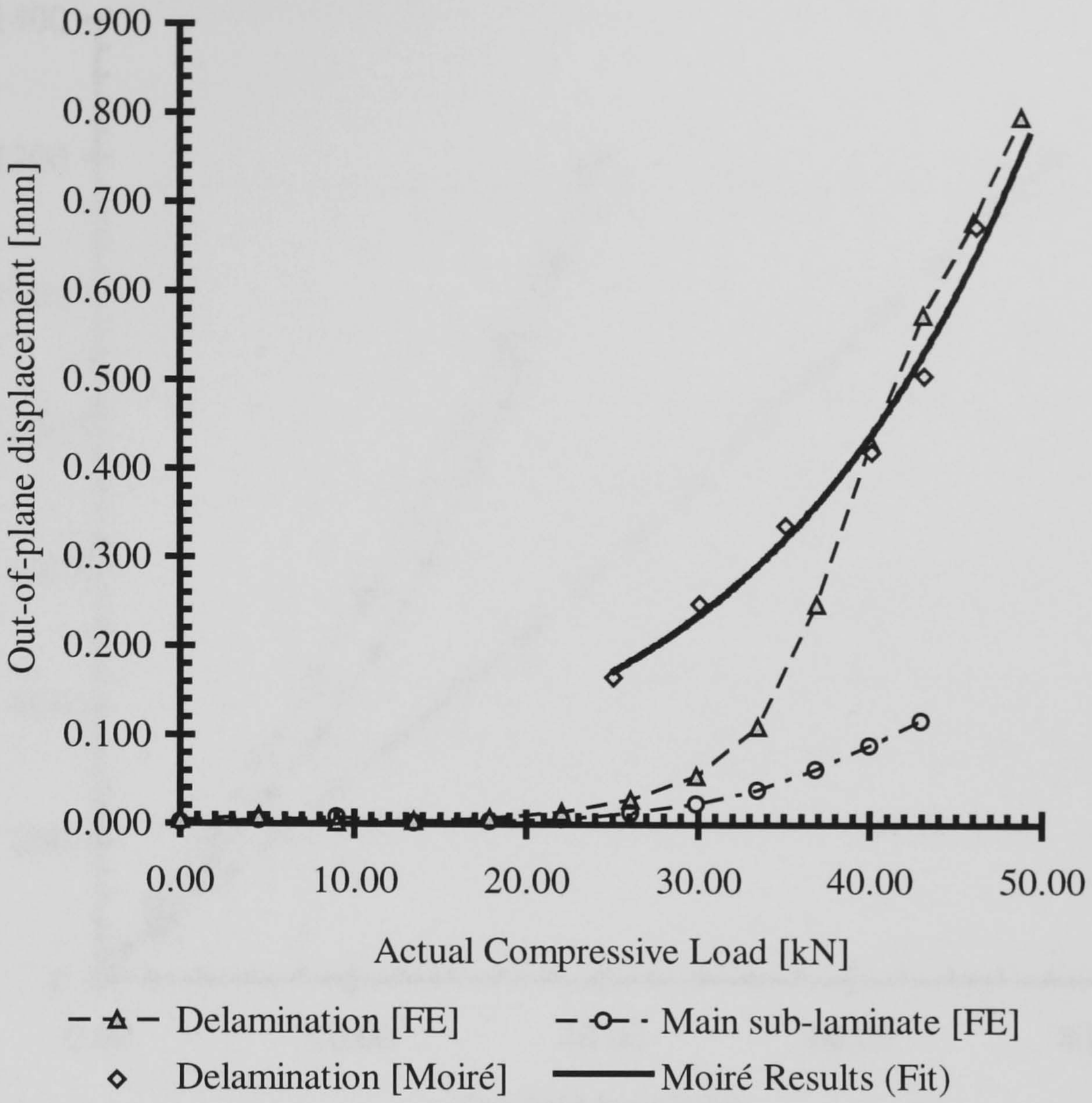

Figure 7.9. Out of plane displacement of central node with applied load. FE results for delamination and sub-laminate are corrected to actual load.

7.6. Prediction of failure of impact specimens

So far the presentation of results has been qualitative. They indicate that the FE model is giving reasonable results that match predictions based on the behaviour of the coupons as they fail. The stress values will now be examined to see how useful the model is in predicting failure.

Figure 7.10 is a graph of the peak compressive stress in the model against the applied load (taken from the applied displacement at far field and corrected for changes in the stiffness of the specimen, using the calibration curve in Figure 7.7).

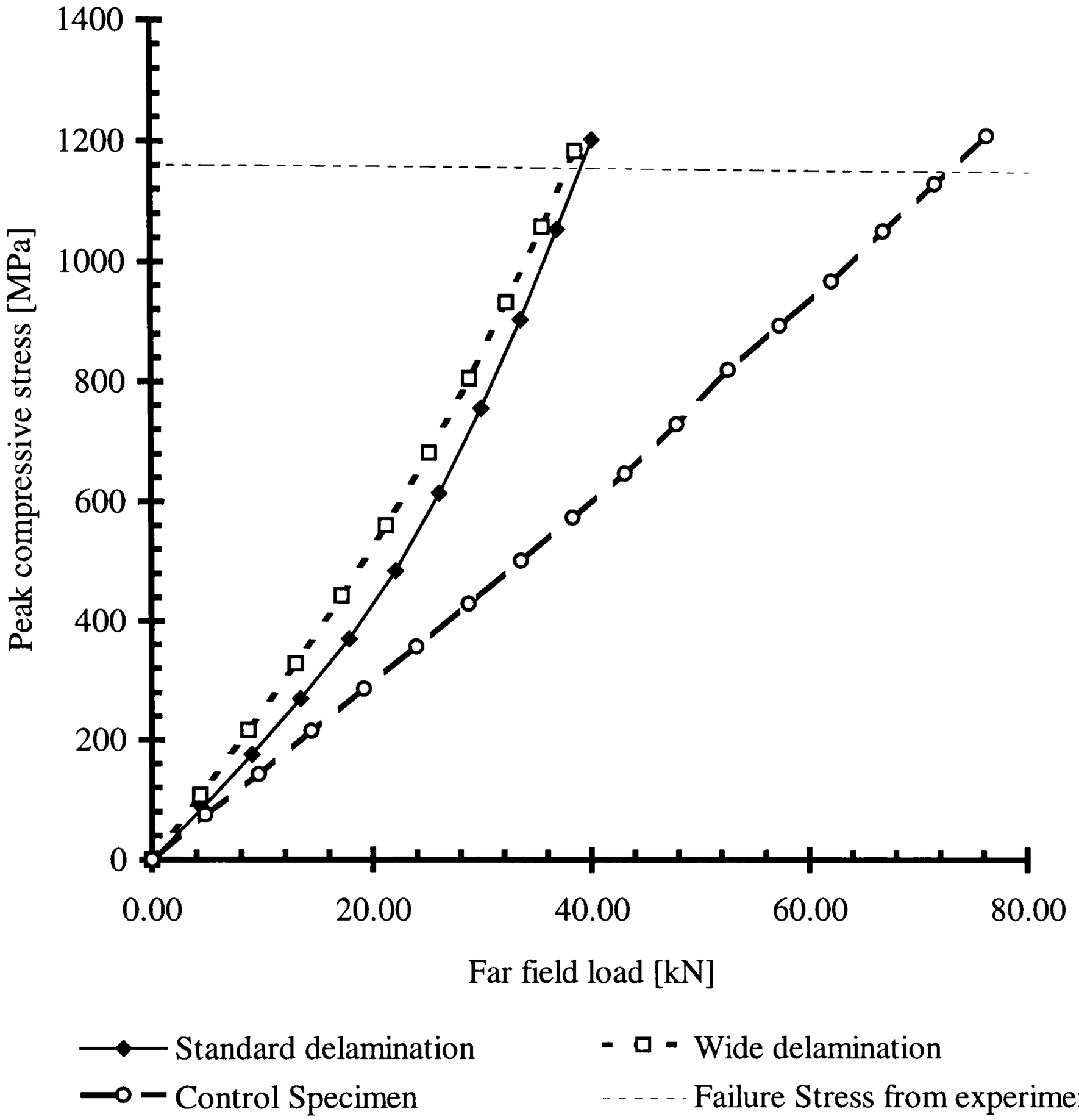

Figure 7.10. Peak stress within the coupon against applied load.

The horizontal line is the stress at which the experimental control specimen (undamaged) fails, taking the failure load from experiment, 72.1 kN from Table 5.3, and reading from the graph here (giving 1160 MPa). The actual far-field stress in the test was 640 MPa, but this experimental result is not a standard compressive stress test. The specimen was enclosed in an antibuckling guide with a large window so some out of plane bending of the specimen is expected, so the peak stress will be greater than the far field stress. There could be additional errors due to material constants used. Since all finite element models used the same material constants the

results from the finite element analysis can be compared to each other. The line can be used to predict the failure load of the other specimens by noting the load at which this stress is reached for other coupons, assuming that failure is caused by compressive failure of the fibres. The stress increases more quickly for applied load in the damaged specimens because of the buckling of the delamination and the remaining plies. The values for a wider delamination are higher at the same applied load, indicating a lower failure load, but the difference is small.

The failure load from this prediction is 38.2 kN for the standard delamination width with ply crack, and 37.5 kN for the wider delamination, which compares well with the experimental value for T300 of 35.7 kN. (a double delamination - assuming that the top delamination has no affect once that the bottom delamination opens up.).

The comparison with T800 is not so good, with a failure from experiment at 52.3 kN.

7.7. Discussion

The finite element work that is described here has given predictions that are close to experiment as far as of failure is concerned. Taking a failure stress in compression of 1200 MPa[2], we get a failure load for an undamaged coupon of 75 kN (compared to experiment, T300, 72.2kN), and for the specimen containing a deep delamination (i.e. 5 plies in sub-laminate) and ply crack 38 kN (compared to experiment, 35.7 kN).

It would not necessarily be expected that the substitution of T800 material properties into the calculation would give the same ratio. This is because the total stress depends on the contribution from bending stresses, which in turn depend on the

---

[2]Ciba Geigy Product Information Sheet Fibre-dux 913c Carbon Pre-preg Vf 60% FTA46F

extent of buckling. It would be informative to repeat the analysis for different material properties.

This is a good agreement and gives confidence in using the compressive failure stress for the fibres as a basis for predicting the failure of the whole specimen. The actual value used for the compressive failure stress of the material is open to question because of the wide variety of methods used in obtaining it, as well as the variation that exists between different manufacturing methods and test specimens. However, the form of the stress-load curve for damaged composites works to reduce these limitations. As can be seen from Figure 7.11, where the stress against applied load increases sharply, a large error in the failure stress produces a smaller error in the predicted failure load.

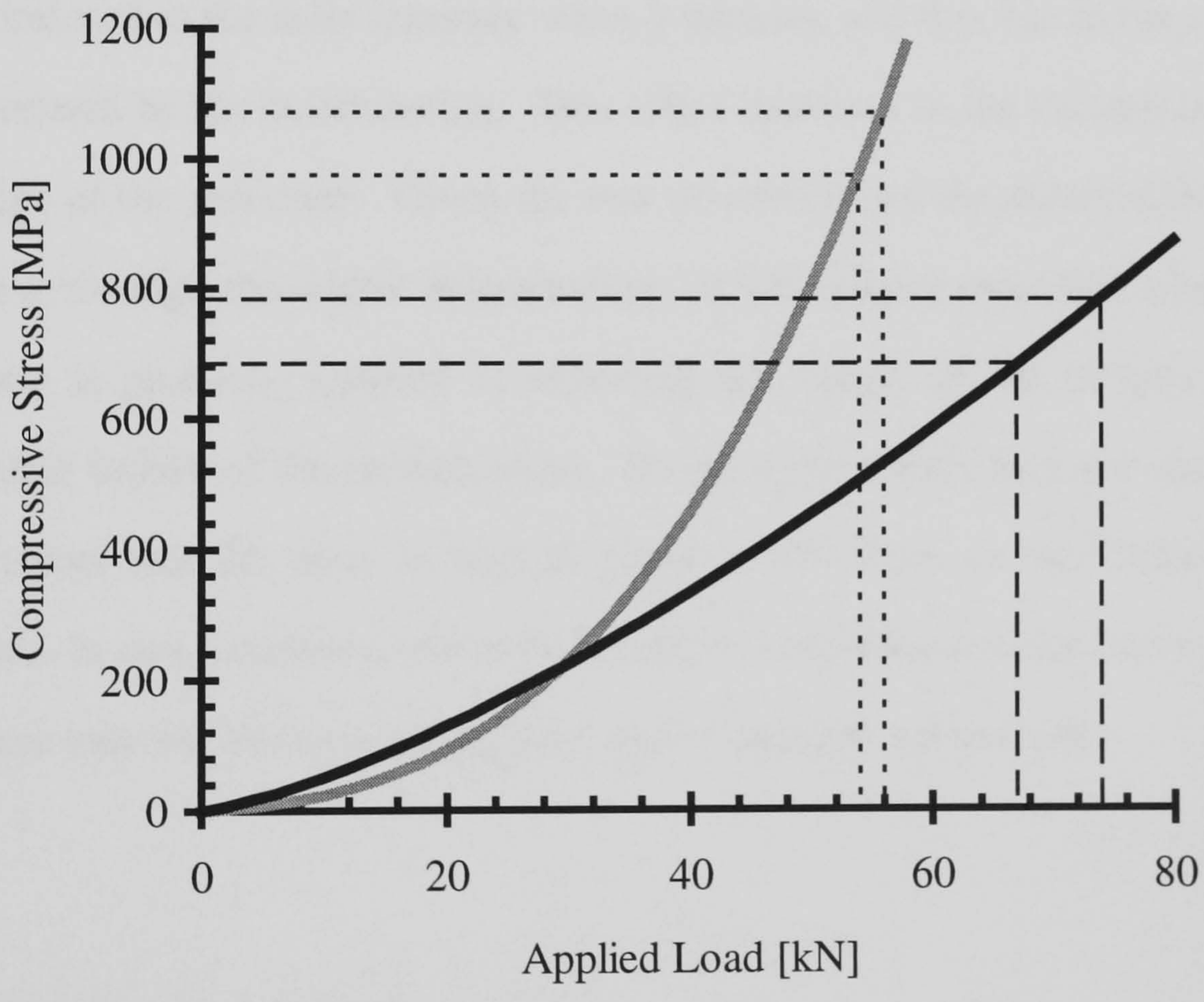

Figure 7.11. *Illustration of how the same error in failure stress can produce different errors in predicted failure load. If failure stress is known to ±50Mpa, for the grey curve the error in predicted failure is ±1.5kN, for the black curve it is ±4.5kN*

The compressive stress in a damaged coupon rises sharply at high loads close to failure due to the buckling of the main laminate, so even if the exact value for the

compressive failure stress is not known, the error in the predicted failure load can be relatively small.

Taking the failure of the undamaged specimen as the baseline it is possible to predict a value for failure of the damaged specimen of 37 kN. This is justified in that both specimens are identical in size and manufacture and the test method is the same. It should be possible to check the validity of this method more thoroughly by looking at different damage configurations and materials.

A further enhancement to the finite element analysis would be to study the effect of the failure of the delaminated layer, which buckles out at low loads, but seems to fail just before initiation of final failure for the coupon. This could be modelled simply by growing the delamination all the way to the edge. The coupon fails due to the stresses induced in the main laminate when it buckles, and this due to the unbalanced loading caused by the delamination. This effect increases as the delamination grows to the edge of the specimen. Given the loss of stability for the delamination when it becomes a 'through-the-width' delamination—it will behave more like a beam than a plate—one is probably justified in expecting the failure of the coupon to follow shortly after failure of the delamination. (In the experiments here the anti-buckling guide ensures that the plate is kept in plane at the edges so this failure mode is prevented. In real situations, where the damage is embedded in the centre of a large plate, there may not be this edge support, unless stringers are present.)

7.8. Concluding Remarks

The finite element analysis described here has predicted deformation of the specimen that is broadly similar to that observed in experiments. The magnitudes of out-of-plane displacements match well at high load (when the delamination has buckled in

the experiments). The stress distribution within the model correlates well with the deformation, and the peak stress zone matches with the position in the model where damage growth is observed to occur during stepped loading.

Predictions made from the finite element results of the expected failure load for damaged specimens, based on the performance of undamaged specimens, were in good agreement with experimental results.

Further work could be carried out to verify this work for other materials and stacking sequences. It could be usefully extended by investigating the effect of multiple delaminations or by modelling growth of the delamination, which can be done by repeating analysis with successive growth of the delamination and calculation of the of the strain energy release rate. Useful information could be gained from a simpler analysis where the width of the delamination is varied.

References

Allix O. and Ladeveze P.

Interlaminar Interface Modelling for the Prediction of Delamination.

Composite Structures **1992** Vol. 22(4) pp. 235-42.

Pavier M.J. and Clarke M.P.

"Experimental techniques for the Investigation of the Effects of Damage on Carbon Fibre Composites."

Composites Science and Technology. Vol. 55 **1994** pp. 157-169

Choi H.Y. and Chang F.K.

"A Model for Predicting Damage in Graphite/Epoxy Laminated Composites Resulting from Low Velocity Impact Damage."

Journal of Composite Materials Vol. 26 November **1992** pp. 2134-69.

Guedra-Degeorges D., Maison S., Trallero D. and Petitniot J.L.

"Buckling and Post-buckling Behaviour of a Delamination in a Carbon-Epoxy Laminated Structure: Experiments and Modelling."

AGARD CP-530 May **1992**; pp. 7.

Kutlu Z. and Chang F.K.

"Modelling Compression Failure of Laminated Composites Containing Multiple Through-the Width Delaminations."

Journal of Composite Materials Vol. 26 March **1992** pp. 350-87.

Lowe A.T.

"The Effect of Single Embedded Delaminations on the Compressive Strength of CFRP."

Undergraduate Project Report 94/2 Bristol University June **1994** pp.1-45.

Nilsson K.F., Storåkers B.

"On Interface Crack Growth in Composite Plates."

Journal of Applied Mechanics Vol. 59 September **1992** pp. 530-8.

Nilsson K.F., Thesken J.C., Sindelar P., Giannakopoulos A.E., Storåkers B.

"A Theoretical and Experimental Investigation of Buckling Induced Delamination Growth."

Journal of the Mechanics and Physics of Solids Vol. 41 **1993** pp. 749-82.

Pavier, M.J.

STYX Users Guide

Department of Mechanical Engineering, University of Bristol, **1993**

Pavier, M.J. and Chester, W.T.

"Compression Failure of Carbon Fibre Reinforced Coupons Containing Central delaminations."

Composites Vol. 21(1) January **1990** pp. 23-31

Reddy J. N.

"An Evaluation of equivalent-single-layer and layerwise theories of composite laminates."

Composite Structures Vol. 25 July **1993** pp. 21-35.

Whitcomb J.D.

"Finite Element Analysis of Instability Related Delamination Growth."

Journal of Composite Materials Vol. 15 September **1981** pp. 403-26.

Whitcomb J.D.

"Approximate Analysis of Post-buckled Through Width Delaminations."

Composites Technology Review Vol. 4(3) September **1982** pp. 71-7.

Whitcomb J.D.

"Parametric Analytical Study of Instability Related Delamination Growth."

Composites Science and Technology Vol. 25 September **1986** pp. 19-48.

Whitcomb J.D.

"Three-Dimensional Analysis of a Post-buckled Embedded Delamination.".

Journal of Composite Materials Vol. 23 September **1989** pp. 862-89.

Whitcomb J.D.

"Analysis of a Laminate with a Post-buckled Embedded Delamination,

Including Contact Effects."

Journal of Composite Materials Vol. 26 September **1992** pp. 1523-35.

CHAPTER 8.

FATIGUE TESTING

8.1. Introduction

Low velocity impacts will cause damage, in the form of delaminations matrix cracks and possibly fibre cracks. It is possible that this damage will be undetectable from the visible surface. The effect of this damage on the static strength of a plate can be measured and predicted. However, under fatigue loading the damage zone is likely to increase in size, and this means that fatigue tests on coupons is necessary if failure predictions are to be meaningful. This investigation is aimed at discovering how the mode of damage growth compares to that under stepped compression loading, in order to ascertain whether findings from static tests and stepped compression can be applied to fatigue regimes. Quantitative information of the relationship between fatigue loads and cycles to failure was not possible in the time frame of this investigation, but information on the mode and rate of damage growth was gained.

This chapter describes the specimens used in fatigue investigations and the techniques employed to measure the extent of damage during cyclic loading. The results of fatigue testing, in the form of diagrams of damage growth and plots of damage against cycles, are also included.

8.2. Fatigue in composites

Fatigue failure of a component is caused by the repeated loading and unloading of the structure during service life. These loads are individually insufficient to cause failure, but their cumulative effect is to cause failure. This cyclic loading can have more than one component, each with its own characteristic time period and load magnitude. As an example, consider the loads on the hull of a submarine. These include loads during surface travel, during underwater travel and during emergency dives, and could be something like those shown in Figure 8.1.

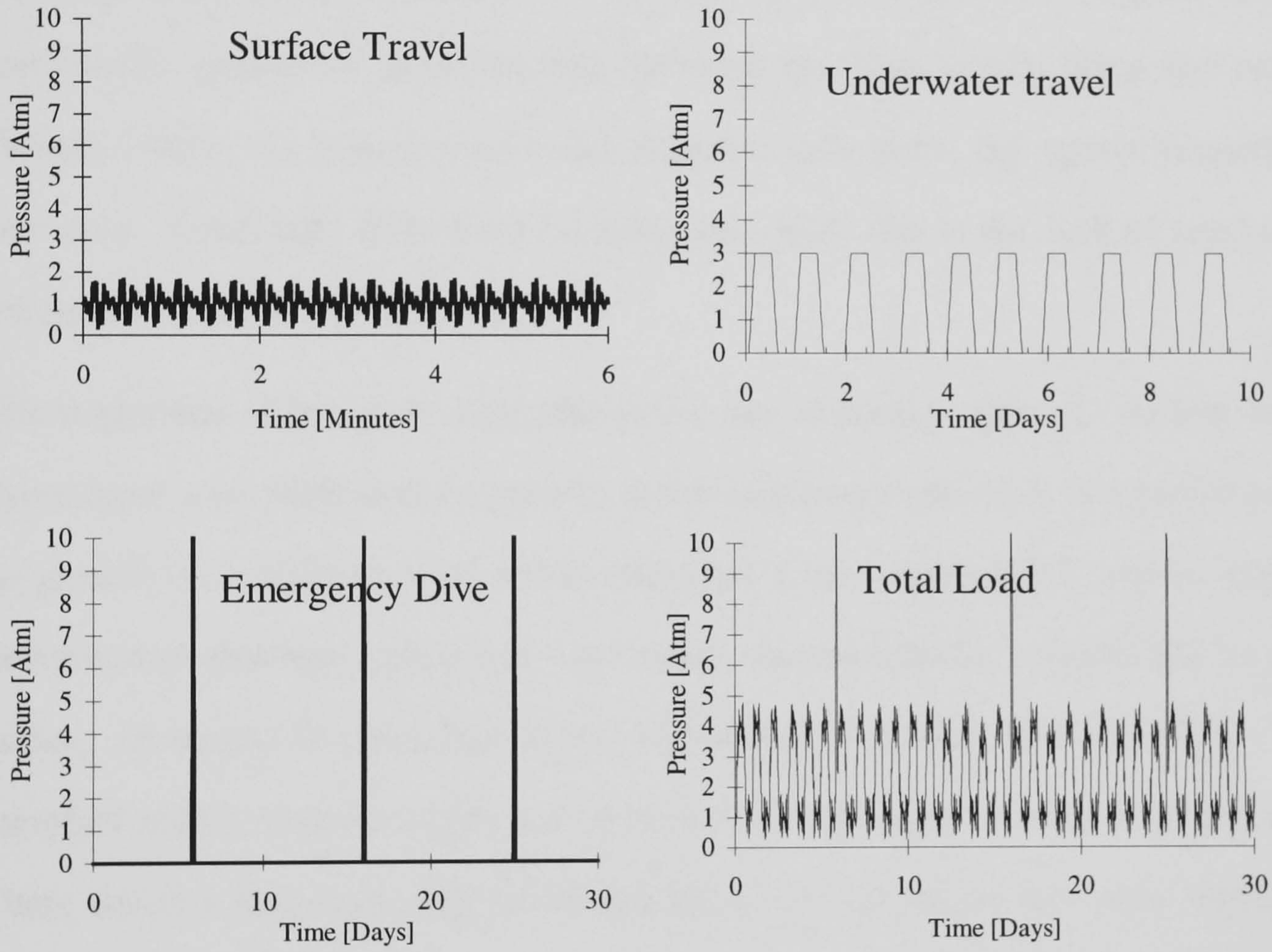

Figure 8.1. Cyclic loading on a submarine hull.

The response of a structure to these repetitive loadings may depend on the load history—the order in which loads occur.

In composites the effect of loading and unloading at loads well below those needed to cause failure may be sufficient to cause damage growth: existing delaminations may increase in size; new delaminations may be initiated at existing matrix cracks or fibre

cracks; matrix cracks may grow in length, or new ones grow from fibre cracks; ply cracks may increase in length due to fibre micro-buckling when matrix cracking reduces the support provided to the fibres. In fact any of the damage growth modes noted in stepped compression and static loading may occur in fatigue. The general sequence in which damage accumulates to cause fatigue failure has been described in previous work (Konur & Matthews, 1989). Matrix cracking starts at low numbers of cycles, initiating at existing damage. The matrix cracks grow along the fibres, reducing in-plane stress concentrations. The matrix cracks are prevented from growing from one ply to the next if the plies have different fibres angles, due to the preferential growth of delaminations between the plies which blunt the crack tip (Soutis, 1989). As matrix cracks and delaminations grow, the matrix properties are degraded. Eventually fibre microbuckling can occur due to the lack of support form the matrix, leading to overall failure.

The magnitude of the cyclic load affects the rate of damage growth. At low levels of stress there is no delamination growth, at intermediate levels there is a period in which no growth occurs(Curtis *et al*, 1993), but after a certain number of cycles growth of delamination damage is observed. Increasing the stress levels reduces this incubation period. (It should be noted that Curtis' evaluation of damage was limited to C-scans, therefore matrix damage would not be detected in the same vicinity as delamination.) There exists a threshold load for delamination growth (Hiley & Curtis, 1992), so it was necessary to ensure that the stress level used in this fatigue work was sufficient to produce damage growth from the artificial inserts.

The fatigue conditions used here, the load magnitude, frequency and numbers of cycles, were chosen in order to ensure that a measurable amount of damage growth occurred within the time frame of the tests, which was limited by the availability of the test machine.

In order to achieve a high enough number of cycles to produce results in a relatively short period of time, a high frequency is needed. Balanced against this is the need to avoid heating the specimen due to energy absorption. (The hysteresis loop for one cycle has an area equal to the energy dissipated by the specimen. The majority of this energy is converted into heat, and in the tests carried out for this study, was approximately 3 Joules—a power input of 30 watts at 10 Hertz. This heat is being produced in the damage zone of the specimen, with a volume of a few cubic centimetres and would therefore be sufficient to raise the temperature considerably if measures were not taken to dissipate the heat.)

The actual load history over one cycle is the next factor to assess. Laminated materials tend to fail differently under tensile and compressive loading. If the fatigue load cycle contains both compressive and tensile components then the failure may occur in either way and there may be some interaction between the different failure modes. The actual failure mechanisms will depend on the damage present as well as the specific lay-up of the composite [Rotem and Nelson, 1989]. Since this study is particularly interested in the comparison between failure modes under static and fatigue conditions a compressive-compressive loading cycle was used.

The peak value for the loading cycle affects not only the time to onset of damage growth, it can also determine the cycles to failure, and work has been done on the characteristic lives of cycles to failure as a function of applied stress [Haque *et al*, 1993; Curtis *et al*, 1993]. On the basis of this work a value for peak stress was chosen, with the aim of reaching failure (defined as the growth of delamination and/or cracks sufficient to reduce the stiffness of the coupon 25%) within approximately 100,000 cycles .

It is possible to use these values for peak stress to calculate the peak strains experienced by the composite, and thus use the limiting strain for no fatigue growth

within a certain number of cycles as a design criteria. It has been shown, on this basis [Curtis *et al*, 1993], that the compressive performance of composites is poorer than the tensile performance in fatigue.

Curtis' work looked at the fatigue response of impact damaged composites, containing a full range of impact damage (delaminations, fibre breaks and matrix cracks). This work tested specimens that contained limited (artificial) damage, which should give an indication of which mode of damage is predominant in deciding the mechanism of failure.

8.3. Test Specimens

The specimens chosen to test in fatigue reflect the concern for qualitative information on failure processes and are shown in Table 8.1. The size and construction of these specimens was identical to that for static testing: 18 ply $(\pm 45°,0°_3,\pm 45°,0°_2)_s$ coupons of nominal thickness 2.25 mm, 250mm by 50 mm wide with centrally located damage.

Material	Description	Cracks	Delaminations
T800/5245	Deep delamination	0°plies - 14,15,16	25 mm x 25 mm between plies 13 and 14
T800/5245	Realistic damage	0°plies - 14,15,16 = 75 mm of cuts	Total of 2500 mm^2 distributed as per Figure 4.1
T800/5245	Actual Impact Damage - 7 Joule		

Table 8.1. Description of specimens used in fatigue tests.

8.4. Test Procedure

The objective was to follow the growth of damage with increasing load cycles. Before each test cycle the coupons were scanned using an ultra-sonic C-scan and also injected with zinc-iodide penetrant and X-rayed. This allowed comparison of the two methods of assessing the extent of damage.

The sequence of loading was selected such that damage could be assessed after two thousand, ten thousand, fifty thousand and one hundred thousand cycles. This necessitated removing the coupon from the test machine in order to carry out X-ray and C-scans of the damage. The time interval involved was at most two hours, so the specimen did not need to be exposed to the penetrant for more than a day. (Work by Soutis [1989] and Spearing [1989] indicate that zinc iodide affects damage growth by increasing the rate of matrix cracking, so reducing exposure time minimises this effect.)

Immediately after scanning, the specimen was fitted into the anti-buckling guide[1] and inserted into a MAYES servo-hydraulic test machine, rated to 100 kN and working at 2500 psi. The specimens were held in place by mechanical grips and subjected to a compression - zero - compression loading cycle. The peak load used was 75% of the ultimate compressive strength of the coupon. Results from the stepped loading tests showed that the specimens could sustain a load of 75% of failure load without significant growth of the delamination, so this was thought a suitable value to be used for the peak load. The aim was to stress the specimen sufficiently to cause damage growth, while avoiding breaking the specimen in the first few cycles - if possible to achieve a specimen life close to the maximum cycles possible in the time available (100,00 cycles).

---

[1] The same anti-buckling guide as was used for the static testing—see Appendix A.

The cycle rate was 10 Hz, the maximum that could be used without excessive heating of the specimen due to the energy absorbed each cycle. A cooling fan was used to reduce the temperature of the specimen (which was kept within 2 degrees of room temperature). At this rate it was possible to complete the test on a specimen within one day, a necessary constraint as the x-ray penetrant is believed to affect the material after prolonged exposure.

The testing was computer controlled and monitored to detect changes in the modulus of the specimen. A change of 0.25% over one cycle caused a print out of the load displacement curve for one cycle, and an overall change of 25% caused a halt in the testing.

The plot of load against displacement shows a hysteresis curve, from which it is possible to calculate the energy absorbed in each cycle. A typical curve is shown in Figure 8.2. The energy absorbed per cycle is of the order of three Joules—most of which is dissipated as heat and only a small amount is responsible for damage growth.

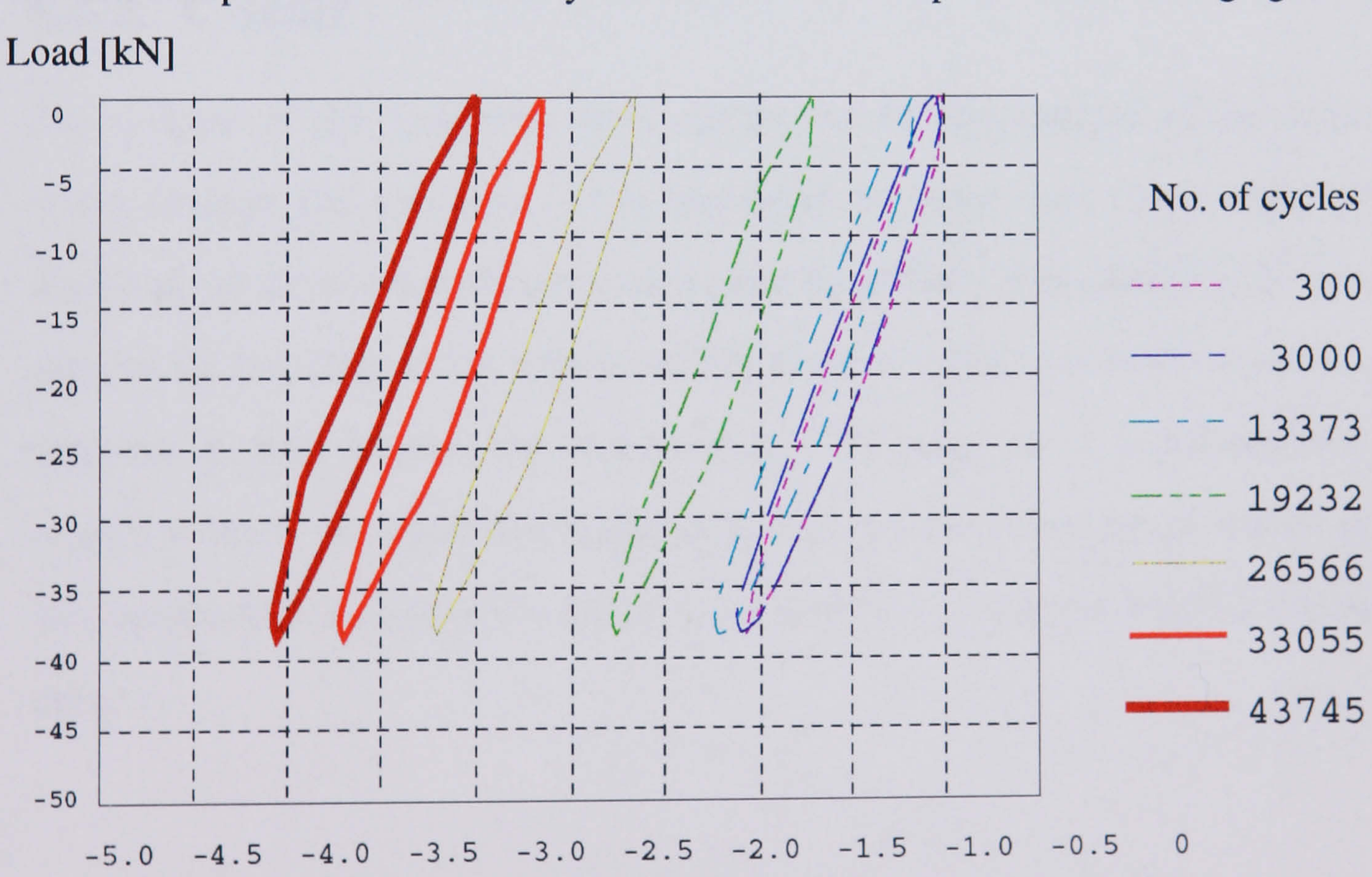

Figure 8.2. Hysteresis curves for fatigue specimen containing deep delamination and crack.

8.5. Results

8.5.1. X-ray evaluation

The specimens were exposed to X-rays at 20 kV and 1.5 mA for 60 seconds. The film used was Agfa-Gaveart OS-RAY M3 (18 cm by 24 cm). The specimen was taped to the paper film envelope at a distance of one metre from the X-ray tube.

The area indicated as delaminated by the X-ray film was close to that shown by the C-scan, although the edge of the delamination was not very easy to determine because the density of the image reduced toward the edge of the damage. (Due to the reducing thickness of penetrant.) This indicates that the X-ray technique can be used with confidence. It was possible to see more detail in the X-ray image, and in particular the presence and growth of ply and matrix cracks.

8.5.2. C-scan

The C-scans of the specimens were carried out by transmission of the ultrasonic waves through the specimen, while immersed in water, and measurement of the amplitude of the waves reflected from a glass base plate. The resolution of the scans allowed for five steps in the transmissibility to be recorded, and in all cases the scans indicated a sharp edge to the delamination. The presence of a delamination was enough to mask any signal that might have been obtained from ply or matrix cracks. This emphasises the usefulness of the X-ray method at revealing detail in the damage zone.

8.5.3. Damage growth with fatigue loading

The growth of damage with increasing cycles was quite clear for the artificially damaged specimens. Figure 8.3 shows tracings of the outline of the x-ray images to indicate the growth of the damage. In Figure 8.4 the area of the delamination is plotted against the number of cycles.

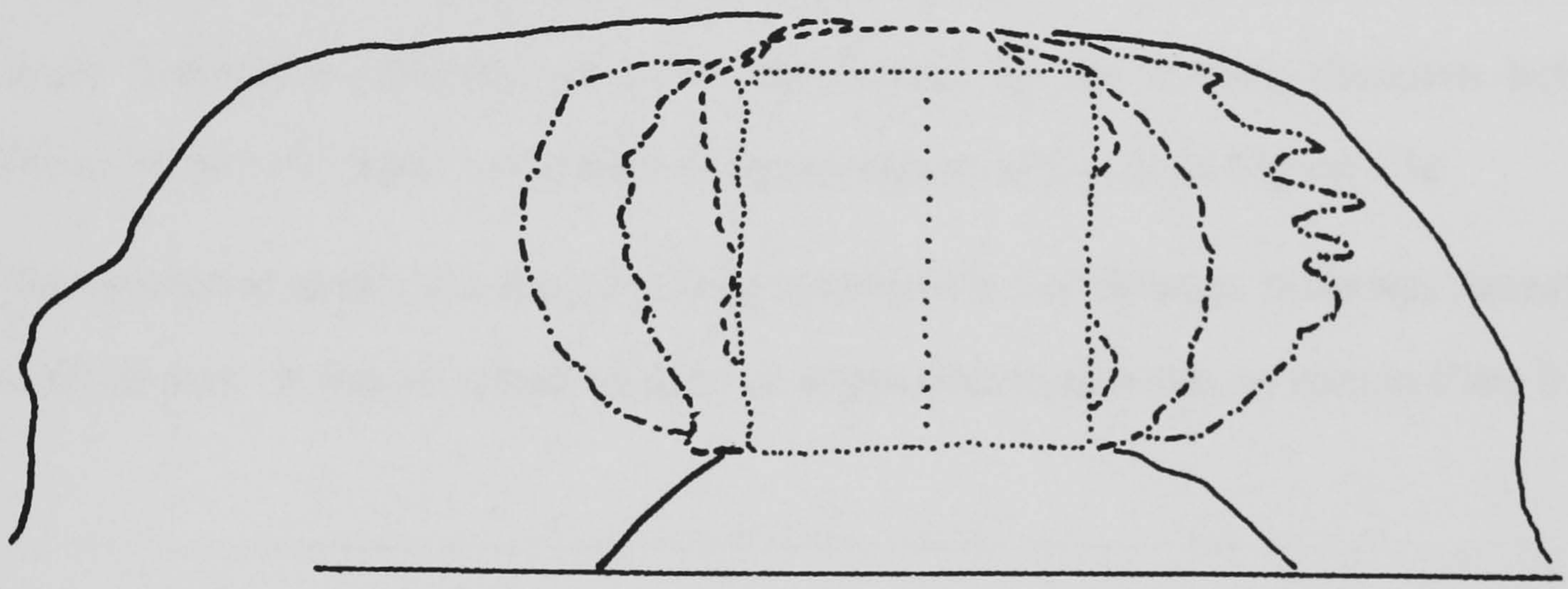

Figure 8.3a. Delamination growth in specimen containing one delamination and crack. Loading axis is horizontal (also in 8b and 8c)

Before test

2 000 cycles

10 000 cycles

50 000 cycles

100 000 cycles

Figure 8.3b Delamination growth in actual impact specimen.

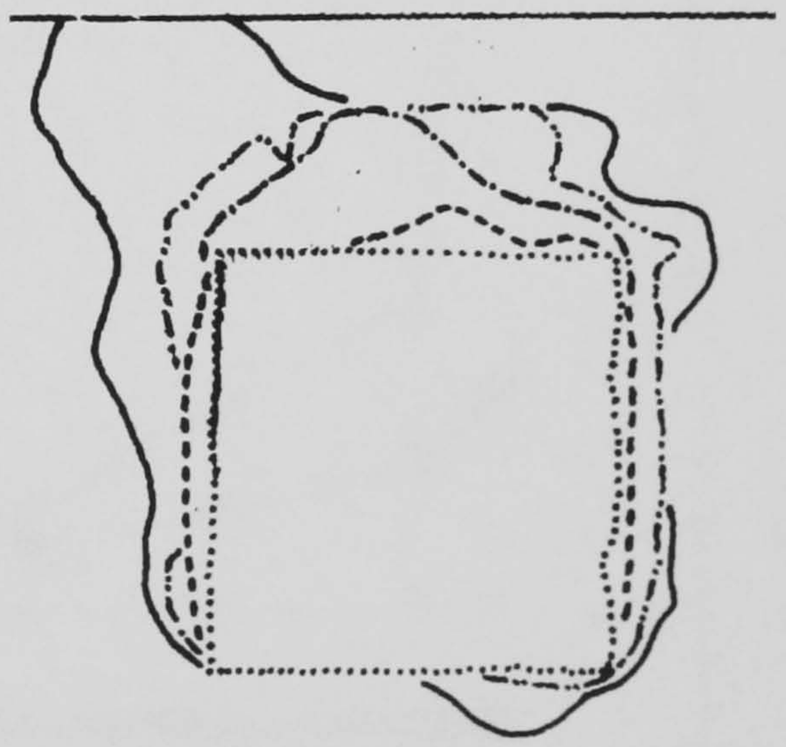

Figure 8.3c. Delamination growth in realistic artificial damage specimen.

The delamination growth in the specimen with actual impact damage was minimal. with only a 13% increase in shadow of the delamination on the X-ray picture for 100,000 cycles (this, of course, does not account for the possibility of increased delamination within the original area). In contrast, the artificially damaged specimens, showed significant delamination growth. The realistic artificial damage showed growth both in the loading direction and across the specimen, whereas the single implanted delamination grew significantly in the loading direction before following the 45° fibres to the edge of the specimen, as shown in Figure 8.3c

The amount of matrix cracking in the specimen with real damage, however, increased considerably. It was so extensive as to be impossible to measure, as seen in Plate 8.3.

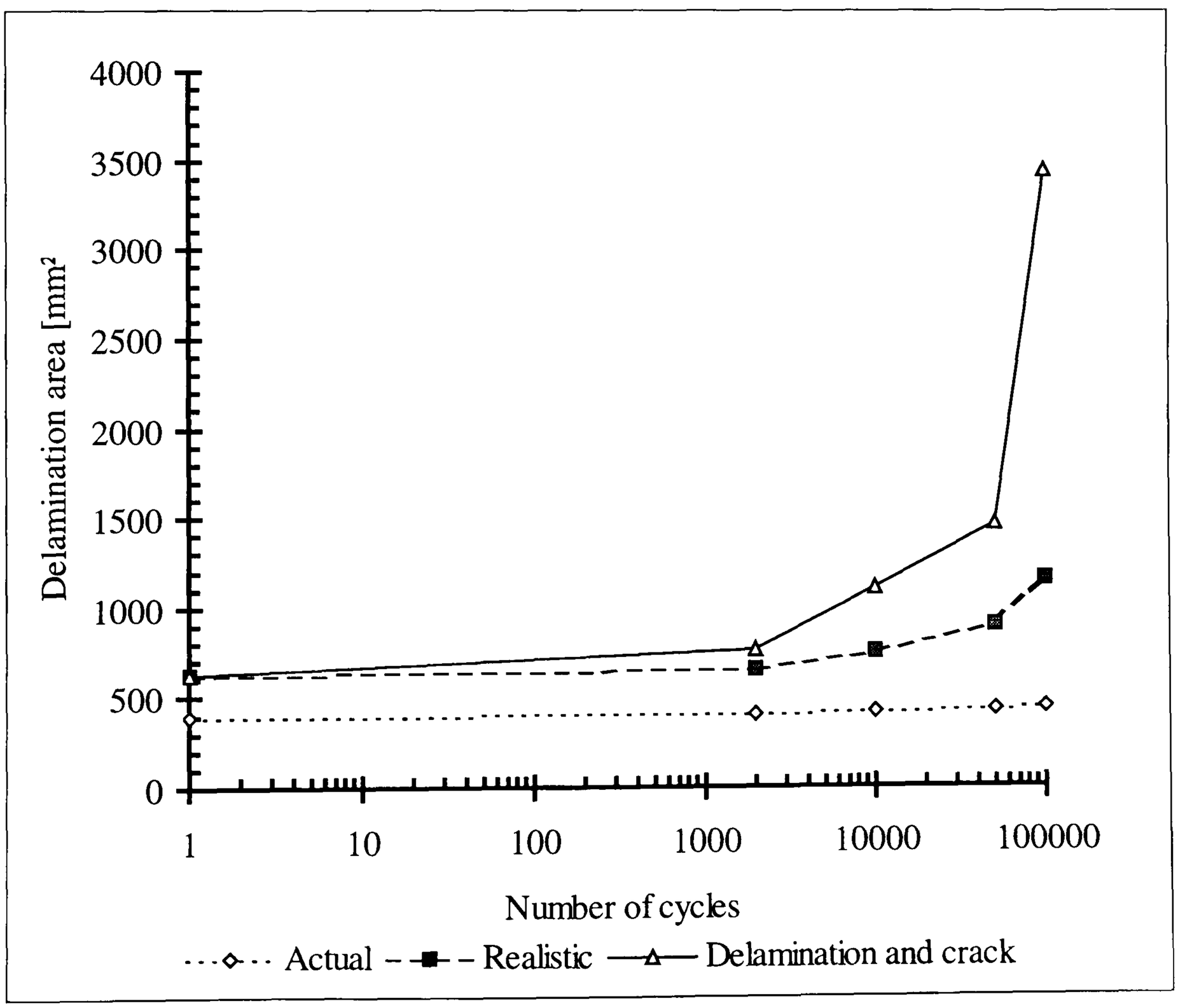

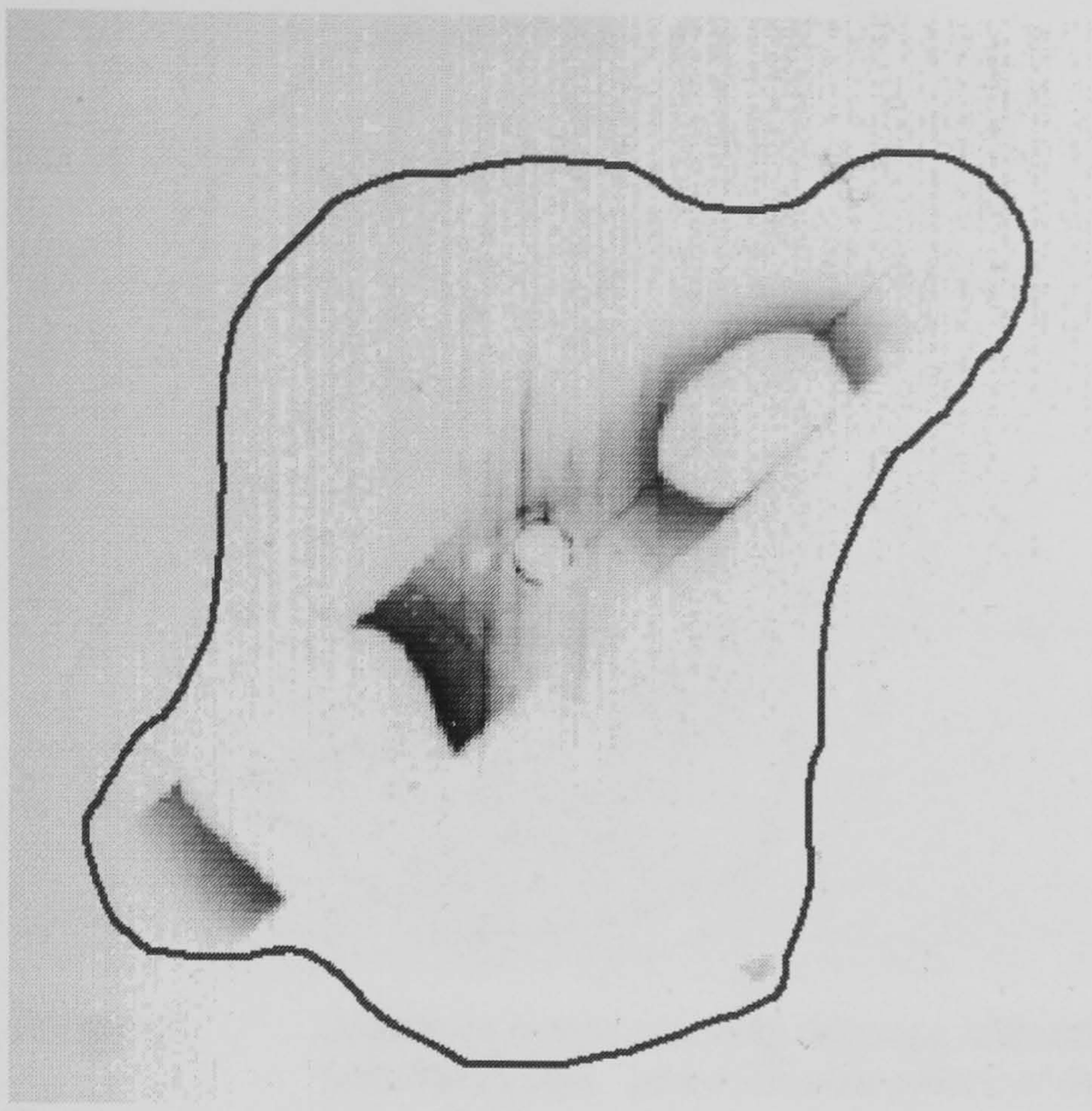

Plate 8.1. *Growth of matrix cracking damage with increasing fatigue cycles - after 2000, cycles. Line indicates extent of delamination from C-scan*

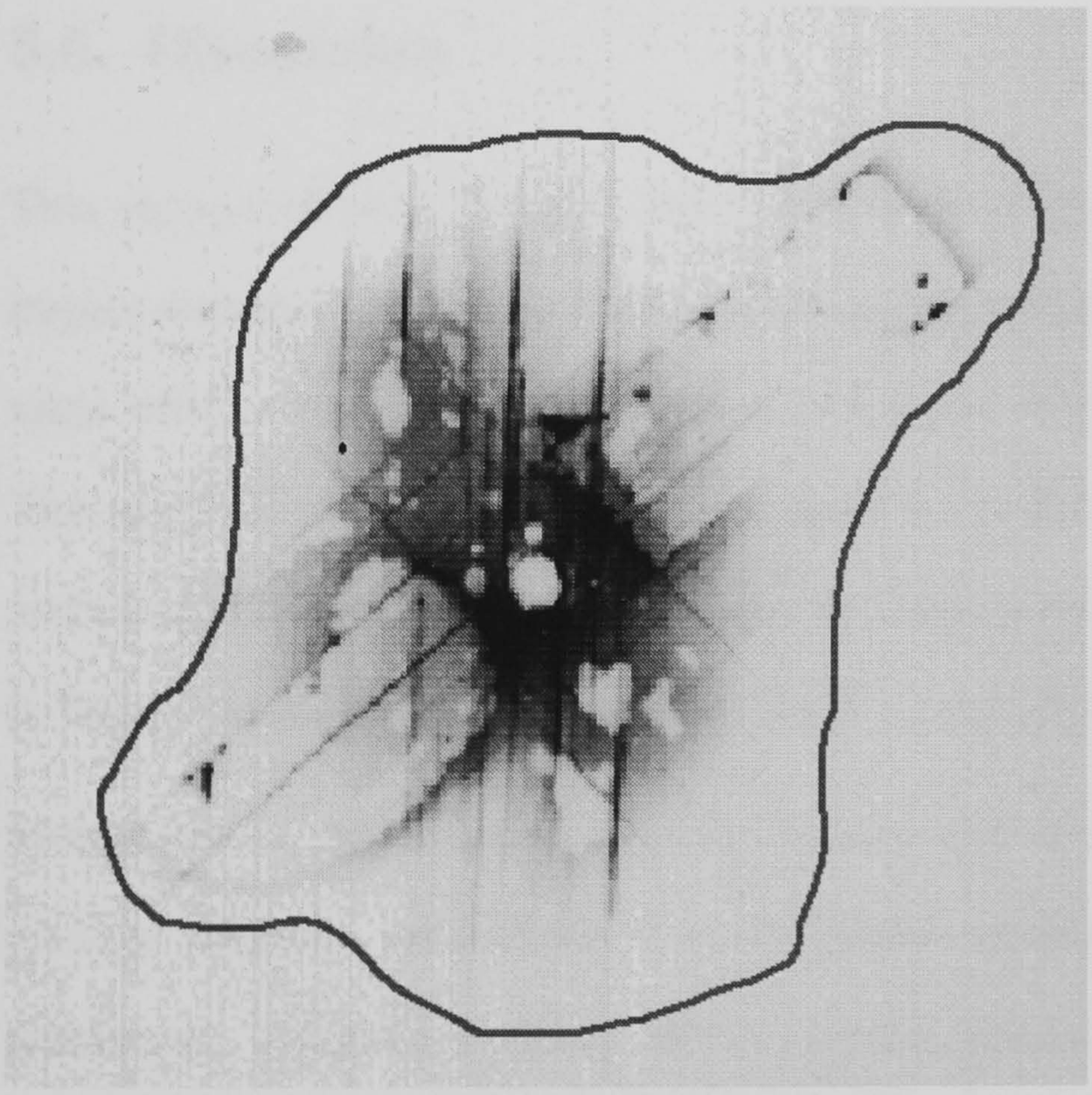

Plate 8.2. *Growth of matrix cracking damage with increasing fatigue cycles - after 50 000 cycles. Line indicates extent of delamination from C-scan*

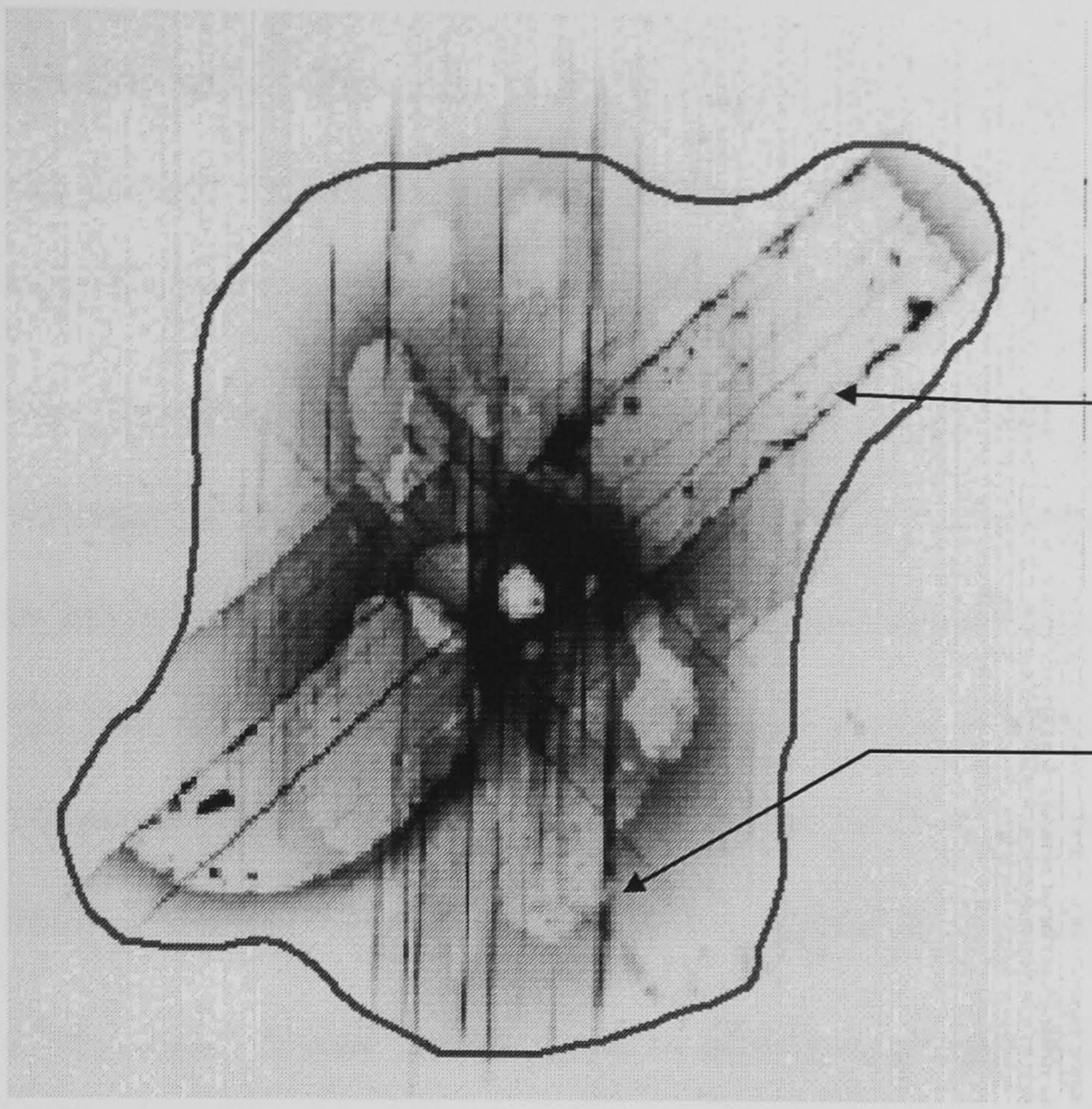

Plate 8.3. *Growth of matrix cracking damage with increasing fatigue cycles - after 100,000 cycles. Line indicates extent of delamination from C-scan*

8.6. Discussion

This section of work gives an indication of the likely outcome of fatigue loading on impact damage. Firstly, simplified artificially implanted damage does not produce the same effect as actual impact damage in fatigue. There are several reasons for this. The mode of damage growth is very sensitive to the initial damage, and the amount and combination of implanted damage does not closely match the real impact damage. In fatigue damage growth is expected to be a critical factor in failure.

Matrix cracks appear to be the main mechanism in damage growth in actual impact damage coupons, and there is little matrix cracking in our artificially damaged specimens. Figure 8.4 clearly shows that the delamination that is initially present in the 7 Joule impact coupon has not grown measurably even after 100,000 cycles at 75% of static failure load. During this time the density of matrix cracks has increased

considerably. Previous work [Curtis *et al*, 1993] also indicates very little increase in the size of the damage zone within this number of cycles, but in their case they used only C-scans, so the amount of matrix cracking could not be measured.

The ply cracks present at the start have not grown during fatigue. In the artificially damaged coupons cut (ply cracks) are a site for the initiation of matrix cracking, so it is likely that matrix cracks form there and effectively blunt the tip of the ply crack. In the impacted specimen this is also seen in the increase of matrix cracking around the impact point. As the matrix cracks grow they reduce the stiffness of the damaged zone and therefore the loads that are carried by that part of the composite.

One would expect the increase in matrix cracking to reduce the lateral restraint on the fibres in the damaged zone, allowing fibres to buckle and delaminations to grow. Within the time-scale of our experiment this has not happened, but other work [Curtis *et al*, 1993] indicates that it does happen before failure, although sometimes more damage growth occurs at free-edges.

In the artificially damaged specimens there was very little matrix cracking (only that at the edge of the delamination, running from the ends of the ply cuts) and a clean fibre break and delamination. The delamination growth is along the specimen, in the loading direction, similar to the growth of a delamination in tensile static loading. The delamination has grown towards the edge and failure occurs after the delamination meets the edge. Since the damage has reached the same edge of the coupon in both directions in which it has grown, it may be that the damage contains multiple delaminations—the damage seems to follow the direction of the ±45° fibres. Deply investigation would be needed to determine this (and this is only possible at the end of the testing).

8.7. Concluding Remarks

Firstly, it is clear that the artificial damage that was implanted does not behave, in fatigue, in the same way as the real impact damage (which is rich in matrix crack damage). Any results for artificial damage composed mainly of delaminations would give a low estimate if used for predicting the failure of real damage specimens.

The presence of matrix cracks in the impact zone have the effect of retarding delamination growth. The increasing density of matrix cracks means that the fibres are losing support, but the zone for this loss of constraint on the fibres is small. It may be the case that the incubation period mentioned by Curtis [1993] is the period in which this matrix cracking is occurring, and that at some later stage, after more cycles, delamination growth will start.

Where there are few matrix cracks (as in our coupons with artificially implanted damage) the mode of delamination growth is different to that observed under static loading conditions (along rather than across the loading direction).

Future work on the fatigue properties of impacted composites could usefully investigate the effect of damage growth during cyclic loading on the static strength. Another extension to the work would be to perform deply on specimens after cyclic loading to determine the exact state of the damage, though this could be difficult if there is extensive matrix cracking and fibre breakage as the plies might not hold together after pyrolysis.

References

Curtis P. T., Gates J. and Molyneux C.G.

"Impact Damage Growth in Carbon Fibre Composites."

RAE Technical Report TR93009 Feb. 1 **1993** pp. 1-14.

Haque A., Krishnagopalan J. and Jeelani S.

"Fatigue Damage in Laminated Composites."

Journal. of Reinforced Plastics and Composites Vol. 12 **1993** pp. 1058-69.

Hiley, M.J. and Curtis, P.T.

"Mode II Damage Development in Carbon Fibre Reinforced Plastics."

AGARD 74th Structures and Materials Meeting, Patras, Greece. CP-530 **1992**

pp. 17.1-17.11

Konur, O. and Matthews, F.L.

"Effect of the Properties of the Constituents on the Fatigue Performance of

Composites: A Review."

Composites Vol. 20 **1989** pp. 317-328

Rotem A. and Nelson H.G.

"Failure of a Laminated Composite under Tension-Compression Fatigue

Loading."

Composites Science and Technology Vol. 36 **1989** pp. 45-62.

Soutis, C.

"Compressive Failure of Notched Carbon Fibre-Epoxy Panels."

Ph.D. Thesis, Cambridge. **1989** pp. 2.15-2.18, 8.1-8.12

Spearing, S.M.

"The fatigue Damage Mechanics of Notched Carbon Fibre-Epoxy Laminates."

Ph.D. Thesis, Cambridge. **1989**

Tsai G.C., Doyle J.F. and Sun C.T.

"Frequency Effects on the Fatigue Life and Damage of Graphite Epoxy Composites."

Journal of Composite Materials **1987** Vol. 21 pp. 2-13.

CHAPTER 9.

DISCUSSION

9.1. Introduction

This chapter summarises and enlarges upon the discussion in each of the previous chapters. The first part of the work investigated techniques for creating artificial damage, and the validity of these methods is discussed. Before these techniques could be used in experiments, it was necessary to measure the damage caused by real impacts, and the experimental results from these investigations are evaluated. Next, the significance of the results of experiments on coupons containing artificial damage is considered. Finally, the application of finite element methods for predicting the effects of damage is discussed.

9.2. Artificial Damage

9.2.1. Evaluation of Artificial Damage Techniques

A variety of different materials were tested for suitability as inserts to create artificial delaminations. No significant advantage was found for using double thicknesses of insert, as the PTFE film (commonly used for this purpose) was shown to have very low adhesion to the matrix and thus modelled a delamination well. Ply cracks were

effectively modelled by cutting plies prior to curing the composite. It was found that loading the specimens in tension, to a level of a few per cent of the failure load, caused a matrix crack to appear at the ply crack, as would be the case in a real impact. This is an important step to take when modelling real damage, as delaminations and matrix cracks grow from existing matrix cracks. This is particularly true for fatigue work, where matrix crack growth is significant.

9.2.2. Evaluation of Impact Damage

Low velocity impact tests were carried out on plates of 18 ply multi-directional carbon-fibre composite. The nominal plate thickness of 2.25 mm is in the range where the impact damage is greatest for a given energy of impact [Rhodes *et al*, 1979]. The results that were obtained from these tests were comparable to that from other studies [Birch and Williams, 1978; Bishop *et al,* 1984]. The results from these tests cannot be used to predict the performance of plates made with different geometries or with different stacking sequence, as longer and thinner plates with a lower stiffness fail in flexure (fibre breakage), while thicker (and shorter) plates receive more interlaminar damage. The stacking sequence chosen for tests has been shown to improve post impact compressive strength (Morton & Godwin, 1989), but this is achieved by reducing the damage from impact—with the 45° plies on the outside the compressive properties are reduced in comparison to a stacking sequence with the 0° plies on the outside, but the improvement in impact resistance more than compensates.

The comparative tests between T300/913c and T800/5245c showed a difference in impact response between the two materials. The same impact energy produced a different damage pattern. Of particular note is that the fibre damage in the T800/5245c was much reduced, and only at the highest energy used here, a 12 Joule impact, was any fibre breakage recorded. The cause of this is a combination of the properties of the fibres and matrix. The T800 fibres have a smaller diameter and are

approximate 50% stronger, have a higher modulus and a greater strain to failure than the T300 fibres. All these factors would help to make them more resistant to breakage under the loading conditions involved in low energy impact. The T800/5245c plate is likely to flex less, therefore shifting the balance of damage mode from fibre fracture to delamination. In terms of fracture toughness, the two matrix materials are quite similar, the mode I critical strain energy release rate for 913c (the resin used with the T300 fibres) is slightly greater than that of 5245c (in mode II the T800 is significantly tougher). This would make creation of matrix cracks in the T800/5245c composite more difficult in mode II and also mode I crack growth would be less because of the lower flexing at comparable impact loads. Further work with identical fibres in the two different matrices would be necessary to ascertain the role of the matrix in reducing fibre cracking during impact.

The general pattern of impact damage was of delaminations between the ±45° plies and the 0° plies. The area of delamination increased towards the rear surface, as is predicted for plates of this size and thickness.

9.2.2. Replication of Impact Damage

Having determined the extent of damage from real impacts, the next step was to replicate this amount of damage, but in a form that would be easier to model analytically. To do this artificial delaminations and artificial ply cracks needed to be produced. The use of PTFE film as a method of introducing a starter crack was widespread [Martin, 1988; Davies *et al*, 1989] but published work did not justify its use. By inserting various materials between plies and using a modified double cantilever beam test it has been shown that the force required to open the delamination is lowest when using a thin PTFE film. Additionally, it was found that the insert does not need to be doubled (a common practice), and that release agents

are not necessary. Within the limits of these measurements the PTFE delaminant behaves as a freshly opened delamination. The simplified geometry used for delamination inserts produced a comparable reduction in compressive strength to that from real damage. The use of a complex geometry of inserts and ply cracks gave a very good match of post impact compressive strength to real damage as far as static tests are concerned, but simplified damage was used in order to allow separation of the effects of delaminations and cracks.

Ply cracks per se did not affect the compressive properties of the specimens, but the matrix crack that is associated with the ply crack was an initiation point for delamination growth.

9.3. Failure processes

9.3.1. Tension

Failure in tension of the damaged composites is initiated by the failure of the 0° fibres. When a critical load is reached (the ultimate tensile strength of the material) and some fibres fail the load is redistributed among the remaining fibres taking them beyond the critical value—there is always some variation in the strength of individual fibres. The failure is controlled by the amount of undamaged 0° fibres in the coupon. The amount of delamination present has no consistent effect on the failure load, as would be expected, as tensile loads would tend to close the delaminations between unbroken plies. The delaminations that occur grow between broken and unbroken plies in the loading direction.

9.3.2. Compression

The first point to note about compressive failures is that artificial damage which is a realistic replication of real impact damage produces a reduction in strength that is very close to that from real damage. This indicates that a simplification in terms of the geometry and position of the damage can be made while retaining realism.

Under static loading the position of the delamination has a large effect, and the position relative to the cut 0° fibres is critical in that it will determine the stage at which these fibres can buckle out. In the case of two delaminations it is important to know where the buckling occurs—if there are multiple delaminations any that are contained in material above the delamination that fails can not buckle out further. The buckled plies are held together, effectively preventing that upper delamination contributing to the failure, or of growing.

Since low velocity impact can produce multiple delaminations it is worth considering what the effect would be of more than one delamination on the post impact compressive strength. From the work carried out on T800, it was seen that the lower of two identical delaminations dominates the failure, as once the lower delamination has buckled out any delaminations above it have no more effect, except to reduce the stiffness of the delaminated plies (and the finite element analysis showed that they do not carry any significant load). (The specimen with a delamination closer to the surface than a delamination five plies in fails at a load that is 1.3% less than one with just the deep delamination.) In real damage the delaminations near to the rear surface tend to be larger than deeper delaminations, so it would be worth investigating further the interaction of multiple delaminations.

It is expected that smaller and deeper delaminations should buckle out at higher loads and this has indeed been shown [Lowe, 1994], and in some cases the initiation of the buckling of the delamination is coincident with the failure of the specimen.

9.4. Failure criteria

9.4.1. Tension

In order to predict the post impact tensile strength of a composite one needs to know the amount of fibre damage that has been created in the 0° plies by the impact. The strength of the composite can be calculated from the net section of undamaged 0° fibres in the stacking sequence used here, and the same would be true of any lay up dominated by 0° plies. The angle plies carry very little load and their contribution to the strength in tension is limited.

9.4.2. Compression

The failure of the coupon in compression can be related to different events in the failure process. The first to be considered is the buckling load for the delamination. It is possible that as the delamination buckles, the load that had been carried by those plies is largely transferred to the remaining plies. If this happens close to the failure load for the remaining plies the initiation of delamination (localised buckling) would cause failure. It was shown that for delaminations that are close to the surface, and are as large as typical delaminations caused by low velocity impact damage, the load at which localised buckling occurs is very low compared to the failure load. This means that load can be transferred safely to the plies below the delamination. For smaller or deeper delaminations, it is sometimes the case that the delamination buckling out coincides with failure [Lowe, 1994].

If the delamination buckles out of plane without causing immediate failure of the specimen, then the next process to occur as the load increases is the buckling of the remaining plies. If multiple delaminations were present, subsequent delamination could also buckle out. Once the delaminated plies have buckled they carry very little load, and the load is mostly carried by the main sub-laminate and the regions of the delaminated plies that have not buckled. The size of the delamination will obviously

affect the contribution made by the latter part of the coupon. The load on the plies below the delamination is unbalanced, including a moment that superimposes a bending compressive load on the plies in addition to the in-plane compressive stress. The magnitude of this moment is related to both the depth and the width of the delamination.

It has been shown in this work that the delamination can grow across the width of the specimen, and the stress distribution calculated using the finite element method indicates that there are increased stresses in the delaminated plies just beyond the edge of the inserted damage.

Eventually, the main sub-laminate will buckle and the combination of in-plane compressive stress and bending compressive stress are sufficient to cause compressive failure of the 0° fibres due to micro-buckling. The peak compressive stresses shown by the finite element work are found in the zone in which failure occurs in the experiments.

The failure of the specimens used in this work is a post-buckling event—the specimen is quite stable at loads that are sufficient to produce quite large buckles of the delamination. It is postulated that the coupon will fail when the stress reaches a level sufficient to cause compressive failure of fibres (in the T300 system of the order of 1200MPa). The compressive stress distribution within the coupon is affected by the configuration of the damage, and the finite element work matches the expected areas of compressive stress concentration due to the combination of in-plane stresses and bending stresses. The values calculated for failure load of damaged specimens, based on a criterion of peak compressive stress within the specimen, correspond very well with experimental results.

The growth of the delamination during the failure of the coupon will have some effect on the stresses that are calculated for the specimen, but these changes are small. The growth of the delamination would tend to lower the failure load of the

coupon. Other work using the same specimen configuration and materials, but varying the delamination size, indicates little change in ultimate compressive strength with delamination size [Lowe, 1994]

Once some fibres have failed in compression, and these fibres have already been shown to be in the same ply as the delaminating material (and have buckled out), the specimen effectively has off-axis loading. The remaining plies will tend to buckle in the opposite direction, as was shown by the finite element model. The coupon then fails because of the same combination of in-plane and bending stresses, but this time in the main laminate.

In other configurations, where for example the laminate is very thick, the failure of the delaminating ply would not necessarily cause failure of the structure. However, it is possible that if there are multiple delaminations, that these could buckle out in succession.

Modelling real damage as far as matrix cracking is concerned is difficult because of the need to refine the mesh to incorporate cracks. It would be very difficult to incorporate matrix cracks in the ±45° plies, as many triangular elements would be needed, in addition to a layer of elements for each angle ply. This work has used two elements through the thickness, and extending this to include multiple delaminations would be useful. Additional care would then be necessary to ensure that contact conditions were observed—in this work the two sub laminates deform in opposite directions, once multiple delaminations are present there is the requirement to prevent elements from penetrating each other. It should be possible to continue the present scheme of analysis for further damage configurations, including depth and size of delamination, as well as thicker and thinner plates.

The actual growth of the delamination was not studied in this work. All that has been done is to look at the effect of a growing delamination on the results that were produced for implanted damage. It is possible to predict the growth of the delamination and others have done this [Pavier and Chester, 1990]. When predicting delamination growth it is necessary to use an energy approach to calculate the strain energy released if the delamination were to grow in a particular direction.

9.5. Concluding Remarks

The finite element analysis carried out has shown that a relatively simple model can follow the behaviour of the actual coupon quite closely. The use of a plate element can significantly reduce the computational time, while still accounting for out-of-plane movement and through-the-thickness damage. It has been verified that the superposition of two specialised plate elements is a valid and useful technique for modelling delaminations.

Techniques such as using a quarter model have been validated. Comparison of quarter and full models results show that even though the delamination and the remaining plies are not balanced the buckling behaviour was identical.

References

Birch M.W. and Williams J.G.

"The effect of rate on the impact fracture toughness of polymers."

International Journal of Fracture Vol. 14 Feb. **1978** pp. 69-84.

Bishop S.M., Howard G.D., and Wood C.J.

"The Notch Sensitivity and Impact Performance of [0,-45,+45] Carbon Fibre Reinforced PEEK."

RAE Technical Report 84066 June **1984** pp. 1-15.

Pavier M.J., Chester W.T.

"Compression Failure of Carbon Fibre-Reinforced Coupons Containing Central Delaminations."

Composites Vol. 21 Jan **1990** pp. 23-31.

Lowe A.T.

"The Effect of Single Embedded Delaminations on the Compressive Strength of CFRP."

Undergraduate Project Report 94/2 Bristol University June **1994** pp. 1-45.

Morton, J. and Godwin, E.W.

"Impact Response of Tough Carbon Fibre Composites."

Composite Structures Vol. 13 **1989** pp. 1-19

Rhodes M.D., Williams J.G. and Starnes J.H.Jr.

"Low Velocity Impact Damage in Graphite Fibre Reinforced Epoxy Laminates".

34th Annual Conference on Reinforced Plastics - Composites Institute Jan **1979** New Orleans, Lou.

CHAPTER 10.

CONCLUSIONS AND FUTURE WORK

10.1. Artificial Damage Techniques

10.1.1. Artificial Delaminations

By inserting various materials between plies and using a modified double cantilever beam test it has been shown that the force required to open the delamination is least when using a thin PTFE film. Additionally, it was found that the insert does not need to be doubled (a common practice), and that release agents are not necessary. Within the limits of our measurements the PTFE insert is the same as a freshly opened delamination. The position of the delamination is unaffected by the curing process.

10.1.2 Artificial Ply Cracks

Cutting the fibres before lay-up and curing of the composite is effective as a means of replicating fibre breakage due to impact damage. For tests in compression it may be necessary to apply a tensile load in order to produce a matrix crack at the point where the fibres are broken. This load is quite low compared to the failure load of the specimen as a whole (approximately 2% is sufficient), and no indication has been

found that the load applied at this point is sufficient to cause delamination growth (if a delamination is present).

10.2. Investigative Techniques

10.2.1. X-radiography

With careful choice of X-ray penetration (kV), intensity (mA) and exposure (time and distance) it is possible to achieve good contrast images of impact damage, if an X-ray opaque penetrant is used for image enhancement. Fine detail of the damage in the form of matrix and ply cracks can easily be seen, and comparison with the C-scan has indicated that the delamination area is accurately represented, although the edge of the delamination is difficult to define because of the tapering thickness of the penetrant layer. Techniques for efficient introduction of the penetrant into damaged specimens were devised to ensure full penetration of the zinc iodide penetrant, without the need for extensive soak times.

10.2.2. Deply

Extensive investigation has indicated that gold chloride, commonly used in the deply technique for indicating the delamination area, is the most effective penetrant. If the same specimen requires X-radiographic inspection the zinc iodide penetrant leaves a residue on the delamination area that is sufficient for recording the damage after deply.

10.2.3. Resin Injection

By using a low viscosity, quick-setting, room temperature cure resin it is possible to 'freeze' the position of delaminated or buckled plies when the specimen is under load.

Similar efforts must be taken as for X-ray and deply penetrants to ensure the resin reaches the full extent of the damage. Sectioning the specimen after the resin has cured gives information on the state of deformation of the specimen while under load.

10.3. Replicating Impact Damage

Penetrant enhanced X-ray examination using zinc iodide, and deply using gold chloride to reveal delamination damage are effective methods for characterising the damage produced by low velocity impacts. Using the information provided by inspection of actual impact damage it was possible to construct specimens with artificially implanted damage. The combinations of delaminations and ply cuts introduced were chosen to give a range of damage from a close representation of the actual damage to a geometrically simple arrangement of PTFE inserts and fibre cuts. The residual strength of the impact damaged specimens could be achieved by using extensive implants of damage (inserts and ply cuts), but a simplified damage arrangement was sufficient to model compressive failure.

10.4. Post-damage residual strength

The results of static testing indicate that the residual tensile strength of the damaged specimens was proportional to the net section of undamaged 0° fibres. (For 15% reduction in fibre cross-section by cutting fibres: T800 had average of 15% stregth reduction, T300 10%—see Tables 5.1 and 5.2) The correlation held for both artificially implanted damage and actual impact damage. The presence of delaminations did not affect the failure load.

The residual compressive strength of the specimens was controlled by the amount of delamination. There was some effect from the fibre cuts, because of their effect on the buckling load of the 0° fibres. The mode of failure was by compressive failure of the fibres. This occurred in the regions of greatest stress caused by the combination of in-plane compressive stress and the bending-compressive stress due to out of plane deflections. Coincident with this was delamination growth laterally toward the edge of the coupon.

The final alignment of the specimen after failure indicates that the laminae below the delamination failed in compression, as the coupon has buckled in the opposite direction to the delamination. This is due to the bending induced in the lower plies because of the off-axis loading caused by a reduction in stiffness in the delamination region.

10.5. Finite Element Modelling

The finite element program was able to demonstrate the stress distribution in a compression of a coupon containing a delamination. Measurement of the load experienced by the model compared with that expected for the applied displacement showed that the stiffness of the coupon decreased as the load increased, which is accounted for by the buckling of the delamination lowering its load carrying capabilities.

Measurement of the stress through the thickness of the FE model indicates a compressive stress distribution consistent with a super-position of compressive and bending-compressive stresses. Within the plane of the coupon, the compressive stresses are greatest in the undamaged part of the 0° ply at the end of the cut plies.

The presence of a matrix crack in the model means that this is not the effect of a stress singularity in the finite element mesh.

The magnitude of predicted stresses at failure matched very closely the failure stresses for the experimental coupons, hence it should be possible to use finite element analysis to predict the failure loads for different materials or stacking sequences and for different damage configurations.

10.6. Fatigue

The effect of the delaminations and the ply-cuts were independent in static tests, but the presence of the fibre crack was a point of initiation for delamination growth at low loads (approximately 1-2% of failure load) in tension. This means that the amount of delamination in a specimen containing ply cracks would change in a fatigue test, if the loading is ever in tension. The mode of delamination growth under the compressive-compressive loading cycle was in the direction of loading, but tending to follow the 45° fibres to the edge of the coupon. This is in contrast to the static specimens where delamination growth was perpendicular to loading. This means that the conclusions from static tests cannot be extended to fatigue regimes.

Experiment also showed that the delamination growth from a real impact was much less than that from artificial damage, due to the presence of multiple matrix cracks. The matrix damage in the specimen with actual impact damage increases significantly under fatigue loading, effectively preventing delamination growth. In order to model the damage in fatigue it would be necessary to include artificial matrix cracking.

10.7. Future Work

The work to date has been limited in its scope as far as size and positioning of the damage through the thickness of the specimen is concerned. The delaminations used have had simple geometries and it would be fruitful to continue these investigations using more realistic configurations of implanted damage.

10.7.1. Specimen geometry

Experimental work to investigate the effect of specimen geometry could include changing the thickness, stacking sequence and include using singly curved specimens (modelling sections of a filament wound tube for example).

As has already been stated, the thickness affects the damage response of a composite plate, so to make predictions on the impact tolerance of a composite of a different thickness to those studied in this work would require further experimentation even if the finite element technique were used to predict the failure loads (as the damage inflicted for the same energy would be different).

Stacking sequence can be varied to improve impact resistance, but it can have a detrimental effect on impact tolerance. Repeating finite element work done here with different ply lay up is straight forward if time consuming, and could be used to verify the results found here.

Using specimens of a different geometry than flat plates would be useful to verify the applicability of the work done here to common configurations of composite used in real life applications, as composite plate structures are seldom completely flat in practise.

10.7.2. Delamination size and position

The size and depth of a delamination has an influence on the effect that it has on residual compressive strength [Lowe, 1994]. Further work could be carried out to determine these relationships, including finite element analysis.

10.7.3. Multiple delaminations

The method here has been proven for single and double delaminations, but in real impacts there may be many more delaminations. The artificial damage method allows full control over damage size, position and quantity, so simplifying the study of the interaction of multiple damage zones.

10.7.3. Fatigue

Fatigue experiments have been restricted in this work, but a fuller understanding of the processes that control composite material's damage tolerance would be useful. As was found here, the actual damage inflicted by an impact did not affect the fatigue life of the coupon as greatly as artificial damage. Other work has shown that notched residual compressive strength can be improved by fatigue loading in compression [Soutis, 1989]. It would be interesting to see if this was also true for impact damage.

The biggest problem with the fatigue analysis of composites is in monitoring the level of damage and the effect of fatigue loading on residual strength. The need to use some sort of penetrant, and ultrasonic scanning or X-radiography, mean that cycling has to be interrupted and the work becomes very laborious. To determine the S-N curve for any material requires many coupons, and with the variability of actual damage, even more would be required for composites. It was hoped that artificially implanted damage would help by allowing consistent damage to be implanted, but the mechanism of failure in fatigue seems to be linked to matrix cracking, and attempts

were not made to implant these. Work on a technique for creating artificial matrix cracks would therefore be helpful.

10.7.4. Finite element analysis

The effect of multiple delaminations and their interaction could also be studied using finite element analysis, though the numerical modelling would be more complex. Other improvements would need to be made in the model as the presence of multiple sub-laminates increases the possibility of one ply penetrating another during analysis, requiring some type of contact constraints to be applied. (In this work the initial displacement of the delaminated plies ensured that the two sets of element did not, initially, move towards each other).

The growth of the delamination sideways could be predicted using a virtual crack closure technique and given the necessary computing power the delamination could be grown during loading, to determine if the delamination growth is a factor in the failure.

Some fatigue analysis could be carried out using FE. This would require a greater understanding of the fatigue properties of the material. Again there are complications if matrix cracks are to be modelled, partly due to the complexity of modelling them, and also due their number and growth during cyclic loading. One approach would be to simplify the problem by using degraded properties for the zones that contain extensive matrix cracking.

10.7.5. Material properties.

This study used two different composites, each with different fibre and matrix.. A useful investigation of the contribution made by fibre and matrix to the post impact

compressive strength would be a comparison of composites with common matrix material and different fibres (or vice versa).

References

Lowe, A.

"The effect of single embedded delaminations on the compressive strength of carbon fibre reinforced plastics."

Report submitted for degree of M.Eng, **1994** University of Bristol.

Soutis, C.

"Compressive failure of notched carbon fibre-epoxy panels."

PhD. Thesis **1989** Jesus College, Cambridge.

APPENDIX A

Anti-buckling guide for static and fatigue tests.

End clamps are attached to the specimen, over the end tabs.

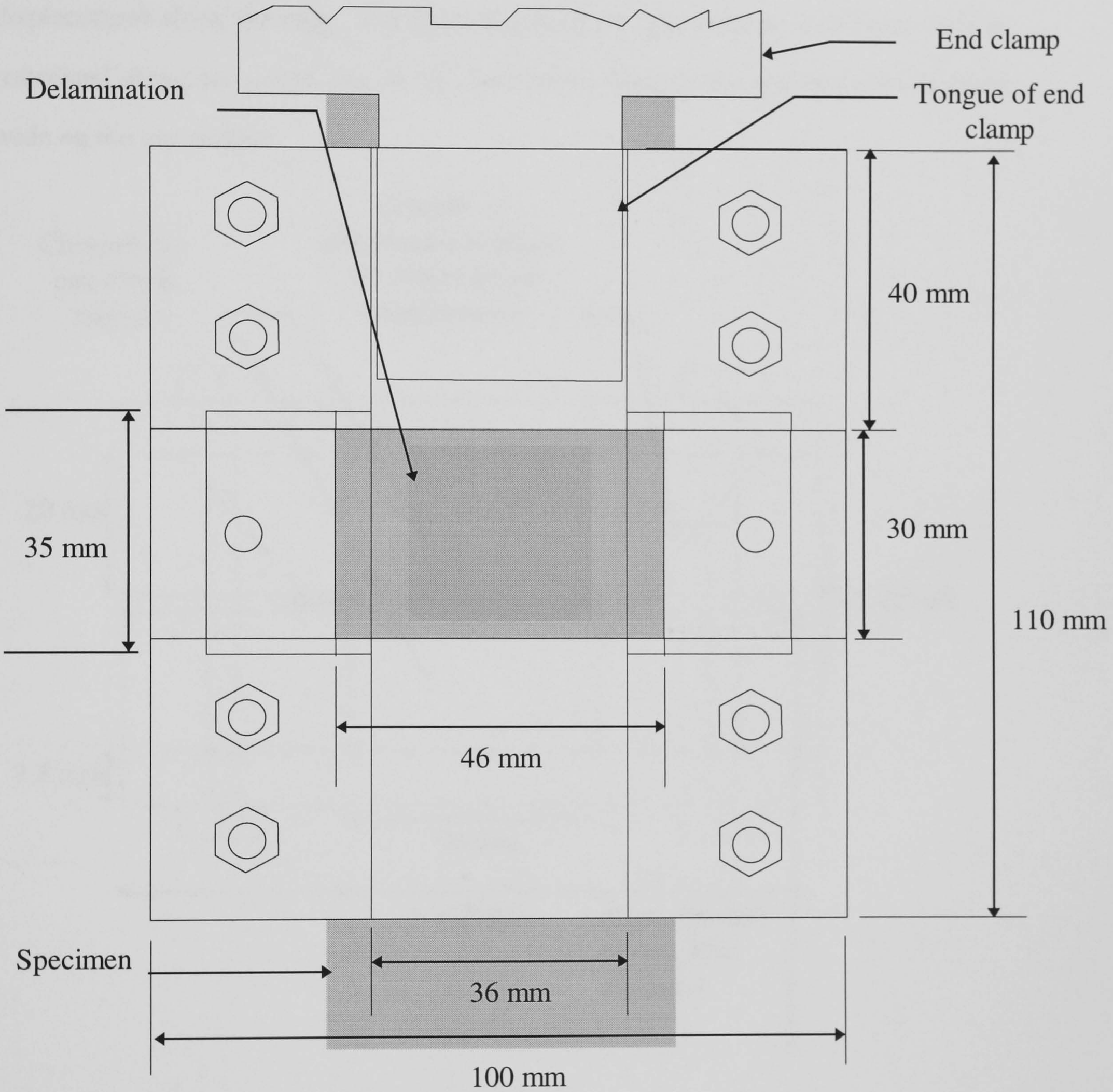

Front view of anti-buckling guide with specimen in place.

The end clamps fit into a fixture on the cross head to ensure alignment of the load with the centreline of the specimen. They also fit into the anti-buckling guide to prevent bending of the specimen at the edge of the anti-buckling guide

The guide prevents the specimen from buckling by limiting the out-of-plane displacement along the edge. For the majority of the specimen an area 5mm wide is restrained along each edge, but at the observation window the restraint area is 2mm wide on the top surface

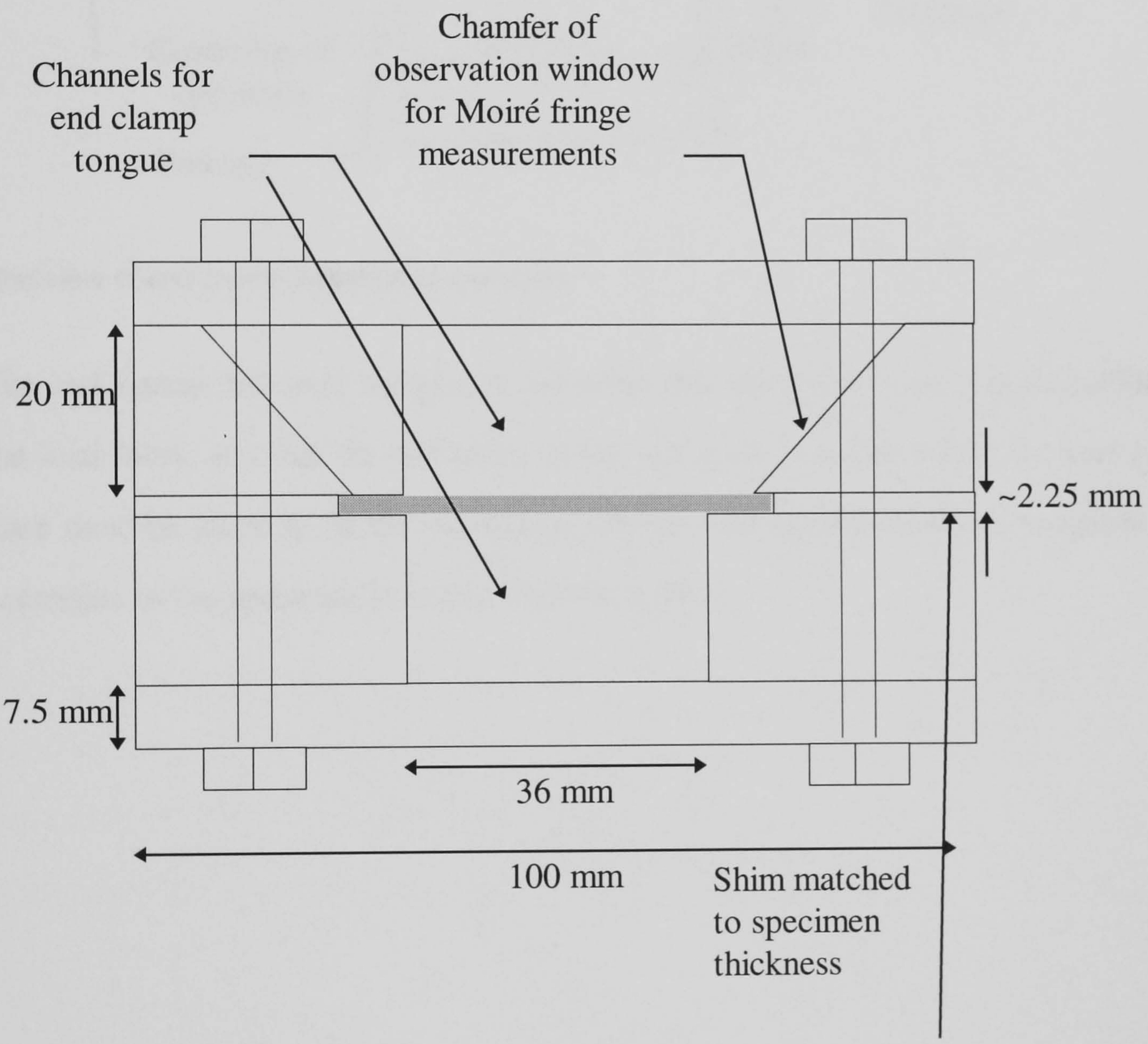

End view of anti-buckling guide.

A pair of end clamps are bolted to each other, gripping the end-tabs, at each end of the specimen. Each pair of clamps has flanges that fit a groove in the end fixture.

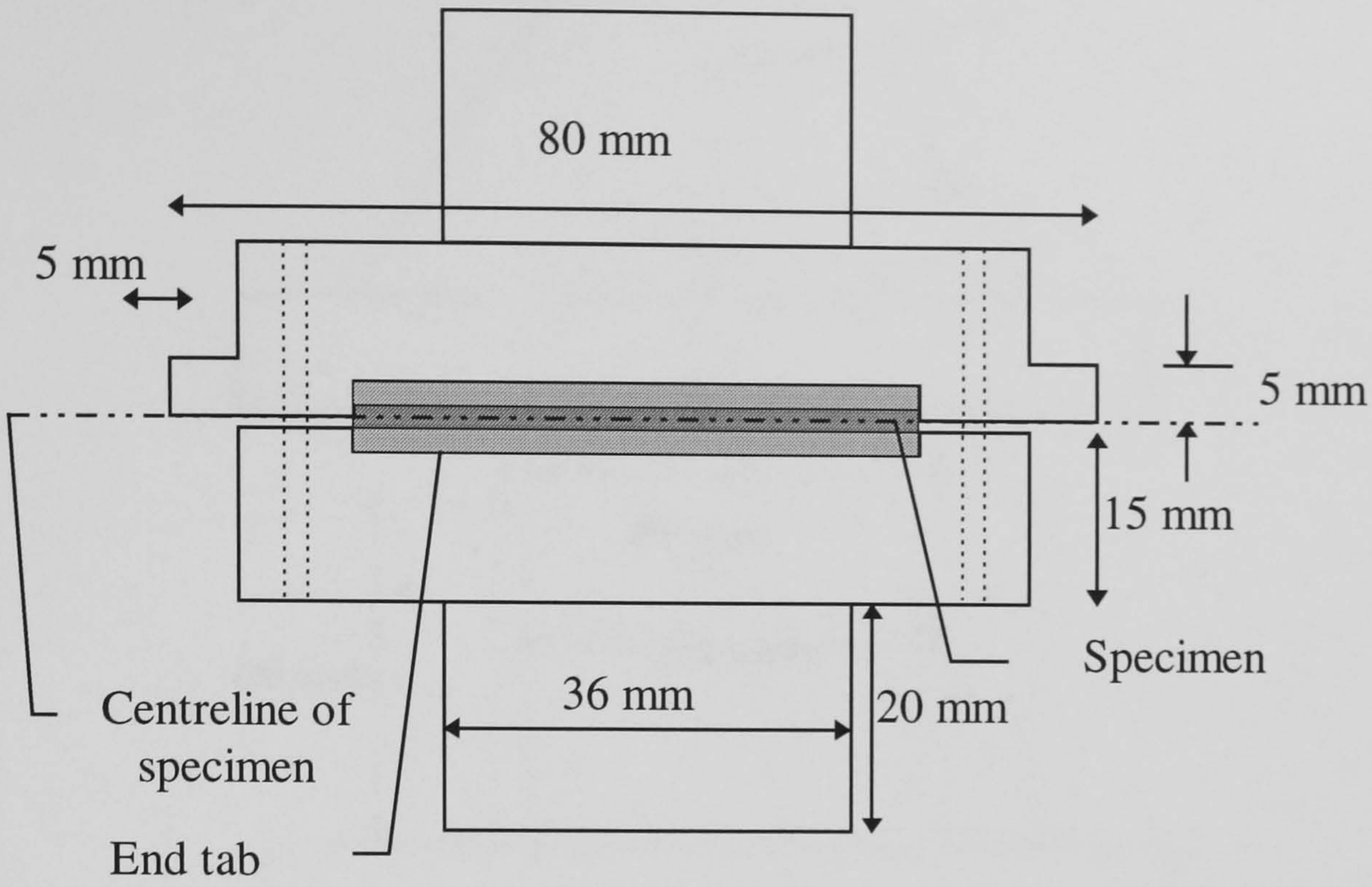

End view of end clamp attached to specimen.

The end fixture fits onto the platens ensuring that the grooves are perpendicular to the load faces, and that the centreline of the specimen is aligned with the load path. Care must be taken to fit the end-clamp into the end fixture correctly to ensure the centreline of the specimen is in line with the loading.

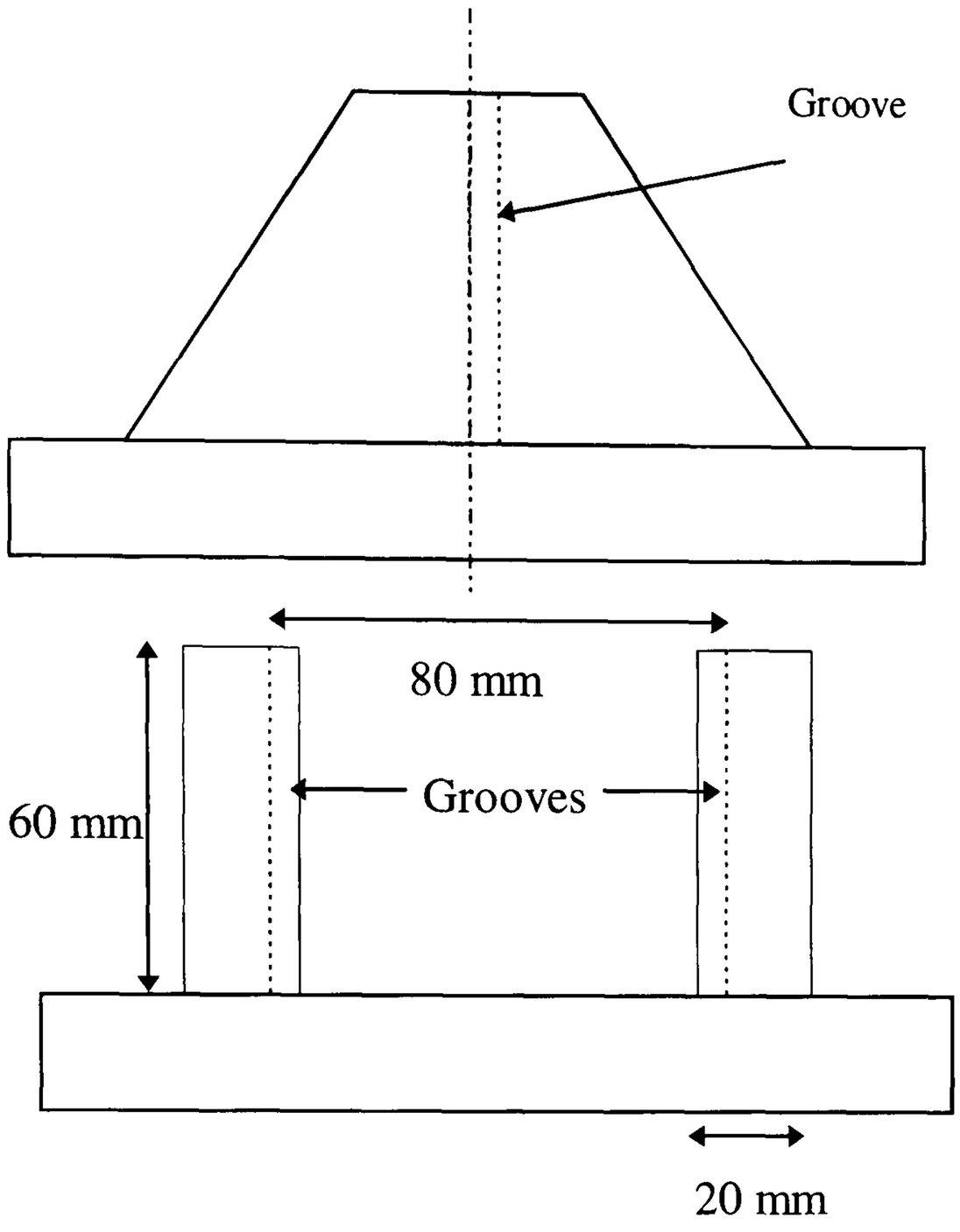

End fixture side view (top) and front view (bottom)

The grooves of the end fixture and the tongues of the end clamp ensure that the specimen remains perpendicular to the loading face. The tolerances of the guide are such that the end clamps can slide smoothly in the grooves of the end fixture. Similarly, the anti-buckling guide can slide up and down the specimen, but in this case the fit is slightly tighter, such that the guide will not slip under its own weight during the test. The end clamp tongues can slide easily in the anti-buckling guide.

APPENDIX B

Derivation of Moiré fringe formula:

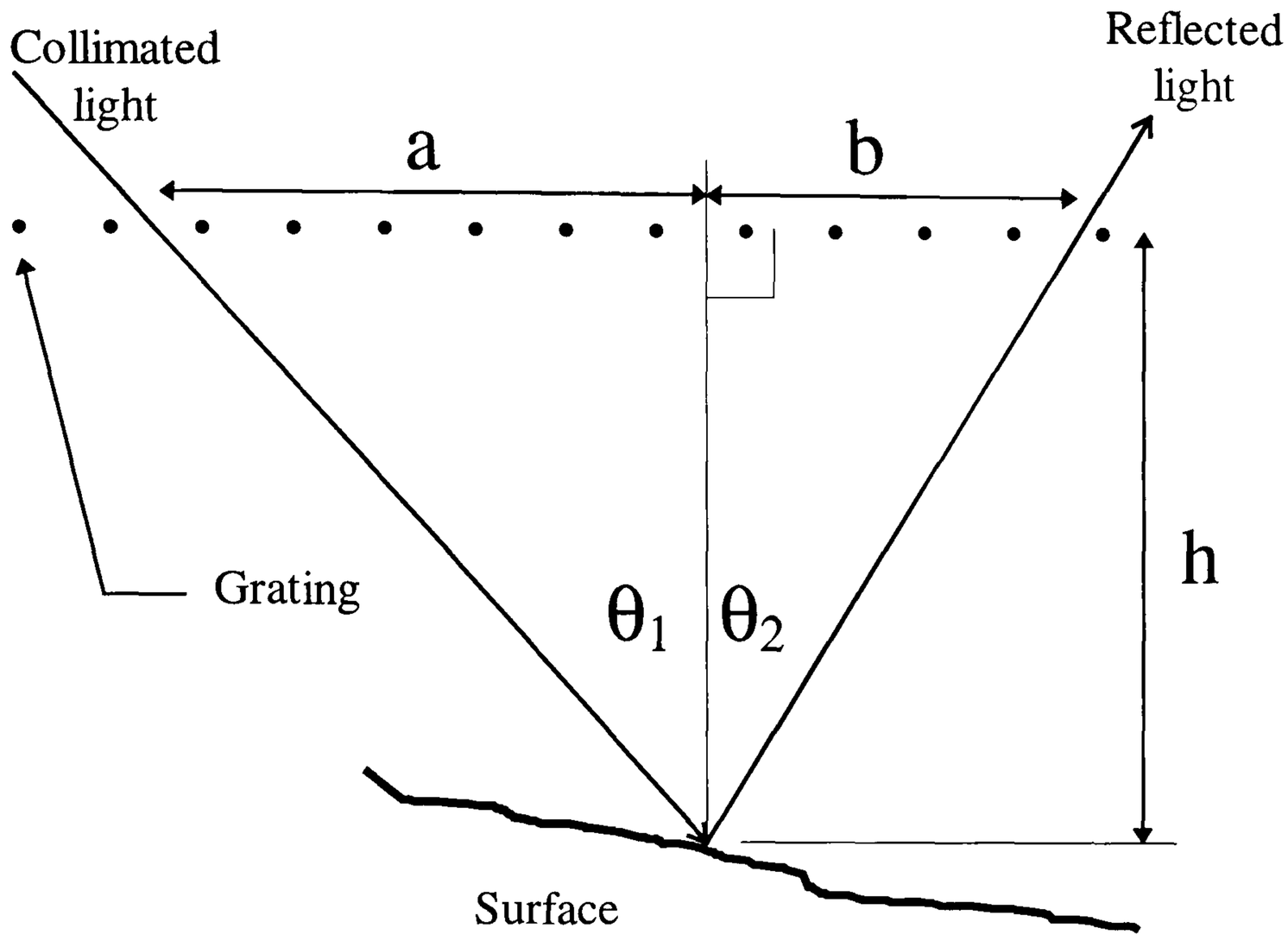

If the light source is at angle θ_1 and the observer is at angle θ_2, then a light region will appear when the shadow of one grating aligns with the line of another grating. (Equivalent to the illuminated parts of the surface being visible through the gaps in the grating.)

In this case $np = a+b$, where n = number of intervening spaces (and is equivalent to the order of the contour), and p = grating pitch).

But we also have that $\tan\theta_1 = a / h$; and $\tan\theta_2 = b / h$.

$$\therefore \tan\theta_1 + \tan\theta_2 = \frac{a+b}{h}$$

$$\therefore h = \frac{a+b}{\tan\theta_1 + \tan\theta_2} = \frac{np}{\tan\theta_1 + \tan\theta_2}$$

$$\therefore \Delta h = \text{height between each contour} = \frac{p}{\tan\theta_1 + \tan\theta_2}$$

since the number of gratings changes by one for each successive contour, as shown in the following diagram:

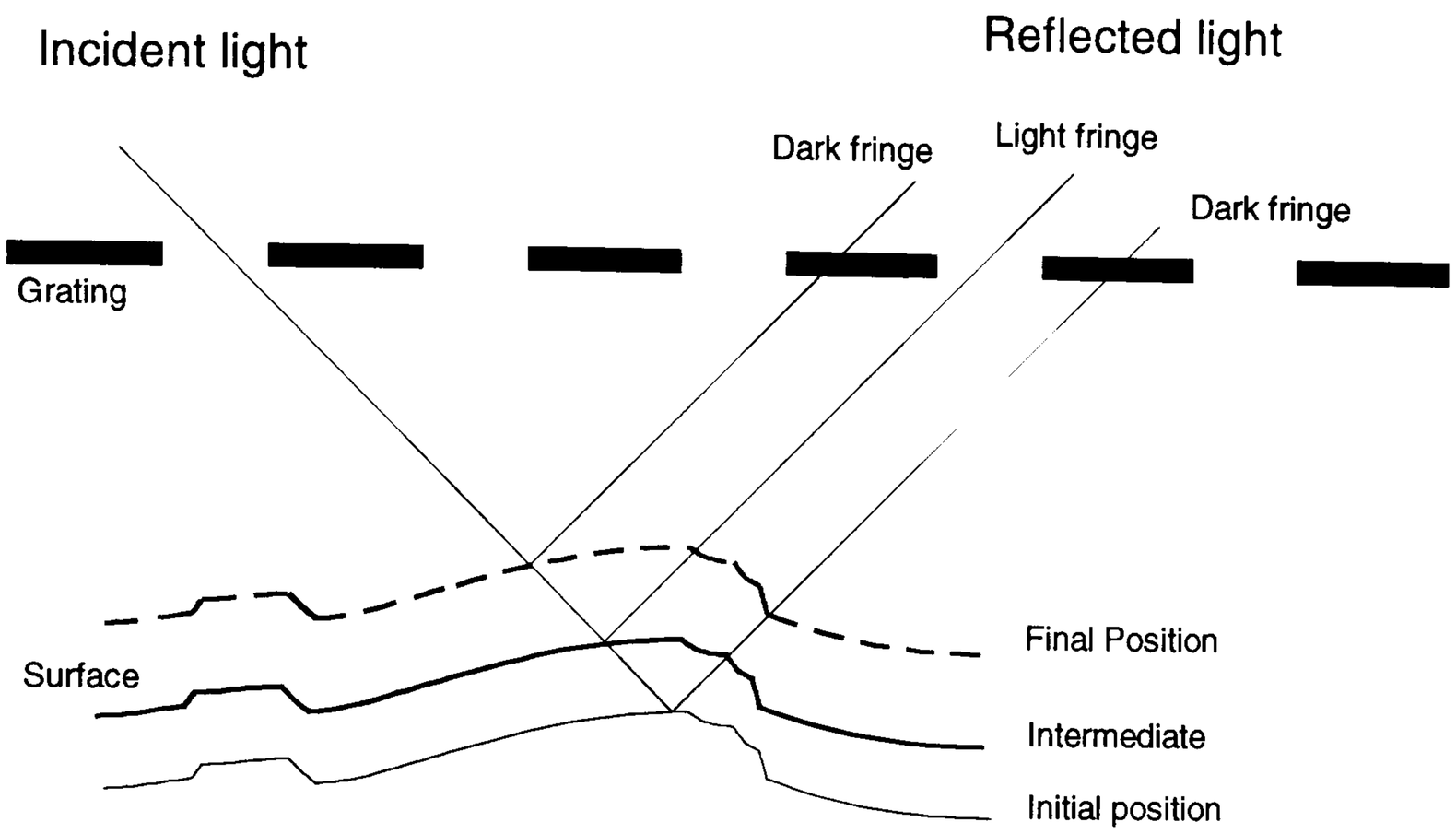

Suitable choice of grating pitch allows a suitable range of contour heights, with the following provisos:

1. As the grating pitch reduces, the diffraction effect increases and so the contrast of the fringes reduces. This effect is greater with a larger gap between surface and grating.

2. The light source must produce parallel light for good contrast, otherwise the distance between grating and surface is limited.

3. Increasing the illuminating and viewing angles reduces the contour height, but is limited by the mechanism by which the grating was produced.

A compromise must be made between the maximum buckle that can be observed and the precision of the measurement, due to the effects (1) and (3). The maximum out-of-plane displacement is limited to the grating-surface separation.

APPENDIX C.

Example of a STYX data file:

A STYX data file is an ASCII file containing information necessary to define the finite element model and the way it is to be loaded. The first data file, *filename*-r0.dat, sets up the model. Subsequent data files, *filename*-r1.dat, *filename*-r2.dat etc, provide information on the loading increments. Additional information can be put in the later data files to change the constraints on the model. There follows a typical data file. The file is broken up into sections, and to help to make clear the purpose of each section a brief description is inserted. The annotation is in italics, and a sketch of the blocking is included.

```
control
title = Buckling of Laminate with Delaminated Plies
Retained
problem = large
solution_file = /temp/solve-std.tmp
end control
```

The title is included in any data output.

The problem is of the large displacement type. This means that the solution routine will require increments of load and each increment will have a number of solution iterations. Successive .dat *files can set the number and size of the increments and the level of iteration required - a user defined variable to achieve convergence of the solution. Depending on the problem between 3 and 7 iterations are required. The more iterations the longer it takes (direct scaling).*

The solution file is placed in a directory other than the one from which STYX has been run. This may be necessary as the file can be quite large - in this case about 10 MBytes. It is deleted after use, leaving a link file in the working directory containing all information necessary for continuing the problem.

```
blocks
type = q8, element_type = q8_pt
block  ply_sequence  d_1  d_2   nodes
  1          1        5    5    1 2 4 5     ! Plies beneath
delamination
  2          2        5    5   10  2 14 5   ! Delamination
  3          3        5    5    2  3 5 6    ! Undamaged laminate
  4          3        5    5    4  5 7 8    ! Undamaged laminate
  5          3        5    5    5  6 8 9    ! Undamaged laminate
  6          3        5    5    3 11 6 12   ! Extended section
  7          3        5    5    6 12 9 13   ! to reduce stress
  8          3        5    5   11 15 12 16  ! concentration.
  9          3        5    5   12 16 13 17  !.
end blocks
```

Here the blocks of elements are defined as 8 noded quadrilateral blocks containging 8-noded quadrilateral plate elements. d_1 and d_2 state the number of elements along the edges of the blocks.

The diagram shows the results of the numbering of nodes.

Care must be taken to preserve the order of numbering the nodes on the corners of the blocks. As only four nodes are provided the program will add the mid-side nodes assuming a straight edge.

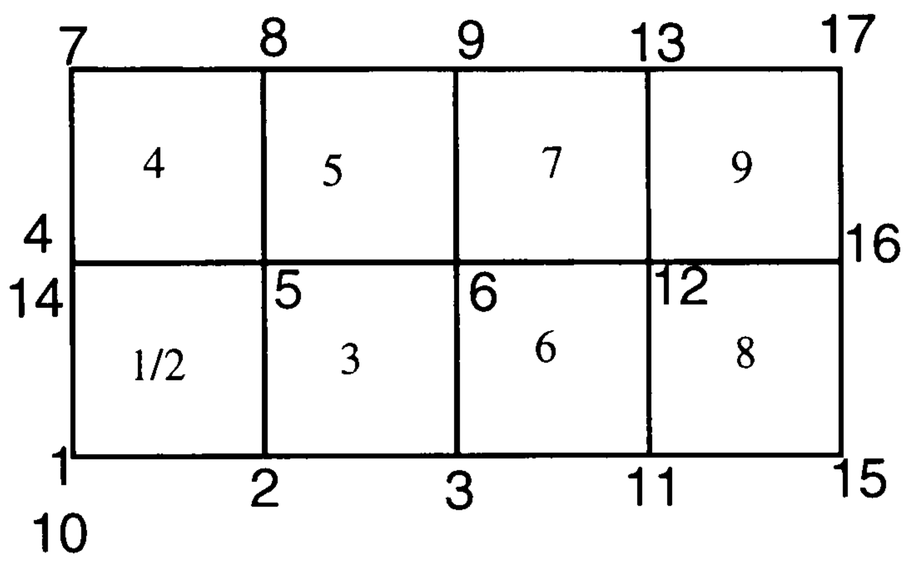

If curved edges are required a further 4 node numbers can be supplied, in which case the sides are parabolic.

Straight sides can be indicated by applying a node number of zero.

The ordering of the node numbers is shown here.

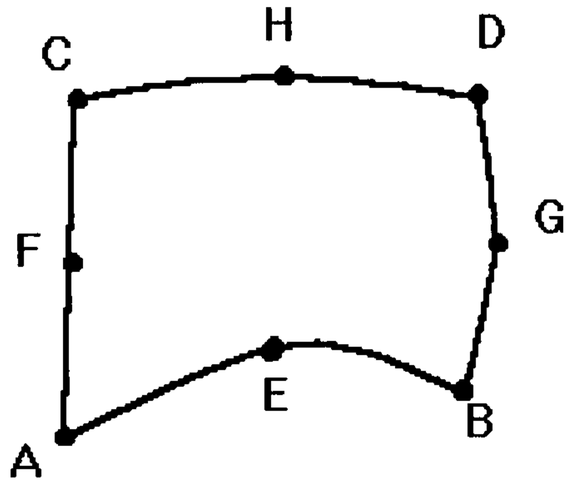

Comments can be placed on any line by inserting an exclamation mark.

```
nodes
z = 0.0
node   x          y
   1    0          0
   2   12.5e-3     0
   3   25.0e-3     0
   4    0         12.5e-3
   5   12.5e-3    12.5e-3
   6   25.0e-3    12.5e-3
   7    0         25.0e-3
   8   12.5e-3    25.0e-3
   9   25.0e-3    25.0e-3
  11   37.5e-3     0
  12   37.5e-3    12.5e-3
  13   37.5e-3    25.0e-3
  14    0         12.4999e-3 ! produces long.1 matrix crack
  15   50.0e-3     0
  16   50.0e-3    12.5e-3
  17   50.0e-3    25.0e-3

z = 2.0e-3
  10    0          0
end nodes
```

All nodes after z=0 are defined to have a z coordinate of 0. Nodes 4 and 14 do not align which means that all the node along the edge 4 to 5 do not equivalence with the nodes along the edge 14 to 5. This produces a (matrix) crack.

Since node 10 is not in the same plane as node 1, and the edges of block 2 are straight, all nodes in block2 have non-zero z-coordinates. This produces a delamination between blocks 1 and 2.

```
materials
type = orthotropic
material   e_1    e_2    e_3    nu_23   nu_31   nu_12   g_23   g_31
g_12
   1     135e9  8.5e9  8.5e9   0.35    0.35    0.35    3e9    3e9    3e9
   2     135e3  8.5e3  8.5e3   0.35    0.35    0.35    3e3    3e3    3e3
end materials
```

The material is defined as orthotropic (the other choice is isotropic) Material properties are defined such that material 2 has reduced properties, by a factor of 1 000 000.

ply_sequences

The lay-up of each ply sequence is defined - e.g. material one has material 1 for the first 8 layers (counting from the bottom up) and then threee layers of material 2. The ampersand indicates that another line of information needs to be read in by the program. The last two numbers on each line are the ply angle and the thickness of the ply respectively.

```
ply_sequence      sequence
     1       1 -45 0.125e-3 & ! Plies beneath delamination
             1  45 0.125e-3 &
             1   0 0.375e-3 &
             1 -45 0.125e-3 &
             1  45 0.125e-3 &
             1   0 0.5e-3   &
             1  45 0.125e-3 &
             1 -45 0.125e-3 &
             2   0 0.375e-3 &
             2  45 0.125e-3 &
             2 -45 0.125e-3

     2       2 -45 0.125e-3 & ! Delaminated plies
             2  45 0.125e-3 &
             2   0 0.375e-3 &
             2 -45 0.125e-3 &
             2  45 0.125e-3 &
             2   0 0.5e-3   &
             2  45 0.125e-3 &
             2 -45 0.125e-3 &
             1   0 0.375e-3 &
             1  45 0.125e-3 &
             1 -45 0.125e-3

     3       1 -45 0.125e-3 & ! Undamaged laminate
             1  45 0.125e-3 &
             1   0 0.375e-3 &
             1 -45 0.125e-3 &
             1  45 0.125e-3 &
             1   0 0.5e-3   &
             1  45 0.125e-3 &
             1 -45 0.125e-3 &
             1   0 0.375e-3 &
             1  45 0.125e-3 &
             1 -45 0.125e-3
end ply_sequences
```

In this case three ply sequences are defined, such that the ply angles and thicknesses remain constant for each block, but the materials properties of some plies are reduced to simulate missing plies. This has the effect of removing plies from blocks 1 and 2 so that block 1 contains only plies below the delamination, and block 2 only plies above. The two blocks are not prevented by the program from moving through each other, but the intial displacements of the delamination disposes it to buckle upward.

displacements

The displacement of nodes during loading is defined in this section. In this example it starts by defining the freedom of movement of the nodes along the edge of the blocks. For example, u_y is the movement in the y-direction. It can be set to zero, some specific value or be left free (the default). t_x is the rotation around the x axis.

```
block   edge      u_y      t_x
  1       1 2       0        0
  2      10 2       0        0
  3       2 3       0        0
  6       3 11      0        0
  8      11 15      0        0
```

The nodes along the bottom of the model, which correspond to the long centre-line of the specimen, are fixed in the y-direction and prevented from rotating around the x-axis. Thsi is equivalent to a plane of symmetry along this edge. Movement in all othe directions/rotations is allowed

```
block   edge      u_x      t_y
  1       1 4       0        0
  2      10 14      0     free
  4       4 7       0        0
```

The nodes along the left hand edge of the model, which correspond to the short centre-line across the specimen, are fixed in the x-direction and prevented from rotating around the y-axis. This is equivalent to a plane of symmetry along this edge. Movement in all othe directions/rotations is allowed. The edge of block 2, the delamination, is allowed to rotate, simulating a crack.

```
block   edge      u_z      t_x      t_y      e_xx        e_yy
  8      15 16      0        0        0  -10.54e-3    6.84e-3
  9      16 17      0        0        0  -10.54e-3    6.84e-3
```

The nodes along the right hand edge of the model, which correspond to the loaded end of the specimen, are strained in the x-direction in compression, with an appropriate lateral strain in the y-direction due to the poisson's ratio effect. The edge is held in the z-direction and prevented from rotating, to replicate the effect of the anti-buckling guide.

```
block   edge      u_z      t_y
  4       7 8       0        0
  5       8 9       0        0
  7       9 13      0        0
  9      13 17      0        0
```

The nodes along the top edge of the model, which correspond to the free edge of the specimen, are held in the z-direction and prevented from rotating, to replicate the effect of the anti-buckling guide.

```
u_x = 0, u_y = 0, t_x = 0, t_y = free ! this prevents overwriting
node
10
u_x = 0, u_y = 0, t_x = 0, t_y = 0    ! no crack in this layer
node
1
```

end displacements

The nodes at the corners have to be redefined to make sure that the information in the earlier statement have not been overwritten by later ones..

```
constraint_equations
active = on,  right_hand_side = 0
constraint            equations
    1       1.0 u_y  14, -1.0 u_y 4
    2       1.0 u_y 183, -1.0 u_y 99
    3       1.0 u_y 180, -1.0 u_y 96
    4       1.0 u_y 186, -1.0 u_y 102
    5       1.0 u_y 184, -1.0 u_y 100
    6       1.0 u_y 112, -1.0 u_y 21
    7       1.0 u_y 187, -1.0 u_y 103
    8       1.0 u_y 191, -1.0 u_y 107
    9       1.0 u_y 189, -1.0 u_y 105
   10       1.0 u_y 192, -1.0 u_y 109
end constraints
```

This last section is used to hold the nodes on either side of the matrix crack together in the y-direction It in effect says that the y-displacement of node 14 minus the y-displacement of node 4 equals zero (right_hand_side). The same applies to the other pairs of nodes along the crack. All these constraints can be added to later incremental data files.

APPENDIX D

This appendix contains the input files for finite element analysis carried out as part of this work. Explanations about the meaning of the files can be found in Appendix C and the *STYX User's Guide.*

.DAT file for FE mesh of control coupon - no delamination or crack

```
control
title = Buckling of Laminate with no damage
problem = large
end control

blocks
type = q8, element_type = q8_pt
block   ply_sequence   d_1   d_2      nodes
  1       1    5      5      1 2 4 5
  2       1    5      5      2 3 5 6
  3       1    5      5      4 5 7 8
  4       1    5      5      5 6 8 9
  5       1    5      5     3 10 6 11 ! Extended section to
  6       1    5      5     6 11 9 12 ! reduce stress conc.
end blocks

nodes
z = 0.0
node  x      y
  2  12.5e-3    0
  3  25.0e-3    0
  4   0        12.5e-3
  5  12.5e-3   12.5e-3
  6  25.0e-3   12.5e-3
  7   0        25.0e-3
  8  12.5e-3   25.0e-3
  9  25.0e-3   25.0e-3
 10  50.0e-3    0
 11  50.0e-3   12.5e-3
 12  50.0e-3   25.0e-3
z = -1.0e-5
node     x       y
  1    0      0
end nodes

materials
type = orthotropic
material  e_1   e_2   e_3   nu_23  nu_31 nu_12  g_23   g_31   g_12
  1      135e9 8.5e9 8.5e9 0.35   0.35  0.35   3e9    3e9    3e9
end materials

ply_sequences
ply_sequence      sequence

      1        1 -45 0.125e-3 & ! Undamaged laminate
           1   45 0.125e-3 &
           1    0 0.375e-3 &
           1  -45 0.125e-3 &
```

```
          1   45 0.125e-3 &
          1    0 0.5e-3   &
          1   45 0.125e-3 &
          1  -45 0.125e-3 &
          1    0 0.375e-3 &
          1   45 0.125e-3 &
          1  -45 0.125e-3
end ply_sequences

displacements
block  edge     u_y     t_x
  1     1 2      0       0
  2     2 3      0       0
  5     3 10     0       0
block  edge     u_x     t_y
  1     1 4      0       0
  3     4 7      0       0
block  edge     u_z     t_x     t_y     e_xx        e_yy
  5    10 11     0       0       0   -10.54e-3    6.84e-3
  6    11 12     0       0       0   -10.54e-3    6.84e-3
block  edge     u_z     t_y
  3     7 8      0       0
  4     8 9      0       0
  6     9 12     0       0
u_x = 0, u_y = 0, t_x = 0, t_y = 0     ! ensure boundary  conditions
node
1
end displacements
```

.DAT file for FE mesh of standard coupon - one delamination (25 mm by 25 mm) between 13 and 14th ply, and ply crack and matrix crack.

```
control
title = Buckling of Laminate with Delaminated Plies Retained no matrix
problem = large
end control

blocks
type = q8, element_type = q8_pt
block   ply_sequence   d_1   d_2      nodes
  1      1    5     5     1 2 4 5 ! Plies beneath delamination
  2      2    5     5    10 2 4 5 ! Delamination
  3      3    5     5     2 3 5 6 ! Undamaged laminate
  4      3    5     5     4 5 7 8 ! Undamaged laminate
  5      3    5     5     5 6 8 9 ! Undamaged laminate
  6      3    5     5     3 11 6 12 ! Extended section to..
  7      3    5     5     6 12 9 13 ! .. reduce stress conc.
  8      3    5     5    11 14 12 15 ! .. reduce stress conc.
  9      3    5     5    12 15 13 16 ! .. reduce stress conc.
end blocks


nodes
z = 0.0
node  x     y
```

```
 1    0      0
 2   12.5e-3    0
 3   25.0e-3    0
 4    0        12.5e-3
 5   12.5e-3   12.5e-3
 6   25.0e-3   12.5e-3
 7    0        25.0e-3
 8   12.5e-3   25.0e-3
 9   25.0e-3   25.0e-3
11   37.5e-3    0
12   37.5e-3   12.5e-3
13   37.5e-3   25.0e-3
14   50.0e-3    0
15   50.0e-3   12.5e-3
 16  50.0e-3   25.0e-3
z = 1.0e-5
 10    0      0
end nodes


materials
type = orthotropic
material e_1   e_2     e_3    nu_23 nu_31 nu_12 g_23   g_31 g_12
  1     135e9   8.5e9   8.5e9   0.35   0.35   0.35   3e9   3e9   3e9
  2     135e3   8.5e3   8.5e3   0.35   0.35   0.35   3e3   3e3   3e3
end materials

ply_sequences
ply_sequence      sequence
     1       1 -45 0.125e-3 & ! Plies beneath delamination
           1  45 0.125e-3 &
           1   0 0.375e-3 &
           1 -45 0.125e-3 &
           1  45 0.125e-3 &
           1   0 0.5e-3   &
           1  45 0.125e-3 &
           1 -45 0.125e-3 &
           2   0 0.375e-3 &
           2  45 0.125e-3 &
           2 -45 0.125e-3

2          2 -45 0.125e-3 & ! Delaminated plies
           2  45 0.125e-3 &
           2   0 0.375e-3 &
           2 -45 0.125e-3 &
           2  45 0.125e-3 &
           2   0 0.5e-3   &
           2  45 0.125e-3 &
           2 -45 0.125e-3 &
           1   0 0.375e-3 &
           1  45 0.125e-3 &
           1 -45 0.125e-3

3          1 -45 0.125e-3 & ! Undamaged laminate
           1  45 0.125e-3 &
           1   0 0.375e-3 &
           1 -45 0.125e-3 &
           1  45 0.125e-3 &
           1   0 0.5e-3   &
           1  45 0.125e-3 &
           1 -45 0.125e-3 &
           1   0 0.375e-3 &
```

```
          1   45 0.125e-3 &
          1 -45 0.125e-3
end ply_sequences


displacements
block  edge     u_y     t_x
  1     1 2      0       0
  2    10 2      0       0
  3     2 3      0       0
  6     3 11     0       0
  8    11 14     0       0
block  edge     u_x     t_y
  1     1 4      0       0
  2    10 4      0      free
  4     4 7      0       0
block  edge     u_z     t_x    t_y     e_xx       e_yy
  8    14 15     0       0      0  -10.54e-3   6.84e-3
  9    15 16     0       0      0  -10.54e-3   6.84e-3
block  edge     u_z     t_x
  4     7 8      0       0
  5     8 9      0       0
  7     9 13     0       0
  9    13 16     0       0

u_x = 0, u_y = 0, t_x = 0, t_y = free  ! this prevents overwriting
node
10
u_x = 0, u_y = 0, t_x = 0, t_y = 0     ! no crack in this layer
node
1
end displacements
```

.DAT file for FE mesh of standard coupon - one delamination (25 mm wide and long) and ply crack, plus fixed matrix crack, at edge of original delamination. (Overlapping prevented)

```
control
title = Buckling of delaminated coupon with ply crack in 0° plies and
matrix crack
problem = large
end control


blocks
type = q8, element_type = q8_pt
block   ply_sequence   d_1   d_2      nodes
  1      1    5     5     1  2  4  5 ! Plies beneath delamination
  2      2    5     5    10  2 14  5 ! Delamination
  3      3    5     5     2  3  5  6 ! Undamaged laminate
  4      3    5     5     4  5  7  8 ! Undamaged laminate
  5      3    5     5     5  6  8  9 ! Undamaged laminate
  6      3    5     5     3 11  6 12 ! Extended section to..
  7      3    5     5     6 12  9 13 ! .. reduce stress conc.
```

```
  8       3     5      5     11 15 12 16 ! .. reduce stress conc.
  9       3     5      5     12 16 13 17 ! .. reduce stress conc.
end blocks

nodes
z = 0.0
node   x       y
  1    0       0
  2   12.5e-3    0
  3   25.0e-3    0
  4    0        12.5e-3
  5   12.5e-3   12.5e-3
  6   25.0e-3   12.5e-3
  7    0        25.0e-3
  8   12.5e-3   25.0e-3
  9   25.0e-3   25.0e-3
 11   37.5e-3    0
 12   37.5e-3   12.5e-3
 13   37.5e-3   25.0e-3
 14    0        12.4999e-3 ! produces long.l matrix crack
 15   50.0e-3    0
 16   50.0e-3   12.5e-3
 17   50.0e-3   25.0e-3
z = 1.0e-5
 10    0      0
end nodes


materials
type = orthotropic
material   e_1   e_2   e_3   nu_23   nu_31   nu_12   g_23 g_31 g_12
  1      135e9   8.5e9   8.5e9   0.35   0.35   0.35   3e9   3e9   3e9
  2      135e3   8.5e3   8.5e3   0.35   0.35   0.35   3e3   3e3   3e3
end materials


ply_sequences
ply_sequence      sequence
     1       1 -45 0.125e-3 & ! Plies beneath delamination
          1  45 0.125e-3 &
          1   0 0.375e-3 &
          1 -45 0.125e-3 &
          1  45 0.125e-3 &
          1   0 0.5e-3   &
          1  45 0.125e-3 &
          1 -45 0.125e-3 &
          2   0 0.375e-3 &
          2  45 0.125e-3 &
          2 -45 0.125e-3

     2       2 -45 0.125e-3 & ! Delaminated plies
          2  45 0.125e-3 &
          2   0 0.375e-3 &
          2 -45 0.125e-3 &
          2  45 0.125e-3 &
          2   0 0.5e-3   &
          2  45 0.125e-3 &
          2 -45 0.125e-3 &
          1   0 0.375e-3 &
          1  45 0.125e-3 &
          1 -45 0.125e-3
```

```
      3       1 -45 0.125e-3 & ! Undamaged laminate
            1  45 0.125e-3 &
            1   0 0.375e-3 &
            1 -45 0.125e-3 &
            1  45 0.125e-3 &
            1   0 0.5e-3   &
            1  45 0.125e-3 &
            1 -45 0.125e-3 &
            1   0 0.375e-3 &
            1  45 0.125e-3 &
            1 -45 0.125e-3
end ply_sequences

displacements
block  edge     u_y     t_x
  1     1 2      0       0
  2    10 2      0       0
  3     2 3      0       0
  6     3 11     0       0
  8    11 15     0       0
block  edge     u_x     t_y
  1     1 4      0       0
  2    10 14     0      free
  4     4 7      0       0
block  edge     u_z     t_x     t_y     e_xx       e_yy
  8    15 16     0       0       0  -10.54e-3   6.84e-3
  9    16 17     0       0       0  -10.54e-3   6.84e-3
block  edge     u_z     t_y
  4     7 8      0       0
  5     8 9      0       0
  7     9 13     0       0
  9    13 17     0       0
u_x = 0, u_y = 0, t_x = 0, t_y = free  ! this prevents
                                       ! overwriting

node
10
u_x = 0, u_y = 0, t_x = 0, t_y = 0     ! no crack in this
                                       ! layer

node
1
end displacements

constraint_equations
active = on,  right_hand_side = 0
constraint       equations
   1      1.0 u_y  14, -1.0 u_y 4
   2      1.0 u_y 183, -1.0 u_y 99
   3      1.0 u_y 180, -1.0 u_y 96
   4      1.0 u_y 186, -1.0 u_y 102
   5      1.0 u_y 184, -1.0 u_y 100
   6      1.0 u_y 112, -1.0 u_y 21
   7      1.0 u_y 187, -1.0 u_y 103
   8      1.0 u_y 191, -1.0 u_y 107
   9      1.0 u_y 189, -1.0 u_y 105
  10      1.0 u_y 192, -1.0 u_y 109
end constraints
```

.DAT file for FE mesh of coupon - no delamination (actually 5 mm, mathematically impossible not to have a delamination at least one element wide) and ply crack, plus matrix crack at edge of delamination (overlapping prevented)

```
control
title = Buckling of Laminate with Delaminated Plies Retained
problem = large
end control

blocks
type = q8, element_type = q8_pt
block   ply_sequence   d_1   d_2      nodes
  1       1     1      5      1  2  4  5  ! Plies beneath delamination
  2       2     1      5     10  2 14  5  ! Delamination
  3       3     9      5      2  3  5  6  ! Undamaged laminate
  4       3     1      5      4  5  7  8  ! Undamaged laminate
  5       3     9      5      5  6  8  9  ! Undamaged laminate
  6       3     5      5      3 11  6 12  ! Extended section to
  7       3     5      5      6 12  9 13  !  reduce stress conc.
  8       3     5      5     11 15 12 16  ! Extended section to
  9       3     5      5     12 16 13 17  !  reduce stress conc.
end blocks

nodes
z = 0.0
node  x      y
  1   0      0
  2  2.5e-3   0
  3  25.0e-3   0
  4   0       12.5e-3
  5  2.5e-3  12.5e-3
  6  25.0e-3  12.5e-3
  7   0       25.0e-3
  8  2.5e-3  25.0e-3
  9  25.0e-3  25.0e-3
 11  37.5e-3   0
 12  37.5e-3  12.5e-3
 13  37.5e-3  25.0e-3
 14   0       12.4999e-3 ! produces long.1 matrix crack
 15  50.0e-3   0
 16  50.0e-3  12.5e-3
 17  50.0e-3  25.0e-3

z = 1.0e-5
node  x      y
 10   0      0
end nodes


materials
type = orthotropic
material  e_1  e_2  e_3  nu_23  nu_31  nu_12  g_23 g_31 g_12
  1    135e9  8.5e9  8.5e9  0.35  0.35  0.35  3e9  3e9  3e9
  2    135e3  8.5e3  8.5e3  0.35  0.35  0.35  3e3  3e3  3e3
end materials


ply_sequences
```

```
ply_sequence      sequence
     1       1 -45 0.125e-3 & ! Plies beneath delamination
           1  45 0.125e-3 &
           1   0 0.375e-3 &
           1 -45 0.125e-3 &
           1  45 0.125e-3 &
           1   0 0.5e-3   &
           1  45 0.125e-3 &
           1 -45 0.125e-3 &
           2   0 0.375e-3 &
           2  45 0.125e-3 &
           2 -45 0.125e-3

     2       2 -45 0.125e-3 & ! Delaminated plies
           2  45 0.125e-3 &
           2   0 0.375e-3 &
           2 -45 0.125e-3 &
           2  45 0.125e-3 &
           2   0 0.5e-3   &
           2  45 0.125e-3 &
           2 -45 0.125e-3 &
           1   0 0.375e-3 &
           1  45 0.125e-3 &
           1 -45 0.125e-3

3          1 -45 0.125e-3 & ! Undamaged laminate
           1  45 0.125e-3 &
           1   0 0.375e-3 &
           1 -45 0.125e-3 &
           1  45 0.125e-3 &
           1   0 0.5e-3   &
           1  45 0.125e-3 &
           1 -45 0.125e-3 &
           1   0 0.375e-3 &
           1  45 0.125e-3 &
           1 -45 0.125e-3
end ply_sequences


displacements
block  edge     u_y     t_x
  1     1 2      0       0
  2    10 2      0       0
  3     2 3      0       0
  6     3 11     0       0
  8    11 15     0       0
block  edge     u_x     t_y
  1     1 4      0       0
  2    10 14     0      free
  4     4 7      0       0
block  edge     u_z     t_x     t_y     e_xx        e_yy
  8    15 16     0       0       0   -10.54e-3    6.84e-3
  9    16 17     0       0       0   -10.54e-3    6.84e-3
block  edge     u_z     t_y
  4     7 8      0       0
  5     8 9      0       0
  7     9 13     0       0
  9    13 17     0       0

u_x = 0, u_y = 0, t_x = 0, t_y = free  ! this prevents
                                       ! overwriting

node
```

```
10
u_x = 0, u_y = 0, t_x = 0, t_y = 0      ! no crack in this
                                                ! layer
node
1
end displacements


!constraint_equations
!active = on,  right_hand_side = 0
!constraint       equations
!  1      1.0 u_y  14, -1.0 u_y 4
!  2      1.0 u_y 180, -1.0 u_y 96
!end constraints
```

.DAT file for FE mesh of coupon - wide delamination (30 mm wide by 25 mm long) and ply crack, plus matrix crack at edge of delamination (overlapping prevented)

```
control
title = Delamination wide + fixed matrix crack + ply crack.
problem = large
end control


blocks
type = q8, element_type = q8_pt
block   ply_sequence   d_1   d_2      nodes
  1         1       5     6      1 2 4 5    ! Plies beneath delamination
  2      2          5     6     10 2 14 5   ! Delamination
  3      3          5     6      2 3 5 6    ! Undamaged laminate
  4      3          5     4      4 5 7 8    ! Undamaged laminate
  5      3          5     4      5 6 8 9    ! Undamaged laminate
  6      3          5     6      3 11 6 12  ! Extended section to..
  7      3          5     4      6 12 9 13  !  reduce stress conc.
  8      3          5     6     11 15 12 16 !  reduce stress conc.
  9      3          5     4     12 16 13 17 !  reduce stress conc.
end blocks


nodes
z = 0.0
node  x       y
  1    0       0
  2   12.5e-3    0
  3   25.0e-3    0
  4    0        15.0e-3
  5   12.5e-3   15.0e-3
  6   25.0e-3   15.0e-3
  7    0        25.0e-3
  8   12.5e-3   25.0e-3
  9   25.0e-3   25.0e-3
 11   37.5e-3    0
 12   37.5e-3   15.0e-3
 13   37.5e-3   25.0e-3
 14    0        14.9999e-3 ! produces long.l matrix crack
```

```
 15   50.0e-3    0
 16   50.0e-3   15.0e-3
 17   50.0e-3   25.0e-3

z = 2.0e-4
 10    0      0
end nodes


materials
type = orthotropic
material   e_1   e_2   e_3   nu_23   nu_31   nu_12   g_23 g_31 g_12
  1      135e9   8.5e9   8.5e9   0.35   0.35   0.35   3e9   3e9   3e9
  2      135e3   8.5e3   8.5e3   0.35   0.35   0.35   3e3   3e3   3e3
end materials


ply_sequences
ply_sequence      sequence
     1       1 -45 0.125e-3 & ! Plies beneath delamination
           1  45 0.125e-3 &
           1   0 0.375e-3 &
           1 -45 0.125e-3 &
           1  45 0.125e-3 &
           1   0 0.5e-3   &
           1  45 0.125e-3 &
           1 -45 0.125e-3 &
           2   0 0.375e-3 &
           2  45 0.125e-3 &
           2 -45 0.125e-3


     2       2 -45 0.125e-3 & ! Delaminated plies
           2  45 0.125e-3 &
           2   0 0.375e-3 &
           2 -45 0.125e-3 &
           2  45 0.125e-3 &
           2   0 0.5e-3   &
           2  45 0.125e-3 &
           2 -45 0.125e-3 &
           1   0 0.375e-3 &
           1  45 0.125e-3 &
           1 -45 0.125e-3

3       1 -45 0.125e-3 & ! Undamaged laminate
      1  45 0.125e-3 &
      1   0 0.375e-3 &
      1 -45 0.125e-3 &
      1  45 0.125e-3 &
      1   0 0.5e-3   &
      1  45 0.125e-3 &
      1 -45 0.125e-3 &
           1   0 0.375e-3 &
           1  45 0.125e-3 &
           1 -45 0.125e-3
end ply_sequences


displacements
block   edge     u_y     t_x
  1      1 2      0       0
```

```
  2     10 2      0       0
  3      2 3      0       0
  6      3 11     0       0
  8     11 15     0       0
block   edge     u_x     t_y
  1      1 4      0       0
  2     10 14     0     free
  4      4 7      0       0
block   edge     u_z     t_x     t_y     e_xx        e_yy
  8     15 16     0       0       0   -10.54e-3   6.84e-3
  9     16 17     0       0       0   -10.54e-3   6.84e-3
block   edge     u_z     t_y
  4      7 8      0       0
  5      8 9      0       0
  7      9 13     0       0
  9     13 17     0       0

u_x = 0, u_y = 0, t_x = 0, t_y = free  ! this prevents overwriting
node
10
u_x = 0, u_y = 0, t_x = 0, t_y = 0     ! no crack in this layer
node
1
end displacements


constraint_equations
active = on,  right_hand_side = 0
constraint       equations
   1       1.0 u_y  14, -1.0 u_y 4
   2       1.0 u_y 215, -1.0 u_y 116
   3       1.0 u_y 212, -1.0 u_y 113
   4       1.0 u_y 218, -1.0 u_y 119
   5       1.0 u_y 216, -1.0 u_y 117
   6       1.0 u_y 129, -1.0 u_y 21
   7       1.0 u_y 219, -1.0 u_y 120
   8       1.0 u_y 223, -1.0 u_y 124
   9       1.0 u_y 221, -1.0 u_y 122
  10       1.0 u_y 224, -1.0 u_y 126
end constraints
```

.DAT file for FE mesh of coupon - wide delamination (30 mm wide by 25 mm long) and ply crack, plus fixed matrix crack at edge of original delamination (overlapping prevented when constraints used)

```
control
title = Delamination wider + matrix and Ply cracks.
problem = large
end control

blocks
type = q8, element_type = q8_pt
block   ply_sequence   d_1   d_2      nodes
  1       1      5     5     1  2  6  7    ! Plies beneath delamination
  2       1      5     1     6  7 11 12    ! Plies beneath delamination
  3       2      5     5    18  2 19  7    ! Delamination
```

```
  4       2       5       1     20  7 11 12   ! Delamination
  5       3       5       4     11 12 13 14   ! Undamaged laminate
  6       3       5       5      2  3  7  8   ! Undamaged laminate
  7       3       5       5      7  8 14 15   ! Undamaged laminate
  8       3       5       5      3  4  8  9   ! Extended section
  9       3       5       5      8  9 15 16   ! to reduce stress
  10      3       5       5      4  5  9 10   ! concentration
  11      3       5       5      9 10 16 17   !
end blocks

nodes
z = 0.0
node   x       y
  1    0       0
  2   12.5e-3   0
  3   25.0e-3   0
  4   37.5e-3   0
  5   50.0e-3   0
  6    0       12.5e-3
  7   12.5e-3  12.5e-3
  8   25.0e-3  12.5e-3
  9   37.5e-3  12.5e-3
 10   50.0e-3  12.5e-3
 11    0       15.0e-3      !  Limit of edge of delamination
 12   12.5e-3  15.0e-3      !  Limit of edge of delamination
 13    0       25.0e-3
 14   12.5e-3  25.0e-3
 15   25.0e-3  25.0e-3
 16   37.5e-3  25.0e-3
 17   50.0e-3  25.0e-3
z = 1.0e-5
 18    0      0       ! produces transverse ply crack
 19    0      12.4999e-3 ! produces long.l matrix crack
 20    0      12.5001e-3 ! produces long.l matrix crack
end nodes

materials
type = orthotropic
material  e_1   e_2   e_3   nu_23  nu_31  nu_12  g_23 g_31 g_12
  1     135e9  8.5e9  8.5e9  0.35  0.35  0.35  3e9  3e9  3e9
  2     135e3  8.5e3  8.5e3  0.35  0.35  0.35  3e3  3e3  3e3
end materials

ply_sequences
ply_sequence     sequence
     1       1 -45 0.125e-3 & ! Plies beneath delamination
             1  45 0.125e-3 &
             1   0 0.375e-3 &
             1 -45 0.125e-3 &
             1  45 0.125e-3 &
             1   0 0.5e-3   &
             1  45 0.125e-3 &
             1 -45 0.125e-3 &
             2   0 0.375e-3 &
             2  45 0.125e-3 &
             2 -45 0.125e-3

2            2 -45 0.125e-3 & ! Delaminated plies
             2  45 0.125e-3 &
             2   0 0.375e-3 &
             2 -45 0.125e-3 &
             2  45 0.125e-3 &
```

```
    2   0 0.5e-3   &
    2  45 0.125e-3 &
    2 -45 0.125e-3 &
    1   0 0.375e-3 &
    1  45 0.125e-3 &
    1 -45 0.125e-3

3       1 -45 0.125e-3 & ! Undamaged laminate
    1  45 0.125e-3 &
    1   0 0.375e-3 &
    1 -45 0.125e-3 &
    1  45 0.125e-3 &
    1   0 0.5e-3   &
    1  45 0.125e-3 &
    1 -45 0.125e-3 &
    1   0 0.375e-3 &
    1  45 0.125e-3 &
    1 -45 0.125e-3
end ply_sequences

displacements
block  edge   u_y   t_x
  1     1  2   0     0      ! Plane of symmetry
  3    18  2   0     0      ! along centre-line
  6     2  3   0     0      ! of the coupon -
  8     3  4   0     0      ! longitudinally
  10    4  5   0     0      !
block  edge   u_x   t_y
  1     1  6   0     0      ! Plane of symmetry
  2     6 11   0     0      ! along centre-line
  4    20 11   0     0      ! of the coupon -
  5    11 13   0     0      ! transverse
block  edge   u_x   t_y
  3    18 19   0   free     ! ply crack edge
block  edge   u_z   t_x   t_y   e_xx      e_yy
 10     5 10   0     0     0  -10.54e-3  6.84e-3   ! Loaded end +
 11    10 17   0     0     0  -10.54e-3  6.84e-3   ! A-B guide
block  edge   u_z   t_y
  5    13 14   0     0      !
  7    14 15   0     0      ! Outside edge - held
  9    15 16   0     0      ! by anti-buckling guide
 11    16 17   0     0      !

! Following lines specify particular nodes:
! this prevents overwriting of constraints.

u_x = 0, u_y = 0, t_x = 0, t_y = free
node
18
u_x = 0, u_y = 0, t_x = 0, t_y = 0      ! no crack in this layer
node
1
end displacements

! Following equations prevent delamination from occupying the
! same space as undamaged material-it may move out of plane.

constraint_equations
active = on,  right_hand_side = 0
constraint        equations
   1       1.0 u_y  19, -1.0 u_y 20
   2       1.0 u_y 201, -1.0 u_y 214
```

```
  3       1.0 u_y 198, -1.0 u_y 213
  4       1.0 u_y 204, -1.0 u_y 217
  5       1.0 u_y 202, -1.0 u_y 216
  6       1.0 u_y 130, -1.0 u_y 115
  7       1.0 u_y 205, -1.0 u_y 219
  8       1.0 u_y 209, -1.0 u_y 222
  9       1.0 u_y 207, -1.0 u_y 221
 10       1.0 u_y 210, -1.0 u_y 224
end constraints
```

.DAT file for FE mesh of coupon - wider delamination (35 mm wide by 25mm long) and ply crack, plus matrix crack at edge of extended delamination (overlapping prevented). For investigation of effect of delamination growth.

```
control
title = Delamination wider ( 35 mm rather than 25) + Ply crack in top 5
plies
!       + matrix along edge of delamination.  Constraints can be applied
to
!       edge of matrix cracks to ensure they do not overlap.
problem = large
end control


blocks
type = q8, element_type = q8_pt
block   ply_sequence    d_1    d_2      nodes
  1         1           5      7       1 2 4 5     ! Plies beneath delamination
  2         2           5      7      10 2 14 5    ! Delamination
  3         3           5      7       2 3 5 6     ! Undamaged laminate
  4         3           5      3       4 5 7 8     ! Undamaged laminate
  5         3           5      3       5 6 8 9     ! Undamaged laminate
  6         3           5      7       3 11 6 12   ! Extended section
  7         3           5      3       6 12 9 13   ! to reduce stress
  8         3           5      7      11 15 12 16  ! concentration
  9         3           5      3      12 16 13 17  ! conc.
end blocks


nodes
z = 0.0
node   x       y
  1    0       0
  2   12.5e-3    0
  3   25.0e-3    0
  4    0        12.5e-3
  5   12.5e-3   12.5e-3
  6   25.0e-3   12.5e-3
  7    0        25.0e-3
  8   12.5e-3   25.0e-3
  9   25.0e-3   25.0e-3
 11   37.5e-3    0
 12   37.5e-3   12.5e-3
 13   37.5e-3   25.0e-3
```

```
 14    0        12.4999e-3 ! produces long.1 matrix crack
 15   50.0e-3    0
 16   50.0e-3   12.5e-3
 17   50.0e-3   25.0e-3

z = 2.0e-5
 10    0      0
end nodes


materials
type = orthotropic
material   e_1   e_2   e_3   nu_23   nu_31   nu_12   g_23 g_31 g_12
  1     135e9   8.5e9   8.5e9   0.35   0.35   0.35   3e9   3e9   3e9
  2     135e3   8.5e3   8.5e3   0.35   0.35   0.35   3e3   3e3   3e3
end materials

ply_sequences
ply_sequence      sequence
      1       1 -45 0.125e-3 & ! Plies beneath delamination
            1  45 0.125e-3 &
            1   0 0.375e-3 &
            1 -45 0.125e-3 &
            1  45 0.125e-3 &
            1   0 0.5e-3   &
            1  45 0.125e-3 &
            1 -45 0.125e-3 &
            2   0 0.375e-3 &
            2  45 0.125e-3 &
            2 -45 0.125e-3

      2       2 -45 0.125e-3 & ! Delaminated plies
            2  45 0.125e-3 &
            2   0 0.375e-3 &
            2 -45 0.125e-3 &
            2  45 0.125e-3 &
            2   0 0.5e-3   &
            2  45 0.125e-3 &
            2 -45 0.125e-3 &
            1   0 0.375e-3 &
            1  45 0.125e-3 &
            1 -45 0.125e-3

3       1 -45 0.125e-3 & ! Undamaged laminate
            1  45 0.125e-3 &
            1   0 0.375e-3 &
            1 -45 0.125e-3 &
            1  45 0.125e-3 &
            1   0 0.5e-3   &
            1  45 0.125e-3 &
            1 -45 0.125e-3 &
            1   0 0.375e-3 &
            1  45 0.125e-3 &
            1 -45 0.125e-3
end ply_sequences


displacements
block   edge     u_y     t_x
  1      1 2      0       0
  2     10 2      0       0
  3      2 3      0       0
```

```
  6      3 11     0       0
  8     11 15     0       0
block   edge     u_x     t_y
  1      1 4      0       0
  2     10 14     0      free
  4      4 7      0       0
block   edge     u_z     t_x     t_y     e_xx        e_yy
  8     15 16     0       0       0   -10.54e-3    6.84e-3
  9     16 17     0       0       0   -10.54e-3    6.84e-3
block   edge     u_z     t_x
  4      7 8      0       0
  5      8 9      0       0
  7      9 13     0       0
  9     13 17     0       0

u_x = 0, u_y = 0, t_x = 0, t_y = free  ! this prevents
                                       ! overwriting
node
10
u_x = 0, u_y = 0, t_x = 0, t_y = 0     ! no crack in this
                                       ! layer
node
1
end displacements


!constraint_equations
!active = on,  right_hand_side = 0
!constraint       equations
!   1       1.0 u_y  14, -1.0 u_y 4
!   2       1.0 u_y 215, -1.0 u_y 116
!   3       1.0 u_y 212, -1.0 u_y 113
!   4       1.0 u_y 218, -1.0 u_y 119
!   5       1.0 u_y 216, -1.0 u_y 117
!   6       1.0 u_y 129, -1.0 u_y 21
!   7       1.0 u_y 219, -1.0 u_y 120
!   8       1.0 u_y 223, -1.0 u_y 124
!   9       1.0 u_y 221, -1.0 u_y 122
!  10       1.0 u_y 224, -1.0 u_y 126
!end constraints
```

.DAT file for FE mesh of coupon - wider delamination (35mm wide and 25 mm long) and ply crack, plus fixed matrix crack at edge of original delamination (overlapping prevented, if constraints applied)

```
control
title = Delamination wider + matrix and Ply cracks.
problem = large
end control

blocks
type = q8, element_type = q8_pt
block   ply_sequence   d_1   d_2      nodes
  1     1    5     5     1  2  6  7   ! Plies beneath delamination
  2     1    5     2     6  7 11 12   ! Plies beneath delamination
```

```
  3     2     5      5     18  2 19  7    ! Delamination
  4     2     5      2     20  7 11 12    ! Delamination
  5     3     5      3     11 12 13 14    ! Undamaged laminate
  6     3     5      5      2  3  7  8    ! Undamaged laminate
  7     3     5      5      7  8 14 15    ! Undamaged laminate
  8     3     5      5      3  4  8  9    ! Extended section to
  9     3     5      5      8  9 15 16    ! reduce stress conc.
  10    3  5    5    4  5  9 10           ! reduce stress conc.
  11    3  5    5    9 10 16 17           ! reduce stress conc.
end blocks

nodes
z = 0.0
node  x      y
  1    0      0
  2   12.5e-3   0
  3   25.0e-3   0
  4   37.5e-3   0
  5   50.0e-3   0
  6    0       12.5e-3
  7   12.5e-3  12.5e-3
  8   25.0e-3  12.5e-3
  9   37.5e-3  12.5e-3
 10   50.0e-3  12.5e-3
 11    0       17.5e-3      !  Limit of edge of delamination
 12   12.5e-3  17.5e-3      !  Limit of edge of delamination
 13    0       25.0e-3
 14   12.5e-3  25.0e-3
 15   25.0e-3  25.0e-3
 16   37.5e-3  25.0e-3
 17   50.0e-3  25.0e-3
z = 1.0e-5
 18    0      0       ! produces transverse ply crack
 19    0      12.4999e-3 ! produces long.l matrix crack
 20    0      12.5001e-3 ! produces long.l matrix crack
end nodes

materials
type = orthotropic
material  e_1   e_2   e_3   nu_23  nu_31  nu_12  g_23 g_31 g_12
  1     135e9  8.5e9  8.5e9  0.35  0.35  0.35  3e9  3e9  3e9
  2     135e3  8.5e3  8.5e3  0.35  0.35  0.35  3e3  3e3  3e3
end materials

ply_sequences
ply_sequence      sequence
     1       1 -45 0.125e-3 & ! Plies beneath delamination
           1  45 0.125e-3 &
           1   0 0.375e-3 &
           1 -45 0.125e-3 &
           1  45 0.125e-3 &
           1   0 0.5e-3   &
           1  45 0.125e-3 &
           1 -45 0.125e-3 &
           2   0 0.375e-3 &
           2  45 0.125e-3 &
           2 -45 0.125e-3
```

```
2       2 -45 0.125e-3 & ! Delaminated plies
      2  45 0.125e-3 &
      2   0 0.375e-3 &
      2 -45 0.125e-3 &
      2  45 0.125e-3 &
      2   0 0.5e-3   &
      2  45 0.125e-3 &
      2 -45 0.125e-3 &
      1   0 0.375e-3 &
      1  45 0.125e-3 &
      1 -45 0.125e-3

3       1 -45 0.125e-3 & ! Undamaged laminate
      1  45 0.125e-3 &
      1   0 0.375e-3 &
      1 -45 0.125e-3 &
      1  45 0.125e-3 &
      1   0 0.5e-3   &
      1  45 0.125e-3 &
      1 -45 0.125e-3 &
      1   0 0.375e-3 &
      1  45 0.125e-3 &
      1 -45 0.125e-3
end ply_sequences

displacements
block  edge   u_y   t_x
  1     1  2    0     0      ! Plane of symmetry
  3    18  2    0     0      ! along centre-line
  6     2  3    0     0      ! of the coupon -
  8     3  4    0     0      ! longitudinally
  10    4  5    0     0      !
block  edge   u_x   t_y
  1     1  6    0     0      ! Plane of symmetry
  2     6 11    0     0      ! along centre-line
  4    20 11    0     0      ! of the coupon -
  5    11 13    0     0      ! transverse
block  edge   u_x   t_y
  3    18 19    0   free     ! ply crack edge
block  edge   u_z   t_x   t_y   e_xx      e_yy
 10     5 10    0     0    0  -10.54e-3  6.84e-3   ! Loaded end +
 11    10 17    0     0    0  -10.54e-3  6.84e-3   ! A-B guide
block  edge   u_z   t_y
  5    13 14    0     0      !
  7    14 15    0     0      ! Outside edge - held
  9    15 16    0     0      ! by anti-buckling guide
 11    16 17    0     0      !

! Following lines specify particular nodes:
! this prevents overwriting of constraints.

u_x = 0, u_y = 0, t_x = 0, t_y = free
node
18
u_x = 0, u_y = 0, t_x = 0, t_y = 0      ! no crack in this layer
node
1
end displacements

! Following equations prevent delamination from occupying the
! same space as undamaged material-it may move out of plane.
```

```
constraint_equations
active = on,  right_hand_side = 0
constraint       equations
   1       1.0 u_y  19, -1.0 u_y 20
   2       1.0 u_y 218, -1.0 u_y 232
   3       1.0 u_y 215, -1.0 u_y 230
   4       1.0 u_y 221, -1.0 u_y 238
   5       1.0 u_y 219, -1.0 u_y 236
   6       1.0 u_y 147, -1.0 u_y 228
   7       1.0 u_y 222, -1.0 u_y 241
   8       1.0 u_y 226, -1.0 u_y 247
   9       1.0 u_y 224, -1.0 u_y 245
  10       1.0 u_y 227, -1.0 u_y 250
end constraints
```

APPENDIX E

Publications Resulting From This Work

Pavier, M.J. and Clarke, M.P. *Accepted for publication in Composite Structures* **1996**.

FINITE ELEMENT PREDICTION OF THE POST IMPACT COMPRESSIVE STRENGTH OF FIBRE COMPOSITES

Abstract:

Low velocity impact damage to composite laminates results in a complicated pattern of fibre cracks, matrix cracks and delaminations. The complexity of the damage has made the prediction of compressive strength reduction difficult since the mechanisms of failure are difficult to discern. In this paper a finite element prediction of post-impact compressive strength is described based on a stress analysis of a laminate containing buckled delaminated plies. The strength reduction mechanisms have been assessed from tests on laminates containing artificial simplified damage similar to real impact damage. Excellent agreement between experimental failure loads and finite element predictions has been found.

Pavier, M.J. and Clarke, M.P. *Composite Structures* 34 **1996**. pp. 43-53

"A SPECIALISED COMPOSITE PLATE ELEMENT FOR PROBLEMS OF DELAMINATION BUCKLING AND GROWTH."

Abstract:

A specialised layered composite finite element for problems of delamination buckling and growth has been developed based on a thick plate element. The element allows delaminated laminae to be joined together easily by using the simple method of shifting the position of the mid-plane of the element relative to the laminae it represents. In addition the element includes a small initial out of plane displacement to enable buckle initiation to take place without requiring normal forces to be applied. The element is demonstrated to function correctly using a number of simple test cases and by comparing the results of an analysis of a circular delamination with those from a full three dimensional analysis.

Pavier, M.J. and Clarke, M.P.

Composites Science and Technology 55
September **1995** pp.157-69.

"EXPERIMENTAL TECHNIQUES FOR THE INVESTIGATION OF THE EFFECTS OF IMPACT DAMAGE ON CARBON FIBRE COMPOSITES."

Abstract:

Low velocity impact damage to composite laminates causes a complicated pattern of matrix cracks, fibre cracks and delamination. A significant effect of this damage is to reduce the strength of the laminate, particularly in compression; however due to the complexity of the damage the precise mechanisms controlling the strength reduction are unclear. In this paper a technique is described for replicating impact damage artificially by including PTFE film delaminants and cut plies during lay-up. Comparisons between real and artificially reproduced damage are made to demonstrate the validity of the technique. Experimental methods of X-ray radiography and resin injection are developed to allow the mechanisms controlling strength reduction to be assessed, both under tensile and compressive loading. Under tensile load the reduction in strength due to impact damage is found to be entirely due to fibre cracks and may be estimated using a net section calculation. Meanwhile under compression, strength reduction is largely due to the redistribution of stress resulting from buckling of delaminated plies and may be predicted by calculating stresses in the undelaminated part of the laminate.

Clarke M.P. and Pavier M.J.

Composite Structures 25
July **1993** pp.113-20

"ARTIFICIAL DAMAGE TECHNIQUES FOR LOW VELOCITY IMPACT IN CARBON-FIBRE COMPOSITES."

Abstract:

Materials and techniques used in artificially induced damage are evaluated and compared. The damage induced by low velocity impacts is characterised using penetrant enhanced radiography and deply techniques. This information is used to construct specimens with simulated damage that will facilitate the study of damage growth. Specimens manufactured match quite closely the properties of specimens which contain actual damage.

Clarke M.P., Pavier M.J. and Kemp, M.

Proceedings ICCM 9
July **1993** pp. 250-7.

"MODELLING OF ARTIFICIAL DAMAGE IN CARBON-FIBRE COMPOSITES."

Abstract:

Low velocity impact damage was modelled artificially to allow study of the effects of delaminations and ply-cracks on residual compressive and tensile strength. Real damage from impacts was characterised using penetrant enhanced radiography and de-ply techniques. Initially, real and artificially damaged specimens were compared. The artificial damage was then simplified so that a finite element model could be used in comparison with actual artificial damage. The mechanisms that initiate failure of the specimen were investigated by varying the position and combination of delaminations and ply-cracks.

APPENDIX F

Details of Matrices for Specialised Plate Element

For completeness all the matrices referred to in chapter 6 are given in detailed form here.

Writing equation, $\delta\varepsilon = \mathbf{B}\delta\mathbf{u}$, as

$$\delta\varepsilon = \sum_{i=1}^{N} \mathbf{B}_i \delta\mathbf{u}_i$$

where N is the number of nodes of the element and $\delta\mathbf{u}_i$ is the incremental displacement of node i we have

$$\delta\varepsilon^{\mathbf{T}} = \begin{bmatrix} \delta\varepsilon_x & \delta\varepsilon_y & \delta\gamma_{yz} & \delta\gamma_{zx} & \delta\gamma_{xy} \end{bmatrix}$$
$$\delta\mathbf{u}_i^{\mathbf{T}} = \begin{bmatrix} \delta u_i & \delta v_i & \delta w_i & \delta\theta_i^x & \delta\theta_i^y \end{bmatrix}$$

and

$$\mathbf{B}_i = \begin{bmatrix} F_{11}\frac{\partial N_i}{\partial x} & F_{21}\frac{\partial N_i}{\partial x} & F_{31}\frac{\partial N_i}{\partial x} & -zF_{21}\frac{\partial N_i}{\partial x} & zF_{11}\frac{\partial N_i}{\partial x} \\ F_{12}\frac{\partial N_i}{\partial y} & F_{22}\frac{\partial N_i}{\partial y} & F_{32}\frac{\partial N_i}{\partial y} & -zF_{22}\frac{\partial N_i}{\partial y} & zF_{12}\frac{\partial N_i}{\partial y} \\ F_{13}\frac{\partial N_i}{\partial x} & F_{23}\frac{\partial N_i}{\partial x} & \frac{\partial N_i}{\partial x} & -F_{21}N_i - zF_{23}\frac{\partial N_i}{\partial x} & F_{11}N_i + zF_{13}\frac{\partial N_i}{\partial x} \\ F_{13}\frac{\partial N_i}{\partial y} & F_{23}\frac{\partial N_i}{\partial y} & \frac{\partial N_i}{\partial y} & -F_{22}N_i - zF_{23}\frac{\partial N_i}{\partial y} & F_{12}N_i + zF_{13}\frac{\partial N_i}{\partial y} \\ F_{12}\frac{\partial N_i}{\partial x} + F_{11}\frac{\partial N_i}{\partial y} & F_{22}\frac{\partial N_i}{\partial x} + F_{21}\frac{\partial N_i}{\partial y} & F_{32}\frac{\partial N_i}{\partial x} + F_{31}\frac{\partial N_i}{\partial y} & -zF_{22}\frac{\partial N_i}{\partial x} - zF_{21}\frac{\partial N_i}{\partial y} & zF_{12}\frac{\partial N_i}{\partial x} + zF_{11}\frac{\partial N_i}{\partial y} \end{bmatrix}$$

where F_{ij} are components of the deformation gradient tensor $\mathbf{F}$ calculated from the displacement gradient tensor $\mathbf{H}$ by

$$\mathbf{F} = \mathbf{H} + \mathbf{I}$$

where $\mathbf{I}$ denotes the unit tensor [Atkin & Fox, 1980]. The components of the displacement gradient tensor are calculated as follows :

$$H_{11}=\sum_{i=1}^{N}\left[u_i\frac{\partial N_i}{\partial x}+z\theta_i^y\frac{\partial N_i}{\partial x}\right],\quad H_{12}=\sum_{i=1}^{N}\left[u_i\frac{\partial N_i}{\partial y}+z\theta_i^y\frac{\partial N_i}{\partial y}\right],\qquad H_{13}=\sum_{i=1}^{N}\left[\theta_i^y N_i\right]$$

$$H_{21}=\sum_{i=1}^{N}\left[v_i\frac{\partial N_i}{\partial x}+z\theta_i^x\frac{\partial N_i}{\partial x}\right],\quad H_{22}=\sum_{i=1}^{N}\left[v_i\frac{\partial N_i}{\partial y}+z\theta_i^x\frac{\partial N_i}{\partial y}\right],\qquad H_{23}=\sum_{i=1}^{N}\left[\theta_i^x N_i\right]$$

$$H_{31}=\sum_{i=1}^{N}\left[w_i\frac{\partial N_i}{\partial x}+z_i\frac{\partial N_i}{\partial x}\right],\qquad H_{32}=\sum_{i=1}^{N}\left[w_i\frac{\partial N_i}{\partial y}+z_i\frac{\partial N_i}{\partial y}\right]$$

An initial displacement gradient tensor $\mathbf{H}^O$ is defined with zero components except for

$$H_{31}^{O}=\sum_{i=1}^{N}\left[w_i^{o}\frac{\partial N_i}{\partial x}\right],\ H_{32}^{O}=\sum_{i=1}^{N}\left[w_i^{o}\frac{\partial N_i}{\partial y}\right]$$

to allow the components of the strain vector

$$\varepsilon^{T}=\left[\varepsilon_x\quad\varepsilon_y\quad\gamma_{yz}\quad\gamma_{zx}\quad\gamma_{xy}\right]$$

to be calculated by

$$\varepsilon_x=H_{11}+\tfrac{1}{2}\left[H_{11}{}^2+H_{21}{}^2+H_{31}{}^2-H_{31}^{O\,2}\right]$$

$$\varepsilon_y=H_{22}+\tfrac{1}{2}\left[H_{12}{}^2+H_{22}{}^2+H_{32}{}^2-H_{32}^{O\,2}\right]$$

$$\gamma_{yz}=H_{23}+H_{32}+H_{12}H_{13}+H_{22}H_{23}$$

$$\gamma_{zx}=H_{13}+H_{31}+H_{11}H_{13}+H_{21}H_{23}$$

$$\gamma_{xy}=H_{12}+H_{21}+H_{11}H_{12}+H_{21}H_{22}+H_{31}H_{32}-H_{31}^{O}H_{32}^{O}$$

The stress vector

$$\sigma^{T}=\left[\sigma_x\quad\sigma_y\quad\tau_{yz}\quad\tau_{zx}\quad\tau_{xy}\right]$$

is calculated from the strain vector by $\sigma=\mathbf{D}\varepsilon$.

The material matrix **D** is derived using $\mathbf{D}=\mathbf{T}\mathbf{Q}\mathbf{T}^{T}$ with the transformation matrix **T** given by

$$\mathbf{T}=\begin{bmatrix} c^2 & s^2 & 0 & 0 & -2sc \\ s^2 & c^2 & 0 & 0 & 2sc \\ 0 & 0 & c & -s & 0 \\ 0 & 0 & s & c & 0 \\ sc & -sc & 0 & 0 & c^2-s^2 \end{bmatrix}$$

where $c=\cos\theta$, $s=\sin\theta$ where θ is the orientation of the current ply and the material matrix **Q** by

$$\mathbf{Q}=\begin{bmatrix} \frac{E_{11}}{1-\nu_{12}\nu_{21}} & \frac{\nu_{12}E_{22}}{1-\nu_{12}\nu_{21}} & 0 & 0 & 0 \\ \frac{\nu_{12}E_{22}}{1-\nu_{12}\nu_{21}} & \frac{E_{22}}{1-\nu_{12}\nu_{21}} & 0 & 0 & 0 \\ 0 & 0 & \frac{G_{23}}{\lambda} & 0 & 0 \\ 0 & 0 & 0 & \frac{G_{31}}{\lambda} & 0 \\ 0 & 0 & 0 & 0 & G_{12} \end{bmatrix}$$

λ in the above matrix is a shear correction factor intended to correct the over-stiff behaviour of the element in shear. The value for the isotropic case of 1.2 is used, but values calculated for orthotropic laminates are not too different [Whitney, 1973].

Finally matrices **G** and **M** have their standard form where the submatrix $\mathbf{G}_i$ corresponding to node *i* is

$$\mathbf{G}_i = \begin{bmatrix} \frac{\partial N_i}{\partial x} & 0 & 0 & 0 & z\frac{\partial N_i}{\partial x} \\ 0 & \frac{\partial N_i}{\partial x} & 0 & -z\frac{\partial N_i}{\partial x} & 0 \\ 0 & 0 & \frac{\partial N_i}{\partial x} & 0 & 0 \\ \frac{\partial N_i}{\partial y} & 0 & 0 & 0 & z\frac{\partial N_i}{\partial x} \\ 0 & \frac{\partial N_i}{\partial y} & 0 & -z\frac{\partial N_i}{\partial y} & 0 \\ 0 & 0 & \frac{\partial N_i}{\partial y} & 0 & 0 \\ 0 & 0 & 0 & 0 & N_i \\ 0 & 0 & 0 & -N_i & 0 \\ 0 & 0 & 0 & 0 & 0 \end{bmatrix}$$

and

$$\mathbf{M} = \begin{bmatrix} \sigma_x & 0 & 0 & \tau_{xy} & 0 & 0 & \tau_{zx} & 0 & 0 \\ 0 & \sigma_x & 0 & 0 & \tau_{xy} & 0 & 0 & \tau_{zx} & 0 \\ 0 & 0 & \sigma_x & 0 & 0 & \tau_{xy} & 0 & 0 & \tau_{zx} \\ \tau_{xy} & 0 & 0 & \sigma_y & 0 & 0 & \tau_{yz} & 0 & 0 \\ 0 & \tau_{xy} & 0 & 0 & \sigma_y & 0 & 0 & \tau_{yz} & 0 \\ 0 & 0 & \tau_{xy} & 0 & 0 & \sigma_y & 0 & 0 & \tau_{yz} \\ \tau_{zx} & 0 & 0 & \tau_{yz} & 0 & 0 & 0 & 0 & 0 \\ 0 & \tau_{zx} & 0 & 0 & \tau_{yz} & 0 & 0 & 0 & 0 \\ 0 & 0 & \tau_{zx} & 0 & 0 & \tau_{yz} & 0 & 0 & 0 \end{bmatrix}$$

REFERENCES

Atkin, R.J. and Fox, N.

"An introduction to theTheory of Elasticity."
Longman, **1980**

Whitney, J.M.

"Shear correction factors for orthotropic laminates under static load."
Journal of Applied Mechanics, 40 **1973** pp. 302-304